

AN INVESTIGATION INTO THE ROLE OF  
SEX CHROMOSOME SYNAPSIS IN MEIOTIC SEX  
CHROMOSOME INACTIVATION AND FERTILITY

Thesis submitted for the degree of Doctor of Philosophy

James Michael Andrew Turner

National Institute for Medical Research

University College London

University of London

2000

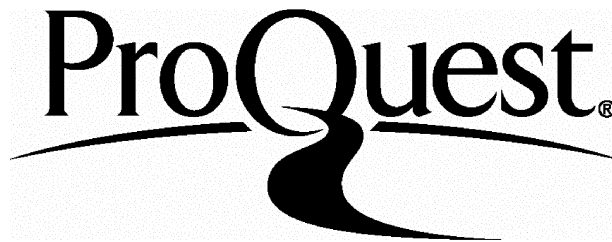
ProQuest Number: 10016064

All rights reserved

INFORMATION TO ALL USERS

The quality of this reproduction is dependent upon the quality of the copy submitted.

In the unlikely event that the author did not send a complete manuscript and there are missing pages, these will be noted. Also, if material had to be removed, a note will indicate the deletion.



ProQuest 10016064

Published by ProQuest LLC(2016). Copyright of the Dissertation is held by the Author.

All rights reserved.

This work is protected against unauthorized copying under Title 17, United States Code.  
Microform Edition © ProQuest LLC.

ProQuest LLC  
789 East Eisenhower Parkway  
P.O. Box 1346  
Ann Arbor, MI 48106-1346

This thesis is dedicated to my parents, Patsy and Mick,  
my sister Emma and my brother Matthew.

## ACKNOWLEDGEMENTS

First and foremost I would like to thank Paul, who has been an excellent supervisor and who has taught me everything I've ever needed to know about sex chromosomes, and more. I would also like to thank Shanthi, who has also been a great source of support and a good friend, even if she does insist that the sex body serves no function. Thanks also to other members of the past and present lab, namely Aine, Tristan, Vladimir, Linda and Sophie.

A very special thank you also goes to the members of Robin's lab, in particular Ariel for her amazing 'ordum puddung', Donald for technical assistance and for joining me in many whistling conversations and Amanda for 'enhunzung' so many amazing 'storuz'. I also thank members of the Division of Neurobiology for making me feel at home when I arrived at the Institute, and the staff of Biological Services, in particular Rachel, for teaching me about respect for animals and for making me laugh so much. I am also indebted to Christa Heyting, with whom I have had many in depth e-mail discussions about the minutiae of meiosis, to Ricardo Benavente, Henri-Jean Garchon and David Elliott for provision of invaluable reagents and to Stamatis Pagakis for help with imaging.

Thanks also goes to those outside the lab that have supported me over the last three years, namely Mum, Dad, Emma, Matthew, Helen, Mike, Phil, Barny, Jenny, Lance, Sue, Paula, Lisa, Simon, Mahreen and Sugi. A very special thank you goes to Helen for spotting the mistakes in my thesis that myself and others would never have noticed.

Finally, I would like to thank the NIMR mice, without which none of this work would have been possible.



## ABSTRACT

During male meiosis in a number of species, the sex chromosomes become transcriptionally inactive (termed meiotic sex chromosome inactivation, or MSCI) and form a peripheral, densely staining structure termed the sex body. The function of MSCI is not known, but it may serve to silence ‘poisonous’ sex-linked genes, or to prevent the asynapsed portions of the sex chromosomes from triggering a checkpoint that monitors synapsis, recombination, or both. It has been postulated that MSCI is mediated by the *Xist* gene, and that Y chromosome inactivation proceeds by ‘*quasi-cis*’ spreading of *Xist* RNA from the X chromosome to the Y chromosome via the synapsed pseudoautosomal regions. The purpose of the present study was to examine the *quasi-cis* hypothesis, by analysing MSCI in *Xist*-disrupted spermatocytes, and Y chromosome inactivation in spermatocytes with high levels of X-Y synaptic failure.

The first two chapters were aimed at identifying an MSCI marker that could be used to carry out the experiments described above. The MSCI-specificity of three sex body proteins: ASY, XMR/XLR and XY77 was examined by analysing the expression of each in oocytes from  $XY^{Tdyml}$  females. The sex chromosomes in these oocytes failed to exhibit MSCI and were therefore suitable as negative controls. ASY and XMR/XLR coated the asynapsed X chromosome in  $XY^{Tdyml}$  oocytes and also the asynapsed autosomes in T(2;5)72H oocytes, indicating that their presence in the sex body is related to the asynaptic and not transcriptionally inactive state of the sex chromosomes. XY77, in contrast, was sex body-specific.

Next, the *quasi-cis* model was investigated by examination of MSCI in *Xist*-disrupted males and in males with sex chromosome synaptic failure ( $XY^{d1}$ ,  $XY^{*X}$ ). MSCI and sex body formation proceeded normally in the absence of *Xist*, but both were disrupted in  $XY^{d1}$

spermatocytes.  $XY Y^{d1}$  spermatocytes exhibiting defects in sex body formation and/or MSCI were eliminated between mid and late pachytene, indicating that MSCI is indispensable for meiosis and that it is disrupted by excess sex chromatin.

Finally, an inherited genetic effect was characterised that could partially circumvent the pachytene checkpoint in  $X^{Y^*}O$  mice. This effect allowed the normally sterile  $X^{Y^*}O$  males to be fertile. The fertility was found to be due to the inheritance of an autosomal, dominant C3H factor (the major factor) together with a recessive MF1 factor. Inheritance of a second, dominantly-acting C3H allele (the minor factor) further augmented the sperm counts of the  $X^{Y^*}O$  males. Neither of the C3H factors was *Hst1*, a gene that confers fertility to interspecific hybrid male mice. Inheritance of these  $X^{Y^*}O$  fertility factors was unable to restore fertility in  $X^{Y^*}Y^{Tdy m1}$  males, possibly due to the additional defects in MSCI that these males would be expected to experience.

## **CONTENTS**

<b>ABSTRACT</b>	<b>4</b>
<b>CHAPTER 1. GENERAL INTRODUCTION.</b>	
1.1. MEIOSIS	16
1.1.1. Overview	16
1.1.2. The synaptonemal complex	16
1.1.3. Presynaptic alignment, homology searching and synapsis	19
1.1.4. Recombination	22
1.1.5. After pachytene	25
1.1.6. Sexual dimorphism in mammalian meiosis	26
1.2. MEIOTIC SEX CHROMOSOME INACTIVATION (MSCI)	30
1.2.1. Properties	30
1.2.2. Function	32
1.2.3. Mechanism	34
1.3. MEIOTIC CHECKPOINTS	36
1.3.1. General features	36
1.3.2. The pachytene checkpoint	37
1.3.3. Unpaired sex chromosomes and gametogenic failure	39
1.4. OUTLINE OF PROJECTS	45

## **CHAPTER 2. AN INVESTIGATION INTO THE MSC1-SPECIFICITY OF A NOVEL SEX BODY PROTEIN, ASYNAPTIN.**

2.1. INTRODUCTION	47
2.2 MATERIALS AND METHODS	51
2.2.1. Mice	51
2.2.2. Squash procedure	52
2.2.3. Surface spread procedure	53
2.2.4. Immunostaining	53
2.2.5. Examination	53
2.2.6. Total RNA extraction from testes and ovaries	53
2.2.7. DNase treatment and reverse transcription of total RNA	53
2.2.8. Genomic DNA extraction	53
2.2.9. PCR procedure	54
2.3 RESULTS	56
2.3.1. MSC1 status of XY <sup>Tdym1</sup> oocytes	56
2.3.2. ASY localisation in XY testis	57
2.3.3. ASY localisation in XY <sup>Tdym1</sup> oocytes	58
2.3.4. ASY localisation in XO oocytes	58
2.3.5. ASY localisation in In(X)/X oocytes	58
2.3.6. ASY localisation in XX oocytes	59
2.3.7. ASY localisation in T(2;5)72H oocytes	59
2.3.8. ASY localisation in XXY <sup>d1</sup> oocytes	60
2.4 DISCUSSION	79

**CHAPTER 3. AN INVESTIGATION INTO THE MSC1-SPECIFICITY  
OF XMR AND XY77.**

3.1. INTRODUCTION	84
3.2. MATERIALS AND METHODS	88
3.2.1. Mice	88
3.2.2. Squash procedure	88
3.2.3. Surface spread procedure	88
3.2.4. Immunostaining	88
3.2.5. Examination	88
3.2.6. Total RNA extraction from testes and ovaries	88
3.2.7. Reverse transcription of total RNA	88
3.2.8. Genomic DNA extraction	89
3.2.9. PCR procedure	89
3.2.10. Cloning and sequencing of PCR products	90
3.3. RESULTS	91
3.3.1. Anti-XLR immunostaining of XY testis	91
3.3.2. Anti-XLR immunostaining of XX oocytes	92
3.3.3. Anti-XLR immunostaining XY <sup>Tdym1</sup> oocytes	92
3.3.4. Anti-XLR immunostaining of T(2;5)72H oocytes	93
3.3.5. <i>Xmr/Xlr</i> expression in male and female gonads	93
3.3.6. Southern analysis of <i>Xmr</i>	95
3.3.7. XY77 in male meiosis	96
3.3.8. XY77 in XX and XY <sup>Tdym1</sup> females	96
3.4. DISCUSSION	119

## CHAPTER 4. AN INVESTIGATION INTO THE QUASI-CIS MODEL OF MSC1.

4.1. INTRODUCTION	124
4.2. MATERIALS AND METHODS	129
4.2.1. Mice	129
4.2.2. Squash procedure	130
4.2.3. Surface spread procedure	130
4.2.4. Immunostaining	130
4.2.5. Examination	130
4.2.6. Quantitation of XLR and RBM levels	131
4.2.7. Total RNA extraction	131
4.2.8. DNase treatment and reverse transcription of total RNA	131
4.2.9. PCR procedure	131
4.3. RESULTS	133
4.3.1. MSC1 status of <i>Xist</i> -targeted mice	133
4.3.2. Sex body formation in $XY Y^{d1}$ and $XY Y^{*X}$ spermatocytes as revealed by XY77 immunostaining	134
4.3.3. Sex body formation and Y chromosomal MSC1 in $XY Y$ , $XY Y^{d1}$ and $XY Y^{*X}$ spermatocytes as revealed by anti-XLR staining and RBM expression analysis	135
4.3.4. Surface spread analysis of $XY Y^{d1}$ males	138
4.4. DISCUSSION	165

## **CHAPTER 5. GENETIC ANALYSIS OF A FERTILE PEDIGREE OF X<sup>Y\*</sup>O MICE.**

5.1. INTRODUCTION	170
5.2. MATERIALS AND METHODS	177
5.2.1. Breeding crosses	177
5.2.1.1. XY* x In(X)/X	177
5.2.1.2. XY* x XO	177
5.2.1.3. X <sup>TaY*</sup> O (fertile) x In(X)/X or XO	177
5.2.1.4. X <sup>TaY*</sup> O (fertile) x XY <sup>Tdym1</sup> or XO (?carrier)	178
5.2.1.5. XY* x XY <sup>Tdym1</sup>	179
5.2.2. Sperm count	179
5.2.3. Genomic DNA extraction	179
5.2.4. PCR procedure	180
5.3. RESULTS	181
5.3.1. <i>Hst1</i> linkage analysis	181
5.3.2. Investigation of the strain source of the fertility factors in the X <sup>TaY*</sup> O pedigree	181
5.3.3. The mode of inheritance of the C3H fertility factors	182
5.3.4. Evidence that a recessive MF1 factor is also required for X <sup>Y*</sup> O fertility	183
5.3.5. Other sex chromosomally aberrant genotypes	184
5.4. DISCUSSION	196
<b>CHAPTER 6. GENERAL DISCUSSION.</b>	200
<b>APPENDIX 1.</b>	208
<b>REFERENCES.</b>	218

## **LIST OF FIGURES**

### **CHAPTER 1.**

Figure 1.1. The synaptonemal complex and homologous recombination 28

### **CHAPTER 2.**

Figure 2.1. ASY expression during male mouse meiosis 49

Figure 2.2. Analysis of MSCI in XY<sup>Tdym1</sup> pachytene oocytes 61

Figure 2.3. ASY expression in squashed and spread XY spermatogenic cells 63

Figure 2.4. ASY expression during XY male meiosis 65

Figure 2.5. High power analysis of ASY in the sex body 67

Figure 2.6. Appearance of ASY and morphological sex bodies during XY male meiosis. 69

Figure 2.7. ASY expression in the absence of MSCI 71

Figure 2.8. ASY expression in the absence of MSCI cont. 73

Figure 2.9. ASY expression in heterozygous T(2;5)72H pachytene oocytes 75

### **CHAPTER 3.**

Figure 3.1. Anti-XLR staining in squashed spermatogenic cells 97

Figure 3.2. Anti-XLR staining in squashed spermatogenic cells cont 99

Figure 3.3. Anti-XLR staining in squashed spermatogenic cells cont 101

Figure 3.4. Anti-XLR staining in squashed XX and XY<sup>Tdym1</sup> oogenic cells 103

Figure 3.5. Anti-XLR staining in squashed XY<sup>Tdym1</sup> oogenic cells cont 105



Figure 3.6. Anti-XLR staining in spread T(2;5)72H oogenic cells	107
Figure 3.7. Comparison of <i>Xlr</i> and <i>Xmr</i> cDNA sequences	109
Figure 3.8. RTPCR analysis of <i>Xmr</i> and <i>Xlr</i> expression in testes and ovaries	111
Figure 3.9. Southern analysis of <i>Xmr</i>	113
Figure 3.10. Anti-XY77 staining in XY spermatogenic and XY <sup>Tdym1</sup> oogenic cells	115

#### CHAPTER 4.

Figure 4.1. <i>Xist</i> gene structure and <i>Xist</i> disruption	127
Figure 4.2. RTPCR analysis of <i>Xist</i> , <i>Pgk2</i> and <i>Pdhal</i> expression in normal and <i>Xist</i> -disrupted testis	139
Figure 4.3. MSCI and sex body formation in <i>Xist</i> - spermatocytes	141
Figure 4.4. XY77 and XMR/XLR staining of sex bodies in XYY <sup>d1</sup> and XYY <sup>*X</sup> spermatocytes	145
Figure 4.5. RBM expression in squashed XY and XYY <sup>*X</sup> spermatogenic cells	147
Figure 4.6. RBM expression in squashed XY <sup>d1</sup> and XY spermatogenic cells	149
Figure 4.7. RBM expression in squashed XYY <sup>d1</sup> spermatogenic cells	151
Figure 4.8. Graph showing percentage of cells with and without sex bodies during meiotic progression in XY and XYY <sup>d1</sup> mice	155
Figure 4.9. Plots of RBM expression vs. whole nuclear XMR/XLR expression during the early-late pachytene transition in XY and XYY <sup>d1</sup> mice	157
Figure 4.10. Surface spread XYY <sup>d1</sup> spermatocytes	161
Figure 4.11. Surface spread XYY <sup>d1</sup> spermatocytes demonstrating that synapsis with the X chromosome is not a prerequisite for Y chromosome inclusion in the sex body	163

## CHAPTER 5.

- Figure 5.1. Diagrammatic representation of the  $XY^*$  rearrangement and of the products of its recombination with the X chromosome 173
- Figure 5.2. Sperm count distribution of  $X^{TaY^*}O$  males generated by mating  $X^{TaY^*}$  males to  $In(X)/X$  and  $XO$  (daughters of fertile  $X^{TaY^*}O$ ) 175
- Figure 5.3. Example of *Hst1* linkage analysis using *Tbp* primers for  $X^{Y^*}O$  males from the pedigree 186
- Figure 5.4. Sperm count distribution of  $X^{Y^*}O$  males generated by mating a) MF1  $XY^*$ , b)  $X^{TaY^*}$ , c) 129/MF1  $XY^*$  and d) C3H/MF1  $XY^*$  males to  $In(X)/X$  females 188
- Figure 5.5. Sperm count distribution of  $X^{Y^*}O$  males generated by mating C3H/MF1  $XY^*$  males to a)  $In(X)/X$  and b) MF1  $XO$  females, or fertile  $X^{Y^*}O$  males to c)  $In(X)/X$  and d) MF1  $XO$  females 190
- Figure 5.6. Sperm count distribution of  $X^{Y^*}O$  males generated by mating a) MF1  $XY^*$  x C3H  $XO$ , b) C3H  $XY^*$  x MF1  $XO$ , c) C3H/MF1  $XY^*$  x C3H  $XO$  and d) MF1/C3H  $XY^*$  x MF1  $XO$  192
- Figure 5.7. Sperm count distribution of fertility factor-carrying  $X^{Y^*}Y^{Tdym1}$  males and of  $X^{Y^*}O$  males 'homozygous' for the C3H fertility factors. 194

## **LIST OF TABLES**

### **CHAPTER 2**

Table 2.1. Appearance of ASY and of morphological sex bodies during XY male meiosis	69
Table 2.2. Appearance of ASY during meiosis I in different female genotypes	77

### **CHAPTER 3**

Table 3.1. Appearance of anti-XLR staining of asynapsed chromatin during meiosis I in different female genotypes	117
--	-----

### **CHAPTER 4**

Table 4.1. Existence of morphological sex bodies and sex chromosome RNA POLII exclusion in <i>Xist</i> <sup>+</sup> and <i>Xist</i> <sup>-</sup> spermatocytes	143
Table 4.2. Changes in sex body morphology during meiotic progression in XY and XYY <sup>d1</sup> spermatocytes	153
Table 4.3. Synaptic configuration and sex chromosomal abnormalities in XY and XYY <sup>d1</sup> spermatocytes	159

CHAPTER 1

GENERAL INTRODUCTION

## 1.1 MEIOSIS

### 1.1.1 Overview

Meiosis is a highly specialised form of cell division that functions primarily to reduce the diploid to the haploid state. Like mitosis, it commences with a single round of DNA replication, but this is followed by a unique series of processes, which include homologous alignment and synapsis, non-sister chromatid recombination and chiasma formation. The result is that at anaphase I, homologues rather than sister chromatids disjoin (the reductional division). Subsequently, at anaphase II, the sister chromatids of each homologue segregate, as in mitosis (the equational division). Prophase I is a long process (6 days in the mouse) that can be divided into a number of substages, each of which is associated with characteristic changes in chromosome morphology.

### 1.1.2 The synaptonemal complex

The synaptonemal complex (SC), which was first identified 44 years ago (Moses, 1956; Fawcett, 1956), is a proteinaceous, ribbon-like structure that holds homologues in close apposition along their entire lengths (Figure 1.1a). It is a tripartite structure consisting of two lateral elements (LEs) that lie 100nm apart and a central element (CE) that runs between and parallel to them. At higher magnification, the lateral elements appear connected by a three to five layer thick series of transverse filaments (TFs). Each of these TFs possesses two centrally located, symmetrically placed thickenings, which are collectively thought to constitute the CE (Roeder, 1997). Formation and dissolution of the SC is associated with important events in meiosis, namely synapsis, recombination and segregation, and is regulated at least in part by phosphorylation of SC-proteins (Lammers *et al.*, 1995; Rockmill and Roeder, 1991). Although the SC is a highly conserved structure, at least two species, *Schizosaccharomyces pombe* and

*Aspergillus nidulans*, carry out meiosis in the absence of SC (Bahler *et al.*, 1993; Egel-Mitani *et al.*, 1982).

Prior to synapsis, the lateral elements of the SC are referred to as axial elements (AEs). These first appear as discrete stretches between the sister chromatids of homologues at leptotene. During zygotene, axial elements extend in length and become closely connected to each other by proteins that constitute the TFs. Completion of SC assembly, and thus of synapsis, marks the transition to pachytene, the substage of prophase during which homologous recombination takes place. This is followed by diplotene, during which TFs disassemble, and homologues disassociate except at the sites of crossover, which are visible cytologically as chiasmata. Although axial elements degenerate at the prophase-metaphase transition, axial element remnants remain associated with the sister kinetochores (the proteinaceous structures flanking the centromeres) until anaphase II (Dobson *et al.*, 1994).

Identification of proteins that constitute structural components of the SC has come from two main sources. In rodents SCs have been purified and used as antigens with which to raise anti-SC antibodies. These antibodies have then been used to derive the sequence (by cDNA expression library screening), molecular weight (Westerns) and expression pattern (immunogold and immunofluorescence labelling) of their corresponding antigens. In contrast, most yeast SC components have been identified through genetic screens for mutants defective in viable spore production. Although the poor cytology and short meiotic cycle of yeast nuclei make the timing of appearance and subcellular localisation of such proteins more difficult to determine than in mammalian meiocytes (Ashley and Plug, 1998), these mutant screens provide invaluable information regarding the function of SC proteins, information which is

lacking in mammals. Components of the TFs of the SC include yeast Zip1 (Sym *et al.*, 1993) and rodent SCP1 (SYN1 in hamsters, Meuwissen *et al.*, 1992; Dobson *et al.*, 1994), SC65 (Chen *et al.*, 1992) and SC48 (Smith and Benavente, 1992), whereas components of the LEs include yeast Hop1 (Hollingsworth *et al.*, 1989) and Red1 (Smith and Roeder, 1997), rodent SCP2 (Offenberg *et al.*, 1998) and SCP3 (COR1 in hamsters, Lammers *et al.*, 1994; Dobson *et al.*, 1994) and an unnamed 55-70kDa protein in *Lilium* (Anderson *et al.*, 1994). A number of proteins with roles in synapsis, recombination, transcription, chromatin silencing and cell cycle control also localise to the SC during prophase, some of these will be discussed later.

The phenotypes of *zip1*, *hop1* and *red1* mutants have provided much information on the function of the SC. During pachytene in *zip1* null mutants, full-length axial elements are formed that undergo homologous pairing but fail to synapse, as reflected by the greater variability in interaxial distances (100nm in wild type vs. 100-400nm in *zip1*, Sym *et al.*, 1993). Mutants that affect the length of Zip1 also affect the distance between axial elements (Sym *et al.*, 1995). Together with the observation that Zip1 localises to synapsed but not unsynapsed axial elements (Sym *et al.*, 1993), these data suggest that Zip1 is a major component of the TFs and that TFs are required for synapsis, but alone they offer little information regarding the role of synapsis per se. However, although *zip1* null mutants display nearly wild-type levels of commitment to recombination, they have reduced levels of crossing over, and those cross overs that do form do not exhibit interference (Sym and Roeder., 1994).

The phenotypes of null mutants for Hop1 and Red1, which code for components of the axial/lateral elements of the SC, also lend support to a role for the SC in recombinatory regulation. In *hop1* mutants, axial element formation is normal but recombination, which is

reduced by 90%, preferentially occurs between sisters and not between homologues (Schwacha and Kleckner, 1994). In *red1* mutants, axial elements fail to form and there is consequently no mature SC. This defect is accompanied by a 75% reduction in crossing over, and those chromosomes that have undergone crossing over nevertheless mis-segregate, suggesting that Red1 functions to convert cross over events into functional chiasmata (Rockmill and Roeder, 1990). The localisation of COR1 in mouse meiocytes is also suggestive of a function in segregation. COR1 remains associated with the pairs of sister kinetochores following SC degeneration and lags between them as they separate at anaphase II, suggesting that the axial elements may serve to prevent sister chromatid disjunction at metaphase I (Dobson *et al.*, 1994). Taken together then, these observations suggest that the SC functions in crossover formation and interference, promotion of interhomologue recombination and segregation.

### 1.1.3 Presynaptic alignment, homology searching and synapsis

In order for homologues to initiate synapsis, some kind of presynaptic alignment must take place (Kleckner and Weiner, 1993). This can be defined as the parallel alignment of homologues at a distance that exceeds the width of the SC, and is genetically separable from synapsis since it can proceed in mutants in which synapsis is defective (e.g. *zip1*, Sym *et al.*, 1993). In *Drosophila* and *Saccharomyces cerevisiae*, homologues pair premeiotically (Hiraoka *et al.*, 1993; Weiner and Kleckner, 1994), while in mouse and humans they occupy distinct domains (Scherthan *et al.*, 1996). Homologous pairing in the mouse initiates by the migration of centromeres and then telomeres to the nuclear envelope during the late leptotene - early zygotene transition (Scherthan *et al.*, 1996). As with many other organisms, these telomeres cluster to form a bouquet, which is thought to facilitate pairing by bringing homologous sequences into alignment within a limited region of the nucleus (Roeder, 1997). Intriguingly,



genes inserted at ectopic locations in *S. cerevisiae* can, in some cases, recombine at nearly wild-type levels with their normally-located counterparts, suggesting that pairing involves a genome-wide homology search in which each sequence probes all other sequences prior to commitment to recombination (Jinks-Roberston and Petes, 1985). In this model, pairing would involve the formation and dissolution of unstable, so-called 'paranemic' joints between intact DNA duplexes as a search for homology was carried out. The reversible nature of these joints would allow connections between ectopic repeats to be discouraged in favour of those between homologous sequences, as well as being a prerequisite for the resolution of the many interchromosomal tangles that would result from multiple pairing interactions between uncondensed homologues (Kleckner, 1996). The fact that the number of pairing sites in *S. cerevisiae* (~190) is similar to the number of recombination events that occur during meiosis, has suggested that recombination may initiate at sites of presynaptic pairing (Weiner and Kleckner, 1994). Moreover, the RecA homologue Rad51 is thought to localise to sites of early pairing and in vitro can form paranemic joints between DNA duplexes of the kind described above (West, 1992), suggesting that it may facilitate these interactions in vivo. However, *rad51* null mutants still undergo significant homologue pairing (Kleckner, 1996). Another possible candidate in this process is Hop2 (see below).

Assembly of mature SC, and hence synapsis, takes place when homologues approach each other at a distance of less than 300nm and marks the leptotene - zygotene transition. Some theoretical and genetic studies have suggested that synapsis initiates at the telomeres (Sen and Gilbert, 1988; Wicky and Rose, 1996). Other studies, mainly involving three dimensional reconstruction of serially sectioned EM prophase nuclei, or immunostaining of surface spread meiocytes with anti-SC antibodies, have indicated that synapsis initiates interstitially. This is

the case in mouse spermatocytes (Moens *et al.*, 1998), human oocytes (Bojko, 1983), wheat (Holboth, 1981) and rye (Abirached-Darmency *et al.*, 1983). Following initiation, synapsis extends in a zipper-like fashion to encompass the length of each homologous pair (Loidl, 1994). The DNA of synapsed bivalents is arranged in a series of chromatin loops, each of which associate at their base with the lateral element of the SC (Weith and Traut, 1980). SC-associated DNA shows a number of unusual characteristics, including reduced sensitivity to DNase treatment and the PRINS (primer in-situ labelling) technique (Moens *et al.*, 1998). Surprisingly however, there are no sequences specific to SC-associated DNA (Pearlman *et al.*, 1992) and the axial element component SCP3 has non-specific DNA-binding properties (Heyting *et al.*, 1989). Although some prokaryotic DNA sequences fail to make SC-attachments when integrated into eukaryotic chromosomes (Heng *et al.*, 1994), the organisation of chromatin loops appears to be largely influenced by chromosomal geography and environmental influences. For instance, telomeric DNA (which forms small loops when at the telomeric ends of the SCs) assumes a larger loop size when integrated at interstitial positions (Heng *et al.*, 1996), and human DNA assumes a loop size characteristic of yeast when integrated into the yeast genome (Loidl *et al.*, 1995).

As mentioned, ectopic recombination events (gene conversions) in *S. cerevisiae* can occur at high frequencies and yet synapsis usually only takes place between regions of long range homology. This discriminative process is likely to involve Hop2 (Leu, *et al.*, 1998). In *hop2* mutants, nearly wild-type levels of SC are formed but most chromosomes are engaged in extensive non-homologous synapsis. Moreover, allelic recombination is reduced in favour of ectopic recombination. Hop2 may actively prevent synapsis from initiating at sites of ectopic recombination by assessing the degree of surrounding short or long range homology (Leu, *et*

*al.*, 1998). Alternatively, Hop2 may participate in the early alignment of homologous chromosomes, as described above, by mediating the unstable interactions between chromosomes engaged in a search for homology (Leu, *et al.*, 1998), a role that was originally proposed for Rad51 (West, 1992). The first model is favoured because it accommodates the fact that ectopic recombination (usually between dispersed repeats) occurs at high frequency during normal yeast meiosis. The timing of these ectopic events suggests that the sequences involved are physically associated during pachytene and therefore that they recombine away from the SC, presumably between chromatin loops (Roeder, 1995). Association between homologous sequences residing in chromatin loops has been discussed previously (Moens *et al.*, 1998).

#### 1.1.4 Recombination

In *S. cerevisiae* and *Caenorhabditis elegans*, recombination is initiated by the formation of double strand breaks (DSBs) which are catalysed by Spo11 (Keeney *et al.*, 1997; Dernberg *et al.*, 1998; Figure 1.1b). Spo11 is homologous to the type II topoisomerases, which induce DSBs via a reversible, transesterification reaction (Keeney *et al.*, 1997). Mutants of Rad50, Mre11, Xrs2 and Mer2 also fail to induce DSBs (Alani *et al.*, 1990; Johzuka and Ogawa, 1995; Nairz and Klein, 1997; Ivanov *et al.*, 1992; Rockmill *et al.*, 1995), suggesting that they cooperate with Spo11 in this process. DSB formation is followed by 5'-to-3' exonucleolytic resection, a process which again involves Rad50 and Mre11 (Alani *et al.*, 1990; Nairz and Klein, 1997; Figure 1.1b). The resulting single-stranded overhang then invades the uncut homologous duplex in a reaction that involves four homologues of the RecA protein, including Rad51 and Dmc1, as well as a single-stranded DNA-binding protein (SSB; Shinohara *et al.*, 1992; Bishop *et al.*, 1992; Sung, 1997; Figure 1.1b). Following recognition of its homologous

sequence, the invading strand then engages in repair synthesis and branch migration, resulting in the formation of two Holliday junctions (Figure 1.1b). The direction in which each of these junctions is resolved will determine whether a crossover or non-crossover (gene conversion) will result (Figure 1.1b). Resolution involves a number of mismatch repair proteins e.g. Msh4, Msh5, Mlh1, as well as SC components such as Zip1 (Ross-MacDonald and Roeder, 1994; Hollingsworth *et al.*, 1995; Hunter and Borts, 1997; Sym and Roeder, 1994).

Meiotic recombination occurs at discrete, electron-dense structures originally termed 'recombination nodules' (Carpenter, 1975). Microscopically, two types of nodule can be visualised. The first, termed early recombination or zygotene nodules are of variable size (30-200nm) and associate with axial elements and newly formed SCs during zygotene and early pachytene. Immunogold labelling has placed RAD51 at these nodules, consistent with their proposed role as the sites at which strand exchange reactions are initiated (Anderson *et al.*, 1997). The second, termed late recombination nodules, are fewer in number and are more consistent in size (100nm). There is a close correlation between the number and distribution of these nodules and the number and distribution of chiasmata, leading to the proposal that late recombination nodules are the sites at which reciprocal recombination takes place (Carpenter, 1988). Recently, immunofluorescence analysis has demonstrated that a subset of early nodules mature into late nodules, consistent with the hypothesis that some strand exchange reactions resolve as crossovers while others resolve as gene conversion events (Plug *et al.*, 1998). In mice, components of early nodules include RAD51, Replication Protein A (RPA; the mammalian homologue of SSB, Wold and Kelly, 1988) and the checkpoint proteins ATM (Ataxia-telangectasia mutated) and ATR (Ataxia-telangectasia *rad3*-related; Plug *et al.*, 1998). As nodules mature, RAD51 and ATR are removed but RPA and ATM remain transiently

associated with the SCs as MLH1, a known component of late nodules, appears (Baker *et al.*, 1996). Thus, RPA and ATM are components of both early and late nodules (Plug *et al.*, 1998).

Although it was traditionally believed that synapsis is a prerequisite for recombination, recent data from *S. cerevisiae* and mouse suggest that the opposite is true. Organisms that fail to make SC (e.g. *S. pombe* and *A. nidulans*) and mutants defective in SC formation (e.g. *zip1*) can nevertheless recombine (Bahler *et al.*, 1993; Egel-Mitani *et al.*, 1982; Sym *et al.*, 1993). Instead, recombination appears to be required for synapsis. Mutants with primary defects in recombination from both *S. cerevisiae* (e.g. *spo11*, *rad50*, *mre11*, *mer2* and *com1*) and mouse (*Dmc1*, *Pms2*, *Msh5*) exhibit defects in synapsis (Cao *et al.*, 1990; Alani *et al.*, 1990; Johzuka and Ogawa, 1995; Nairz and Klein, 1997; Rockmill *et al.*, 1995; Prinz *et al.*, 1997; Yoshida *et al.*, 1998; Pittman *et al.*, 1998; Baker *et al.*, 1995; Edelmann *et al.*, 1999; de Vries *et al.*, 1999). In *S. cerevisiae*, DSBs appear prior to and are resolved concomitant with synapsis (Padmore *et al.*, 1991). A possible link between these two processes is provided by Zip2 (Chua and Roeder, 1998); Zip2 colocalises extensively with Zip1, and mutants for these two genes display similar phenotypes, i.e. homologues pair but fail to synapse. Zip2 assembles at early pairing sites in a DSB-dependent fashion and colocalises with proteins involved in recombination in a *rad50S* mutant. Furthermore, Zip1 fails to assemble in the absence of Zip2. These data suggest that Zip2 binds to sites at which recombination initiates and then ‘nucleates’ Zip1 at these sites, thereby permitting synapsis (Chua and Roeder, 1998).

Data from other organisms suggest that synapsis can occur in the absence of DSBs and/or recombination. Homologous synapsis proceeds normally in female *Drosophila* deficient in recombination (e.g. *mei-W68* and *mei-P22*, McKim *et al.*, 1998). Furthermore, *C. elegans*

deficient in Spo11 (and therefore DSB formation) nevertheless undergo normal synapsis (Dernberg *et al.*, 1998). Even in mice, some data are inconsistent with recombination events preceding synapsis. In vitro, RAD51 is inefficient at carrying out strand exchange without RPA (Baumann *et al.*, 1996). In mouse surface spreads, RAD51 coats axial elements prior to synapsis, but RPA appears concomitant with synapsis, suggesting that RAD51 may be 'search inactive' prior to this point (Plug *et al.*, 1997). It has therefore been reasoned that DSB induction prior to synapsis would be unlikely as it would encourage extensive chromosomal rearrangements (Plug *et al.*, 1998). Furthermore, surface spreads from mice deficient for the PIK-like checkpoint protein ATM (which exhibit moderate levels of asynapsis) exhibit fragmentation of synapsed but not asynapsed axes. Should these fragments be the result of unresolved DSBs (as suggested by the assembly of RPA at their ends), these observations suggest that DSBs are inflicted only after synapsis (Plug *et al.*, 1997). Finally, the fact that translocated sequences frequently recombine with their homologous counterparts in *S. cerevisiae* but not *Drosophila*, *C. elegans* or mouse, suggests fundamental recombinational differences between these organisms (McKim *et al.*, 1998).

#### 1.1.5 After pachytene

Following pachytene, the SC disassembles and homologues remain associated by chiasmata, which hold homologues together because sister chromatids remain associated at sites distal to chiasmata (Roeder, 1997). Bivalents undergo a dramatic condensation and congress at the equator where they form bipolar spindle attachments. Maintenance of sister chromatid cohesion through meiosis I ensures that homologues and not sister chromatids segregate (Moore and Orr-Weaver, 1998). By meiosis II, sisters remain associated only at their centromeres, and at

anaphase this association is lost, permitting disjunction of sisters (Miyazaki and Orr-Weaver, 1994).

Commitment to both anaphase I and II is regulated by mechanical tension at the kinetochores (LeMaire-Adkins *et al.*, 1997). Tension, which results from the pulling of conjoined chromosomes to opposite poles of the cell by the spindles, is probably monitored by protein phosphorylation. This is suggested by the observation that an unidentified kinetochore-associated protein becomes phosphorylated when spindle tension is defective but dephosphorylates once tension is achieved (Nicklas *et al.*, 1995).

#### 1.1.6 Sexual dimorphism in mammalian meiosis

Under normal circumstances, mammalian sex is determined by the presence or absence of the *Sry* gene. In the mouse, *Sry* transcription at 10.5dpc diverts the bipotent genital ridge along a testis-forming pathway (Koopman *et al.*, 1991). Since *Sry* resides on the short arm of the Y chromosome, mammals with an XY and XX sex chromosome constitution develop as males and females, respectively.

Mammalian meiosis is extremely sexually dimorphic. In females, meiosis is initiated once, during foetal life, with all germ cells entering prophase more or less synchronously, whereas in males, meiosis initiates postnatally and continues throughout life. In females, meiosis results in one gamete, and gametogenic differentiation commences prior to meiotic completion, whereas in males, meiosis results in four gametes, which differentiate postmeiotically. In females, prophase I is followed by a meiotic arrest that can last years, whereas in males meiosis normally proceeds uninterrupted. In male mice, pachytene takes 6 days whereas in females, it

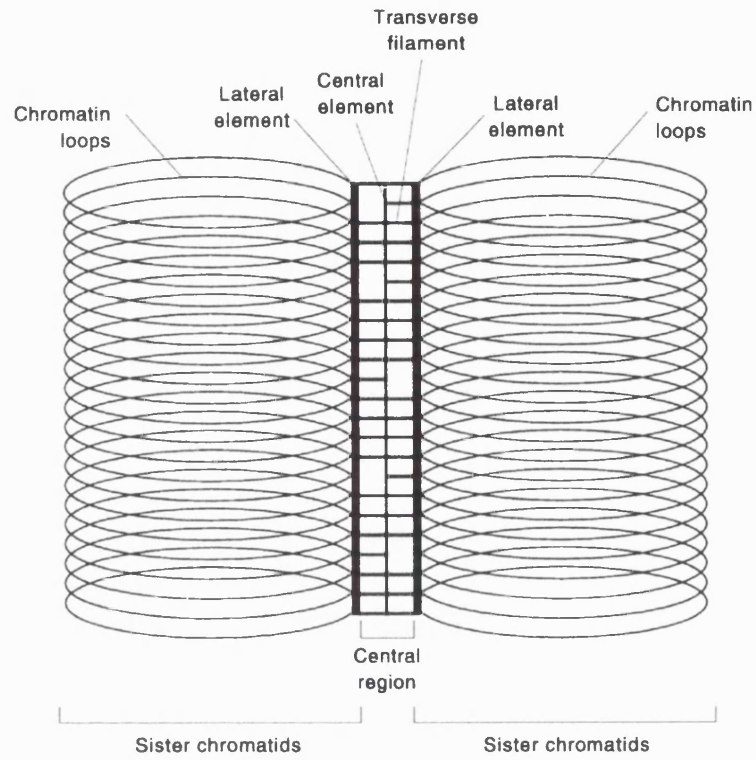
takes only 3 days (Goetz *et al.*, 1984; Speed *et al.*, 1982). It is during this stage that males and females display a particularly dimorphic feature, regarding the behaviour of the sex chromosomes. That is, in males but not females the sex chromosomes are transcriptionally inactivated and form a peripheral, densely-staining structure termed the sex body, XY body or sex vesicle (Solari, 1974). This is discussed in section 1.2.



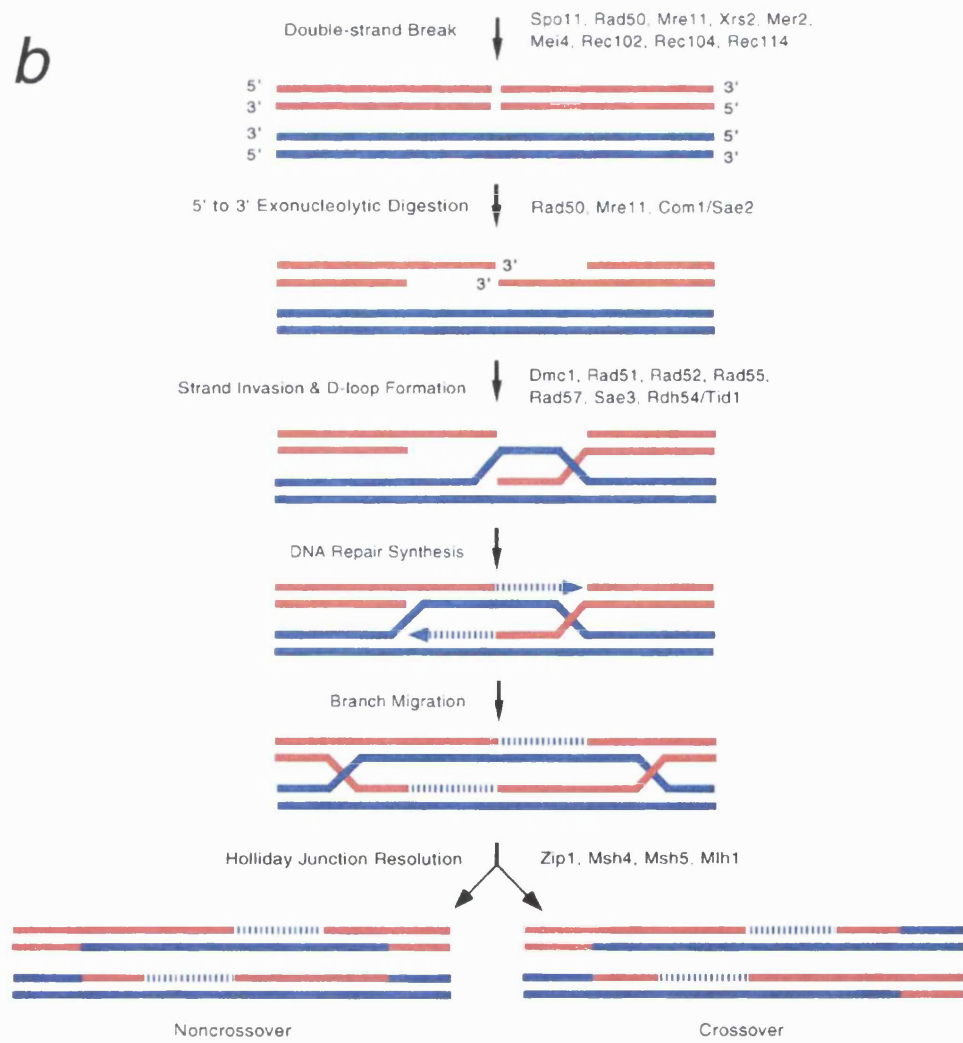
Figure 1.1. The synaptonemal complex and homologous recombination (reproduced from Roeder, 1997).

- a) The synaptonemal complex (SC). The mature SC consists of two lateral elements connected by multiple transverse filaments. The base of the sister chromatid loops are connected to the SC; it is at these points that homologous recombination takes place.
- b) DSB repair model of meiotic recombination (Szostak *et al.* 1983; Sun *et al.* 1991). Shown are two double-stranded DNA molecules (one in red, the other in blue). Gene products are indicated where a corresponding mutant has been demonstrated to be defective at a specific step.

*a*



*b*



## 1.2 MEIOTIC SEX CHROMOSOME INACTIVATION (MSCI)

### 1.2.1 Properties

During male meiosis in a number of species, the X and Y chromosomes become transcriptionally inactive (termed meiotic sex chromosome inactivation, or MSCI) and form a peripheral, densely-staining structure termed the sex- or XY body (Solari, 1974). This is in contrast to the female in which, following the reactivation of the inactive X of oogonia, the two X chromosomes appear euchromatic and indistinguishable from the autosomes (Monk and McLaren, 1981, Ohno, 1964). Although the sex body can be visualised as early as zygotene, it is most conspicuous at late pachytene, when the sex chromosomes undergo a further increase in chromatin condensation (Solari, 1974). That the sex chromosomes are largely transcriptionally inactive during meiosis was first shown by the observation that tritiated-uridine is excluded from the sex body (Monesi, 1965). Moreover, the sex body was thought to be protein-rich, based on its strong positivity for basic proteins using the alcoholic phosphotungstic technique (Solari, 1974).

These early observations have since been corroborated by a number of studies. RNA polymerase II is excluded from the sex body and meiotic initiation is associated with the inactivation of several X-linked (e.g. *Pgk1*, *Pdha1*, *Phka*, *Zfx*) and Y-linked (e.g. *Rbm*, *Ube1y*) genes (Richler *et al.*, 1994; McCarrey *et al.*, 1992; Mahadevaiah *et al.*, 1998; Odorisio *et al.*, 1996), some of which are reactivated postmeiotically (Hendriksen *et al.*, 1995). A number of sex body-associating proteins have also been identified. By immunostaining, some have been shown to be restricted to the sex body (e.g. XY40, XY77 and GCNF; Smith and Benavente, 1992; Kralewski *et al.*, 1997; Bauer *et al.*, 1998) while others display preferential enrichment in this domain (e.g. p51, M31 and XMR; Smith and Benavente, 1995; Motzkus *et al.*, 1999;

Calenda *et al.*, 1994). The temporal differences in appearance of each of these proteins have demonstrated that the sex body undergoes dynamic changes in protein expression between zygotene and diakinesis. For instance, XMR labels the X chromosome prior to formation of the sex body proper (during zygotene, Calenda *et al.*, 1994 and present study), while XY77 coats the sex body later, during late pachytene and diplotene (Kralewski *et al.*, 1997). Although each protein has been proposed to play a role in some aspect of the transcriptional inactivation or condensation of the sex chromosomes, these hypotheses remain to be proven.

Other proteins whose meiotic function is better understood have also been shown to associate with the sex body. KU70, MRE11 and RAD50 all accumulate in the sex body at pachytene (Goedecke *et al.*, 1999). MRE11 and RAD50 function in DSB repair both by homologous recombination (in meiotic cells, Roeder, 1997) and together with KU70 in non-homologous end-joining (in mitotic cells, Lustig, 1999). Since the X and Y chromosomes are largely devoid of a pairing partner during meiosis, one might expect DSBs (should they be inflicted in the absence of synapsis) to be repaired by the non-homologous end-joining pathway (Goedecke *et al.*, 1999). Thus the appearance of certain proteins in the sex body might be a consequence of the asynaptic behaviour of the sex chromosomes. Bloom's protein (BLM), a single-stranded DNA helicase, mutations of which cause male sterility, also associates with the sex body (and less so the autosomes) during late pachytene (Walpita *et al.*, 1999). BLM has been proposed to play a number of roles during meiosis, including the resolution of chromatid interlocks prior to disjunction at metaphase I (Walpita *et al.*, 1999). The apparently high levels of BLM in the sex body vs. the autosomal compartment is likely to be secondary to the dense nature of the chromatin of the sex chromosomes during meiosis.

### 1.2.2 Function

Although the function of MSCI is unknown, a number of hypotheses have been proposed to explain its existence. Lifschytz and Lindsley (1972) interpreted the male-specificity of MSCI as indicating that certain X-linked gene products are inhibitory to spermatogenesis. The sterility of males with X-autosome translocations was thought to be due to the defective inactivation of these genes caused by the associated autosomal chromatin. This concept was later extended to explain the sterility of autosome-autosome translocation males by Forejt (1982), who proposed that unpaired autosomes might disturb MSCI through their abnormal associations with the X chromosome. In support of the hypothesis is the finding that X-autosome (e.g. T(X;4)37H) and autosome-autosome (e.g. T(5;12)31H) heterozygous male mice retain higher X-linked gene activities than their siblings during meiosis (Hotta and Chandley, 1982), and that anchoring of the sex chromosomes in the autosomal compartment (with accompanying defects in sex body formation) are frequently observed in sterile T(11;19)42H heterozygotes (Richler *et al.*, 1989). However, tritiated-uridine uptake analysis in Ts(1<sup>13</sup>)70H and Ts(5<sup>12</sup>)31H tertiary trisomics (Speed *et al.*, 1985) and T(X;16)16H heterozygotes (Jaafar *et al.*, 1989) indicate that the transcriptional activity of the X chromosome is unaffected by chromosomal rearrangements.

A number of arguments oppose the Lifschytz and Lindsley hypothesis. Firstly, inactivation of the whole X chromosome may be an inappropriately exaggerated response to the requirement to silence selected genes. In addition, there has been no demonstration that expression of sex-linked genes during meiosis is inherently disruptive to spermatogenesis. On the contrary, the male germline appears to have evolved means to provide spermatocytes with X gene products during MSCI. In grasshopper and *Brachysola magna*, MSCI is preceded by a compensatory hyperactivation of the X chromosome (White, 1973, Church, 1979), and in mammals,

inactivation of genes with vital metabolic functions (e.g. *Pgk1*, *Pdhal*) coincides with the activation of autosomal 'backups'. These are retroposon-derived copies of their X-linked counterparts whose expression is strictly male meiosis-specific (e.g. *Pgk2*, *Pdhal*, McCarrey *et al.*, 1992; Iannello and Dahl, 1992). Also, the hypothesis fails to consider that MSCI does not occur in species where the male is the homogametic sex (e.g. birds and reptiles) or that meiotic initiation in the female germline coincides with X (or W) chromosome reactivation (Monk and McLaren, 1981; Beçak and Beçak, 1981).

Alternative hypotheses for the function of MSCI have been proposed by both Jablonka and Lamb (1988) and McKee and Handel (1993). The former hypothesis suggests the inactivation of the sex chromosomes is a response to them being largely asynapsed during meiosis. In general, deficient synapsis triggers a highly conserved pachytene checkpoint that precipitates meiotic arrest and/or apoptosis (Roeder, 1997, Odorisio *et al.*, 1998). In mice, synapsis between the X and the Y chromosomes is limited to the distal pseudoautosomal region (PAR), and while autosomal or PAR synaptic failure triggers the checkpoint (Odorisio *et al.*, 1998), the unpaired regions of the X and Y do not. Thus, Jablonka and Lamb viewed MSCI as the means by which the asynapsed non-PAR X and Y axes avoided checkpoint recognition. This model also takes into account the fact that the heterochromatic X of female oogonia is reactivated on entry to meiosis, because this would allow it to synapse with its euchromatic partner and thereby prevent arrest. In situations where the female is the heterogametic sex (e.g. birds), the inactive W chromosome reactivates and undergoes extensive non-homologous synapsis with the Z chromosome (Solari, 1992). Jablonka and Lamb attributed this choice to reactivate and not to undergo MSCI as a reflection of a requirement for Z-linked gene products during oogenesis (Jablonka and Lamb, 1988).

Although based on a similar argument, McKee and Handel viewed MSCI as a means of preventing the X and Y chromosomes from engaging in non-PAR recombination events. They viewed the reactivation of the X chromosome in females as a means of permitting recombination between the sex chromosomes, and thus preventing both nondisjunction at metaphase I and the accumulation of deleterious mutations. In their model, synaptic failure in non-inactivated chromosomes would result in an inability to resolve DSBs, which would in turn be the trigger for the pachytene checkpoint. Unlike the Jablonka and Lamb model, their model accounts for the fact that some organisms do not undergo MSCI despite having heteromorphic sex chromosomes, because in many cases they are achiasmatic (e.g. *Drosophila*, McKee and Handel, 1993). Evidence against this hypothesis is that recombination occurs between the short arm of the Y chromosome and the Sxr<sup>a</sup> fragment in XSxr<sup>a</sup>Y males (Laval *et al.*, 1995), although it is possible that in these circumstances these segments do not undergo MSCI.

### 1.2.3 Mechanism

Very little is known about the genetic and cellular control of MSCI. Mice with single sex chromosomes, (e.g. XSxr<sup>a</sup>O) or disrupted XY pairing, (e.g. interspecific hybrid males) synthesise morphologically 'normal' sex bodies, with tritiated-uridine uptake values not statistically different from controls (Handel *et al.*, 1994). Thus MSCI depends neither on the presence of a pairing partner nor efficient X-Y pairing. Sex bodies are also formed in T(X;16)16H males, precluding a requirement for an intact X chromosome (Handel *et al.*, 1994). Other data suggest that a testis environment is required for MSCI. SC analysis of oocytes from XY<sup>POS</sup> females revealed a lack of sex body formation (which is generally accepted as a morphological correlate of MSCI; Kundu *et al.*, 1983). Ectopic germ cells in the

adrenal gland of XY males also fail to form sex bodies (Hogg and McLaren, 1985), but foetal male gonocytes forced into premature meiosis do (Whitten *et al.*, 1979).

Other studies have suggested a role for *Xist* in MSCI. *Xist* is located in the X-inactivation centre (XIC) on the human and mouse X chromosome (Brown *et al.*, 1991) and encodes a 15kb transcript that is not translated. It is required in *cis* for the propagation of X-inactivation, although how it performs this function is unknown (Penny *et al.*, 1996). In males, *Xist* is expressed exclusively in the testis (McCarrey and Dilworth, 1992; Salido *et al.*, 1992; Kay *et al.*, 1993). Using purified spermatogenic populations, McCarrey and Dilworth (1992) demonstrated that *Xist* transcription commences in type A spermatogonia and persists throughout pachytene, before diminishing in round spermatids. Furthermore, *Xist* transcripts were shown to coat the X and Y axes of late pachytene nuclei using in situ RTPCR (Ayoub *et al.*, 1997). Taken together, these data suggested a common mechanism between somatic and germline X-inactivation. Ayoub *et al.* (1997) suggested that inactivation of the X chromosome in the male germline was dependent on *Xist*, and that Y chromosome inactivation might proceed by a so-called 'quasi-*cis*' spreading of *Xist* from the X chromosome via the PAR.

A number of observations are at conflict with a common somatic/germline mode of X-inactivation. Both the timing and expression levels of *Xist* are inconsistent with a primary role for *Xist* in MSCI. *Xist* transcripts can be detected at birth; preceding MSCI by approximately one week (Salido *et al.*, 1992). *Xist* is transcribed at considerably lower levels in both whole testis and purified spermatogenic populations than in female liver (Kay *et al.*, 1993, McCarrey and Dilworth, 1992). This has been attributed to both the transient nature of MSCI (with low levels being a prerequisite for reactivation following meiosis) and to the long term nature of somatic X-inactivation (that may permit the build-up of *Xist* transcripts, McCarrey and



Dilworth, 1992). Nevertheless, male mice with a targeted disruption of *Xist* are fertile, implying either that MSCI is *Xist*-independent, or that it is *Xist*-dependent but is not required for spermatogenesis (Marahrens *et al.*, 1997). Whether these *Xist*-deficient males undergo MSCI has not been examined. The low level transcription of *Xist* in the testis may be spurious, as suggested for other genes expressed during spermatogenesis (Willison and Ashworth, 1987).

Somatic and germline X-inactivation also differ in a number of other important respects. Somatic X-inactivation involves the methylation of cytosine residues at CpG dinucleotides in the 5' region of a number of X-linked genes, but methylation at these sites is not a feature of MSCI (Grant *et al.*, 1992). Moreover, packaging of the inactive somatic X chromosome involves hypoacetylation of histone H4, but hypoacetylated H4 is not enriched in the sex body (Armstrong *et al.*, 1997). Once again, these differences may reflect the transient vs. permanent nature of germline vs. somatic X-inactivation.

### 1.3 MEIOTIC CHECKPOINTS

#### 1.3.1 General features

A checkpoint is a surveillance mechanism, that controls cell cycle events by preventing the initiation of a later event if an earlier one has not been completed (San-Segundo and Roeder, 1999). When cells are defective in a critical cell cycle event, disruption of the corresponding checkpoint circumvents arrest, the result being daughter cells with reduced viability (San-Segundo and Roeder, 1999).

At least two checkpoints operate during meiosis to ensure the success of chromosome segregation. The first, termed the 'pachytene checkpoint', monitors homologous synapsis and

recombination, and the second, termed the 'metaphase checkpoint', monitors orientation of the chromosomes on the metaphase spindle (Roeder, 1997). The focus of the next section will be the pachytene checkpoint.

### 1.3.2 The pachytene checkpoint

Most information regarding the molecular nature of the pachytene checkpoint has arisen from genetic studies on meiotic mutants of *S. cerevisiae*. Mutants with defects in recombination (e.g. *zip1*, *dmc1*, *sae3*) arrest during pachytene with unresolved recombination intermediates (Bishop *et al.*, 1992; Sym *et al.*, 1993; Storlazzi *et al.*, 1996; McKee and Kleckner, 1997). This arrest can be circumvented either by preventing the initiation of recombination (e.g. *spo11/dmc1* double mutants) or by disrupting those proteins that couple defective recombination to cell cycle arrest (Lydall *et al.*, 1996). The latter group of proteins include Rad17, Rad24 and Mec1, which are also required for the mitotic DNA damage checkpoint (Weinert, 1998). Rad17 and Rad24, together with Rad9, Mec3 and Ddc1, have all been postulated to function in sensing DNA damage. In the presence of these proteins, Mec1 (together with other checkpoint proteins) induces cell cycle arrest, synthesis of DNA repair proteins and relocation of Sir3 from telomeres to the sites of DNA damage (where it functions in DNA repair; Weinert, 1998; Mills *et al.*, 1999).

While defects in recombination (e.g. unresolved DSBs) are clearly capable of triggering pachytene arrest, evidence from other mutants suggest that defects in synapsis can do the same. The major defect in *zip1* and *zip2* mutants is a failure in synapsis, while that of the *dmc1* mutant is the failure to convert processed DSBs into joint molecules. A recent study searching for mutants which bypass the *zip1* arrest led to the discovery of Pch2, an ATPase of the AAA

family (ATPases associated with diverse cellular activities; San-Segundo and Roeder, 1999). While mutation of *PCH2* completely alleviates the *zip1* and *zip2* arrests, it only partially rescues that of *dmc1*, suggesting that both a synapsis and a recombination checkpoint operate during pachytene, and that *PCH2* is of primary importance in the former (San-Segundo and Roeder, 1999). During normal meiosis, most Pch2 localises to the nucleolus, with small amounts colocalising with Zip1 on synapsed bivalents. In the absence of functional Zip1 however, Pch2 is present only in the nucleolus. Moreover, the nucleolar localisation of Pch2 is critical to its checkpoint function, since disruption of Sir2 (which tethers Pch2 to the nucleolus) results in diffuse Pch2 nuclear staining and defective checkpoint function. It appears that Pch2 requires tandemly repeated genomic DNA for its checkpoint function, since replacement of the rDNA array on chromosome XII with rDNA on multi-copy circular plasmids also disrupts checkpoint function, even though the plasmids form a 'pseudonucleolus' in which Pch2 is located. Under these circumstances, the checkpoint function of Pch2 can be partially restored by overexpressing Sir3, which drives Pch2 away from the pseudonucleolus to the telomeres.

In vertebrates there is also strong evidence for the existence of a pachytene checkpoint, although whether this monitors synapsis or recombination or both is unclear. Mice with asynapsed sex chromosomes or autosomes suffer from an arrest during the first meiotic prophase (Burgoyne and Mahadevaiah, 1993; de Boer and de Jong, 1989). Furthermore, mice defective in *Dmc1*, *Pms2* and *Msh5* gene function exhibit defects in synapsis and accompanying arrest (Pittman *et al.*, 1998; Baker *et al.*, 1995; Edelman *et al.*, 1999; de Vries *et al.*, 1999). Compared to yeast however, there is less information regarding checkpoint proteins in higher eukaryotes. While *MEC1* disruption permits meiotic progression in yeast, disruption of the mammalian *MEC1* homologue *Atm* results in pachytene arrest, with abnormal

homologous synapsis and fragmentation (Xu *et al.*, 1996). Although disruption of *p53* can partially rescue the *Atm*-null arrest (Barlow *et al.*, 1997), it cannot circumvent the arrest of mice with sex chromosomal or autosomal pairing failure (Odorisio *et al.*, 1998). This suggests that, as in yeast, the mammalian ‘pachytene checkpoint’ may be a combination of both a recombination and a synapsis checkpoint, with *p53* operating in the former but not the latter.

How asynapsis might trigger cell cycle arrest remains unclear. Miklos (1974) proposed the existence of chromosomal ‘pairing sites’ that must be saturated by synapsis, and that would trigger arrest when in the unsaturated state. Pairing of the X and Y chromosomes in *Drosophila* is mediated by the repeated sequences specifying the ribosomal RNAs (McKee and Karpen, 1990) but these may function to ensure correct segregation in the absence of recombination, rather than as monitors of asynapsis. It has been suggested that the ‘pairing sites’ proposed by Miklos might in fact be early recombination nodules, since these are the sites at which homology is checked and recombination takes place (Ashley, 2000). A likely candidate in the synapsis checkpoint is ATR, an ATM-related kinase that appears as foci on SCs prior to synapsis (Keegan *et al.*, 1996). As synapsis proceeds, ATR disappears from the SC, but if synapsis fails, it accumulates and appears to coat the axis (Plug *et al.*, 1998).

### 1.3.3 Unpaired sex chromosomes and gametogenic failure

Perhaps the most extensive evidence for the existence of a synapsis checkpoint in mammals derives from studies of sex chromosome aberrations. In 1974, Miklos proposed that the presence of an unpaired sex chromosome during prophase would result in elimination of the cell with that particular error. This concept was then extended by Burgoyne and Baker to

include female meiosis (1984). A summary of different sex chromosome variants is shown in Appendix 1.10.

#### *Mice with one sex chromosome*

The simplest model highlighting the relationship between sex chromosome pairing failure and gametogenic arrest is the  $X^{Y^*}O$  mouse. The  $X^{Y^*}$  chromosome is one of two products generated by recombination in the  $XY^*$  male. These males possess a Y chromosome that has been hijacked by a non-Y centromere added distally to the PAR, the original centromere being inactivated (Eicher *et al.*, 1991; Hale *et al.*, 1991). Recently, it has been shown that the  $Y^*$  PAR has been created by an X PAR-Y PAR fusion event. The compound PAR has a region of proximal X-derived PAR, together with a region of proximal Y-derived PAR in opposite orientations (Figure 5.1, Burgoyne *et al.*, 1998). Crossing-over is preferentially within the region of X-derived PAR and this generates two new products, the  $X^{Y^*}$  and  $Y^{*X}$  chromosomes. The  $X^{Y^*}$  chromosome comprises a complete X and Y chromosome, joined by a single PAR (which is identical to the paternal PAR) and the  $Y^{*X}$  chromosome is essentially a complete PAR with no Y-specific DNA.  $X^{Y^*}O$  mice can be generated by mating  $XY^*$  males to females capable of producing 'O' gametes, such as XO or In(X)1H heterozygotes. The  $X^{Y^*}$  chromosome has no pairing partner and self-synapsis is rarely achieved (Burgoyne and Mahadevaiah, 1993).  $X^{Y^*}O$  mice are sterile, with an almost total spermatogenic block during the meiotic metaphases (Eicher and Washburn, 1986; Burgoyne and Mahadevaiah, 1993; Odorisio *et al.*, 1998).

$XSx^aO$  mice possess an X chromosome attached via a single PAR to the small chromosomal fragment  $Sx^a$  (Cattanach *et al.*, 1971), which comprises most of the short arm of the Y

chromosome including the testis-determinant *Sry*. These mice have a similar meiotic block to  $X^{Y^*}O$  males (Burgoyne and Mahadevaiah, 1993). By restoring synapsis in  $XSx^a$  males using the  $Y^{*X}$  chromosome, this meiotic block is overcome (Burgoyne *et al.*, 1992), providing clear evidence for the existence of a checkpoint monitoring synapsis and/or recombination in mice.

XO females also suffer from a partial meiotic failure. Burgoyne and Baker (1985) demonstrated that XO mice have less than half the number of oocytes of XX females, and that this results from an elevated level of atresia at late pachytene. The fact that some XO oocytes avoid elimination may be related to the ability of the X chromosome to self synapse (termed non-homologous, or heterologous synapsis) and thereby satisfy the requirements of the synapsis checkpoint (Speed, 1986).

#### *Mice with two sex chromosomes*

Much of the evidence relating sex chromosome asynapsis to gametogenic impairment has arisen from studies of mice with two sex chromosomes. PAR-pairing failure can arise through evolutionary divergence of PAR-related sequences (e.g. interspecific hybrid males; Matsuda *et al.*, 1991), through rearrangement of the PAR (e.g.  $XY^*$  males; Eicher *et al.*, 1991; Hale *et al.*, 1991), or through interference with synaptic initiation (e.g.  $XYSx^a$ ,  $XSx^aY$  and  $X^{Y^*}Y^{*X}$  males; Chandley and Fletcher, 1980; Evans *et al.*, 1980; Mahadevaiah *et al.*, 1988; Tease and Cattanach, 1989; Cattanach *et al.*, 1990; Burgoyne *et al.*, 1992). In all of these cases, the degree of spermatogenic impairment is related to the number of cells in which PAR synapsis has failed (Burgoyne and Mahadevaiah, 1993). As mentioned in section 1.1.3, synapsis is preceded by clustering of telomeres at the nuclear envelope (Scherthan *et al.*, 1996). In the third instance,

synapsis is probably disrupted because the addition of Y chromosomal material to the X or Y PARs prevents the PARs from achieving close alignment during this critical period.

Females with sex chromosome pairing failure also display a reduced oocyte count and a resulting shortened reproductive lifespan. These include In(X)/X females (which are heterozygous for a large X chromosome inversion In(X)1H, Burgoyne and Baker, 1985; Tease and Fisher, 1988), XY<sup>Tdym1</sup> females (which are female due to a deletion encompassing *Sry* and display deficient XY pairing, Gubbay *et al.*, 1990; Mahadevaiah *et al.*, 1993) and XY<sup>\*X</sup> females (Hunt, 1991). In contrast to the male, the non-PAR regions of the X chromosome in females appear capable of triggering the synapsis checkpoint when unpaired. This is suggested by an analysis of pairing configurations in In(X)/X females from Tease and Fisher (1988), which demonstrated a selection against oocytes with incompletely paired loops as pachytene proceeded (highlighted by Burgoyne and Mahadevaiah, 1993). It should be noted that XY<sup>Tdym1</sup> females are particularly poor breeders, despite suffering a similar level of asynapsis-mediated germ cell loss as other females with sex chromosome pairing failure (Szot and Burgoyne, unpublished). This suggests that the expression of Y chromosomal genes may have an additional detrimental effect on oogenesis (Burgoyne, unpublished).

#### *Mice with three sex chromosomes*

Assessing the effect of sex chromosome asynapsis on spermatogenesis in males with additional doses of Y chromosomal material has been hampered by the possible additional effects of excess Y-gene expression. XYY males are almost invariably sterile, while XYY<sup>\*X</sup> males are fertile (Hunt and Eicher, 1991). XYY and XYY<sup>\*X</sup> males have similar trivalent frequencies at metaphase I (MI), and this led Hunt and Eicher (1991) to conclude that excess Y-dosage is a

major factor in the infertility of XYY males. However, Burgoyne and Mahadevaiah (1993) pointed out that equivalent MI trivalent frequencies may not be a reliable indicator of equivalent trivalent synapsis at pachytene; they suggested that the difference in fertility between XYY and XYY<sup>\*X</sup> mice might be associated with different levels of trivalent synapsis. Recently Rodriguez *et al.* (2000) showed that XYY<sup>\*X</sup> males do indeed have much higher levels of trivalent synapsis (58%) than XYY males (29%). These data suggested that the differences in levels of sex chromosome synapsis at pachytene were sufficient to account for the differences in fertility between these two genotypes. However, they did not rule out an additional deleterious effect of Y-gene dosage on fertility.

Studies on females with three sex chromosomes further support the relationship between sex chromosome asynapsis and gametogenic failure. Both XY<sup>Tdym1</sup>Y<sup>Tdym1</sup> and XXY<sup>Tdym1</sup> females have levels of sex chromosome asynapsis similar to XY<sup>Tdym1</sup> females and display equivalent levels of oocyte loss as a result of the synapsis checkpoint (Mahadevaiah *et al.*, 1993; Burgoyne and Palmer, unpublished). In XXY<sup>Tdym1</sup> females, synapsis normally occurs between the two X chromosomes but the univalent Y<sup>Tdym1</sup> chromosome is capable of self-synapsis. Analysis of configurations through pachytene suggests that cells with self-synapsed Y<sup>Tdym1</sup> chromosomes escape elimination in favour of those in which the Y<sup>Tdym1</sup> chromosome has failed to self-synapse (Mahadevaiah *et al.*, 1993). Despite the similarities in levels of asynapsis, XY<sup>Tdym1</sup>, XY<sup>Tdym1</sup>Y<sup>Tdym1</sup> and XXY<sup>Tdym1</sup> females nevertheless display differences in their fertility, with XXY<sup>Tdym1</sup> females being the best breeders, followed by XY<sup>Tdym1</sup> females and finally, XY<sup>Tdym1</sup>Y<sup>Tdym1</sup> females (Mahadevaiah *et al.*, 1993). These data suggest that the detrimental effect of the Y chromosome on oogenesis operates in a dose-dependent fashion that



can be partially antagonised by excess X-gene dosage, although how this is achieved remains undetermined.

#### *Mice with four sex chromosomes*

In order to investigate in more detail the possible effects of excess Y gene dosage on spermatogenesis, Rodriguez *et al.* (PhD thesis, 1997) analysed synapsis and fertility in  $XYYY^{*X}$  and  $XYY^{*X}Y^{*X}$  males.  $XYYY^{*X}$  males have the potential to form two bivalents in the presence of two doses of Y-specific genes, whilst  $XYY^{*X}Y^{*X}$  males have the potential to form two bivalents in the presence of only one dose of Y-specific genes. At pachytene in  $XYYY^{*X}$  males, 9% of cells had quadrivalents (all sex chromosomes synapsed together), 34% had  $XY^{*X}$  plus  $YY$  bivalents, and 8% had  $XY$  plus  $YY^{*X}$  bivalents. Despite this relatively high level of PAR synapsis (51%), all the  $XYYY^{*X}$  males were sterile with testis weights of 46mg or less. In the one  $XYY^{*X}Y^{*X}$  male analysed, 10% of the pachytene cells contained quadrivalents, 17% had  $XY^{*X}$  plus  $YY^{*X}$  bivalents and 13% had  $XY$  plus  $Y^{*X}Y^{*X}$  bivalents. As with the  $XYYY^{*X}$  males, this male was sterile. These data proved that the addition of an extra sex chromosome, not necessarily a Y chromosome, was deleterious to spermatogenesis.

The way in which excess sex chromosome dosage disrupts spermatogenesis is at present not known. The fact that the  $XYY^{*X}Y^{*X}$  male studied by Rodriguez *et al.* (PhD thesis, 1997) was sterile indicated that extra sex chromatin could disrupt spermatogenesis even when the Y gene dose was equivalent to normal XY males. This was particularly interesting in light of the hypothesis that inactivation of the Y chromosome proceeds by *quasi-cis* spreading of *Xist* from the X chromosome via the PAR (Ayoub *et al.*, 1997 and see sections 1.2.3 and 1.3.3). Rodriguez *et al.* (pers.comm.) proposed that bivalents not including the X chromosome in

$XYYY^{*X}$  and  $XYY^{*X}Y^{*X}$  mice (i.e.  $YY$  or  $YY^{*X}$ ) would fail to undergo MSCI. If one of the roles of MSCI were to prevent the unpaired regions of the sex chromosomes from triggering the pachytene checkpoint, then these non-inactivated bivalents would trigger such a checkpoint. By extrapolation, any meocyte with X-Y synaptic failure (e.g.  $XYY$ ,  $XYSxr^a$ ) would be expected to experience defective Y chromosome MSCI.

#### 1.4 OUTLINE OF PROJECTS

Little is known about how asynapsed sex chromosomes trigger the synapsis checkpoint and whether such asynapsis also disrupts Y chromosome inactivation. The experiments described in this thesis are aimed at addressing these issues. Particular attention is given to investigating the *quasi-cis* model of MSCI.

The first two chapters describe a novel screening procedure that was designed to check for the MSCI-specificity of three sex body proteins. It was hoped that at least one of these proteins would be a suitable marker with which to analyse X and Y chromosome inactivation in *Xist*-null spermatocytes, and Y chromosome inactivation in spermatocytes with sex chromosome pairing failure. Such experiments are the subject of the third chapter. In view of the high levels of pairing failure in  $XYY$  spermatocytes,  $XYY$  male mice are used to test various aspects of the *quasi-cis* model.

The fourth chapter describes a series of classical genetic experiments that are aimed at identifying the molecular components of the mammalian synapsis checkpoint, using the  $X^{Y*}O$  mouse as a model.

CHAPTER 2

AN INVESTIGATION INTO THE MSC1-SPECIFICITY OF A NOVEL SEX

BODY PROTEIN, ASYNAPTIN

## 2.1 INTRODUCTION

Asynapsis of the X and Y PARs triggers a pachytene checkpoint that results in spermatocyte apoptosis (Burgoyne and Mahadevaiah, 1993; Odorisio *et al.*, 1998). A recent study on mice with four sex chromosomes has demonstrated that excess sex chromatin is also disruptive to spermatogenesis (Rodriguez, T.A; PhD thesis, 1997; see section 1.3.3).  $XYYY^{*X}$  and  $XYY^{*X}Y^{*X}$  mice are sterile, despite having high levels of PAR synapsis (either quadrivalent or bivalent-plus-bivalent configurations). Based on the hypothesis that inactivation of the Y chromosome proceeds by *quasi-cis* spreading of *Xist* from the X chromosome via the PAR (Ayoub *et al.*, 1997 and see sections 1.2.3 and 1.3.3), Rodriguez *et al.* suggested that bivalents not including the X chromosome in  $XYYY^{*X}$  and  $XYY^{*X}Y^{*X}$  mice might fail to undergo MSCI, and that the failure in MSCI would disrupt meiosis. They extended this hypothesis by suggesting that any meiocyte with X-Y synaptic failure (e.g.  $XYY$ ,  $XYSxr^a$ ) would be experience defective Y chromosome MSCI.

If Y chromosomes that fail to synapse with the X chromosome do fail to undergo MSCI, then this should be manifested as exclusion of univalent Y chromosomes from the sex body. Moreover, *Xist*-disrupted spermatocytes should display defective sex body formation. These possibilities could be readily tested by using antibodies to the chromosome axes (e.g. anti-SCP3) and to the sex body, to double label spermatocytes from mice with sex chromosomal anomalies and from those that are *Xist*-null.

The present study describes the detailed expression analysis of a novel, 90kDa sex body-located protein, termed Asynaptin (ASY, see discussion and Figure 2.1). The antibody to this protein, 2E3, was thought to be suitable as an MSCI marker for the studies described above. It

was generated by injecting mice with purified rat synaptonemal complexes (Heyting and Dietrich, 1991). Immunolabelling of testis sections with 2E3 had revealed that ASY was expressed exclusively in pachytene and diplotene spermatocytes of stage IX, X and XI tubules, where it associated with a discrete, peripheral domain thought to be the sex body (Christa Heyting, pers.comm, Figure 2.1).

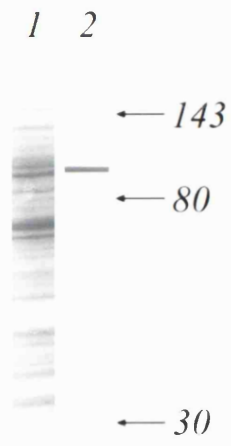
Theoretically, the most suitable control for assessing the MSCI-specificity of any sex body protein is to analyse its expression in pachytene cells with a male sex chromosome constitution (i.e. XY) but where MSCI is absent. An early observation had suggested that the sex chromosomes of XY<sup>POS</sup> female pachytene oocytes fail to assume a sex body-like configuration (Kundu *et al.*, 1983). With this in mind, XY<sup>Tdym1</sup> females (which are deleted for the testis-determining gene *Sry*; Gubbay *et al.*, 1992) were analysed for features of MSCI and were then used as 'sex body-negative' controls.

Figure 2.1 ASY expression during male mouse meiosis.

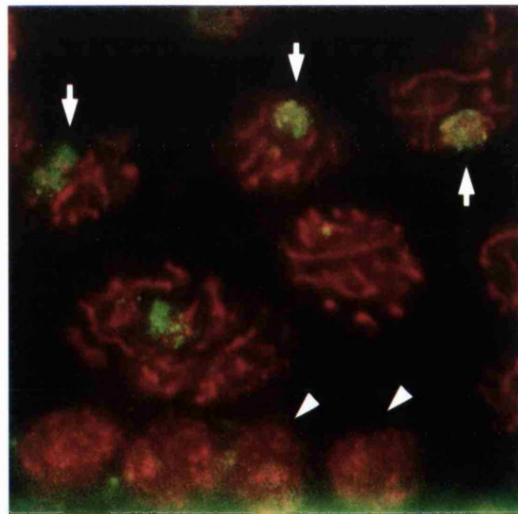
a) Western analysis. Lane 1, polyacrylamide-SDS gel of Coomassie blue-stained spermatocyte nuclear proteins; lane 2, strip of an immunoblot of the same gel probed with 2E3, which detects a ~ 90 kDa protein referred to as 'Asynaptin' (see text. Antibodies to proteins of known molecular weights were used to provide bands of known size). Numbers indicate molecular weights in kDa.

b) Stage X-XI testis tubule section stained for the axial/lateral element protein SCP3 (red) and ASY (green). ASY is present in the sex bodies of late pachytene nuclei (short arrows) but not zygotene nuclei (arrowheads)

*a*



*b*



## 2.2 MATERIALS AND METHODS

### 2.2.1 Mice

Adult MF1 XY males were processed at the age of 2 to 3 months. All females were processed at 18.5dpc.

#### *XY<sup>Tdym1</sup> females*

XY<sup>Tdym1</sup> females (Lovell-Badge and Robertson, 1990; Gubbay *et al.*, 1992) were generated by mating MF1 XX females to MF1 XY<sup>Tdym1</sup> males carrying the *Sry* transgene (Mahadevaiah *et al.*, 1998).

		SPERM			
		X	Y <sup>Tdym1</sup>	X <i>Sry</i> tg	Y <sup>Tdym1</sup> <i>Sry</i> tg
		FEMALE OFFSPRING		MALE OFFSPRING	
EGGS	X	XX	XY <sup>Tdym1</sup>	XX <i>Sry</i> tg	XY <sup>Tdym1</sup> <i>Sry</i> tg

XX and XY<sup>Tdym1</sup> female offspring were distinguished by PCR using YMT2/B primers, which amplify a subfamily of the Y chromosomal *Ssty* multigene family (A. Rattigan, pers.comm). The autosomal *myogenin* gene was used as a control (see section 2.2.8).

#### *XO females*

XO females were generated by mating MF1 XX females to MF1 X<sup>Paf</sup>Y\* males (that generate, amongst others, 'O' gametes; Burgoyne *et al.*, 1998). XX and XO female offspring were distinguished by karyotyping liver cells using standard procedures (see Appendix 1.1).



### *In(X)/X females*

Females heterozygous for the X inversion In(X)1H (Evans and Phillips, 1975) were generated by mating MF1 XX females to MF1 In(X)/Y males. All female offspring from this cross are In(X)/X.

### *T(2;5)72H females*

Heterozygous T(2;5)72H females were generated by mating F<sub>1</sub> (C3HeH X 101/H) XY males to F<sub>1</sub> (C3HeH X 101/H) carrier females (courtesy of Colin Beechey, MRC Harwell).

### *XXY<sup>d1</sup> females*

XXY<sup>d1</sup> females were generated by mating MF1 XY<sup>d1</sup> females (Laval *et al.*, 1995) to MF1 XY males.

		SPERM	
		X	Y
		FEMALE OFFSPRING	MALE OFFSPRING
E	X	XX	XY
G	Y <sup>d1</sup>	XY <sup>d1</sup>	-
G	XY <sup>d1</sup>	XXY <sup>d1</sup>	XXY <sup>d1</sup>
S	O	XO	-

XXY<sup>d1</sup>, XY<sup>d1</sup>, XX and XO females were distinguished by a combination of karyotyping of liver cells using standard procedures (see Appendix 1.1) and PCR for the Y chromosome multiple-copy *YMT2B* gene with the autosomal *myogenin* gene as a control (see section 2.2.8).

### 2.2.2 Squash procedure

Squashed spermatocytes and oocytes were prepared as described in Appendix 1.6.

### 2.2.3 Surface spreading procedure

Surface spread spermatocytes and oocytes were prepared as described in Appendix 1.7.

### 2.2.4 Immunostaining

Meiocytes were immunostained as described in Appendix 1.8. Where detection of SCP3 and RNA POLII was required (both primaries being raised in rabbit), primaries were used sequentially, with SCP3 being detected with goat anti-rabbit Cy2 (Amersham). In controls, 2E3 was replaced either by a hybridoma supernatant control (fish brain tubulin, gift from Christa Heyting) or by PBS.

### 2.2.5 Examination

Immunostained meiocytes were examined as described in Appendix 1.9.

### 2.2.6 Total RNA extraction from testes and ovaries

Total RNA was extracted as described in Appendix 1.3.

### 2.2.7 DNase treatment and reverse transcription of total RNA

DNase treatment and reverse transcription of total RNA was carried out as described in Appendix 1.4.

### 2.2.8 Genomic DNA extraction

Genomic DNA was extracted from tail tips as described in Appendix 1.2

### 2.2.9 PCR procedure

Genomic PCRs and RT PCRs were carried out as described in Appendix 1.5. Genomic PCR primers used were:

YMT2/B (YMTFP1 5' CTG GAG CTC TAC AGT GAT GA 3', YMTRP1 5' CAG TTA CCA ATC AAC ACA TCA 3',  $T_m = 60^{\circ}\text{C}$ , product = 342bp; A. Rattigan, pers. comm).

*Myogenin* (Omla 5' TTA CGT CCA TCG TGG ACA GCA T 3', Omlb 5' TGG GCT GGG TGT TAG TCT TAT 3',  $T_m = 60^{\circ}\text{C}$ , product = 245bp; Wright *et al.*, 1989).

RTPCR primers used were:

*Ube1y* (oMJ95 5' CCT CCT AGT CCG TAT GTC TG 3', oMJ96 5' GAC CCC AAG TTC ATG GAG CG 3',  $T_m = 60^{\circ}\text{C}$ , product = 330bp; courtesy of Mike Mitchell).

*Rbm* (4.2F1 5' CAA GAA GAGF ACC ACC ATC CT 3', 1.8R2 5' CCA GAA GAA CTC ACA TTG AA 3',  $T_m = 58^{\circ}\text{C}$ , product = 159bp; Mahadevaiah *et al.*, 1998).

*Pgk1* (Pgk1F 5' AAG CGC ACG TCT GCC GCG CTG TTC T 3', Pgk1R 5' GTT GGC TCC ATT GTC CAA GCA GAA T 3',  $T_m = 54^{\circ}\text{C}$ , product = 238bp; McCarrey *et al.*, 1992).

*Pgk2* (Pgk2F 5' AGG AGA TAC TGC TAC TTG CTG CGC C3', Pgk2R 5' GAT GAT GAC AGA ATT AAG ACT TGC T 3',  $T_m = 54^{\circ}\text{C}$ , product = 300bp; McCarrey *et al.*, 1992).

*Pdha1* (mPDH-12 5' CAA GTG TTG AAG AAT TAA AG 3', mPDHS-3 5' TTC AAG CCT TTT GTT GTC TG 3',  $T_m = 56^{\circ}\text{C}$ , product = 286bp; Iannello and Dahl., 1992).

*Pdhal* (mPDHT-A 5' TTC GGG AGG CAA CCA AGT TT 3', mPDHT-3 5' GAA GTT TCC TAG AGT ACA CC 3',  $T_m = 56^{\circ}\text{C}$ , product = 459bp; Iannello and Dahl., 1992).

*Hprt* (HPRT1A 5' CCT GCT GGA TTA CAT TAA AGC ACT G 3', HPRT1B 5' GTC AAG GGC ATA TCC AAC AAC AAA C 3',  $T_m = 56-60^{\circ}\text{C}$ , product = 352bp; Melton *et al.*, 1984).

## 2.3 RESULTS

### 2.3.1 MSCI status of XY<sup>Tdym1</sup> oocytes

As previously described (Mahadevaiah *et al.*, 1993), XY<sup>Tdym1</sup> oocytes showed a low level of XY PAR pairing (17%), and in no cells analysed did the X or Y chromosome assume a conspicuous, peripheral location (Figure 2.7a,b,c). Combined staining with anti-SCP3, anti-RNA POLII and DAPI demonstrated that pachytene XY<sup>Tdym1</sup> oocytes stained uniformly for RNA POLII and there was no indication of either RNA POLII-deficient chromatin or sex bodies (as stained with DAPI; Figure 2.2a,b).

Next, the expression of *Rbm* and *Ube1y* was analysed in XX and XY<sup>Tdym1</sup> oocytes. These genes are Y-linked and germ cell-specific, and in males their transcripts become undetectable during pachytene as a result of MSCI (Mahadevaiah *et al.*, 1998; Odorisio *et al.*, 1996). Since meiosis in the ovary occurs in a single, largely synchronous wave, most germ cells have reached mid-late pachytene by 18.5dpc. If MSCI were occurring in these cells, little or no transcription of these genes would be detectable at this age. Contrary to this, both *Rbm* and *Ube1y* were expressed in 18.5dpc XY<sup>Tdym1</sup> oocytes, implying that inactivation of the Y chromosome had not occurred (Figure 2.2c). However, in the *quasi-cis* model described in section 2.1, inactivation of the Y chromosome might fail due to its inability to pair with the X chromosome. Since there are no known X-linked genes that are germ cell-specific, X chromosome transcription in XY<sup>Tdym1</sup> oocytes was indirectly assayed by performing RTPCR for the autosomal backups *Pgk2* and *Pdhal* (McCarrey *et al.*, 1992; Iannello and Dahl, 1992). If X-linked *Pgk1* and *Pdhal1* were inactivated, their autosomal counterparts *Pgk2* and *Pdhal* would have to be activated in order for the oocytes to survive. Neither *Pgk2* nor *Pdhal* were transcribed in 18.5dpc XY<sup>Tdym1</sup> oocytes, indirectly implying

that MSCI had not taken place (Figure 2.2c). Thus both the immunocytochemical and transcriptional analyses demonstrated that MSCI was absent in XY<sup>Tdym1</sup> oocytes. They were therefore used as a sex body-negative control.

### 2.3.2 ASY localisation in XY testis (n=4)

By the squash technique (Page *et al.*, 1998), the expression profile of ASY was consistent with that reported by C. Heyting. It was present only in the nuclei of pachytene spermatocytes, in a peripheral structure reminiscent of the sex body (Figure 2.3a,b). By surface spreading, ASY staining colocalised with the morphological sex body as stained with DAPI, and was associated with a marked deficiency of RNA polymerase II (RNA polII), implying its location on transcriptionally inactive chromatin (Figure 2.3e,f). ASY was first detectable as a faint signal in the sex bodies of half of mid pachytene cells; slightly earlier than reported by C. Heyting (Figure 2.4d). Mid pachytene also represented the earliest stage at which sex bodies (stained with DAPI) first became apparent (Figure 2.6, Table 2.1). ASY was then strongly visible in the sex body at late pachytene and early diplotene, and abruptly disappeared at late diplotene (Figures 2.4e,f,g, 2.6, Table 2.1). ASY formed punctate dots that localised exclusively with the chromatin of the XY bivalent, and showed no preferential localisation to the axial elements (Figure 2.5). It was also excluded from the X centromeric heterochromatin (Figures 2.3e,f, 2.4e,f, 2.5).

No nuclear staining was seen in spermatocytes when 2E3 had been replaced either by a hybridoma supernatant control or by PBS (Figure 2.3c,d).

### 2.3.3 ASY localisation in XY<sup>Tdym1</sup> oocytes (n=3)

Despite the absence of MSCI, surface spread XY<sup>Tdym1</sup> pachytene oocytes of all stages were positive for ASY, which coated the X-chromatin, thus implying a non MSCI-related function for this protein (Figure 2.7a-d, Table 2.2). The Y chromosome, which failed to synapse with the X, usually lay separate and was consistently negative for ASY (Figure 2.7a-c). The X-associated 2E3 staining was not seen in pachytene oocytes in which 2E3 had been replaced either by a hybridoma supernatant control or by PBS (Figure 2.7g,h). Formally, the presence of ASY in XY<sup>Tdym1</sup> oocytes could be explained in two ways. Firstly, ASY production may be 'genetically' controlled, with either the presence of a Y chromosome or of a single X dose controlling its expression. Secondly, its expression may reflect the asynaptic behaviour of the X chromosome.

### 2.3.4 ASY localisation in XO oocytes (n=2)

These oocytes allowed the requirement for a Y chromosome in ASY assembly to be tested. As in XY<sup>Tdym1</sup> pachytene oocytes, the asynapsed X chromosome of early, mid and late XO pachytene oocytes stained positively for ASY (Figure 2.7e, Table 2.2). Thus ASY localisation was not dependent on an XY constitution.

### 2.3.5 ASY localisation in In(X)/X oocytes (n=1)

These oocytes allowed the requirement for a single X chromosome in ASY assembly to be tested. As in XY<sup>Tdym1</sup> and XO pachytene oocytes, a number of In(X)/X oocytes stained positively for ASY (Figure 2.7f, Table 2.2). Thus the presence of ASY was not dependent on a single-X constitution.

### 2.3.6 ASY localisation in XX oocytes (n=4)

These oocytes allowed the requirement for asynapsis in ASY assembly to be tested. In contrast to XY<sup>Tdym1</sup>, XO and In(X)/X pachytene oocytes, there were very few ASY-positive XX pachytene oocytes (Figure 2.8a,c,d, Table 2.2). Where staining was present, ASY was associated with one partially asynapsed bivalent. On closer examination, ASY could be seen to selectively coat the asynapsed but not synapsed segments of these chromosomes (Figure 2.8c,d). Thus assembly of ASY did not occur on X chromatin indiscriminately, but only as a response to asynapsis.

### 2.3.7 ASY localisation in T(2;5)72H oocytes (n=2)

The presence of ASY-positive partially synapsed bivalents in XX females raised the possibility that asynapsed autosomal chromatin might also accumulate ASY protein. ASY localisation was therefore analysed in pachytene oocytes from T(2;5)72H/+ females (Tease, Fisher and Evans, pers.comm) in which heterozygosity for a reciprocal autosome-autosome translocation between chromosomes 2 and 5 leads to regular autosomal asynapsis (Figure 2.9a). ASY was absent in oocytes in which complete synapsis of the translocated autosomes had been achieved (Figure 2.9b,c). In oocytes where synapsis had not been completely achieved, ASY was present. In these circumstances, ASY associated with the chromatin of asynapsed autosomes, but was excluded from segments where synapsis was complete (Figure 2.9d,e,f,g, Table 2.2). Thus ASY coats the chromatin of asynapsed segments of sex chromosomes and autosomes in a sex- and MSCI-independent manner. It was based on this affinity for asynapsed chromatin that the protein was named Asynaptin.



### 2.3.8 ASY localisation in $XXY^{d1}$ oocytes (n=1)

During meiosis in  $XXY$  females, synapsis is preferentially between the X chromosomes and the Y chromosome is normally present as a univalent (Mahadevaiah *et al.*, 1993). Immunostaining of these oocytes with ASY allowed the observation that ASY fails to label the asynapsed Y in  $XY^{Tdyml}$  oocytes to be further investigated. Consistent with this observation, the  $Y^{d1}$  univalents of  $XXY^{d1}$  oocytes were consistently ASY-negative (Figure 2.8b, Table 2.2). Of those cells that were ASY-positive, ASY associated with partially or completely asynapsed bivalents, as described for XX females (Figure 2.8e,f).

Figure 2.2. Analysis of MSCI in XY<sup>Tdym1</sup> pachytene oocytes.

- a) XY<sup>Tdym1</sup> pachytene oocytes stained for DAPI. There are no sex bodies in the upper three pachytene nuclei.
- b) Same nuclei stained for RNA polII (red) and SCP3 (green), with colocalisation showing as yellow. All chromosomes lie in the RNA polII positive domain.
- c) RTPCR analysis of the Y-linked genes *Ube1y* and *Rbm*, the X-linked genes *Pdhal* and *Pgk1* and the autosomal back-ups *Pdhal* and *Pgk2* in 18.5dpc XX, XY<sup>Tdym1</sup> (denoted 'XY') ovaries and adult XY<sup>RIII</sup> testes. *Hprt*, used as an amplification control, is X-linked, but the transcripts are stable and remain detectable throughout pachytene. Arrows denote 500bp.

Product sizes:

*Ube1y* = 330bp

*Rbm* = 159bp

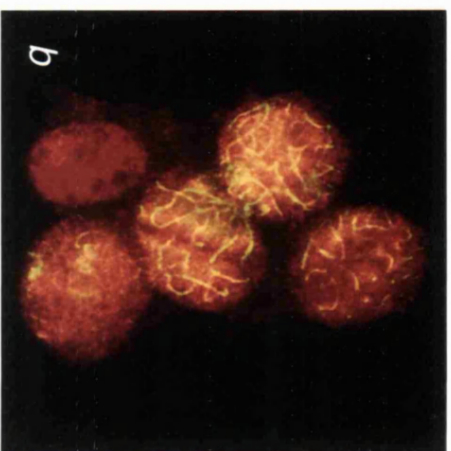
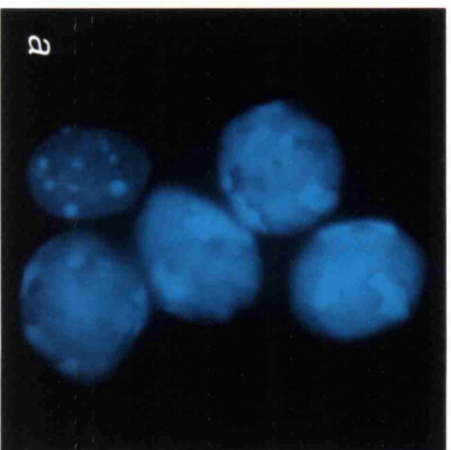
*Pdhal* = 287bp

*Pgk1* = 238bp

*Pdhal* = 459bp

*Pgk2* = 300bp

*Hprt* = 352bp



**C**

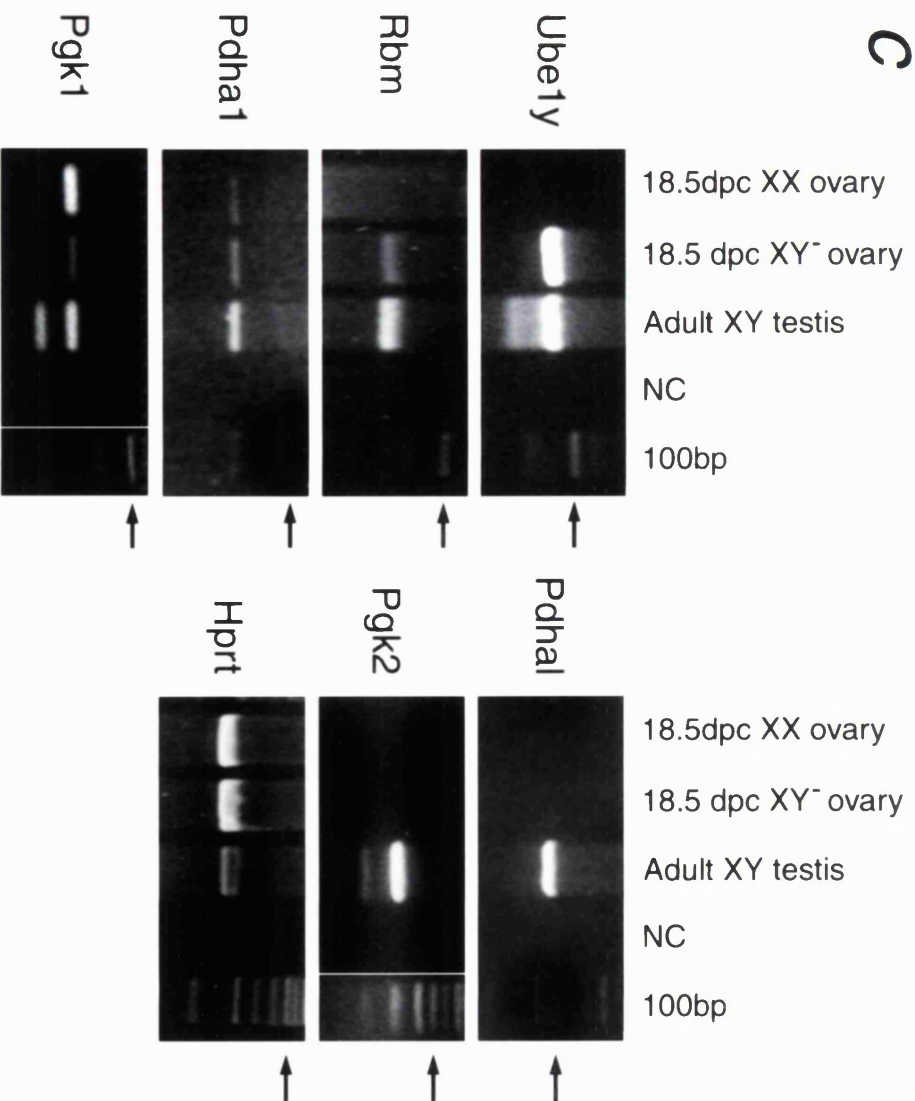


Figure 2.3. ASY expression in squashed (a-d) and spread (e,f) XY spermatogenic cells.

a) XY cells stained for SCP3 (red) and ASY (green). ASY localises to a peripheral nuclear domain in late pachytene (arrowheads) but not leptotene/zygotene (short arrows) nuclei.

b) Same field stained for DAPI. ASY is also absent in Sertoli cells (long arrow), spermatogonia (empty arrowhead) and spermatids (white bracket), cell types that do not stain with SCP3.

c) XY cells stained for SCP3 (red) and control hybridoma supernatant (green).

d) XY cells stained for SCP3 (red) and PBS in place of 2E3 (green)

e) Early diplotene nucleus stained for DAPI, which allows the sex body (white arrowhead), the X-centromere (short arrow) and autosomal centromeric heterochromatin (black arrowheads) to be distinguished.

f) Same nucleus stained for ASY (green) and RNA polIII (red), with colocalisation showing as yellow. ASY coats the sex body, which is RNA polIII-deficient. ASY is largely excluded from the X-centromere.

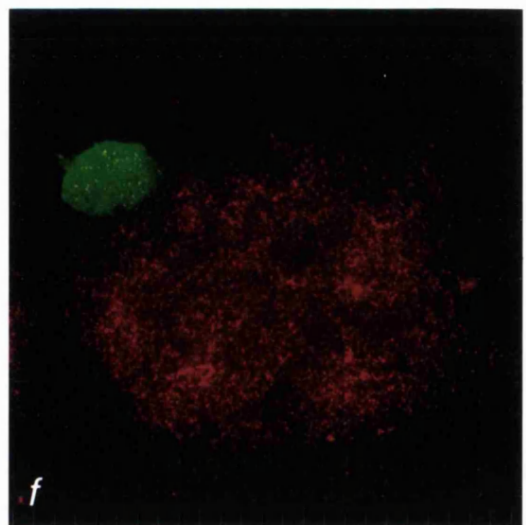
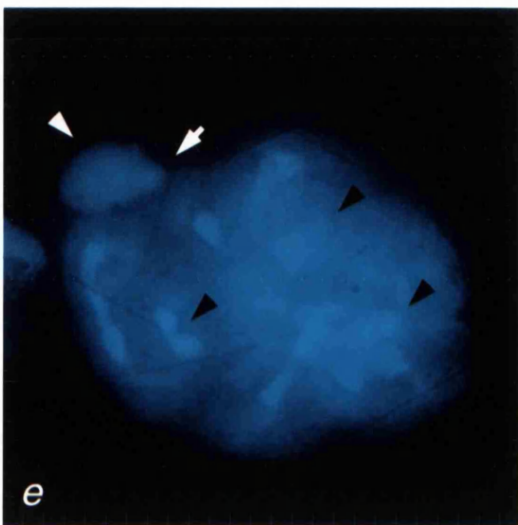
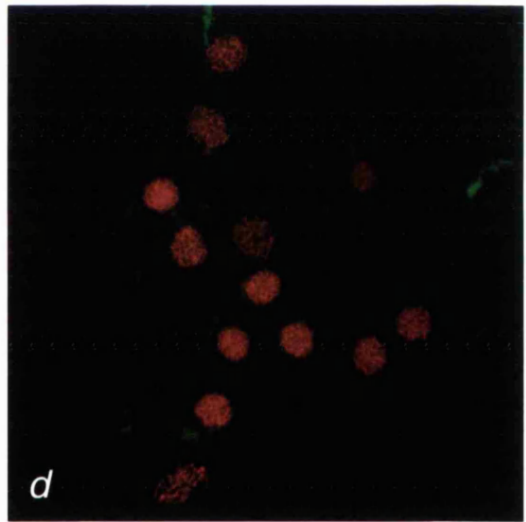
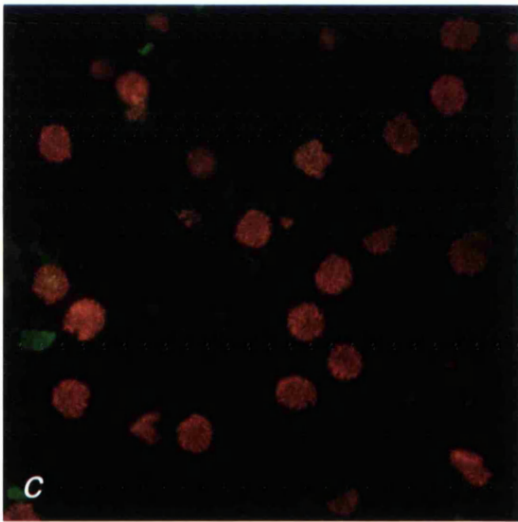
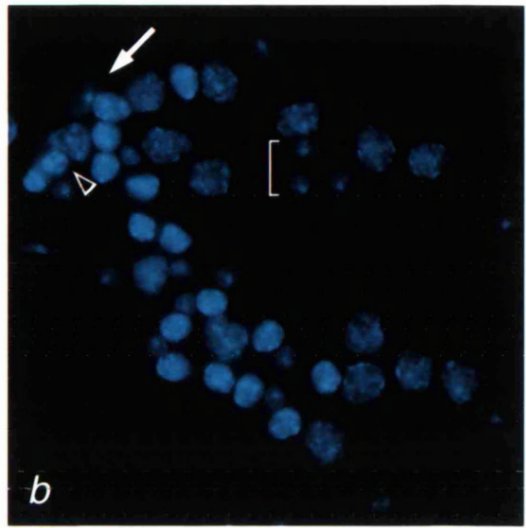
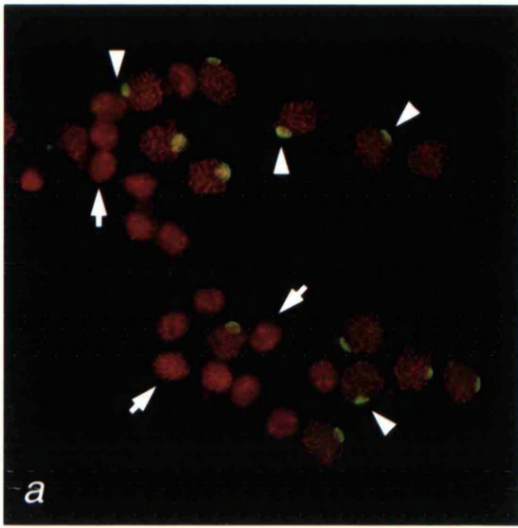


Figure 2.4. ASY expression during XY male mouse meiosis. SCP3 = red, ASY = green.

Arrowhead = Y chromosome, short arrow = X chromosome, long arrow = X-centromere.

a) Leptotene nucleus.

b) Zygotene nucleus.

c) Early pachytene nuclei.

d) Mid pachytene nuclei. ASY first becomes apparent around the sex chromosomes.

e) Late pachytene nucleus. ASY coats the chromatin of the whole sex body except the X-centromere.

f) Early diplotene nucleus. ASY coats the sex body.

g) Mid-late diplotene nucleus. ASY disappears.

h) MI nucleus.

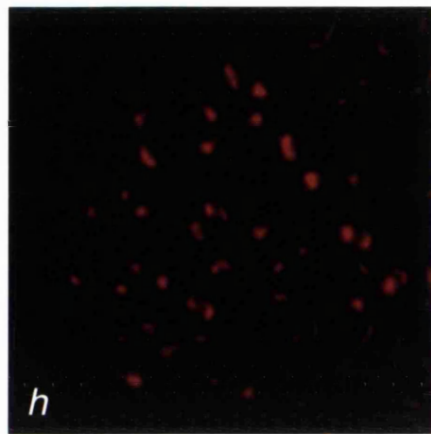
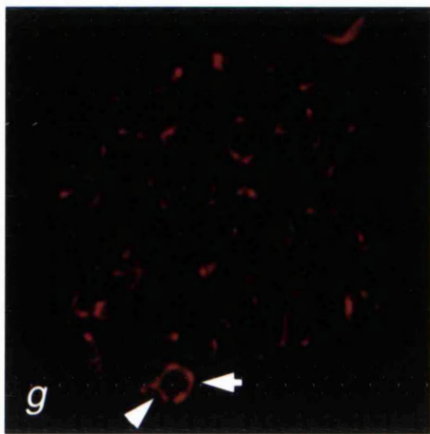
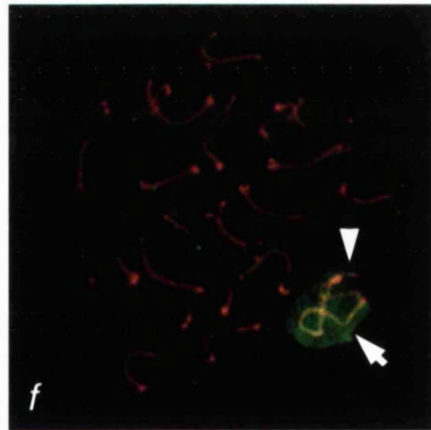
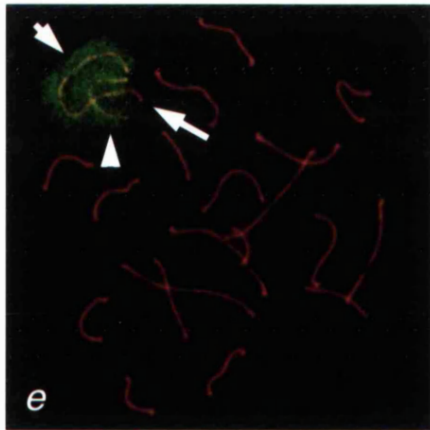
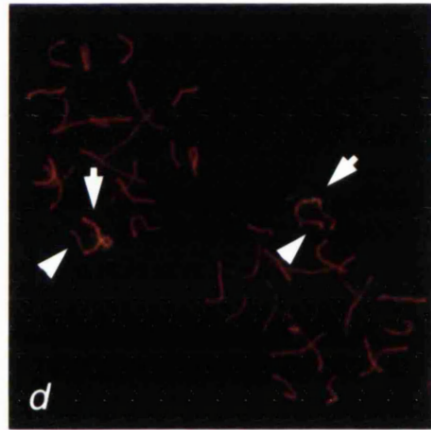
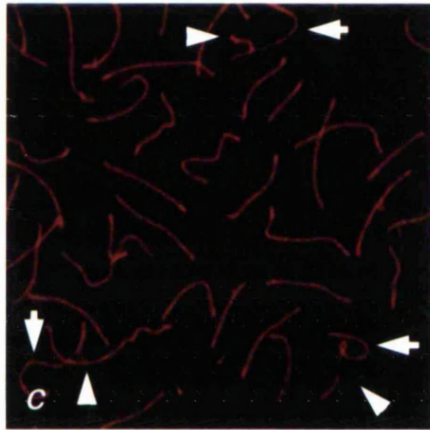
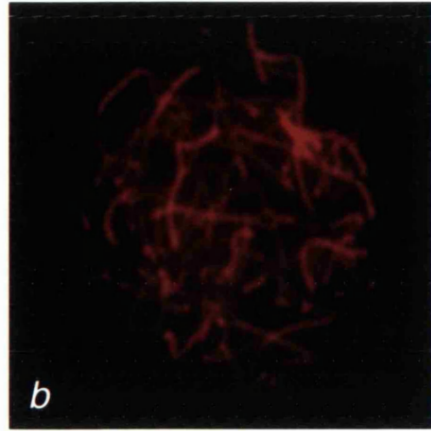
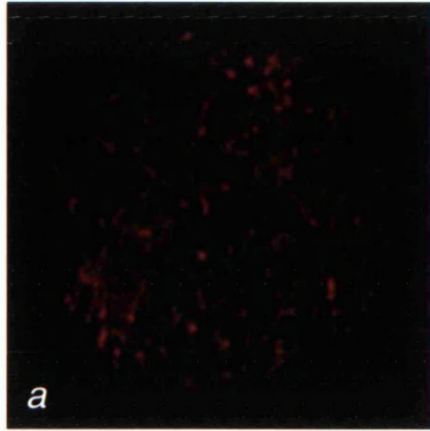


Figure 2.5. High power analysis of ASY in the sex body. SCP3 = red, ASY = green.

Arrowhead = Y chromosome, short arrow = X chromosome, long arrow = X-centromere.

a) Late pachytene sex body stained for ASY and SCP3. ASY forms punctate dots over the chromatin of the X and Y chromosomes.

b) Same nucleus without SCP3. ASY shows no preference for axial cores.

c) Late pachytene sex body stained for ASY and SCP3. Comments as above.

d) Same nucleus without SCP3. Comments as above.



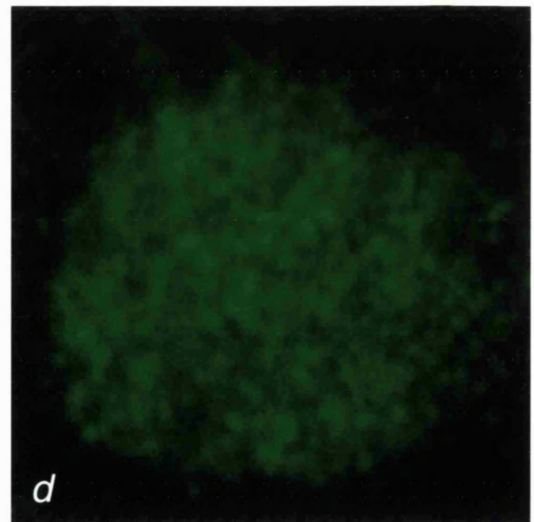
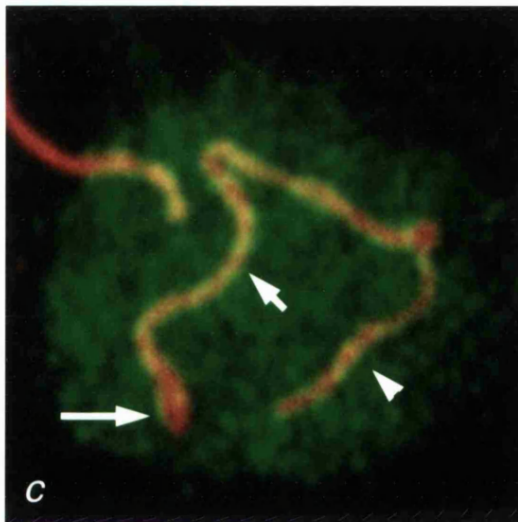
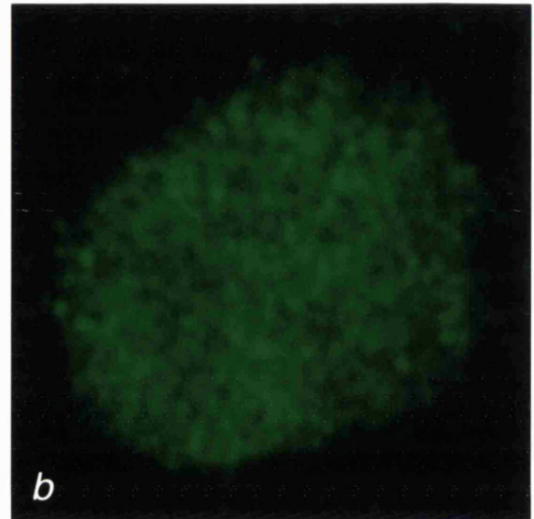
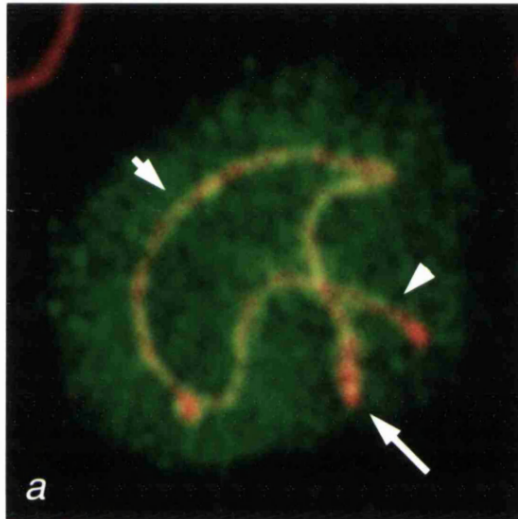
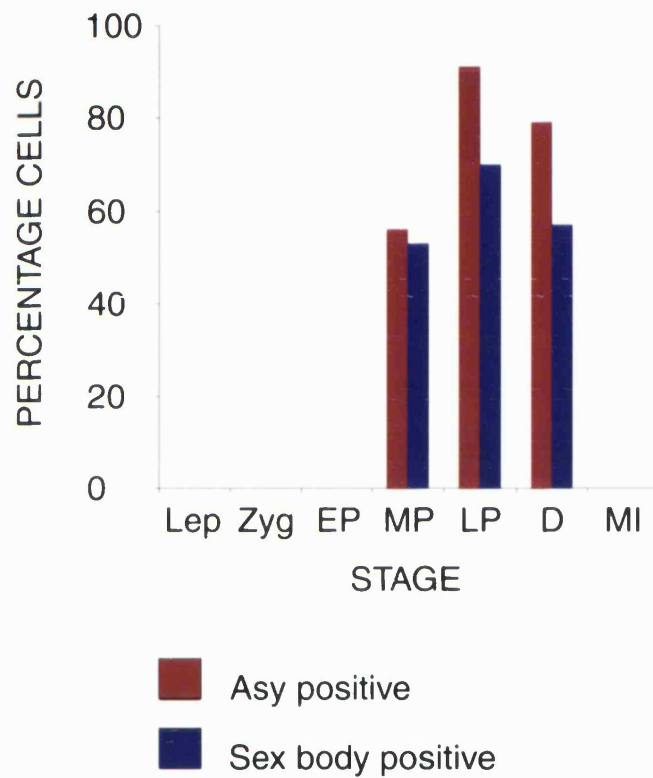


Figure 2.6. Appearance of ASY (red columns) and morphological sex bodies as stained with DAPI (blue columns) during XY male meiosis I, based on data from Table 1.1 below. Lep = leptotene, Zyg = zygotene, EP = early pachytene, MP = mid pachytene, LP = late pachytene, D = diplotene, MI = metaphase I.

Table 2.1. Appearance of ASY and morphological sex bodies as stained with DAPI during XY male meiosis I.



	N <sup>o</sup> cells	N <sup>o</sup> Asy +	N <sup>o</sup> SB +
Leptotene	15	0	0
Zygotene	45	0	0
E. pachytene	9	0	0
M. pachytene	32	18(56%)	17(53%)
L. pachytene	33	30(91%)	23(70%)
Diplotene	14	11(79%)	8(57%)
Metaphase I	7	0	0

Figure 2.7. ASY expression in the absence of MSCI. Arrowhead = Y chromosome, short arrow = X chromosome, long arrow = X-centromere, empty arrowhead = partially asynapsed bivalent.

a)  $XY^{Tdyml}$  early pachytene nucleus stained for SCP3 (red) and ASY (green). ASY coats the X chromatin but is excluded from the X-centromere. X-Y pairing is rare and the asynapsed Y is unstained.

b)  $XY^{Tdyml}$  mid pachytene nucleus. Comments as above.

c)  $XY^{Tdyml}$  early pachytene nucleus. Comments as above.

d)  $XY^{Tdyml}$  early pachytene nucleus. The X chromosome associates with a partially asynapsed bivalent and possibly the Y chromosome as well.

e) XO late-early pachytene nucleus. The asynapsed X chromosome forms a loop.

f) In(X)/X early pachytene nucleus.

g)  $XY^{Tdyml}$  meiocytes stained for SCP3 (red) with 2E3 replaced by control hybridoma supernatant (green).

h)  $XY^{Tdyml}$  meiocytes stained for SCP3 (red) with 2E3 replaced by PBS (green).

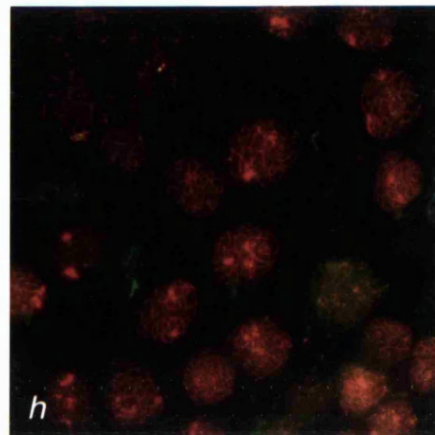
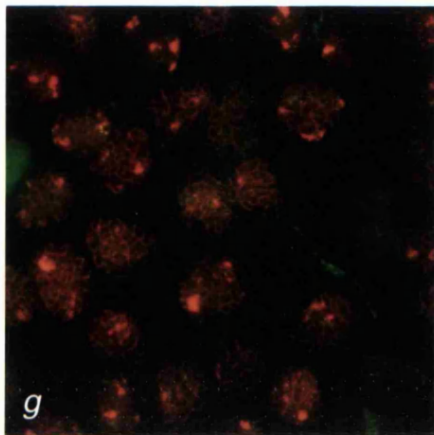
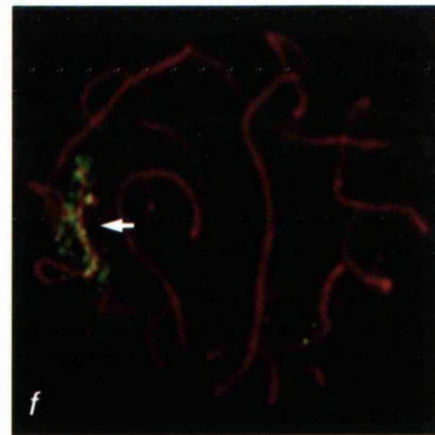
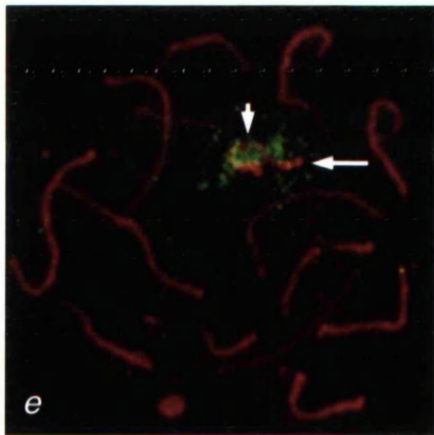
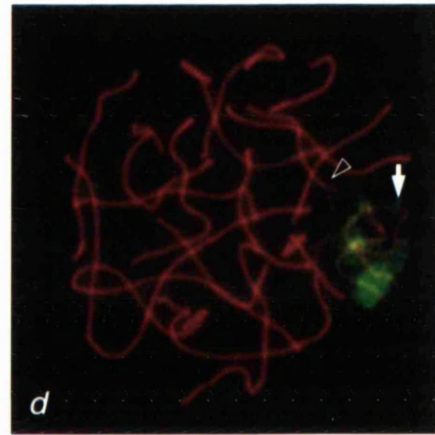
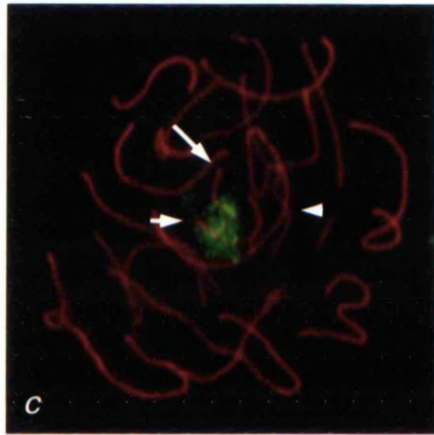
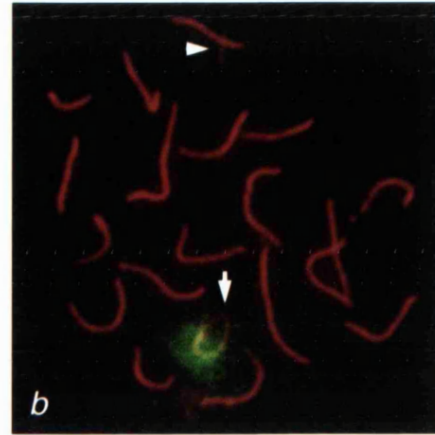
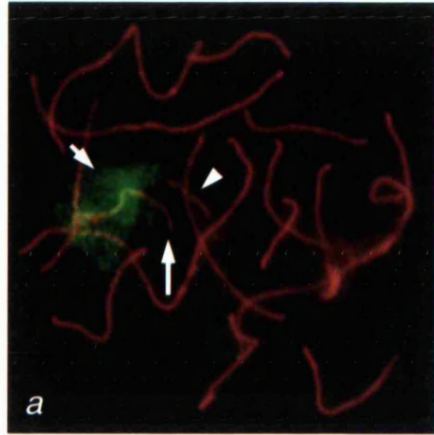


Figure 2.8. ASY expression in the absence of MSCI cont. SCP3 = red, ASY = green.

Arrowhead = synapsed bivalent, short arrow = asynapsed bivalent, long arrow = centromere, empty arrowhead = Y chromosome.

a) XX mid pachytene nucleus. All bivalents have synapsed and ASY is undetectable.

b)  $XXY^{d1}$  late-mid pachytene nucleus. All bivalents have synapsed, but the Y remains a univalent and is unstained.

c) XX mid pachytene nucleus with partial asynapsis of one bivalent (open arrow).

d) Same nucleus at high power. ASY coats the chromatin of the asynapsed but not synapsed part of the bivalent.

e)  $XXY^{d1}$  mid pachytene nucleus with partial asynapsis of one bivalent (open arrow).

f) Same nucleus at high power. Comments as with d).

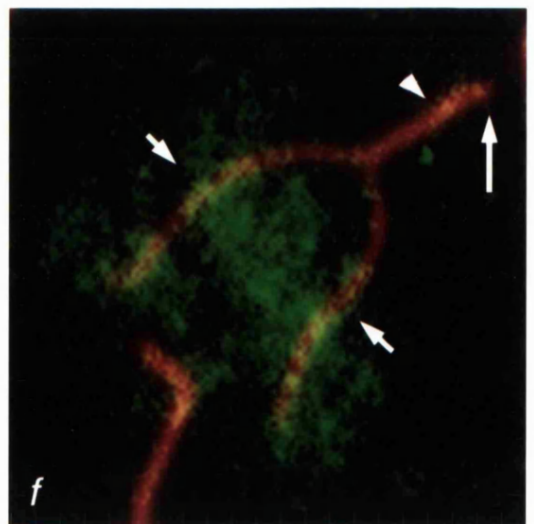
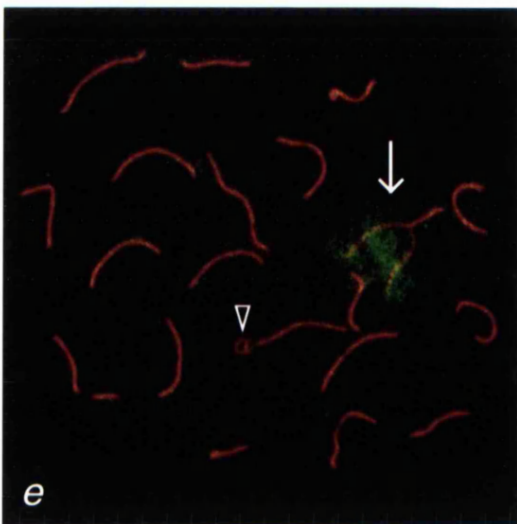
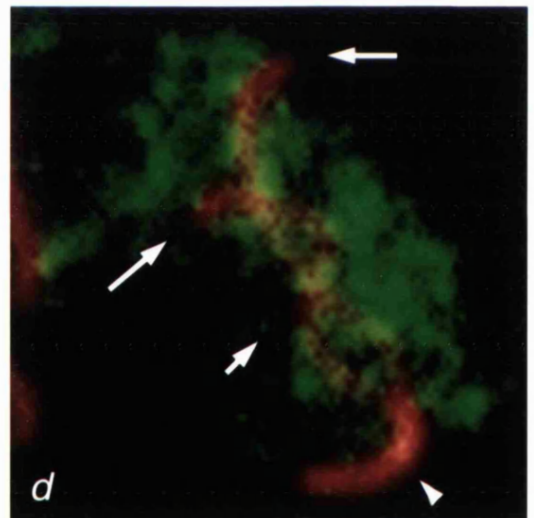
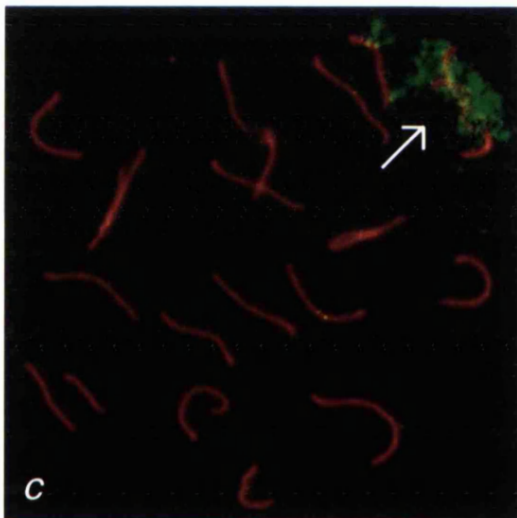
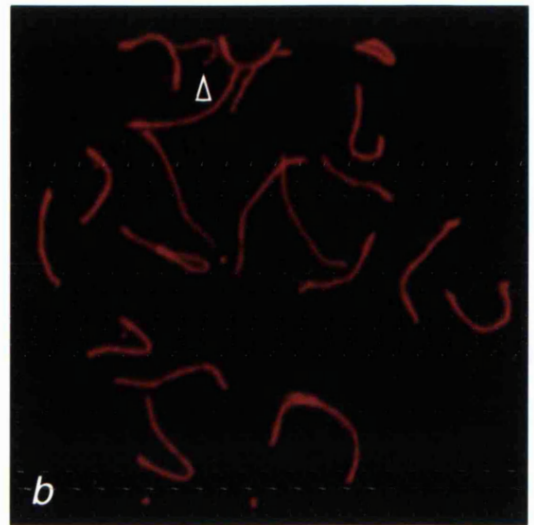
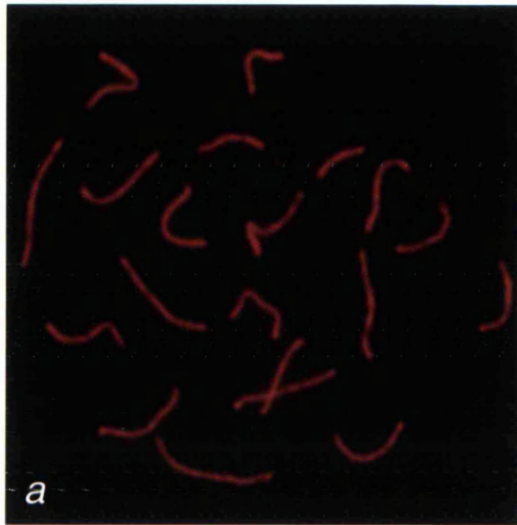
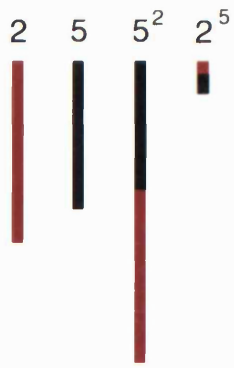


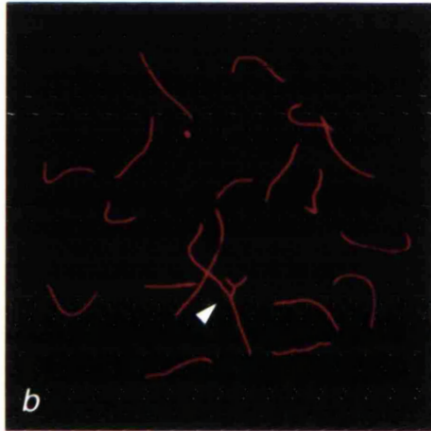
Figure 2.9. ASY expression in heterozygous T(2;5)72H pachytene oocytes. SCP3 = red, ASY = green. Arrowhead = synapsed bivalent, short arrow = asynapsed bivalent.

- a) Schematic representation of the T(2;5)72H reciprocal autosomal translocation.
- b) T(2;5)72H mid pachytene oocyte with complete autosomal synapsis
- c) Configuration of completely synapsed T(2;5)72H quadrivalent from b)
- d) Early T(2;5)72H pachytene oocyte with incomplete autosomal synapsis. ASY coats the asynapsed but not synapsed segments of the T(2;5)72H quadrivalent.
- e) Configuration of incompletely synapsed T(2;5)72H quadrivalent from d)
- f) Early T(2;5)72H pachytene oocyte with incomplete synapsis. Comments as with d).
- g) Early T(2;5)72H pachytene oocyte with incomplete synapsis. Comments as with d).

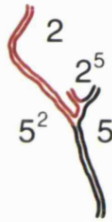




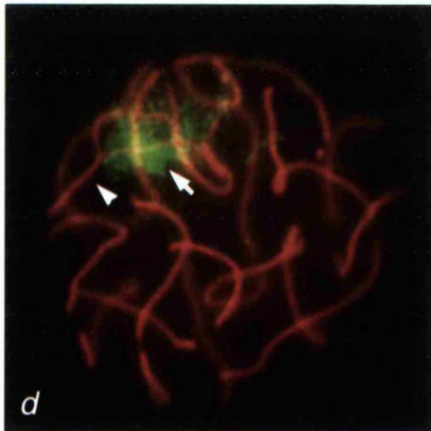
*a*



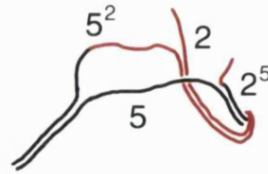
*b*



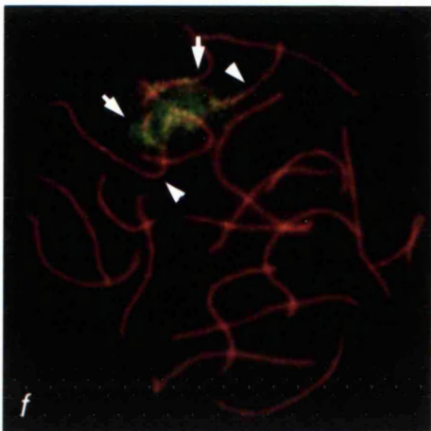
*c*



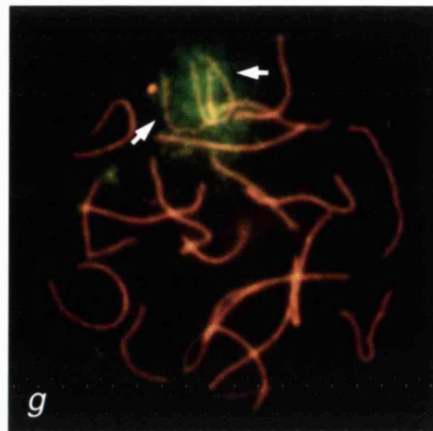
*d*



*e*



*f*



*g*

Table 2.2. Appearance of ASY during meiosis I in different female genotypes.

STAGE	NUMBER CELLS ASY POSITIVE					
	XY <sup>Tdym1</sup> (n=3)	XO (n=2)	In(X)/X (n=1)	XX (n=4)	T(2;5)72H (n=2)	XXY (n=1)
LEPTOTENE	-	-	-	0/8	-	-
ZYGOTENE	-	0/1	2	0/12	0/1	-
EARLY PACH	8/31 (26%)	4/18 (22%)	2/5 (40%)	0/10	1/12 (8%)	0/9
MID PACH	2/15 (13%)	1/5 (20%)	2/9 (22%)	2/28 (7%)	9/30 (30%)	1/16 (6%)
LATE PACH	7/27 (26%)	4/9 (44%)	2/7 (29%)	0/45	2/20 (10%)	0/13
DILOTENE	-	-	1/4 (25%)	0/23	1/4 (24%)	0/8
UNCLASSIFIED	9	-	9	35	1	1
TOTAL CELLS	82	33	36	161	68	47

## 2.4 DISCUSSION

As discussed in section 1.2.1, an increasing number of proteins have been characterised that localise to the sex body. While some are restricted to the sex body (e.g. XY40, XY77, GCNF; Smith and Benavente, 1992; Kralewski *et al.*, 1997; Bauer *et al.*, 1998), others show preferential enrichment in this domain (e.g. p51, M31, Xmr; Smith and Benavente, 1995; Motzkus *et al.*, 1999; Calenda *et al.*, 1994). In light of the highly condensed state of the sex chromosomes during pachytene, it is not surprising that an MSCI-related role has been postulated for many of these proteins (Smith and Benavente, 1992; Kralewski *et al.*, 1997; Bauer *et al.*, 1998; Smith and Benavente, 1995; Motzkus *et al.*, 1999; Calenda *et al.*, 1994). However, in all of these cases this hypothesis remains unproven. The original aim of this study was to identify whether ASY was a true marker of MSCI.

In this study, XY<sup>Tdym1</sup> females were used as sex body-negative controls. The original study that indicated a lack of sex body formation in XY pachytene oocytes was based on silver-stained SC analysis (Kundu *et al.*, 1983). In the present study, sex body formation and MSCI was analysed both morphologically (DAPI staining) and functionally (RNA POLII and X/Y gene expression). The data indicated that MSCI does not take place in XY<sup>Tdym1</sup> oocytes, implying either that the ability to undergo MSCI is programmed in germ cells entering a male sex determination pathway, or that it is conferred by testis-specific factors. Nevertheless, ASY coated the asynapsed X chromosome. Analysis of other sex chromosomally aberrant females indicated that ASY bound the chromatin of chromosomes that had failed to synapse at pachytene. Its existence in the sex body of normal males is therefore likely to reflect the asynaptic, and not transcriptionally inactive nature of the sex

chromosomes. These results with ASY highlight the inadequacy of using XX ovaries as controls, as has been the case in other studies of sex body proteins.

ASY represents the first protein described that is specific for chromatin that fails to synapse. Based on this property, it may serve a number of functions. ASY may be involved in DSB repair in the absence of homologous recombination (so-called non-homologous end joining pathway, or NHEJ, Daza *et al.*, 1996). Consistent with this possibility is the finding that other proteins involved in NHEJ, including Ku70, Mre11 and Rad50, also localise to the sex body (Goedecke *et al.*, 1999). However, whereas these proteins are also expressed in mitotic cells (eg spermatogonia), ASY expression is restricted to meiotic prophase. Should ASY serve a DNA repair role, it must therefore be a meiosis-specific one.

An alternative possibility is that ASY is involved in some aspect of the synapsis checkpoint. The putative checkpoint protein ATR has also been postulated to be involved in alerting meiotic cells to asynapsis (Keegan *et al.*, 1996; Plug *et al.*, 1998; Moens *et al.*, 1999). In contrast to ASY, ATR appears along axial elements *prior* to completion of synapsis, disappearing as synapsis proceeds, but like ASY it accumulates when chromosomes fails to synapse (including the X and Y non-PAR axes; Keegan *et al.*, 1996; Plug *et al.*, 1998; Barlow *et al.*, 1998). An anti-ATR antiserum also labels apoptotic cells (Baart *et al.*, submitted). Under this model, ASY would act downstream of ATR in the checkpoint pathway.

In contrast to male meiosis, where ASY-staining was most clearly observed at late pachytene, ASY stained asynapsed chromatin in oocytes at all pachytene substages. This probably reflects the difference in duration of pachytene (three days versus six days) in

oocytes (Speed *et al.*, 1982) versus spermatocytes (Goetz *et al.*, 1984); this explanation has previously been used to explain the sexual dimorphism in the timing of meiotic MLH1 expression (Ashley and Plug, 1998). Thus, if the process in which ASY participates spans a three day period in both male and female meiosis (late pachytene lasts about three days in the male, Goetz *et al.*, 1984), ASY would be expected to appear at all substages of pachytene in the female.

ASY failed to label univalent Y chromosomes in both  $XY^{Tdym1}$  and  $XXY^{d1}$  oocytes. Although the whole sex body of XY males appeared ASY-positive, the intermingling of X and Y chromatin under these circumstances made it impossible to state categorically whether Y chromatin accumulates ASY. It is formally possible that Y-associated ASY is dispersed during the surface spreading of oocytes. This is partly supported by the fact that not all pachytene oocytes with asynapsed X or autosomal chromatin were ASY-positive (Figure 1.9, Table 1.2). However, bearing in mind that 129 pachytene oocytes (representing  $XY^{Tdym1}$  and  $XXY^{d1}$ ) were imaged, the more likely explanation is that Y chromatin does not accumulate ASY. RAD51/DMC1 and BLM, both of which are implicated in recombination, are also thought not to be present on the Y chromosome, while proteins with checkpoint functions (ATR and hRAD1) are (Moens *et al.*, 1997; Moens *et al.*, 2000; Freire *et al.*, 1998; Moens *et al.*, 1999). Should the absence or presence of a protein on the Y chromosome reflect a recombination versus checkpoint-related role for that protein (Moens *et al.*, 2000), then ASY could function in recombination. Alternatively, the accumulation of ASY on Y chromatin may require juxtaposition of the X and Y chromosomes.

Undermining the potential roles of ATR and ASY in the synapsis checkpoint is the fact that they accumulate on the non-PAR regions of the X and Y chromosomes in male meiosis, and yet these chromosomes fail to trigger checkpoint-mediated arrest. Two possibilities could explain this finding. Firstly, the anti-ATR antibody used by Keegan *et al.* fails to distinguish between the phosphorylated and unphosphorylated forms of this protein (Ashley, 2000). It is therefore possible that the phosphorylation status of sex chromosome-bound ATR differs from that which binds asynapsed autosomes (the same argument could apply for ASY). Alternatively, the XY pair may associate with additional proteins that disrupt the checkpoint pathway.

The results with ASY highlight the importance of using XY female controls for establishing whether other sex body proteins are truly sex body-specific, or whether their location to the sex body is due to the presence of asynapsed chromatin. For future experiments, it is clearly important that the gene coding for ASY be identified. Nevertheless, the present data indicate that ASY is not a marker of MSCI, and therefore is unsuitable for analysing the role of synapsis and of *Xist* in Y chromosome MSCI.

CHAPTER 3

AN INVESTIGATION INTO THE MSCI-SPECIFICITY

OF XMR AND XY77



### 3.1 INTRODUCTION

Results from the previous chapter demonstrated that ASY coats the chromatin of asynapsed axes, and that this was the most likely explanation for its appearance in the sex body of normal male meiocytes. Although an interesting protein, ASY is clearly not a marker of MSCI, and is therefore unsuitable for our proposed studies of MSCI in males with asynapsed Y chromosomes (see introduction to Chapter 2).

As mentioned in section 1.2.1, a number of other proteins (XY40, XY77, p51, GCNF, M31 and XMR) have been identified that locate to the sex body, most of which have been postulated to be involved in MSCI (Smith and Benavente, 1992; Kralewski *et al.*, 1997; Smith and Benavente, 1995; Bauer *et al.*, 1998; Motzkus *et al.*, 1999; Calenda *et al.*, 1994; Escalier *et al.*, 1999). However, none of these proteins have been checked for expression in XY pachytene oocytes; thus, like ASY, their association with the sex chromosomes may not be MSCI-specific. This chapter describes studies using antisera to two of these proteins, XY77 and XMR, that were undertaken in order to begin the task of checking the MSCI-specificity of these other proteins and in the hope of identifying an MSCI-specific sex body marker.

*Xmr* is a member of the *Xlr* (X-chromosome linked, lymphocyte-regulated) multigene family (Calenda *et al.*, 1994). The original member of this family, *Xlr*, was identified by a subtractive cDNA screen aimed at identifying T cell-specific transcripts, and was subsequently shown to be closely linked to the murine *xid* (X-linked immunodeficiency) mutation (Cohen *et al.*, 1985). It is expressed in the most mature stages of both B- and T-cell development (Cohen *et al.*, 1985; Siegel *et al.*, 1987) and, in addition, in immature

thymocytes just prior to T-cell rearrangement (TCR; Escalier *et al.*, 1999). Although between 50 and 75 *Xlr*-related sequences are distributed on both the X and Y chromosomes, most of these do not encode functional transcripts (Garchon *et al.*, 1989). An exception is the testis-specific *Xmr* (*Xlr*-related *meiosis-regulated*) transcript. *Xmr* and *Xlr* are 94% identical at the nucleotide level; both possess an N-terminal acidic domain suggestive of a role in transcriptional activation and a C-terminal coiled-coil domain suggestive of an ability to dimerise (Calenda *et al.*, 1994). However, *Xmr* differs from *Xlr* in that it possesses an additional 388 bp N-terminal sequence with no close homology to any other protein and is deleted at three positions relative to *Xlr* (Calenda *et al.*, 1994).

Published results indicate that *Xmr* transcription and protein expression both begin around the time that germ cells enter meiosis (Calenda *et al.*, 1994). The protein, as detected by an anti-XLR antibody, was visible immunohistochemically in spermatocytes from preleptotene to diplotene. The pattern of staining has two components; first, from preleptotene to early pachytene, there is uniform staining throughout the nucleus, and second, from zygotene to diplotene, there is also a progressively more intense staining of the sex body (Calenda *et al.*, 1994).

The association of XMR with autosomal chromatin in early prophase and the subsequent concentration in the sex body led to speculation that it may play a role in chromatin condensation (Escalier *et al.*, 1999 and H. Garchon, pers. comm); alternatively it has been suggested that XMR may serve a role in meiotic recombination (Escalier *et al.*, 1999). This latter possibility is suggested by its similarity to the yeast *mer2* gene, disruption of which abolishes meiotic recombination, due to an inability to create DSBs (Rockmill *et al.*, 1995).

A recombination-related role is supported by the fact that XLR is highly expressed just prior to TCR (Escalier *et al.*, 1999). XMR also shares significant amino acid homology with SCP3 (Escalier *et al.*, 1999). Although the exact function of SCP3 is unknown, it may be involved in a number of meiotic functions, including homology searching, recombination, chiasma interference, sister chromatid cohesion and prevention of sister chromatid exchange (Lammers *et al.*, 1994). The likely function of XMR therefore remains a matter of debate.

XY77 was identified by generating a monoclonal antibody (mAb 4c6) to protein fractions of rat pachytene spermatocytes (Kralewski *et al.*, 1997). This antibody recognises a number of structures in mouse testis cryosections, namely: the sex body chromatin of late pachytene and diplotene spermatocytes, cytoplasmic dots in spermatids and nuclear dots in Sertoli cells. The latter staining pattern is identical to that found in a control rat vein smooth muscle cell line (termed RV-SMC, Kralewski *et al.*, 1997). On Western blot analysis, mAb 4c6 recognises a 77kDa protein in purified pachytene spermatocytes, a 50kDa protein in RV-SMC cells and no product, even after overloading, in purified spermatids. The absence of an mAb 4c6-positive protein in the spermatid fraction could be due to low levels of expression; alternatively the protein detected by immunofluorescence in spermatids could be a different protein that is more unstable or is subject to conformational changes during the PAGE procedure. The 50kDa protein from RV-SMC cells was thought likely to be the same as the protein present in Sertoli cells in view of the similar pattern of nuclear staining in these cell types. The 77kDa protein from pachytene spermatocytes was considered to be the sex (or 'XY') body-located protein and was hence termed XY77.

In this study, anti-XLR and mAb 4c6 antisera were used to compare XMR and XY77 expression in spermatocytes with that in pachytene XY<sup>Tdym1</sup> oocytes or oocytes with autosomal asynapsis.

## 3.2 MATERIALS AND METHODS

### 3.2.1 Mice

All mice were generated as described in section 2.2.1

### 3.2.2 Squash procedure

Squashed spermatocytes and oocytes were prepared as described in Appendix 1.6.

### 3.2.3 Surface spreading procedure

Surface spread spermatocytes and oocytes were prepared as described in Appendix 1.7.

### 3.2.4 Immunostaining

Meiocytes were immunostained as described in Appendix 1.8. In controls, anti-XLR was replaced by MOPC21 IgG $\kappa$  (purified myeloma immunoglobulin; Sigma), as described by Calenda *et al.* (1994) or PBS, and mAb 4c6 was replaced with PBS.

### 3.2.5 Examination

Immunostained meiocytes were examined as described in Appendix 1.9.

### 3.2.6 Total RNA extraction from testes and ovaries

Total RNA was extracted as described in Appendix 1.3.

### 3.2.7 Reverse transcription of total RNA

Reverse transcription of total RNA was carried out as described in Appendix 1.4.

### 3.2.8 Genomic DNA extraction

Genomic DNA was extracted from tail tips as described in Appendix 1.2

### 3.2.9 PCR procedure

Genomic PCRs and RT PCRs were carried out as described in Appendix 1.5. Genomic PCR primers are described in section 2.2.4. RT PCR primers used were *Hprt* (see section 2.2.4) and *Xmr/Xlr* primers (Calenda *et al.*, 1994):

A: 5' CTT GAG AGA CAA CAA TGG AAA AC 3'

B: 5' AGT CTG AAG ATG GGA AAC TAG AAG 3'

C: 5' TAA CTT GCT GTT CAC CAC TTA ACA AAT T 3'

D: 5' ATT GAG GAG TTG AGC ACG GAA 3'

All primer pairs were used at  $T_m = 58^{\circ}\text{C}$ . Product sizes were:

B + D: *Xmr* = 812bp (extension time = 1 min).

D + C: *Xmr* = 427bp.

A + B: *Xmr* = 420bp, *Xlr* = 630bp.

### 3.2.10 Cloning and sequencing of PCR products

20µl of PCR products, prepared as described in section 3.2.4, were run on a 2% agarose gel as described in Appendix 1.5. Bands were excised using sterile scalpel blades (Swann-Morton) and PCR products extracted using the Qiaex II DNA Extraction Kit according to manufacturer's instructions (Qiagen). Purified PCR products were cloned using the TOPO™ TA Cloning Kit® according to manufacturer's instructions (Invitrogen). White colonies were grown in LB medium containing 50µg ml<sup>-1</sup> kanamycin (Sigma) overnight at 37°C. Plasmid DNA was then extracted using the Hybaid Recovery™ Plasmid Mini Prep Kit according to manufacturer's instructions (Hybaid). The resulting DNA was denatured and sequenced using the Sequenase™ Version 2.0 Sequencing kit according to manufacturer's instructions (USB, Amersham Life Sciences).

### 3.3 RESULTS

#### 3.3.1 Anti-XLR immunostaining of XY testis (n=3)

Anti-XLR immunostaining was carried out on both squashed and surface spread spermatogenic nuclei. For detailed analysis, the squash procedure was used because it retained the whole nuclear staining described by Calenda *et al.* (1994); this staining was lost in the surface spreading procedure. In view of the complex expression pattern seen with anti-XLR, immunostaining was carried out in combination with both anti-SCP3 and anti-SCP1 (which binds only synapsed chromosomes and therefore allows early spermatocytes to be more accurately substaged).

Consistent with published results (Calenda *et al.*, 1994), the anti-XLR antibody first showed whole nuclear staining at leptotene and this increased in intensity during zygotene (Figure 3.1 a-d, 3.2 a-f). At late zygotene a second, more intense signal, possibly representing the condensing X chromosome could also be seen (Figure 3.2 f). Ovoid, peripheral sex bodies were first stained as such at early pachytene and remained so until diplotene, while the nuclear staining decreased in intensity, becoming absent at late pachytene (Figures 3.1 a-d, 3.2 g,h, 3.3 a-d). Although not mentioned by Calenda *et al.* (1994), a third staining pattern was also noted. During diplotene, diffuse XMR staining was seen throughout the nucleus, which at MI was concentrated around the centromeric heterochromatin (Figure 3.1 a-d, 3.3 c-f). No nuclear staining was seen when anti-XLR was replaced by either MOPC21 IgGκ or PBS (Figure 3.1 e,f).



### 3.3.2 Anti-XLR immunostaining of XX oocytes (n=2)

Using the squash procedure, selected XX oogenic cells showed positive immunoreactivity to the anti-XLR antiserum. Staining was restricted to meiocytes (as judged by its complete overlap with SCP3) and began with a whole nuclear staining, which was first evident at leptotene, increased in intensity during zygotene, and then decreased during pachytene, before being absent at late pachytene (Figure 3.4 a-f).

### 3.3.3 Anti-XLR immunostaining of XY<sup>Tdym1</sup> oocytes (n=2)

Whole nuclear immunostaining in XY<sup>Tdym1</sup> oocytes was identical to that of XX oocytes (Figure 3.4 g,h). In addition, there was a more intense, subnuclear signal present at all pachytene substages (Figure 3.4 h, Table 3.1). Examination of well spread cells at high power revealed that this signal represented anti-XLR binding of the asynapsed X chromosome (Figure 3.5 a-f). In contrast to 2E3 (section 2.3.3), anti-XLR showed a particular affinity for the chromosomal axes. The fact that the more intense signals seen in XY<sup>Tdym1</sup> oocytes were rarely observed in XX oocytes (Figure 3.4, Table 3.1) indicated that the protein recognised by anti-XLR accumulated on the X chromosome in XY<sup>Tdym1</sup> oocytes as a response to asynapsis. Neither the whole nuclear nor the asynapsis-related staining was seen when anti-XLR was replaced by either MOPC21 IgGκ or PBS (Figure 3.5 g,h).

#### 3.3.4 Anti-XLR immunostaining in T(2;5)72H oocytes (n=1)

As in the ASY study, the finding that anti-XLR bound asynapsed X chromosomes in XY<sup>Tdym1</sup> oocytes raised the possibility that it might also accumulate on asynapsed autosomes. Analysis of pachytene oocytes from females heterozygous for the reciprocal autosomal translocation T(2;5)72H showed that this was indeed the case (Figure 3.6, Table 3.1).

#### 3.3.5 Xmr/Xlr expression in male and female gonads

The immunostaining results demonstrated that anti-XLR detects a protein with an almost identical expression pattern during meiotic prophase in XY males and XY<sup>Tdym1</sup> females, and suggested that, like ASY, the concentration of the protein in the sex body is asynapsis-related.

In order to verify that the oocyte protein was XMR, RTPCR was performed using *Xmr*-specific primers B and D (Calenda *et al.*, 1994) on 18.5dpc XX and XY<sup>Tdym1</sup> oocytes, with adult XY testis and adult liver as positive and negative controls (Figure 3.7, 3.8). The expected 812bp *Xmr* product was observed in adult XY testes and was absent from adult liver; however, *Xmr* transcripts were not detected in 18.5dpc XX or XY<sup>Tdym1</sup> ovaries. In order to investigate this further, RTPCR was then carried out using primers D and C (Calenda *et al.*, 1994), that amplify an *Xmr*-specific N-terminal sequence (Figure 3.7, 3.8). Once again, the correctly sized (427bp) product was observed in adult XY testes and was absent in adult liver. A product of similar size was detected in some, but not all RTPCRs on 18.5dpc XX and XY<sup>Tdym1</sup> ovaries. To determine whether this was *Xmr*, the PCR products from XX and XY<sup>Tdym1</sup> ovaries and from XY testes were sequenced. Although the XY testis

product matched *Xmr* exactly, the XX and XY<sup>Tdym1</sup> products were neither *Xmr* nor any related *Xlr*-like gene. Next, primers A and B, which give a 420bp product for *Xmr* and a 630bp product for *Xlr* (Calenda *et al.*, 1994), were used on the same samples (Figure 3.7, 3.8). In this PCR, high-level expression of a product of size consistent with *Xlr* was detected in ovaries and testes and, to a lesser extent, in liver. In agreement with the RTPCR using primers B and D, the *Xmr* product was present in XY testes only. 281bp of the *Xlr*-like RTPCR product from XY male, XY<sup>Tdym1</sup> female and XX female were then sequenced. All of these sequences were identical and all matched the published *Xlr* sequence exactly.

While the immunocytochemical results suggested that the same protein, presumed to be XMR, is present in XY testes and XY<sup>Tdym1</sup> ovaries, the RTPCR results show that *Xlr* is transcribed in both, while *Xmr* is restricted to the testis. Since the staining with the anti-XLR antibody is restricted to spermatocytes, the germ line specificity of *Xlr* and *Xmr* transcription was checked with the same three sets of primers using RNA samples from XXSxr<sup>a</sup> and XXSxr<sup>b</sup> testes (Figure 3.8). Spermatogenesis in XXSxr<sup>a</sup> males arrests at the spermatogonial stage due to the incompatibility of spermatogenesis with two doses of X chromosomal material (reviewed by Burgoyne, 1988). However, mitotic non-disjunction can result in the generation of XSxr<sup>a</sup>O cell lines, which are proficient in spermatogonial proliferation but arrest at MI as a result of the synapsis checkpoint (Sutcliffe *et al.*, 1991). Although mitotic disjunction could also theoretically take place in the XXSxr<sup>b</sup> testis, the resulting cells cannot proliferate due to the absence of a gene or genes (present in the Sxr<sup>b</sup> deletion interval) required for spermatogonial mitosis (Burgoyne *et al.*, 1986; Sutcliffe *et al.*, 1989). XXSxr<sup>a</sup> testes therefore may have a limited number of spermatocytes while XXSxr<sup>b</sup> testes totally lack spermatocytes. With all three sets of primers XXSxr<sup>a</sup> testes were positive for *Xmr* while

XXSxr<sup>b</sup> testes were negative. With primers A and B, XXSxr<sup>a</sup> and XXSxr<sup>b</sup> testes (like XY testes) were positive for the 630bp *Xlr* product. Thus *Xmr* appears to be germ cell-dependent while *Xlr* is not.

Finally, the timing of *Xmr* expression was reanalysed by performing RTPCR using all three sets of primers on pre- and postnatal testis at different ages (Figure 3.8). For primer pairs A/B and D/C *Xmr* transcripts were detected from 14.5dpc onwards. Based on the B/D primer PCR, *Xmr* expression was most obvious from 18dpp onwards, although even in this reaction faint PCR products were detected from 14.5dpc. *Xlr* was expressed at all ages from as early as 11.5dpc.

In summary, although *Xmr* was transcribed in a male germ cell-restricted pattern, *Xlr* was present in testes with and without germ cells and in XX and XY<sup>Tdym1</sup> ovaries.

### 3.3.6 Southern analysis of *Xmr*.

As described in the introduction, MSCI results in the large-scale inactivation of many X-linked genes, some of which serve vital metabolic functions (e.g. *Pgk1*, *Pdhal*). In many cases, these genes possess autosomal 'backups' (e.g. *Pgk2*, *Pdhal*) which are transcribed specifically during meiosis and which compensate functionally for their X-linked counterparts. Considering that *Xlr* is X-linked, one possible explanation for the RTPCR data described in section 3.3.5 was that the protein observed during female meiosis was XLR and that XMR might represent another example of a testis-specific autosomal backup. To address this, a Southern containing various genotypes of varied X and Y chromosome copy number was hybridised with an *Xmr* probe generated by PCR using primers D and C (Figure

3.9). Contrary to the autosomal back-up hypothesis, the *Xmr* signal dosed with the X chromosome, indicating that it was X-linked.

### 3.3.7 XY77 in male meiosis (n=2)

XY77 expression was analysed in testis squash preparations using mAb 4c6, in order to verify the male expression pattern described by Kralewski *et al.* (1997, Figure 3.10). Mab 4c6 stained the sex bodies of late pachytene and diplotene spermatocytes, as well as many fine dots in Sertoli cell nuclei. No signals were observed in any other cell types. The sex body-associated signals were lost on surface spreading of spermatocytes.

### 3.3.8 XY77 in XX (n=2) and XY<sup>Tdym1</sup> females (n=5)

When mAb 4c6 was used on squashes of 18.5dpc ovaries from XY<sup>Tdym1</sup> and XX females, no signals were detected in either meiotic or follicular cells (Figure 3.10).

Figure 3.1. Anti-XLR staining in squashed XY spermatogenic cells.

a) XY cells stained for SCP3, showing leptotene/zygotene (bracket A), pachytene (bracket B), diplotene (arrowheads) and MI (short arrow) nuclei.

b) Same nuclei stained with anti-XLR. Anti-XLR stains the whole nucleus during early prophase, the sex body during pachytene, both during diplotene, and the centromeric heterochromatin at MI.

c) Superimposition of a) and b), with colocalisation in yellow.

d) Same nuclei stained with DAPI. Anti-XLR does not stain Sertoli cells (asterisks) or spermatids (long arrows).

e) XY cells stained for SCP3 with anti-XLR replaced by MOPC21.

f) XY cells stained for SCP3 with anti-XLR replaced with PBS.

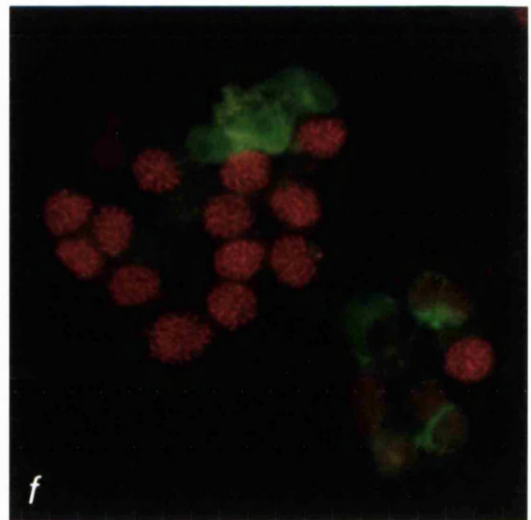
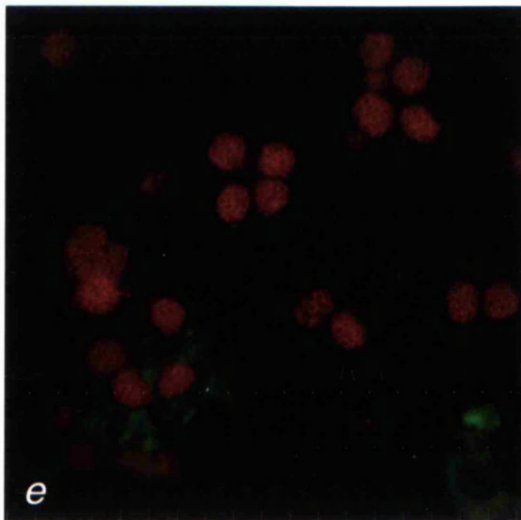
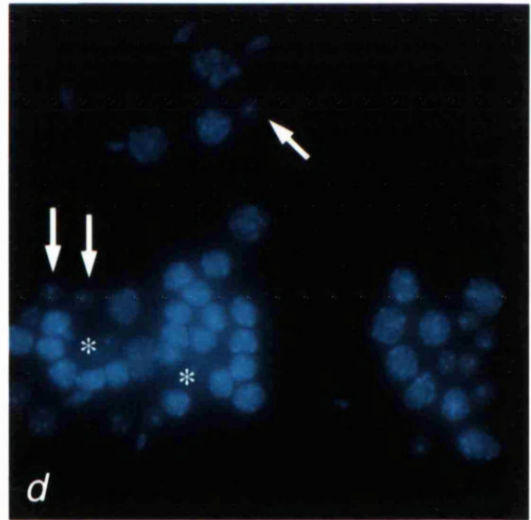
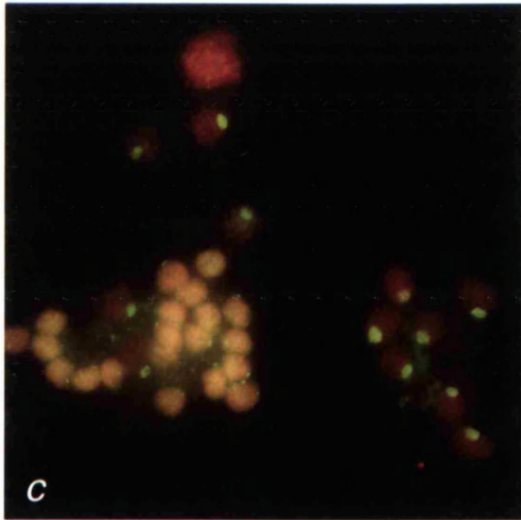
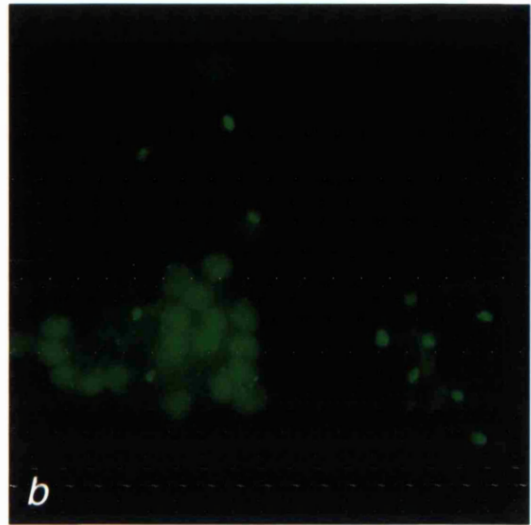
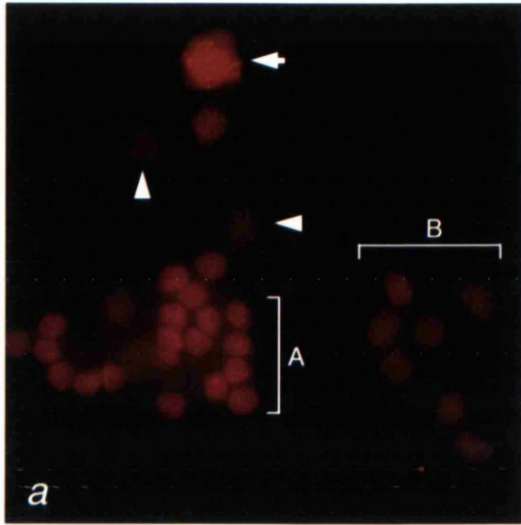


Figure 3.2. Anti-XLR staining in squashed XY spermatogenic cells cont. Anti-SCP1 = red, anti-XLR = green.

- a) Leptotene nucleus stained with anti-SCP1. Synapsis has not yet begun so there is no SCP1 staining.
- b) Same nucleus stained with anti-XLR, which forms multiple punctate dots.
- c) Early zygotene nuclei stained with anti-SCP1. Synapsis has just commenced.
- d) Same nuclei stained with anti-XLR. Comments as in b)
- e) Late zygotene nuclei stained with anti-SCP1.
- f) Same nuclei stained with anti-XLR. A more intensely-staining structure is seen (short arrow). Since an SCP1 signal is absent at this position in e), this is likely to be the X chromosome prior to/in the process of condensation.
- g) Early pachytene nucleus. PAR synapsis (arrowhead) is extensive, indicating early pachytene.
- h) Same nucleus stained with anti-XLR. The sex body is apparent and the whole nuclear staining is reducing.



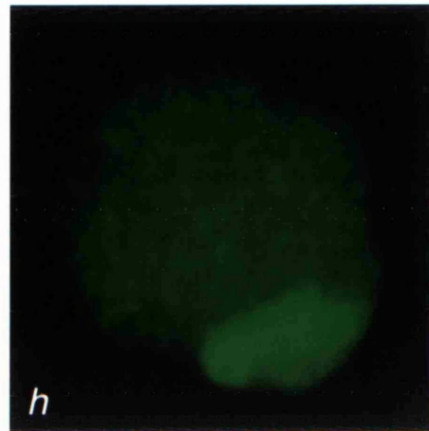
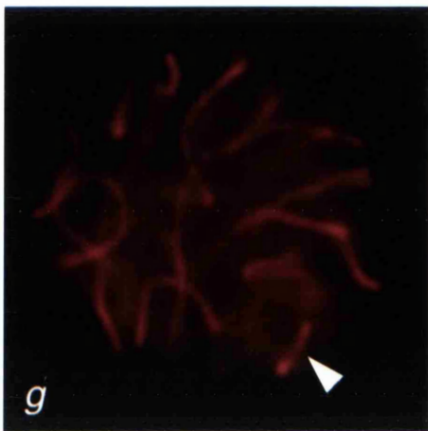
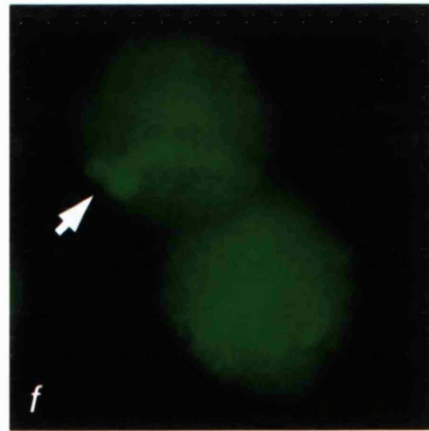
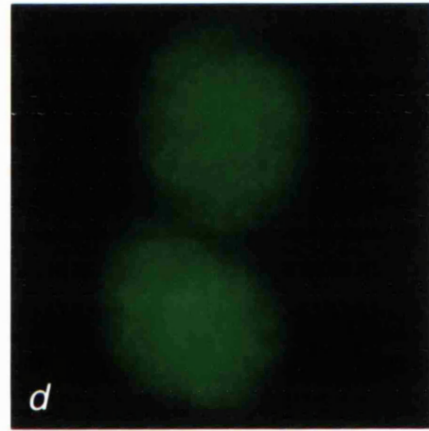
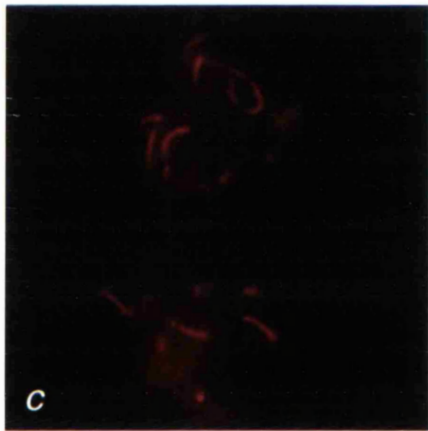
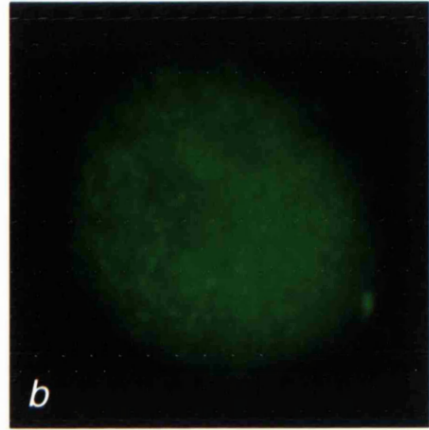
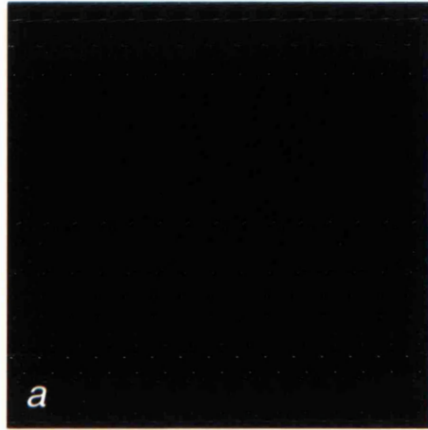


Figure 3.3. Anti-XLR staining in squashed XY spermatogenic cells cont. Anti-SCP1 = red, anti-XLR = green.

- a) Early diplotene nucleus stained with anti-SCP1. Interstitial desynapsis has begun, leaving terminal SCP1 signals (short arrows).
- b) Same nucleus stained with anti-XLR. Only the sex body is stained.
- c) Mid-late diplotene nucleus stained with anti-SCP1. Only a few stretches of SC remain.
- d) Same nucleus stained with anti-XLR. The sex body is beginning to assume a central position and the whole nuclear stain has returned.
- e) MI nucleus stained with DAPI. Asterisks indicate centromeres. SCP1 is absent at this point.
- f) Same nucleus stained with anti-XLR, which shows preferential enrichment at the centromeres.

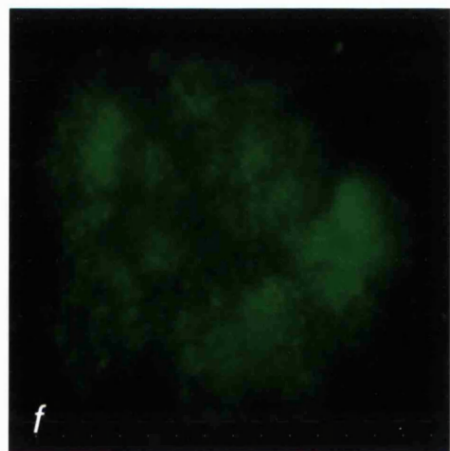
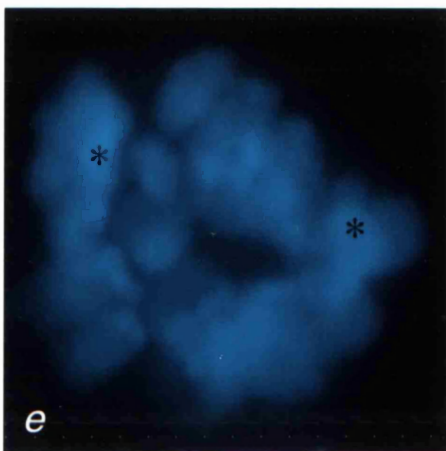
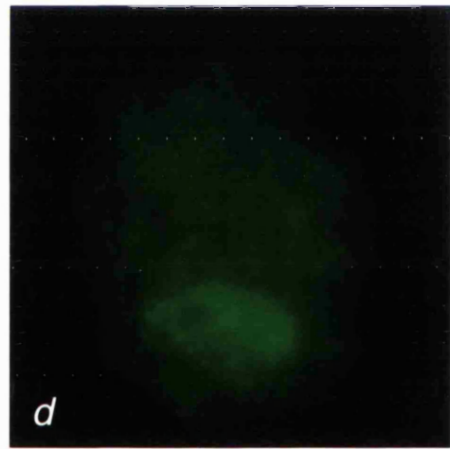
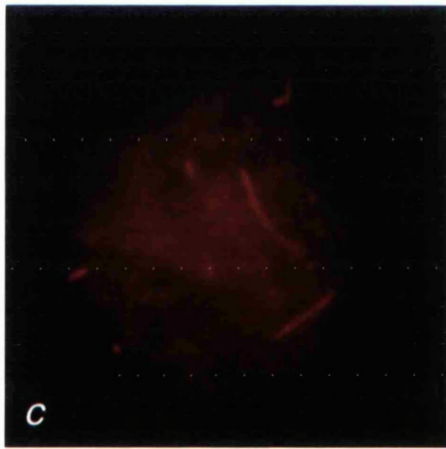
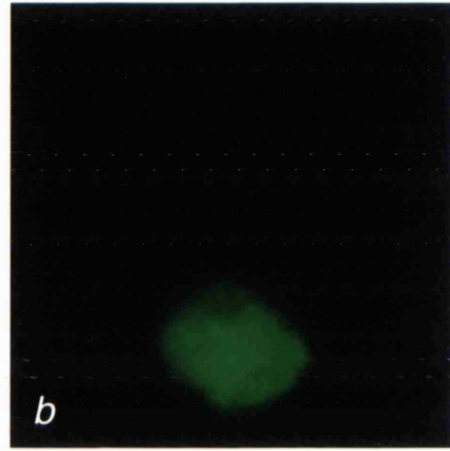
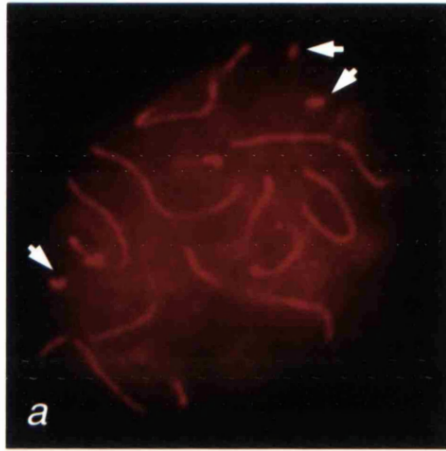


Figure 3.4. Anti-XLR staining in squashed XX and XY<sup>Tdym1</sup> oogenic cells. Anti-SCP3 = red, anti-XLR = green.

a) XX cells stained with anti-SCP3, showing early pachytene (arrowhead), mid pachytene (short arrow) and late pachytene (long arrow) nuclei.

b) Same cells stained with anti-XLR. The staining is abundant at early pachytene, decreases in mid pachytene, and is absent at late pachytene.

c) Superimposition of a) and b).

d) Same cells stained with DAPI. Follicular cells (asterisks) are anti-XLR negative.

e) XX cells stained with anti-SCP3, showing leptotene (long arrows) and zygotene (arrowhead) nuclei.

f) Same cells stained with anti-XLR. The staining increases during the leptotene-zygotene transition.

g) Same cells as c), shown for comparison with h).

h) XY<sup>Tdym1</sup> cells stained with anti-SCP3 and anti-XLR. In addition to the whole nuclear staining, XY<sup>Tdym1</sup> cells have an additional bright, anti-XLR signal (short arrows).

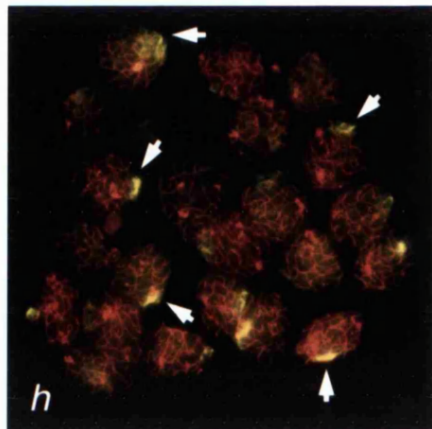
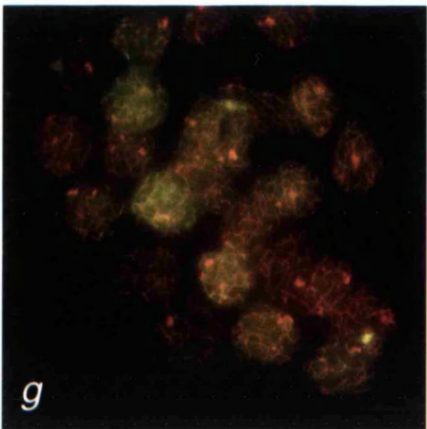
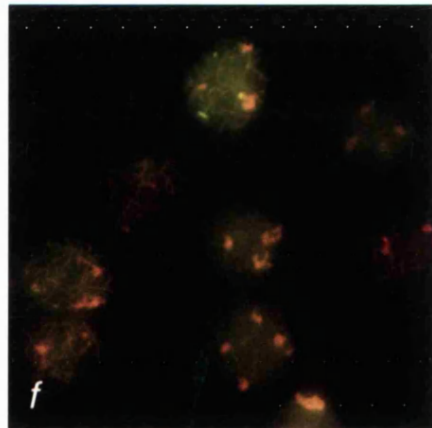
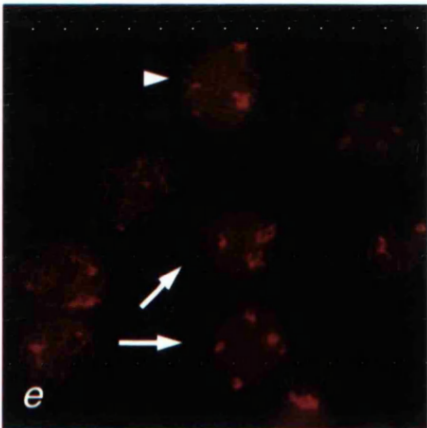
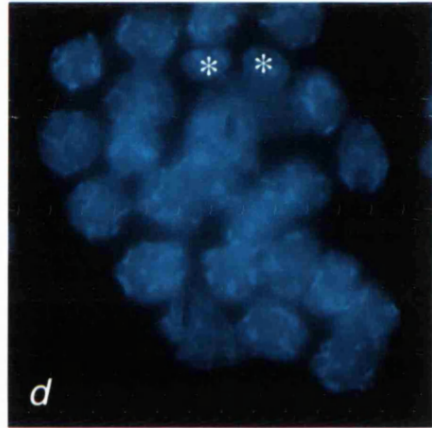
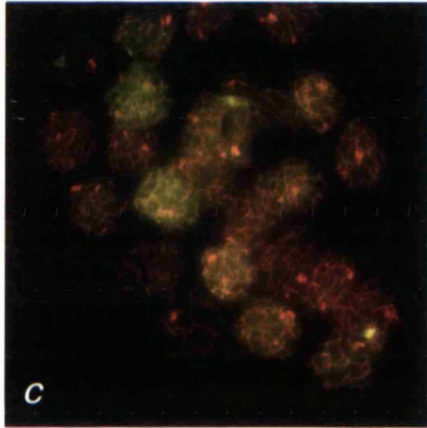
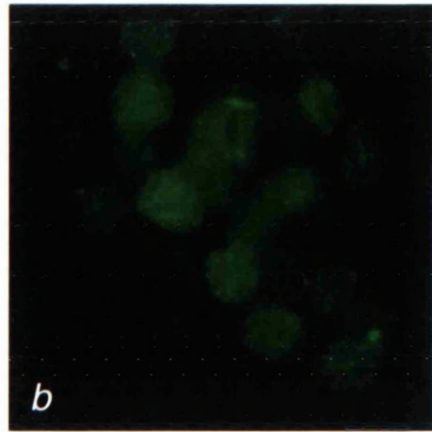
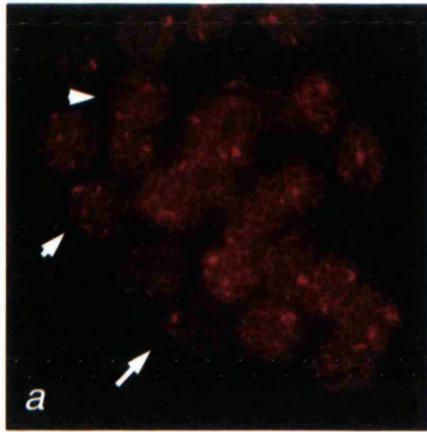


Figure 3.5. Anti-XLR staining in squashed  $XY^{Tdyml}$  oogenic cells cont. Anti-SCP3 = red, anti-XLR = green. Arrowhead = Y chromosome, short arrow = X chromosome. Nucleoli are preserved in squash preparations and appear SCP3-positive.

- a)  $XY^{Tdyml}$  early pachytene nucleus.
- b) Same nucleus stained with anti-XLR, which coats the asynapsed X-axis and surrounding chromatin.
- c)  $XY^{Tdyml}$  early pachytene nucleus with X-Y synapsis.
- d) Same nucleus stained with anti-XLR, which coats the asynapsed X-axis but appears reduced or absent on that of the Y chromosome.
- e)  $XY^{Tdyml}$  early pachytene nucleus.
- f) Same nucleus stained with anti-XLR. Comments as in b).
- g)  $XY^{Tdyml}$  cells with anti-XLR replaced by MOPC21.
- h)  $XY^{Tdyml}$  cells with anti-XLR replaced by PBS.

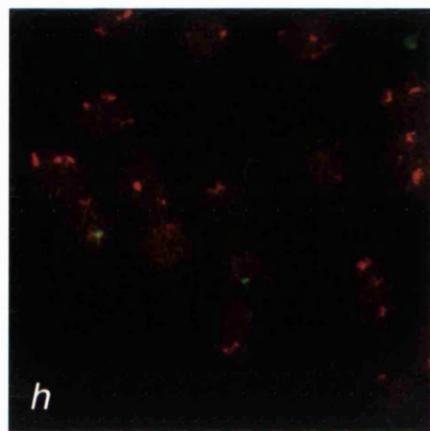
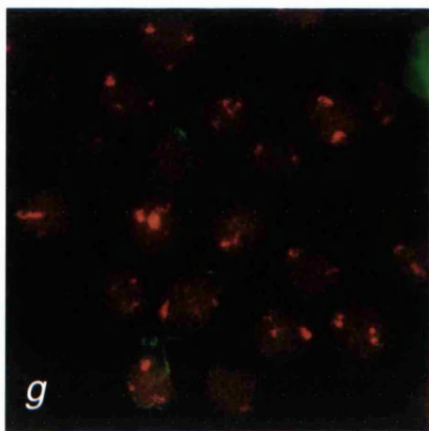
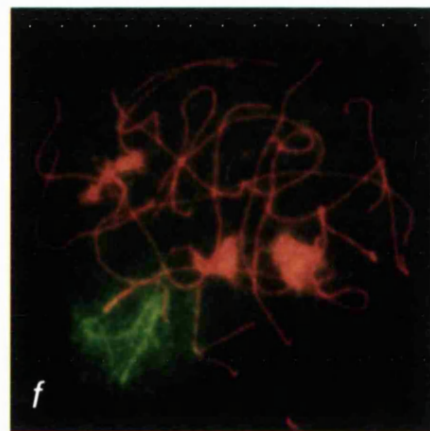
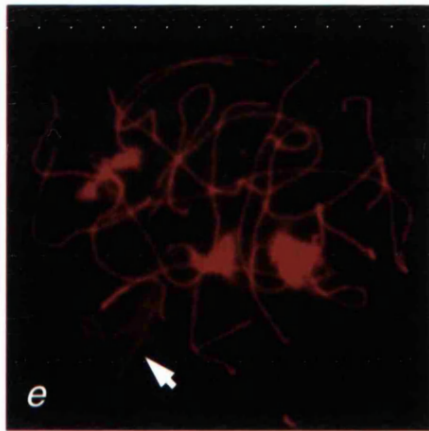
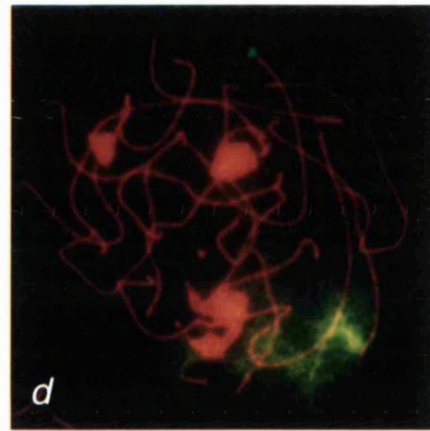
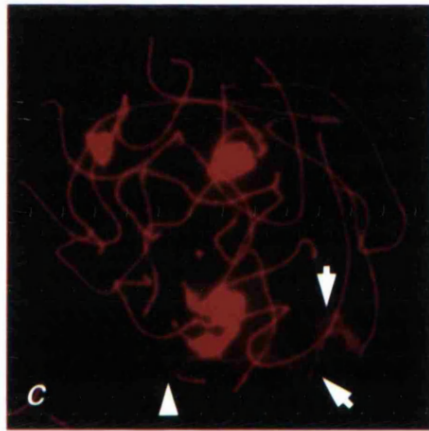
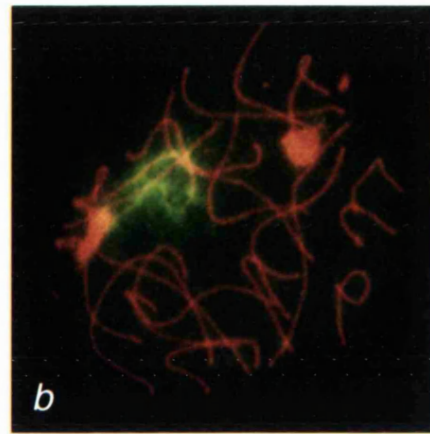
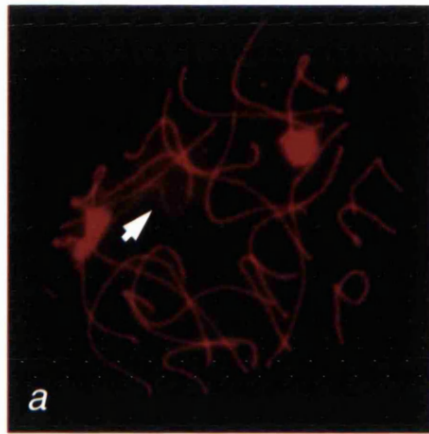


Figure 3.6. Anti-XLR staining in spread T(2;5)72H oogenic cells. Anti-SCP3 = red, anti-XLR = green, short arrows = asynapsed axes.

a) T(2;5)72H mid pachytene nucleus.

b) Same nucleus stained with anti-XLR, which coats the asynapsed axes and surrounding chromatin.

c) T(2;5)72H mid pachytene nucleus.

d) Same nucleus stained with anti-XLR. Comments as in b)

e) T(2;5)72H mid pachytene nucleus.

f) Same nucleus stained with anti-XLR. Comments as in b).



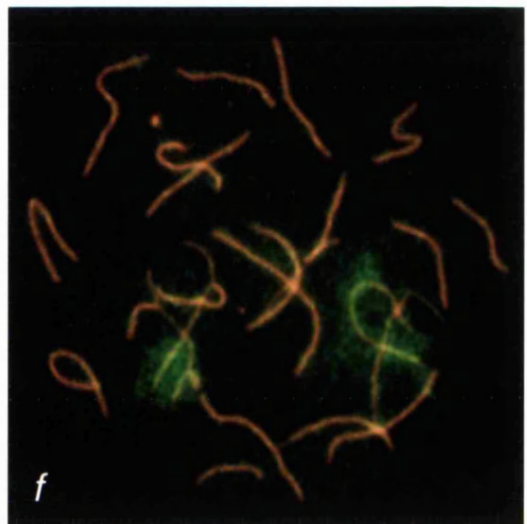
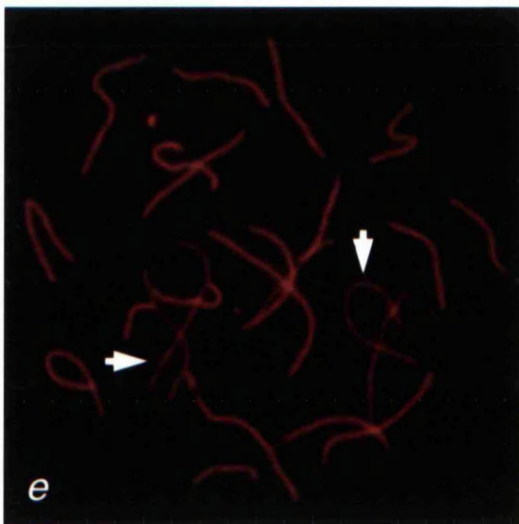
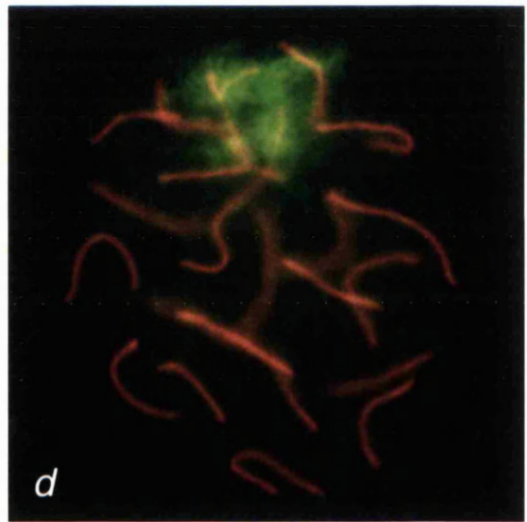
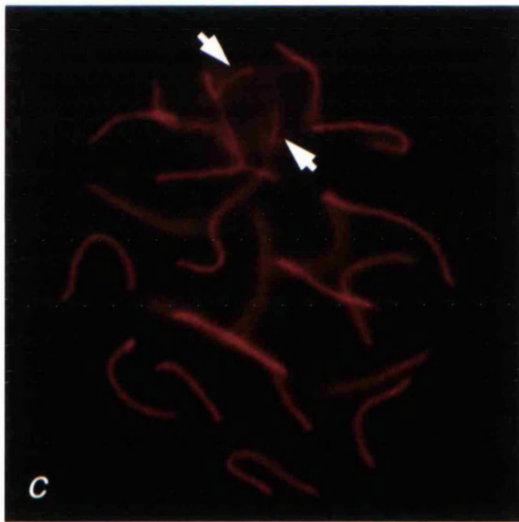
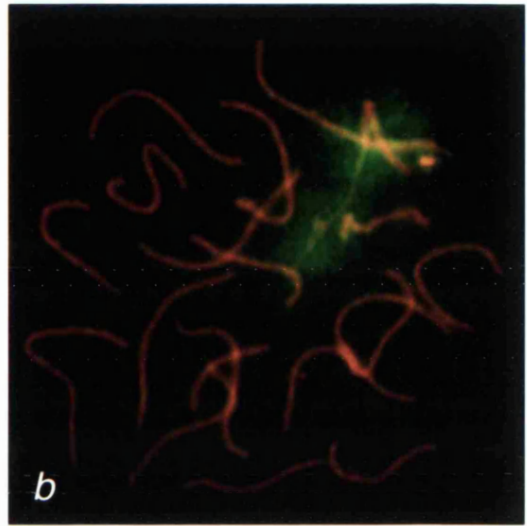
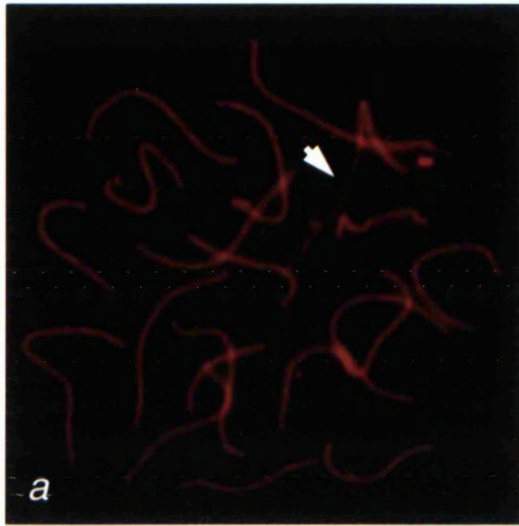


Figure 3.7. Comparison of *Xlr* (denoted pT1) and *Xmr* (denoted pM1) cDNA sequences reproduced from Calenda *et al.* (1994).

Thin line = untranslated regions, thick bar = coding regions, black regions = homologous segments between *Xlr* and *Xmr*, hatched region = *Xmr*-specific sequence, white regions = *Xlr*-specific sequence,  $\Delta 1$ ,  $\Delta 2$  and  $\Delta 3$  = segments of *Xlr* deleted in *Xmr*. Arrows indicate positions at which primers A-D reside.

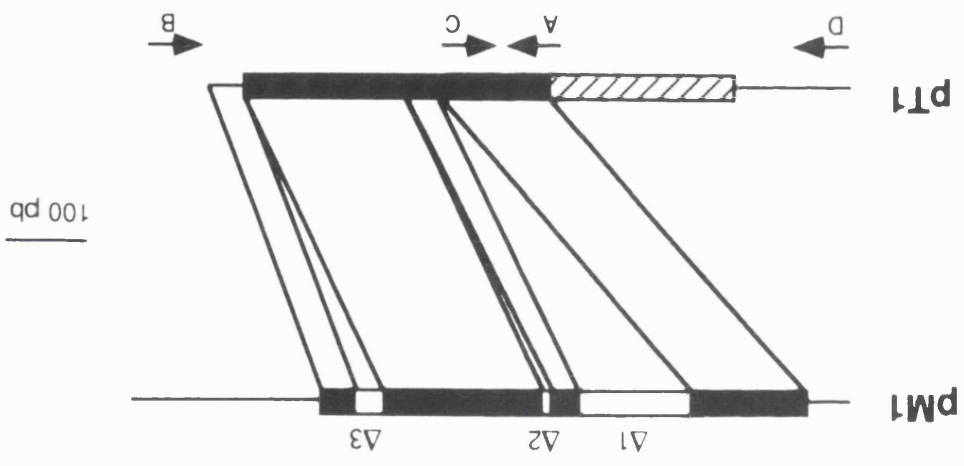


Figure 3.8. RTPCR analysis of *Xmr* and *Xlr* expression in testes and ovaries.

a) In adult XY, XXSxr<sup>a</sup> and XXSxr<sup>b</sup> testes and 18.5dpc XX and XY<sup>Tdym1</sup> (denoted 'XY').

White asterisks denote 500bp.

b) During XY male gonadal development. Arrows indicate 500bp.

Product sizes:

B + D: *Xmr* = 812bp

D + C: *Xmr* = 427bp

A + B: *Xmr* = 420bp, *Xlr* = 630bp

*Hprt* = 352bp

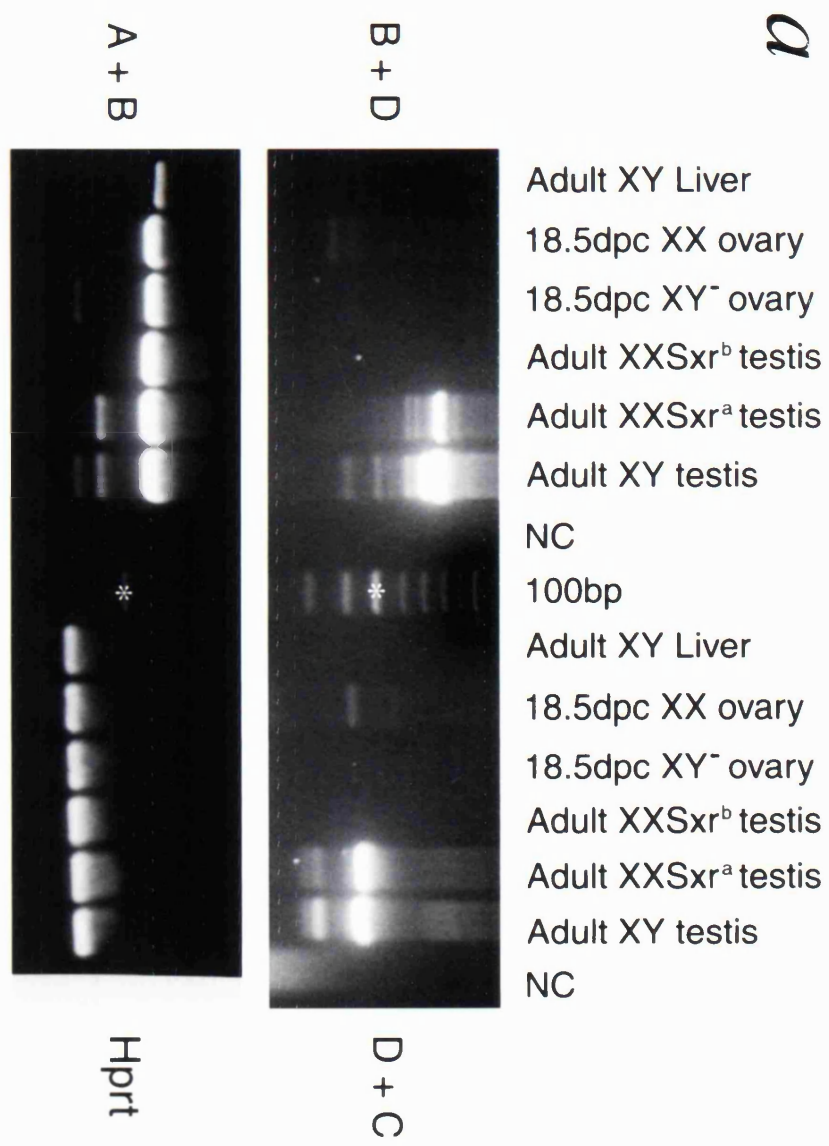
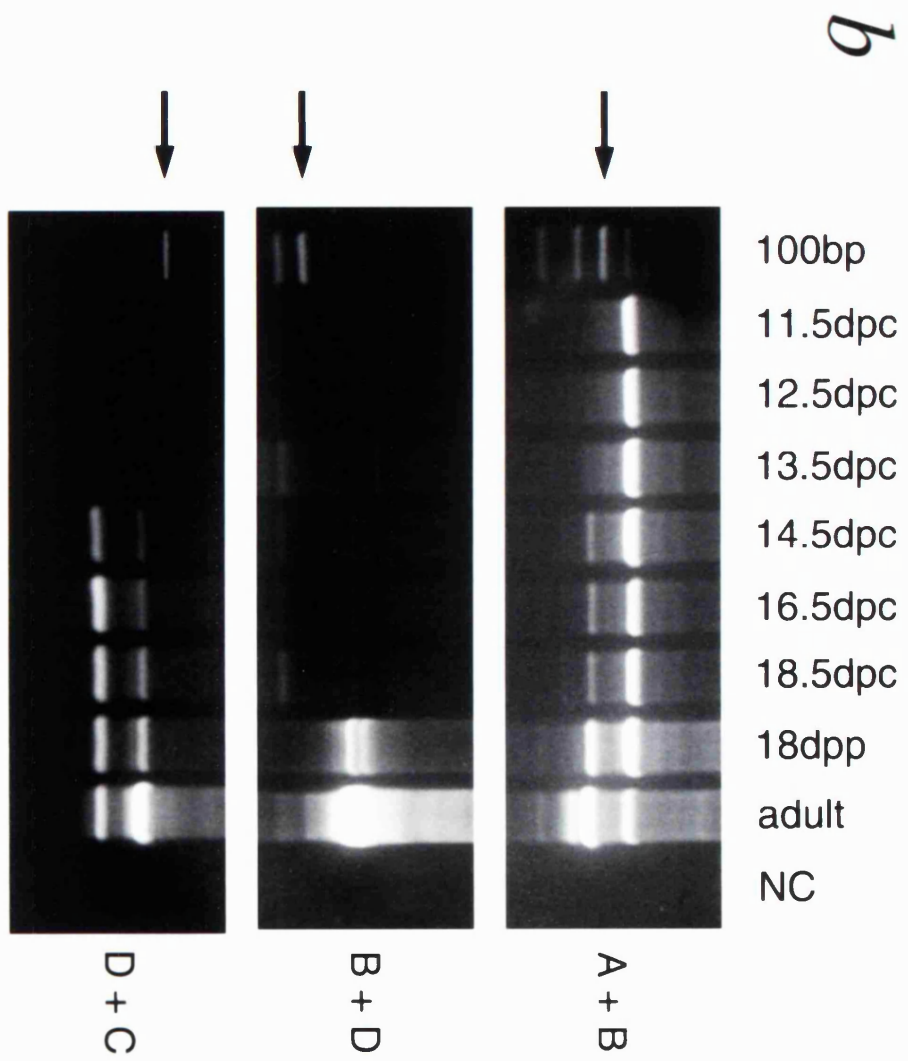


Figure 3.9. Southern analysis of *Xmr* carried out by S. Mahadevaiah. Genomic DNA from mice with varying X and/or Y doses was probed with the PCR product from RTPCR 'D + C' (see section 3.2.8) and with the autosomal control probe HEX (courtesy of P.Thomas, NIMR).

Genotype	X-dose	Y-dose	PAR-dose
XX	2	0	2
XY	1	1	2
XY*	1*	1	2**
XY* <sup>X</sup>	1*	0	2
X <sup>Y*</sup> O	1	1	2**

\* Both the Y\* and the Y\*<sup>X</sup> chromosomes possess a small amount of X-derived material (Burgoyne *et al.*, 1998).

\*\* Both the Y\* and the X<sup>Y\*</sup>O chromosomes have a compound PAR due to a PAR-PAR fusion with deletion of some distal PAR sequences including *Sts* gene (Burgoyne *et al.*, 1998).

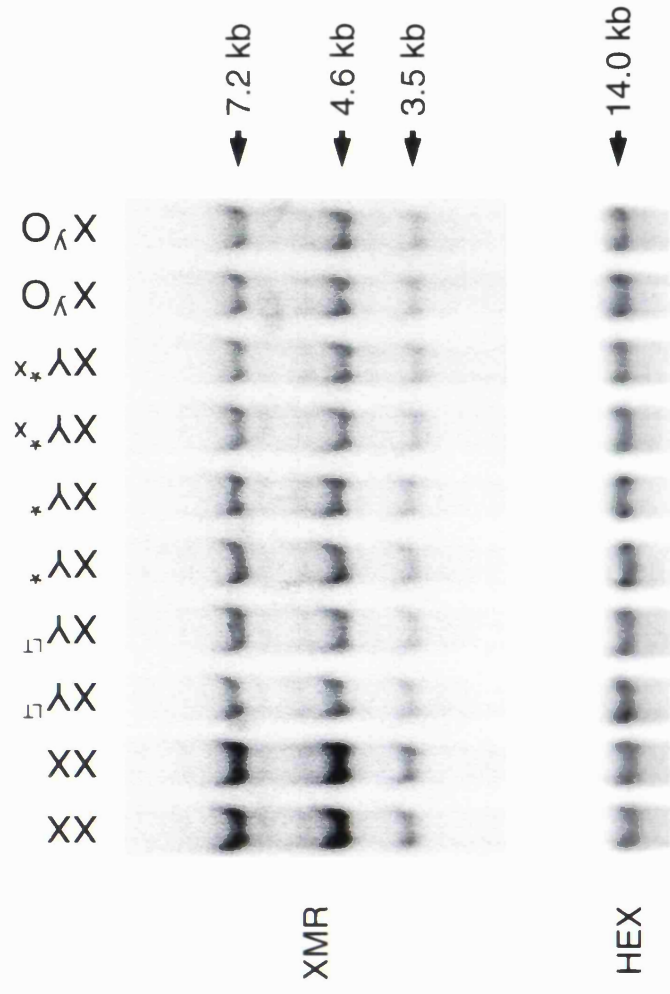


Figure 3.10. Anti-XY77 staining in XY spermatogenic and XY<sup>Tdym1</sup> oogenic cells. Anti-SCP3 = red, anti-XY77, aka mAb 4c6 = green.

- a) XY cells stained with DAPI, showing Sertoli cells (upper left box), spermatids (short arrows) and spermatocytes (others).
- b) Same cells stained with anti-SCP3 and mAb 4c6. MAb 4c6 staining is restricted to late pachytene and diplotene spermatocytes and Sertoli cells.
- c) XY<sup>Tdym1</sup> cells stained with DAPI, showing follicular cells (asterisks) and oocytes (others).
- d) Same cells stained with anti-SCP3 and mAb 4c6. MAb 4c6 staining is absent in all cell types.



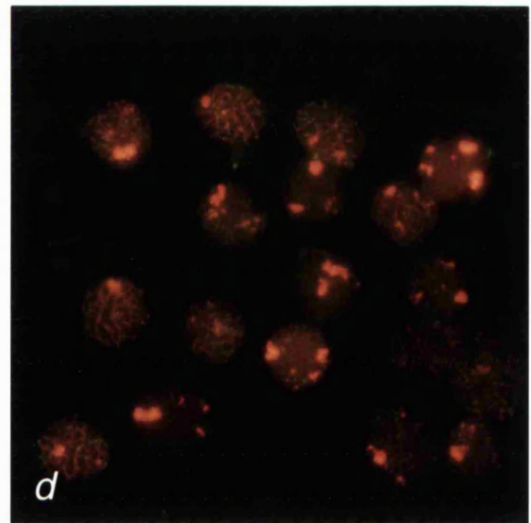
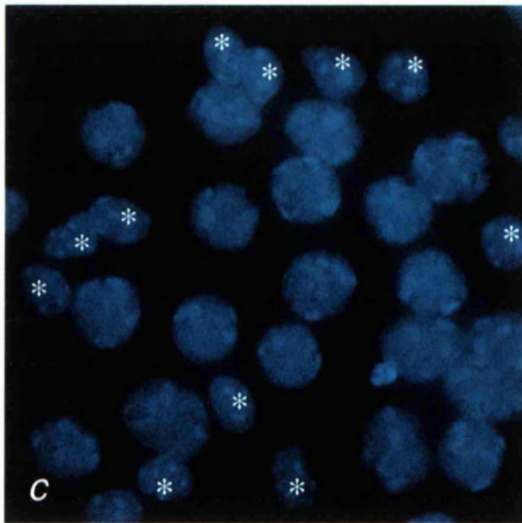
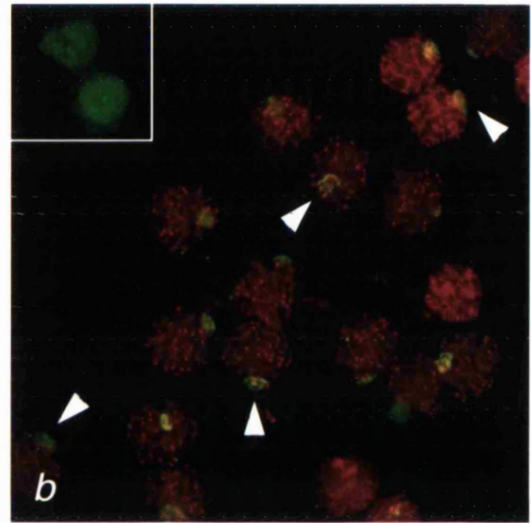
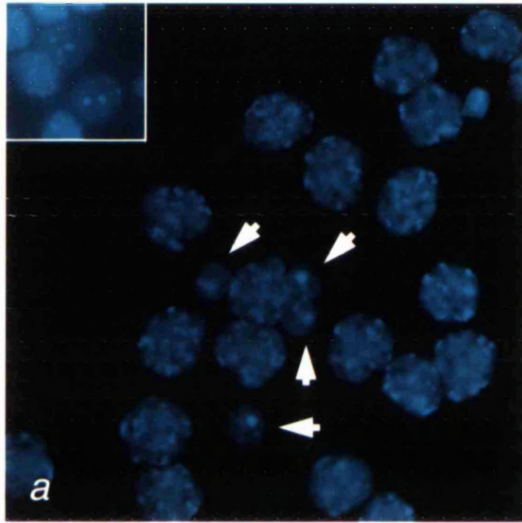


Table 3.1. Appearance of anti-XLR staining of asynapsed chromatin during meiosis I in different female genotypes

STAGE	NUMBER OF CELLS WITH ANTI-XLR STAINING OF ASYNAPSED AXES		
	XY <sup>Tdym1</sup> (n=2)	XX (n=2)	T(2;5)72H (n=1)
LEPTOTENE	0/1	0/7	-
ZYGOTENE	0/7	0/17	0/1
EARLY PACH	11/37 (30%)	0/12	3/7 (43%)
MID PACH	5/21 (24%)	0/11	12/22 (55%)
LATE PACH	14/20 (70%)	2/12 (17%)	5/7 (71%)
DILOTENE	-	0/1	0/1
UNCLASSIFIED	5	2	-
TOTAL CELLS	91	62	38

### 3.4 DISCUSSION

This study sought to check the credentials of two sex-body located proteins, XMR and XY77, that have been postulated to play a role in MSCI. *Xmr* expression was analysed using an anti-XLR antibody that was previously reported to recognise XMR in the testis. In addition to the sex body staining in pachytene spermatocytes, this antibody was known to produce whole nuclear staining in leptotene and zygotene spermatocytes (Calenda *et al.*, 1994). In XX and XY<sup>Tdym1</sup> oocytes an essentially identical pattern of whole nuclear staining was observed. In addition, anti-XLR labelled asynapsed chromatin in XY<sup>Tdym1</sup> and T(2;5)72H females. These results suggest that, as with ASY, the protein detected by anti-XLR binds asynapsed axes in a sex- and MSCI-independent manner, and that this accounts for the location of the protein to the sex body.

Although these immunocytochemical results suggested that XMR was present during female meiosis, RTPCR analysis together with sequence analysis, showed that *Xlr* but not *Xmr* was present. Furthermore, because *Xlr* and *Xmr* transcripts were identified in whole testis RNA (Calenda *et al* reported only *Xmr* as being present), it seemed possible that it was XLR that was being recognised in both cases. Counter to this was the finding that transcription of *Xmr* (but not *Xlr*) was germ cell-specific, which is in agreement with the germ cell specificity of the antibody staining.

One possible resolution to this problem would be if *Xmr* was an autosomal back-up for *Xlr* (which is X-linked and therefore likely to be subject to MSCI), just as *Pgk2* is an autosomal back-up for *Pgk1*. Contrary to this, Southern analysis showed that *Xmr* was X-linked. However, since there are so many *Xlr*-family members on the X chromosome, it is

conceivable that one (*Xmr*) may have integrated into a site that for some reason escapes MSCI (just as some X-linked genes escape X-inactivation in females). Clearly this is a complicated issue that might be partially resolved by studying *Xmr/Xlr* expression in purified pachytene populations and by generating an XMR-specific antiserum.

The observation that XMR/XLR accumulates on asynapsed chromatin independent of MSCI implies that its appearance in the sex body is functionally unrelated to the marked condensation of the sex chromosomes. Unlike ASY, XMR/XLR is detectable during leptotene and zygotene prior to and during synapsis, and is therefore not likely to be playing a role primarily related to asynapsis. The disappearance of XMR/XLR from normally synapsing chromatin coincides temporally with its accumulation on asynapsed axes, suggesting that XMR/XLR may be relocalising at this point.

One possible role for XMR/XLR derives from the observation that members of the *Xlr* multigene family are expressed at stages of germ cell and lymphoid differentiation that are associated with DNA rearrangements. In particular, their expression coincides temporally with TCR in immature thymocytes (Escalier *et al.*, 1999) and the initiation of homologous recombination in leptotene/zygotene meiocytes (Calenda *et al.*, 1994), both of which are associated with the formation and processing of DSBs. Rogakou *et al.* (1999) have demonstrated that somatic cells from a wide variety of organisms respond to agents that induce DSBs with the phosphorylation of histone H2AX. Antibody staining shows that this phosphorylated form ( $\gamma$ -H2AX) colocalises exactly with XMR/XLR on the sex chromosomes, and at selected sites with XMR/XLR on the autosomes during the transition from zygotene to diplotene (Mahadevaiah, Turner and Burgoyne, work in progress). The

finding of phosphorylated H2AX in the sex body is of particular interest because it suggests that MSCI does not prevent the initiation of DSBs in the X and Y chromosomes, as suggested by McKee and Handel (1993). Together with the sequence similarity of *Xmr* with *mer2*, these data support a recombination-related role for XMR/XLR. However, the present finding that XMR/XLR relocates to the whole nucleus at diplotene and then preferentially to the centromeric heterochromatin at metaphase I means that this is unlikely to be the only role for this protein(s).

In agreement with published results, XY77 was present in the sex body chromatin of late pachytene and diplotene spermatocytes and an additional, punctate signal (thought to represent a different antigen, see introduction) was evident in Sertoli cell nuclei. Unlike ASY and XLR, XY77 was not detected in any cell type in XX or XY<sup>Tdym1</sup> oocytes. XY77 is therefore totally sex body-specific and may serve an MSCI-specific role. One of the proposed roles of MSCI is in preventing the non-PAR X and Y axes that remain asynapsed during normal male meiosis from triggering the synapsis checkpoint (Jablonka and Lamb, 1988). Indeed, the presence of XY77 represents the first biochemical distinction between asynapsed axes that trigger the synapsis checkpoint and those that don't. The sex body undergoes a dramatic increase in condensation during late pachytene and diplotene and XY77 may be involved in this process.

In conclusion, as with ASY, the presence of XLR/XMR in the sex body appears to be asynapsis-related rather than MSCI-related. XY77, in contrast to ASY and XMR/XLR, is MSCI-specific, and as such is suitable for the studies we have proposed to test the *quasi-cis*

model of sex body formation (Ayoub *et al.*, 1997) with particular reference to males with additional and/or asynapsed Y chromosomes.

## CHAPTER 4

### AN INVESTIGATION INTO THE QUASI-CIS MODEL OF MSCI



#### 4.1 INTRODUCTION

Asynapsis of the X and Y PARs in mice results in meiotic arrest and apoptosis (Odorisio *et al.*, 1998); this has been taken to indicate the existence of a pachytene checkpoint that may have a long evolutionary pedigree (Roeder, 1997). It has also been proposed that excess Y gene dosage leads to meiotic impairment. The most compelling evidence comes from Hunt and Eicher (1991) who found that although XYY and XYY<sup>\*X</sup> males have similar trivalent frequencies at MI (which they took to indicate similar levels of 'full' trivalent PAR synapsis at pachytene), XYY males suffer severe meiotic impairment and consequent sterility whereas XYY<sup>\*X</sup> males are regularly fertile. Since these mice differ by one dose of Y-specific chromatin, it was concluded that the meiotic failure in XYY mice must, in part, be due to an excess dosage of Y-linked genes (Hunt and Eicher, 1991). However, Burgoyne and Mahadevaiah (1993) pointed out that equivalent MI trivalent frequencies may not be a reliable indicator of equivalent trivalent synapsis at pachytene. They therefore suggested that the difference in fertility between XYY and XYY<sup>\*X</sup> mice might be associated with different levels of trivalent synapsis. Recently Rodriguez and Burgoyne (2000) have shown that XYY<sup>\*X</sup> males do indeed have much higher levels of trivalent synapsis (58%) than XYY males (29%).

Although a low level of trivalent PAR-synapsis is sufficient to explain the severe meiotic impairment and consequent infertility of XYY males, studies of males with four sex chromosomes suggest that this is not the whole story. In XYY<sup>-Y<sup>\*X</sup></sup> and XYY<sup>\*X</sup>Y<sup>\*X</sup> mice, full PAR synapsis can be achieved by the formation of either a quadrivalent, or two bivalents. SC analysis has demonstrated that full PAR synapsis occurs in about one half of pachytene cells from these mice, with most being of the 'bivalent plus bivalent' configuration

(Rodriguez, T.A; PhD thesis, 1997). Despite this, both  $XYY\cdot Y^{*X}$  and  $XYY^{*X}Y^{*X}$  mice have an even more severe meiotic failure than  $XYY$  mice. One possible explanation for this finding invokes the *quasi-cis* hypothesis of Ayoub *et al.* (1997). This hypothesis states that MSCI is mediated by *Xist* transcripts and that inactivation of the Y chromosome proceeds through a '*quasi-cis*' spreading of *Xist* transcripts from the X chromosome to the Y chromosome via the synapsed PARs. Rodriguez and Burgoyne (pers.comm.) reasoned that the *quasi-cis* spreading mechanism would lead to a failure of Y chromosome inactivation if it was not synapsed with the X chromosome. They surmised that it was this failure of Y chromosomal MSCI in the  $YY$  and  $YY^{*X}$  bivalents in  $XYYY^{*X}$  and  $XYY^{*X}Y^{*X}$  mice that was further disrupting meiosis.

In the present chapter experiments are described that were undertaken to test: 1) the proposal that *Xist* mediates MSCI and 2) that there is defective Y chromosomal MSCI in situations where a Y chromosome is not synapsed with the X chromosome.

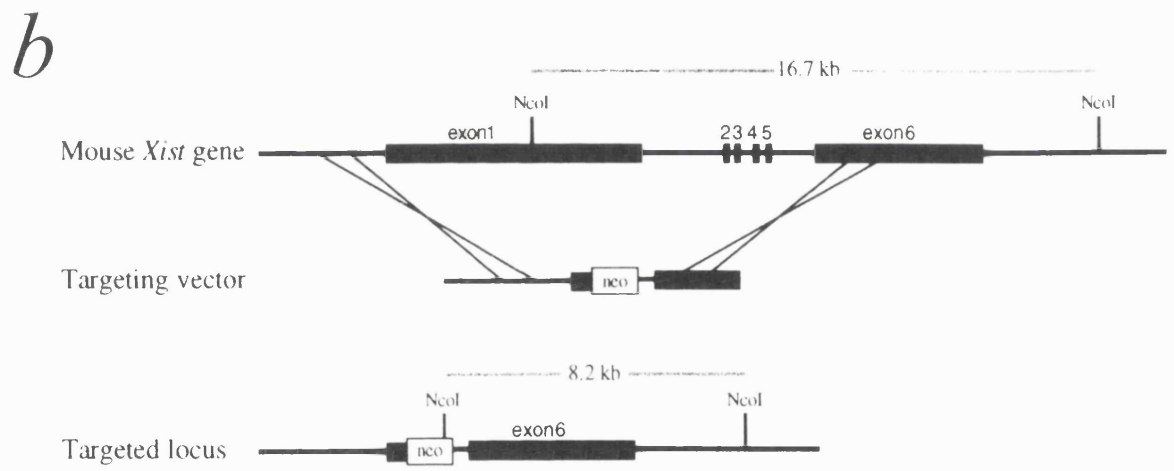
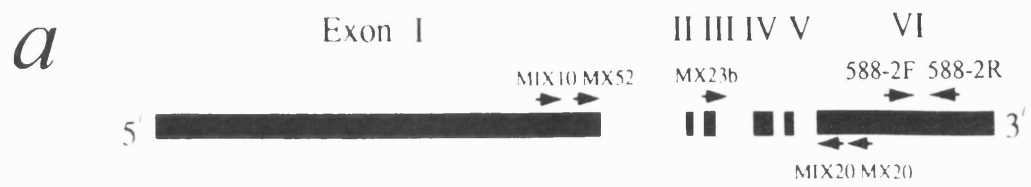
In the first experiment, the MSCI status of *Xist*-disrupted spermatocytes was assessed. The *Xist*-disruption analysed was that created by Marahrens *et al.* (1997), in which most of exon 1 and all of exons 2-5 are deleted, while leaving both exon 6 and the *Xist* promoter intact (Figure 4.1). The disruption abolishes somatic X-inactivation in females but does not affect the fertility of males, implying either that MSCI is *Xist*-independent or that it is *Xist*-dependent but is not essential for spermatogenesis (Marahrens *et al.*, 1997).

In the second experiment sex body formation and Y chromosomal MSCI were analysed in  $XYY^{*X}$  and  $XYY$  males. In  $XYY$  males many pachytene cells have univalent Y

chromosomes while  $XY Y^{*X}$  males are more moderately affected (Rodriguez and Burgoyne, 2000). Mice with four sex chromosomes were not available at the time of this study, but the 'quasi-cis spreading model' predicts that single Y chromosomes that are not synapsed with the X chromosome will also fail to undergo MSCI. In order to assay for a failure of Y chromosomal MSCI, the expression of a multiple copy Y chromosomal gene *Rbm* (Laval *et al.*, 1995; Mahadevaiah *et al.*, 1998) was monitored using an RBM specific antibody; in normal males RBM expression is not normally seen beyond the zygotene stage. In  $XY Y$  males, it is possible that RBM might be detected beyond early prophase because of the increased time taken to degrade the RBM produced in the presence of two Y chromosomes. In order to counter this criticism, the  $XY Y$  males used had one Y chromosome carrying a deletion (the ' $Y^{d1}$ ' deletion) removing the majority of *Rbm* copies; this deletion abolishes the expression of RBM in spermatogonia and early prophase spermatocytes (Mahadevaiah *et al.*, 1998, D.Elliott, personal communication).

Figure 4.1.

- a) *Xist* gene structure (reproduced from Kay *et al.*, 1993). Primer pair positions are indicated.
- b) *Xist* disruption (reproduced from Marahrens *et al.*, 1997). Approximately 15kb of genomic sequence have been replaced with a *neo* expression cassette.



## 4.2 MATERIALS AND METHODS

### 4.2.1 Mice

All males were processed at between 2 and 3 months of age.

#### *Xist-disrupted males*

The *Xist*-disruption was that described by Marahrens *et al.* (1997). *Xist*-disrupted males were provided courtesy of Rudolf Jaenisch (Whitehead Institute for Biomedical Research).

#### *XY, XYY<sup>d1</sup> and XYY<sup>\*X</sup> males*

All three genotypes were generated from a cross between MF1 XY<sup>d1</sup> females and MF1 X<sup>Paf</sup>YY<sup>\*X</sup> males. The *Paf* mutation (Lane and Davisson, 1990) is associated with extensive hair loss in hemizygous males (XY) and females (XO) and patchy hair loss in heterozygous females. XY<sup>d1</sup> females produce 4 genotypes of gametes, namely, X, Y<sup>d1</sup>, XY<sup>d1</sup> and O. X<sup>Paf</sup>YY<sup>\*X</sup> males produce 6 genotypes of sperm, namely, X<sup>Paf</sup>, Y, Y<sup>\*X</sup>, X<sup>Paf</sup>Y<sup>\*X</sup>, X<sup>Paf</sup>Y and YY<sup>\*X</sup> (Hunt and Eicher, 1991). The male offspring generated are shown below:

		SPERM		
		Y	X <sup>Paf</sup> Y	YY <sup>*X</sup>
		MALE OFFSPRING		
E	X	XY	X <sup>Paf</sup> XY	XYY <sup>*X</sup>
G	Y <sup>d1</sup>	-	X <sup>Paf</sup> YY <sup>d1</sup>	-
G	XY <sup>d1</sup>	XYY <sup>d1</sup>	X <sup>Paf</sup> XYY <sup>d1</sup>	XYY <sup>d1</sup> Y <sup>*X</sup>
S	O	-	X <sup>Paf</sup> Y	-

All hemizygous and heterozygous *Paf* males were killed. Due to the higher frequency of Y over YY<sup>\*X</sup> gametes, no XYY<sup>d1</sup>Y<sup>\*X</sup> males were generated during this study. XY, XYY<sup>d1</sup> and XYY<sup>\*X</sup> males were distinguished by karyotyping of bone marrow cells using standard procedures (see Appendix 1.1).

#### 4.2.2 Squash procedure

Squashed spermatocytes were prepared as described in Appendix 1.6.

#### 4.2.3 Surface spreading procedure

Surface spread spermatocytes were prepared as described in Appendix 1.7.

#### 4.2.4 Immunostaining

Spermatocytes were immunostained as described in Appendix 1.8. Where detection of SCP3 and RNA POLII was required (both primaries being raised in rabbit), primaries were used sequentially, with anti-SCP3 being detected with goat anti-rabbit Cy2 (Amersham). The RBM antiserum was different to that used by Mahadevaiah *et al.* (1998), which was no longer available. It was raised against amino acids 113-232 of mouse RBM, fused to GST. The antisera was affinity purified against the same region fused to thioredoxin (D.Elliott, pers.comm.) This new antiserum gave the same staining pattern as the original antiserum except that it did not stain spermatids (D. Elliott, pers. comm.). As a control for non-specific RBM staining, the antiserum was used firstly to immunostain spermatogenic cells from XY<sup>d1</sup> males, which are depleted for most copies of the *Rbm* family (Mahadevaiah *et al.*, 1998) and secondly after preabsorbing with recombinant RBM protein.

#### 4.2.5 Examination

Immunostained meiocytes were examined as described in Appendix 1.9.

#### 4.2.6 Quantitation of XLR and RBM levels

Levels of XLR and RBM staining were quantitated using the Deltavision Examine Data program. This program measures the emission intensity for each fluorophore at every pixel within a selected image (an 11 x 25 pixel window was chosen) and presents the result as the mean of the individual pixel values. This procedure was used to obtain relative intensity values for nuclei at various meiotic substages; in the case of the anti-XLR estimates, the 11 x 25 pixel window was placed to avoid the sex body compartment.

#### 4.2.7 Total RNA extraction from testes

Total RNA was extracted as described in Appendix 1.3.

#### 4.2.8 DNase treatment and reverse transcription of total RNA

DNase treatment and reverse transcription of total RNA was carried out as described in Appendix 1.4.

#### 4.2.9 PCR procedure

RT PCRs were carried out as described in Appendix 1.5. RTPCR primers for *Pgk2*, *Pdhal* and *Hprt* are described in section 2.2.9. *Xist* RTPCR primers are:

588-2 (588-2F 5' ATC TAA GAC AAA ATA CAT CAT TCC G 3'. 588-2R 5' CTT GGA CTT AGC TCA GGT TTT GTG TC 3',  $T_m = 58^{\circ}\text{C}$ , product = 249bp; Borsani *et al.*, 1991).



MIX10/MX20 (MIX10 5' CAT CAC AAC AGC AGT TCT CC 3', MX20 5' TTT AAG ATG CTG CAG TCA GG 3',  $T_m = 55^{\circ}\text{C}$ , product = 844bp, extension time = 1 min; Kay *et al.*, 1993).

MX23b/MIX20 (MX23b 5' ACT GCC AGC AGC CTA TAC AG 3', MIX20 5' GTT GAT CCT CGG GTC ATT TA 3',  $T_m = 55^{\circ}\text{C}$ , product = 578bp; Kay *et al.*, 1993).

## 4.3 RESULTS

### 4.3.1 MSCI status of *Xist*-targeted mice

RTPCR for *Xist* was first performed on adult XY *Xist*<sup>+</sup> and *Xist*<sup>-</sup> testes using the published primers of McCarrey *et al.* (1992, termed 588 2F and 588 2R; see Figure 4.1). Since both primer sequences lie in the same exon (exon 6), RNA was pre-treated with DNase to remove contaminating genomic DNA. *Xist* transcripts were detected in XY *Xist*<sup>+</sup> testis and *Xist*<sup>-</sup> testis (Figure 4.2a), consistent with the idea that these *Xist*<sup>-</sup> mice produce a deleted *Xist* transcript that nevertheless includes exon 6. In order to verify that these *Xist*<sup>-</sup> transcripts were indeed deleted, RTPCR was then carried out using the nested PCR primer pairs MIX10/MX20 and MX23b/MIX20 that lie in exons 1/6 and 3/6, respectively (Kay *et al.*, 1993, and Figure 4.1). *Xist* was detected in *Xist*<sup>+</sup> but not *Xist*<sup>-</sup> testes in both the first and second round reactions (Figure 4.2a). Together, these results are consistent with these *Xist*<sup>-</sup> mice producing an *Xist* transcript that includes exon 6 but is deleted for sequences lying in exons 1-5.

The MSCI status of *Xist*<sup>-</sup> mice was then analysed using RTPCR for the MSCI-dependent autosomal backups *Pgk2* and *Pdhal*. These genes were transcribed in *Xist*<sup>+</sup> and *Xist*<sup>-</sup> testes, indirectly inferring that MSCI had taken place (Figure 4.2b). In order to verify this, surface spread and squashed spermatocyte preparations from *Xist*<sup>+</sup> and *Xist*<sup>-</sup> testes were compared by DAPI staining, RNA POLII exclusion and using the sex body marker XY77. In *Xist*<sup>+</sup> testes, combined immunolabelling for SCP3 and RNA POLII demonstrated that autosomal transcription levels increased throughout meiosis, peaking at late pachytene/early diplotene. It was at these stages (when the sex body becomes most obvious using DAPI) that the sex chromosomes were most clearly RNA POLII-negative. An essentially identical pattern of

RNA POLII staining was seen in meiotic cells from *Xist*<sup>-</sup> males (Figure 4.3a,b). 84% and 87% of the late pachytene/early diplotene cells analysed from the *Xist*<sup>+</sup> and *Xist*<sup>-</sup> males, respectively, showed obvious RNA POLII exclusion from the sex body (Table 4.1, Figure 4.3c,d). When the cells were scored for sex bodies based on DAPI-staining and then checked by visualising the SCP3 and RNA POLII signals, sex bodies were correctly identified in 71% and 61% of *Xist*<sup>+</sup> and *Xist*<sup>-</sup> late pachytene/early diplotene cells, respectively (Table 4.1). Using mAb 4c6, XY77-positive sex bodies were readily detected in squashed spermatocytes from *Xist*<sup>-</sup> males (Figure 4.3e,f). Taken together, these results indicate that MSCI, as measured by a number of parameters, proceeds normally in mice with a targeted disruption of *Xist* (Figure 4.3, Table 4.1).

#### 4.3.2 Sex body formation in $XY Y^{d1}$ (n=3) and $XY Y^{*X}$ (n=2) spermatocytes as revealed by XY77 immunostaining

As in XY males, XY77 was restricted to the sex bodies of late pachytene and diplotene spermatocytes in  $XY Y^{d1}$  and  $XY Y^{*X}$  males (Figure 4.4a-d). In all of the 68  $XY Y^{d1}$  and 106  $XY Y^{*X}$  late pachytene/diplotene spermatocytes analysed, only one sex body structure was noted per cell. At first sight, this seems to indicate (as predicted by the *quasi-cis* spreading model), that univalent Y chromosomes are not forming a separate sex body. However, there are two caveats. First, since XY77 is a late pachytene marker, and apoptotic elimination of cells with asynapsed sex chromosomes begins during pachytene, there is the possibility that cells with two sex bodies have already been eliminated. Second, there is ample prior evidence that univalent chromosomes are attracted to and may become partially incorporated in the sex body. Unfortunately squash preparations are inadequate for resolving the sex chromosome configurations, and XY77 is not detectable in spread spermatocytes.

### 4.3.3 Sex body formation and Y chromosomal MSCI in XY (n=2), XYY<sup>dl</sup> (n=3) and XYY\*<sup>X</sup> (n=2) spermatocytes as revealed by anti-XLR staining and RBM expression analysis

In the light of the limitations of using XY77 as an MSCI-specific sex body marker, it was decided to use combined anti-XLR and RBM immunostaining in order to test the predictions of the *quasi-cis* model in XYY<sup>dl</sup> and XYY\*<sup>X</sup> meiosis. Although anti-XLR staining is not MSCI-specific, it does provide a useful sex-body marker from zygotene onwards and it also allows accurate meiotic substaging (it was not convenient to use SCP3 for substaging since the SCP3 and RBM antibodies were both raised in rabbit). Monitoring expression of RBM, which is shut down at pachytene in normal males, provides a direct assay for a failure of Y chromosomal MSCI.

#### *XY males*

The pattern of anti-XLR staining in normal males is described in Chapter 3. RBM was strongly expressed in spermatogonia (which were easily identifiable from their size, their DAPI-staining pattern and their negativity for XLR) and this staining continued into leptotene and zygotene spermatocytes (Figure 4.5a-d). For both RBM and XLR the intensity of staining in the condensed zygotene nuclei was greater than in the less condensed leptotene nuclei. Spermatogenic cells beyond zygotene together with Sertoli cells showed no staining above background (Figure 4.5a-d). No nuclear RBM staining was seen when the RBM antiserum was preabsorbed with recombinant RBM protein (Figure 4.6c,d). These results are in agreement with previous results with this antibody using sectioned material (D.Elliott personal communication) and with the published results (aside from the lack of spermatid staining) on sectioned material using a different RBM antibody (Mahadevaiah *et al.*, 1998).

### *XY<sup>d1</sup> males*

Anti-XLR staining was indistinguishable from that of normal males, but RBM staining was absent at all spermatogenic stages (Figure 4.6a,b). The lack of RBM staining in these *Rbm*-deficient mice is important in that it confirms the specificity of the antibody; it also means that  $XY Y^{d1}$  mice (see below) should have a single Y chromosomal dose of RBM expression.

### *XY Y<sup>\*X</sup> males*

The anti-XLR staining and RBM expression (in terms of germ cell-specificity and timing of expression) in  $XY Y^{*X}$  testes was indistinguishable from that of XY males (Figure 4.5e-h).

### *XY Y<sup>d1</sup> males*

Only a very low percentage (3%, n=185) of pachytene cells (all early or mid) contained two sex body-shaped signals, one of which was moderately larger than the other (Figure 4.4e,f). However, even under initial examination at low power, two other major defects were readily detectable in the  $XY Y^{d1}$  spermatocytes. The first was that a number of cells had entered pachytene (as identified by low whole nuclear anti-XLR staining) despite having incompletely formed sex bodies (Figure 4.7). To verify this delay in sex body formation, anti-XLR staining intensity values for spermatocytes from  $XY Y^{d1}$  and XY males were first sorted in descending order. Three arbitrary ranges of <700->500, <500->300 and <300 units (representing progression through prophase based on the whole nuclear anti-XLR staining alone) were then selected and the spermatocytes were classified as to the anti-XLR staining of the sex-body domain. As can be seen from Table 4.2 and Figure 4.8, by the time anti-XLR staining intensity values had declined to <700 - >500, most XY spermatocytes (87%) had fully formed sex bodies, whereas only 51% of  $XY Y^{d1}$  spermatocytes had fully formed

sex bodies. This retardation in sex body formation in  $XY Y^{d1}$  males persisted into the <500- >300 range, but on reaching <300 (late pachytene), all of the  $XY Y^{d1}$  cells had normal sex bodies. This is consistent with the observations on XY77 staining in  $XY Y^{d1}$  spermatocytes, which showed only morphologically normal sex bodies at late pachytene (section 4.3.2 and Figure 4.4a,b).

The second major defect in the  $XY Y^{d1}$  spermatocytes was that many early and mid pachytene cells were very strongly stained for RBM, suggesting a failure of *Rbm*-inactivation (Figure 4.7). This resulted in a number of pachytene cells with low whole nuclear anti-XLR staining intensities of <700 having grossly elevated RBM levels (Figure 4.9). In many cases, the intensity of RBM in these cells was similar to that of the surrounding spermatogonia (Figure 4.7). This inappropriate RBM expression was seen in pachytene cells with and without abnormal sex bodies. In order to see if cells with abnormal sex bodies were preferentially affected, the 151 cells showing X chromosome XMR/XLR signals (i.e. late zygotene and pachytene) from Figure 4.9b were classified as to sex body morphology, and the proportion in each class with RBM values greater than 835 units (the upper limit for XY pachytene cells) was counted. Based on this criterion, RBM overexpression was present in 25% of spermatocytes with normal sex bodies (n=99) and 23% of those with abnormal sex bodies (n=52).

As was the case for the sex body abnormality, the RBM expression anomaly had disappeared by late pachytene (XLR <300 units - Figure 4.9).

#### 4.3.4 Surface spread analysis of $XY Y^{d1}$ males (n=2)

The results from sections 4.3.3 show that both sex body formation and Y chromosome MSCI were defective in  $XY Y^{d1}$  spermatocytes, which is in agreement with the predictions of the *quasi-cis* model. However, there was no correlation between abnormal sex body formation and RBM expression, as would have been expected if the sex body abnormality was a manifestation of a failure of Y chromosome inactivation. Indeed, the projecting tail of the abnormal sex bodies was so long that it was suggestive of a failure of X condensation and inactivation rather than the predicted failure of Y chromosome inactivation. In order to investigate the sex body formation defect in greater detail,  $XY Y^{d1}$  surface spread spermatocytes were immunostained for SCP3 (to allow accurate staging) and RNA POLII and analysed under high power.  $XY Y^{d1}$  meiocytes displayed a number of abnormalities (Figure 4.10 and Table 4.3). Sex body abnormalities were present in 82% of early pachytene and 39% of mid pachytene cells, and significantly the defects included many clear examples of a failure of X chromosome condensation (Figure 4.10). Furthermore, other predictions of the *quasi-cis* model were clearly contradicted. Thus, analysis of cells with normally formed sex bodies demonstrated that pairing with the X chromosome was not a prerequisite for inclusion of Y material in the sex body (Figure 4.11). Moreover, cells with trivalent synapsis were equally susceptible to defective sex body formation as those in which synapsis had failed (Figure 4.10c,d).

Figure 4.2. RTPCR analysis of *Xist* and autosomal backups *Pgk2* and *Pdhal* expression in normal and *Xist*-disrupted testis (Marahrens *et al.*, 1997). Arrows indicate 500bp.

a) *Xist* expression.

Product sizes:

588 2F/2R = 249bp.

MIX10/MX20 = 844bp.

MX23b/MIX20 = 578bp.

b) *Pgk2* and *Pdhal* expression.

Product sizes:

*Pgk2* = 300bp.

*Pdhal* = 459bp.

*HPRT* = 352bp.



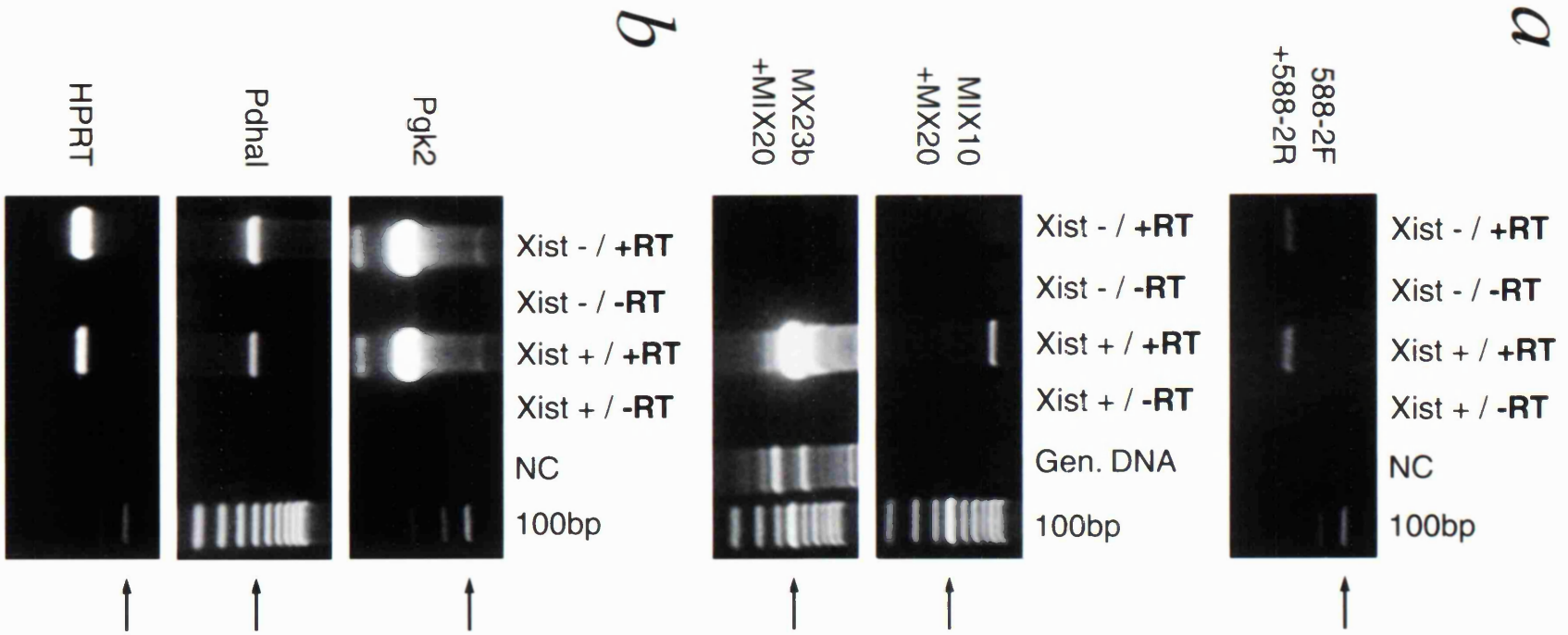


Figure 4.3. MSCI (a-d) and sex body formation (e, f) in *Xist*- spermatocytes. SCP3 = red, DAPI = blue.

a) Surface spread zygotene (arrowhead), late pachytene (long arrow) and diplotene (short arrow) nuclei from an *Xist*- testis.

b) Same nuclei stained for RNA POLII (green). As in *Xist*+ males, transcriptional activity is low at zygotene, higher at late pachytene, and highest at diplotene.

c) *Xist*- early diplotene nucleus, showing peripheral sex body (arrowhead) and X centromere (long arrow).

d) Same nucleus stained for RNA POLII (green). The sex chromosomes occupy a peripheral domain that excludes RNA POLII.

e) Squashed spermatogenic nuclei from *Xist*- testis.

f) Same nuclei stained for XY77 (green), showing XY77-positive sex bodies.

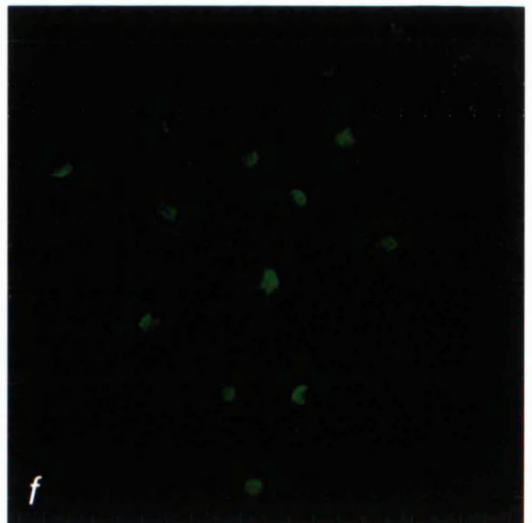
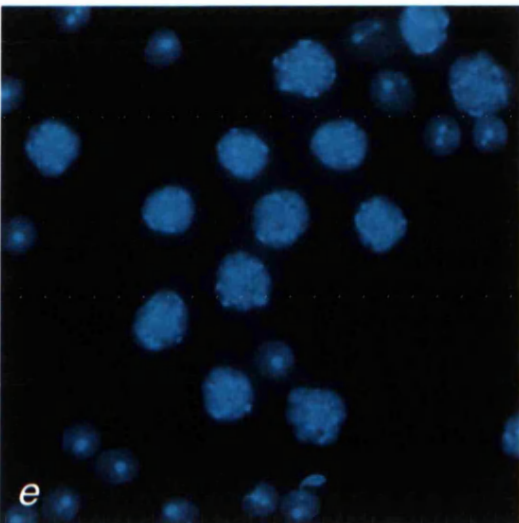
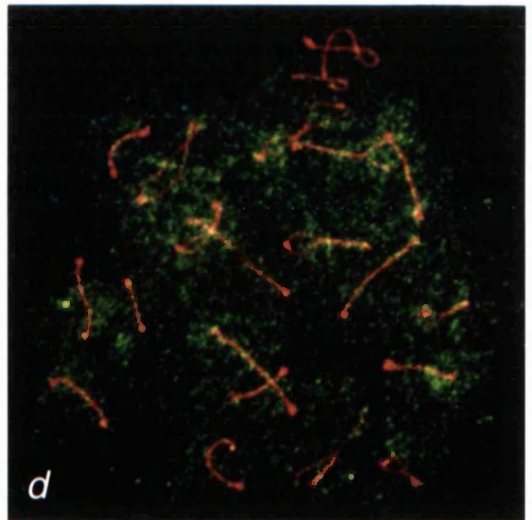
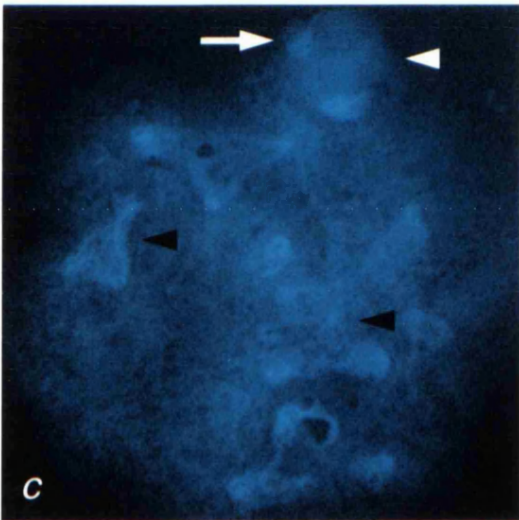
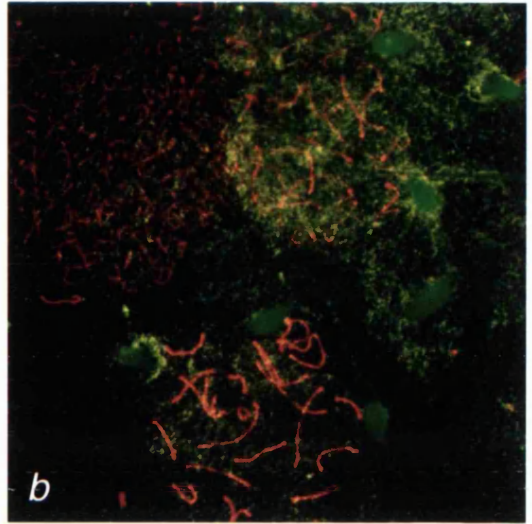
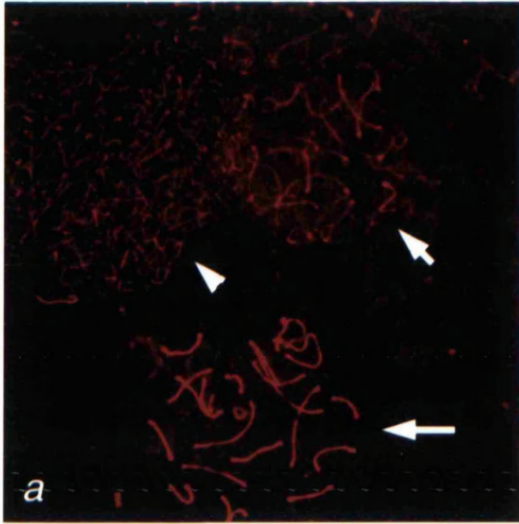


Table 4.1. Existence of morphological sex bodies (DAPI) and sex chromosomal RNA POLII exclusion in *Xist*<sup>+</sup> and *Xist*<sup>-</sup> spermatocytes.

	<i>Xist- 1</i>	<i>Xist- 2</i>	<i>Xist+ 1</i>
<b>Sex body</b>	22 (55%)	26 (67%)	32 (71%)
<b>RNAPolIII-exclusion</b>	32 (80%)	37 (95%)	38 (84%)
<b>Total</b>	40	39	45

Figure 4.4. XY77 and XMR/XLR staining of sex bodies in  $XY Y^{d1}$  and  $XY Y^{*X}$  spermatocytes.

- a)  $XY Y^{d1}$  spermatocytes stained with DAPI. Arrowheads indicate Sertoli cells.
- b) Same cells stained for XY77. XY77 is present in Sertoli cells and late pachytene/diplotene nuclei (closed arrowheads). Note that each late pachytene/diplotene cell has only one sex body signal.
- c)  $XY Y^{*X}$  spermatocytes stained with DAPI. Note the many postmeiotic cells (spermatids and sperms).
- d) Same cells stained for XY77. Note that each late pachytene/diplotene cell has only one sex body signal.
- e)  $XY Y^{d1}$  spermatocytes stained for XMR/XLR showing a rare example of a double sex body signal (arrowheads). This cell is an early or mid pachytene cell based on its whole nuclear signal.
- f) High power mid pachytene  $XY Y^{d1}$  spermatocyte stained for XMR/XLR, again showing double sex body signal.

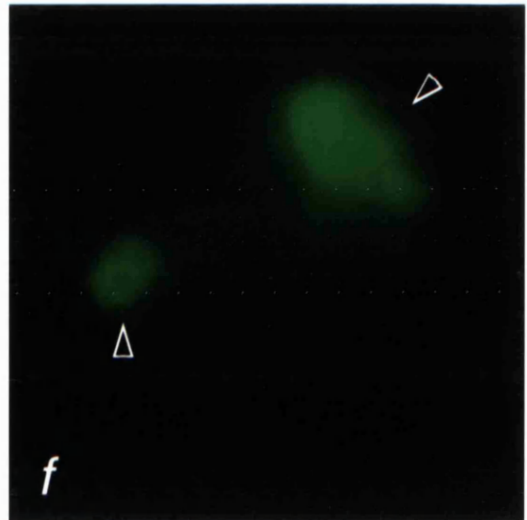
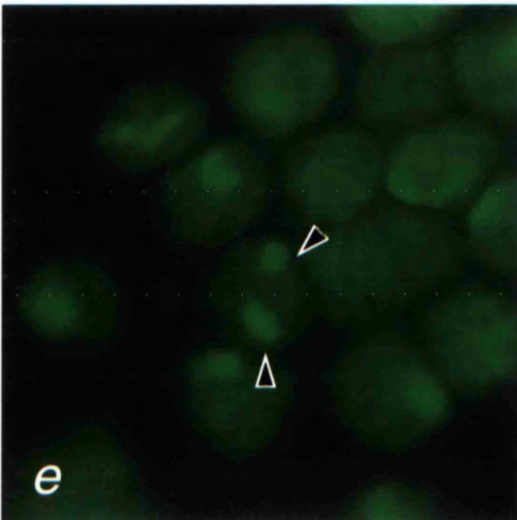
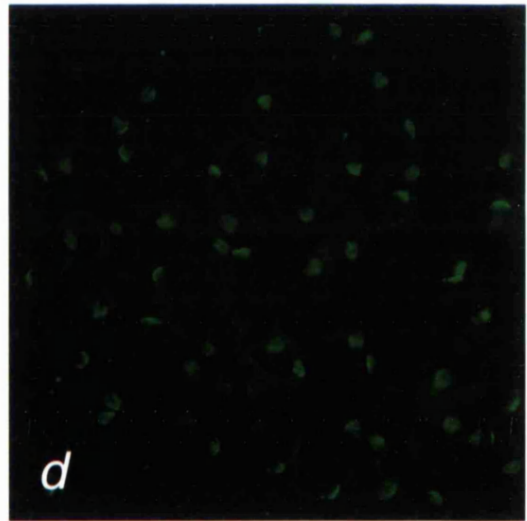
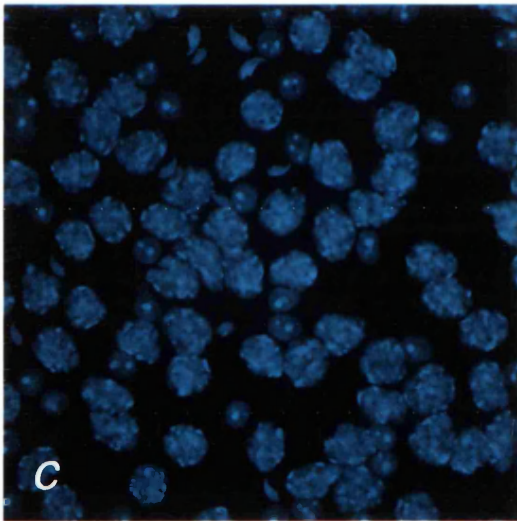
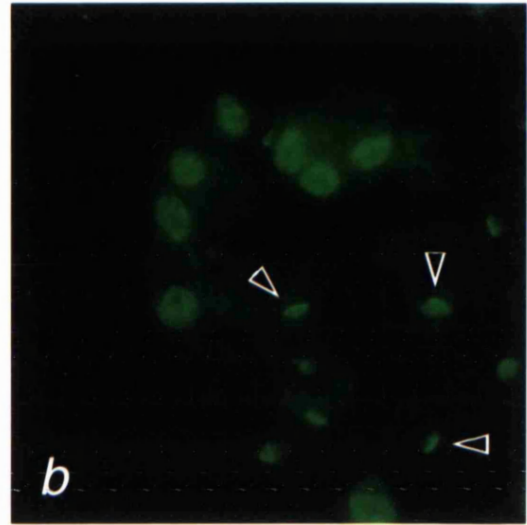
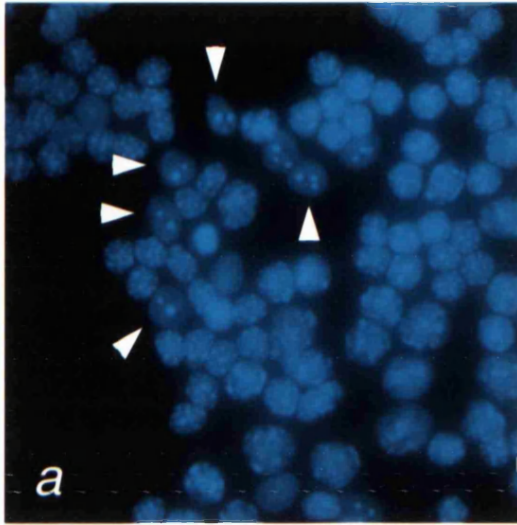


Figure 4.5. RBM expression in XY and XYY<sup>\*X</sup> squashed spermatogenic cells. RBM = red, XMR/XLR = green, DAPI = blue. Long arrow = leptotene/early zygotene nucleus, arrowhead = mid zygotene nucleus, short arrow = late zygotene nucleus, empty arrowhead = late pachytene nucleus, asterisk = spermatogonium.

- a) XY nuclei stained for XMR/XLR. Whole nuclear XMR/XLR staining is most abundant at mid zygotene, and decreases in late zygotene before disappearing in pachytene. Spermatogonia are XMR/XLR-negative.
- b) Same nuclei stained for RBM. Aside from its presence in spermatogonia, the dynamics of RBM expression mirrors that of whole nuclear XMR/XLR expression.
- c) Same nuclei stained for DAPI. A Sertoli cell is marked by the open arrow.
- d) Superimposition of a) and b). Neither RBM nor XMR/XLR are expressed in Sertoli cells.
- e) Nuclei from XYY<sup>\*X</sup> testis stained for XMR/XLR. XMR/XLR levels increase during the leptotene-zygotene transition.
- f) Same nuclei stained for RBM. As in XY testis, meiotic RBM levels are highest during mid-zygotene.
- g) Nuclei from XYY<sup>\*X</sup> testis stained for XMR/XLR.
- h) Same nuclei stained for RBM. As in XY testis, meiotic RBM levels decrease on transition to late zygotene and RBM is absent at late pachytene.



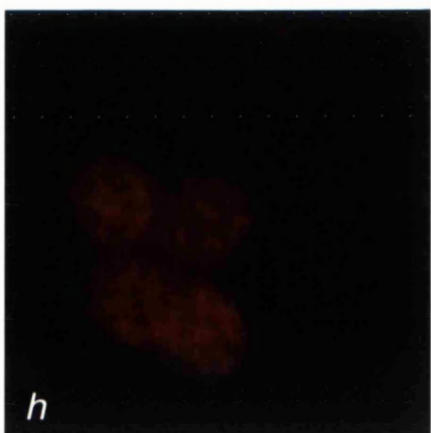
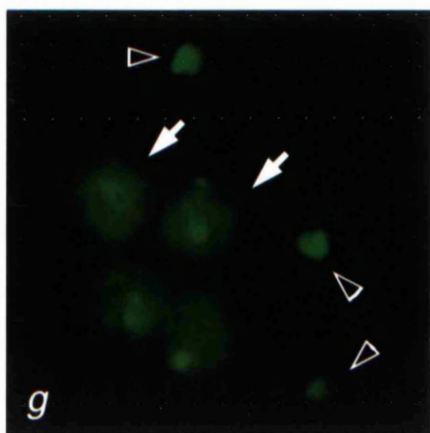
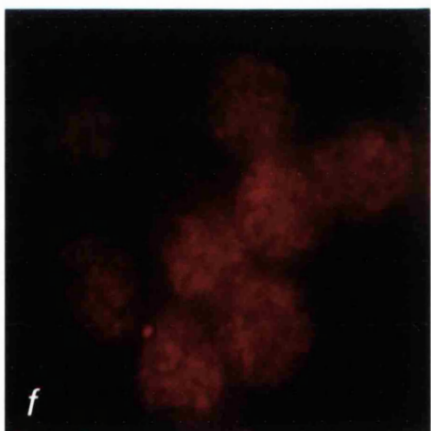
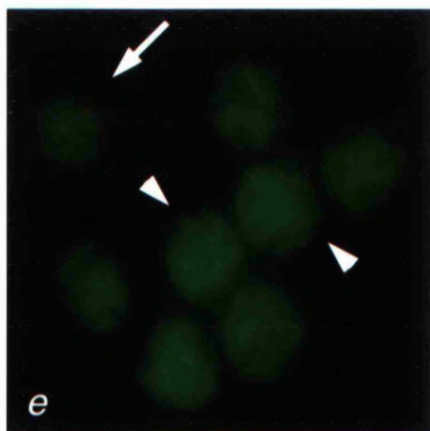
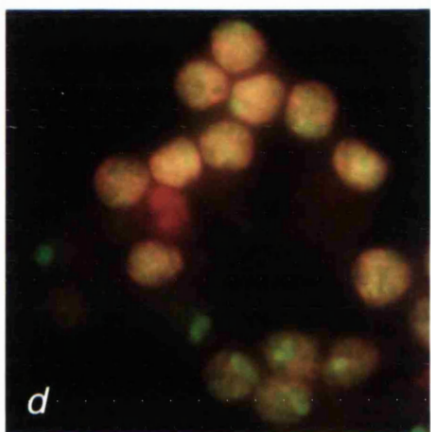
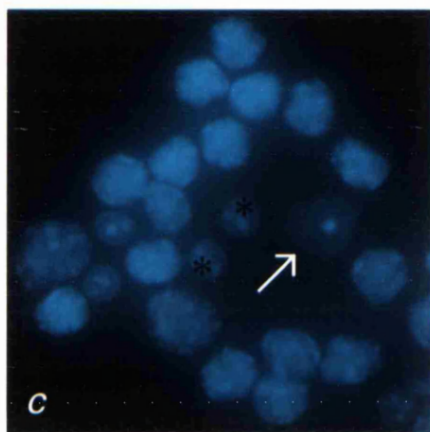
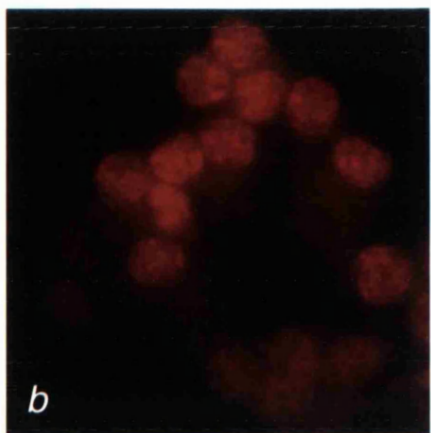
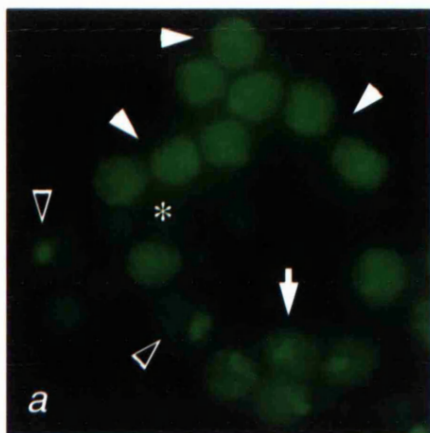


Figure 4.6. RBM expression in squashed  $XY^{d1}$  and XY spermatogenic cells. RBM = red, DAPI = blue.

- a) Nuclei from  $XY^{d1}$  testis.
- b) Same nuclei stained for RBM.
- c) Nuclei from XY testis.
- d) Same nuclei stained for RBM after preabsorption with RBM protein.

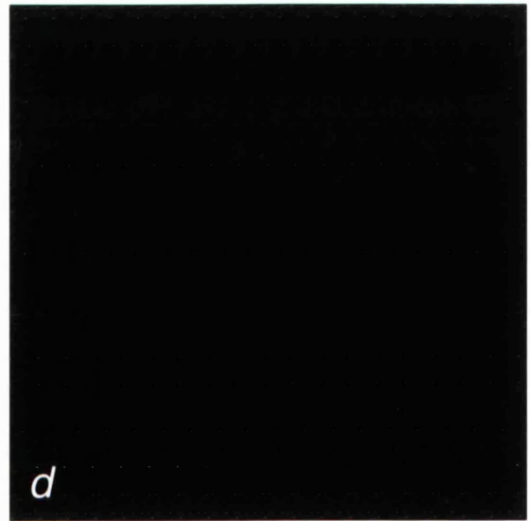
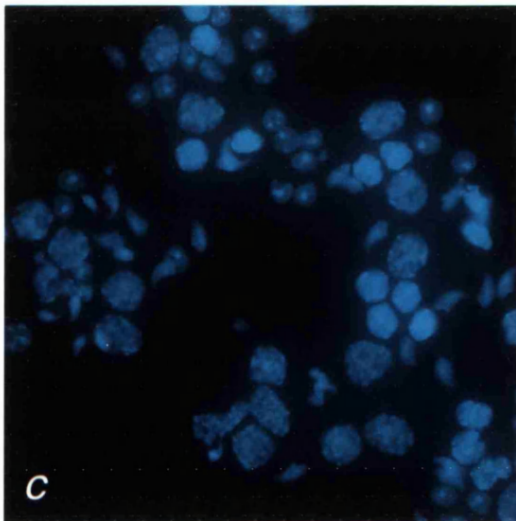
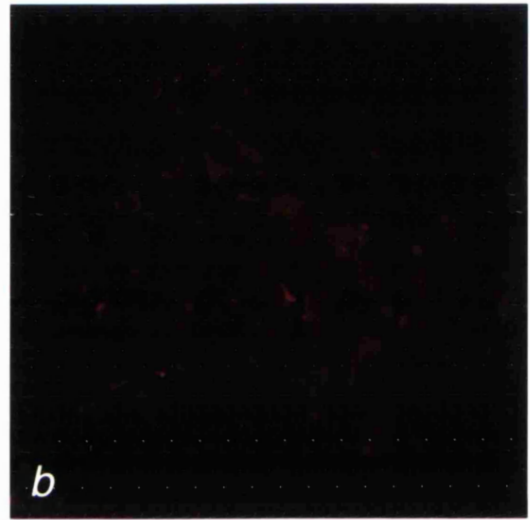
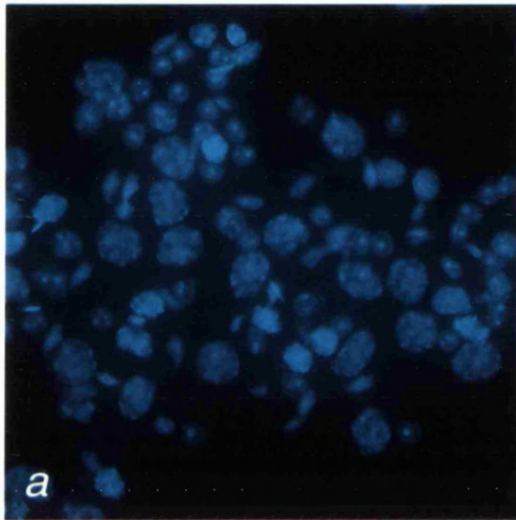


Figure 4.7. RBM expression in squashed  $XYY^{d1}$  spermatogenic cells. RBM = red, XMR/XLR = green. Arrowhead = early/mid pachytene nucleus with normal sex body, short arrow = early/mid pachytene nucleus with abnormal sex body, long arrow = zygotene nucleus, empty arrowhead = late pachytene nucleus, asterisk = spermatogonium.

a) Nuclei stained for XMR/XLR, showing early/mid pachytene nuclei with normal and abnormal sex bodies. The abnormal sex bodies have a tadpole shape that is normally only seen during mid-late zygotene in XY nuclei.

b) Same nuclei stained for RBM. RBM is overexpressed in early/mid pachytene nuclei with normal and abnormal sex bodies.

c) Nuclei stained for XMR/XLR.

d) Same nuclei stained for RBM. RBM expression in abnormal early/mid pachytene nuclei exceeds that of zygotene nuclei and is comparable to spermatogonial expression levels. Late pachytene nuclei are nevertheless RBM-negative.

e) Nuclei stained for XMR/XLR. One quarter of  $XYY^{d1}$  early/mid pachytene nuclei have abnormal sex bodies.

f) Same nuclei stained for RBM.

g) Nuclei stained for XMR/XLR.

h) Same nuclei stained for RBM.

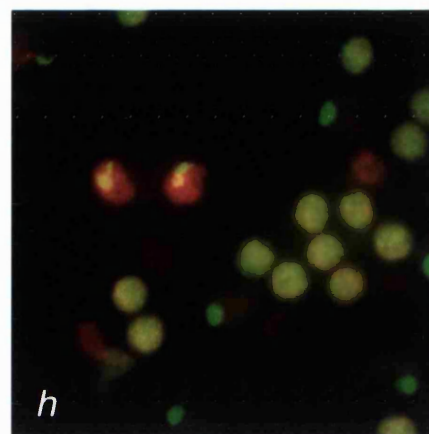
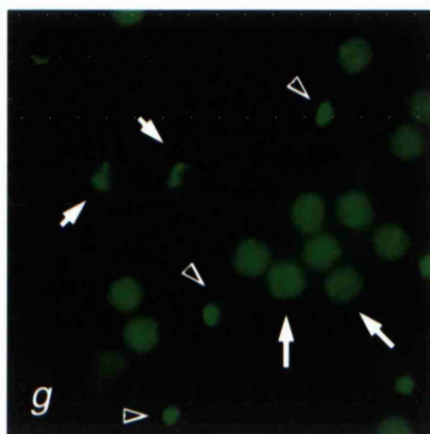
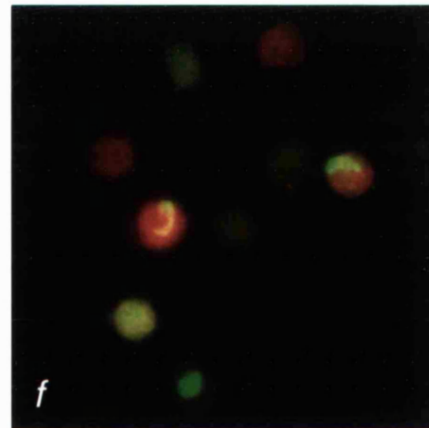
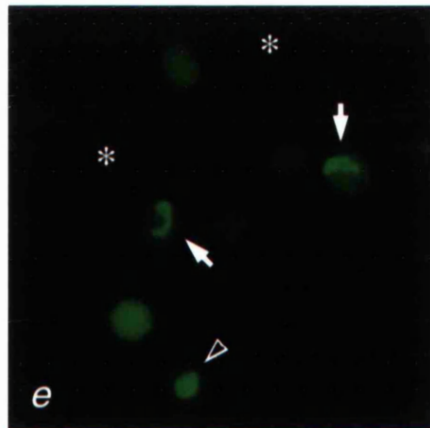
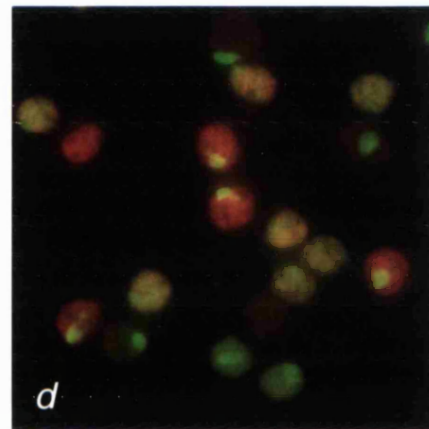
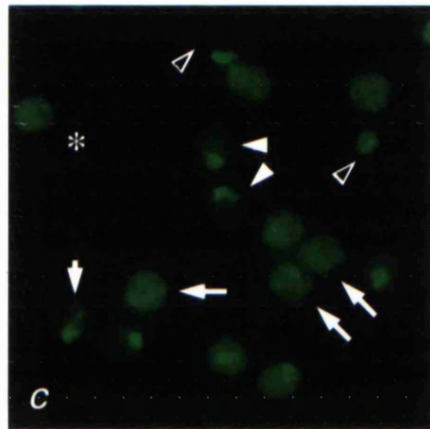
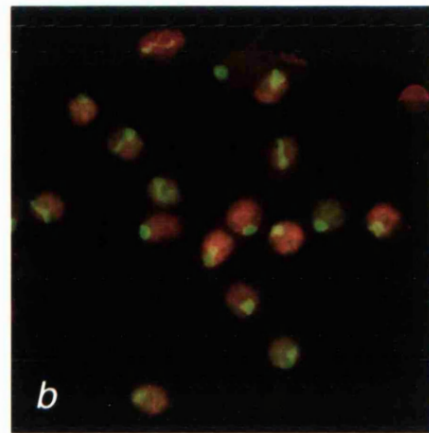
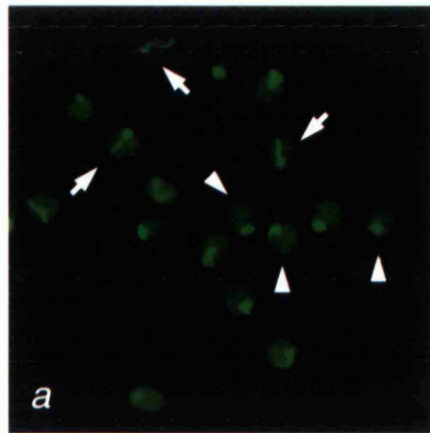


Table 4.2. Changes in sex body morphology (expressed as category 1-4) during meiotic progression (expressed as a function of whole nuclear XMR/XLR values) in XY and XYY<sup>d1</sup> spermatocytes. Individual values are shown in Figure 4.9.

Category 1 = no X chromosome staining (leptotene / early zygotene) - sex body not fully formed.

Category 2 = faintly labelled X chromosome (mid zygotene) - sex body not fully formed.

Category 3 = Clearly labelled X chromosome - sex body not fully formed.

Category 4 = Clearly labelled X chromosome - sex body fully formed.

XY (n = 87)

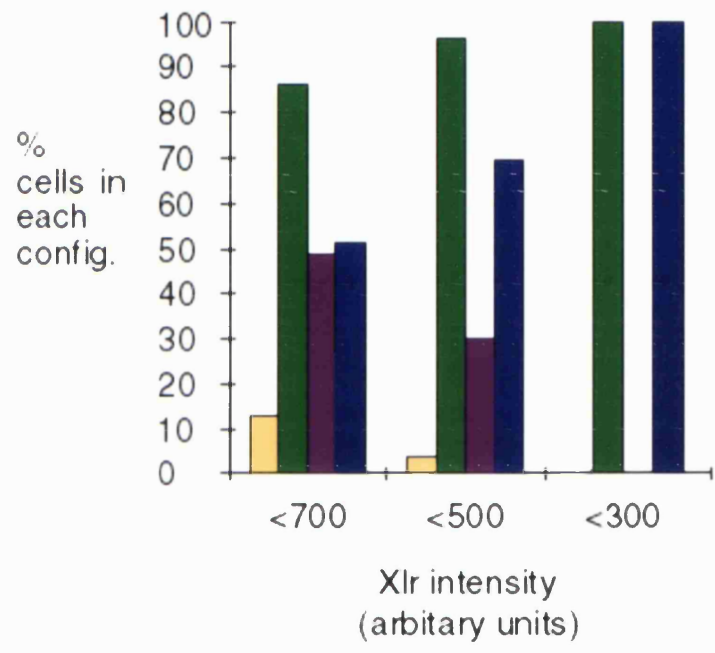
	Category			
XMR/XLR range	1	2	3	4
<700->500	9 (10%)	0	3 (3%)	75 (87%)
<500->300	1 (2%)	0	1 (2%)	58 (96%)
<300	0	0	0	16 (100%)

XY<sup>d1</sup> (n = 194)

	Category			
XMR/XLR range	1	2	3	4
<700->500	23 (12%)	20 (10%)	52 (27%)	99 (51%)
<500->300	4 (4%)	1 (1%)	23 (25%)	63 (70%)
<300	0	0	0	16 (100%)

Figure 4.8. Graph showing percentage of cells with and without sex bodies (derived from Table 4.2) during meiotic progression in XY and XYY<sup>d1</sup> spermatocytes.





- XY    Sex body not fully formed
- XY    Sex body fully formed
- XYY<sup>d1</sup>    Sex body not fully formed
- XYY<sup>d1</sup>    Sex body fully formed

Figure 4.9. Plots of RBM expression vs. whole nuclear XMR/XLR expression during the early - late pachytene transition in XY and  $XY Y^{d1}$  mice. RBM levels are grossly elevated in a subpopulation of  $XY Y^{d1}$  early/mid pachytene spermatocytes, but by late RBM levels are comparable to those of the XY control.

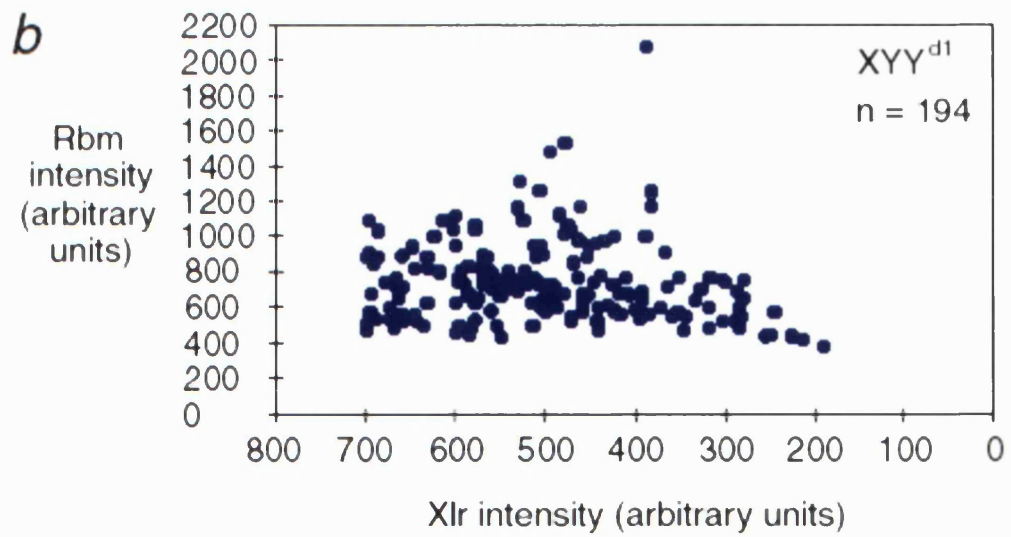
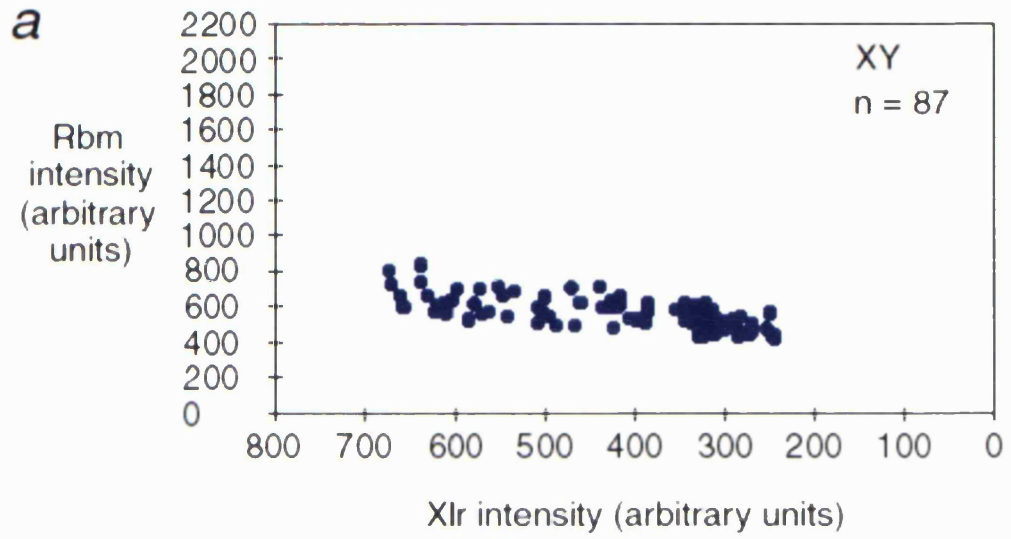


Table 4.3. Synaptic configurations and sex chromosomal abnormalities in XY (a,c) and XYY<sup>d1</sup> (b,d) spermatocytes.

'Abnormal X' = failure in X chromosome condensation.

'X asynchrony' = X chromosome displays a morphology indicative of an earlier stage than the autosomes.

'XY separation' = Y univalent/s is significantly spatially separated from X chromosome / XY bivalent.

'Aut. Asynapsis' = asynapsis of at least one autosomal bivalent.

*a*

	<b>Early pachytene</b>	<b>Mid pachytene</b>	<b>Late pachytene</b>
<b>Paired</b>	20 (100%)	34 (97%)	39 (100%)
<b>Unpaired</b>	-	1 (3%)	-
<b>N° cells scorable</b>	20	35	39
<b>Total N° cells</b>	21	35	39

*b*

	<b>Early pachytene</b>	<b>Mid pachytene</b>	<b>Late pachytene</b>
<b>Trivalents</b>	26 (38%)	24 (43%)	2 (22%)
<b>Chains</b>	6 (9%)	6 (11%)	2 (22%)
<b>XY + Y</b>	24 (35%)	21 (38%)	2 (22%)
<b>X + YY</b>	8 (12%)	3 (5%)	1 (12%)
<b>Univalents</b>	4 (6%)	2 (3%)	2 (22%)
<b>N° cells scorable</b>	<b>68</b>	<b>56</b>	<b>9</b>
<b>Total N° cells</b>	<b>73</b>	<b>59</b>	<b>9</b>

*c*

	<b>Early pachytene</b>	<b>Mid pachytene</b>	<b>Late pachytene</b>
<b>Abnormal X</b>	2 (10%)	1 (3%)	-
<b>X asynchrony</b>	2 (10%)	-	-
<b>Aut. association</b>	1 (5%)	1 (3%)	2 (5%)
<b>XY separation</b>	-	-	-
<b>Aut. asynapsis</b>	-	-	-
<b>Normal</b>	17 (85%)	33 (94%)	37 (95%)
<b>N° cells scorable</b>	20	35	39
<b>Total N° cells</b>	21	35	39

*d*

	<b>Early pachytene</b>	<b>Mid pachytene</b>	<b>Late pachytene</b>
<b>Abnormal X</b>	34 (50%)	12 (21%)	-
<b>X asynchrony</b>	23 (34%)	14 (25%)	-
<b>Aut. association</b>	20 (29%)	4 (7%)	-
<b>XY separation</b>	14 (21%)	9 (16%)	1 (11%)
<b>Aut. asynapsis</b>	4 (6%)	1 (2%)	-
<b>Normal</b>	12 (18%)	34 (61%)	8 (89%)
<b>N° cells scorable</b>	<b>68</b>	<b>56</b>	<b>9</b>
<b>Total N° cells</b>	<b>73</b>	<b>59</b>	<b>9</b>

Figure 4.10. Surface spread  $XYY^{dl}$  spermatocytes. SCP3 = red. Arrowhead = Y chromosome, short arrow = X chromosome, long arrow = X-centromere, empty arrowhead = asynapsed autosome. Abnormalities are classified in the following way:

- 1) Failure of the X chromosome to assume its usual sex body conformation. The X chromosome stretches across the autosomal compartment.
- 2) Absence of a discrete domain containing all three sex chromosomes. Y chromosomes spatially separated from the X chromosome or the XY bivalent.
- 3) Meiotic progression of the X chromosome delayed with respect to autosomes. Cells classified as early or mid pachytene based on their autosomal axes have X chromosome axes reminiscent of very early or early pachytene, respectively.
- 4) Inappropriate associations between the sex chromosomes (most notably the X) and the autosomes.
- 5) Autosomal asynapsis.

Images demonstrate the following abnormalities:

- a) Mid pachytene spermatocyte with XY bivalent plus Y univalent. There is no discrete domain containing all three sex chromosomes. Instead, the Y-univalent is spatially separated from the XY bivalent.
- b) Early/mid pachytene spermatocyte with XY bivalent plus Y univalent. Comments as in a).
- c) Mid pachytene spermatocyte with XYY trivalent. The X chromosome is stretching across the autosomal compartment and has formed a centromeric association with an autosome. The X chromosome morphology is reminiscent of early pachytene.
- d) Early pachytene spermatocyte with XYY trivalent. The X chromosome stretches across the autosomal compartment, and its morphology is reminiscent of very early pachytene.
- e) Early pachytene spermatocyte with XY bivalent plus Y univalent. Comments as in d).
- f) Mid pachytene spermatocyte with XY bivalent plus Y univalent. The X chromosome stretches into the autosomal compartment and has a morphology reminiscent of early pachytene. There is also spatial separation of a univalent Y chromosome and asynapsis of one autosomal bivalent.

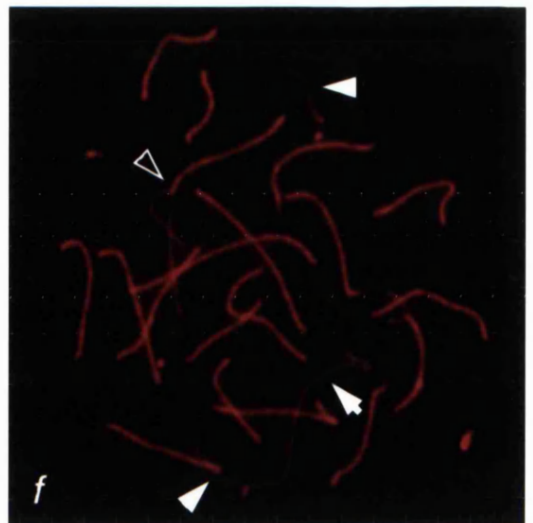
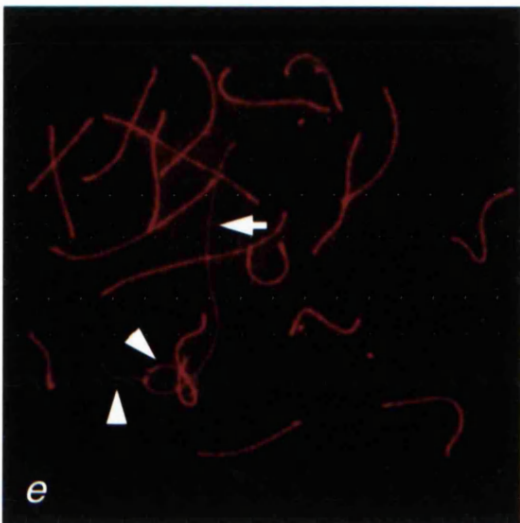
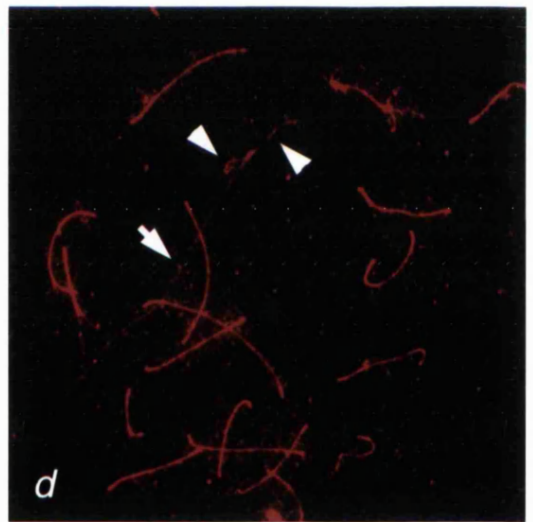
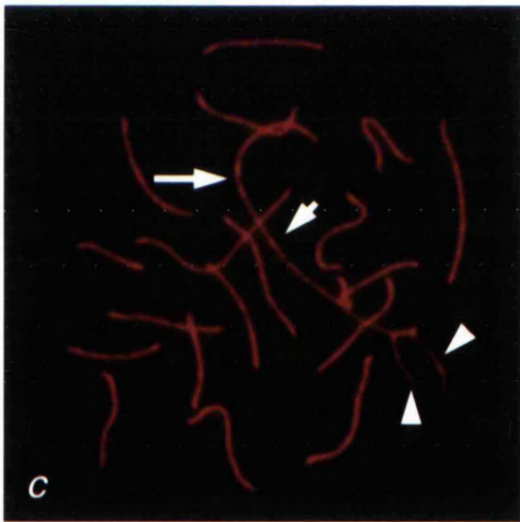
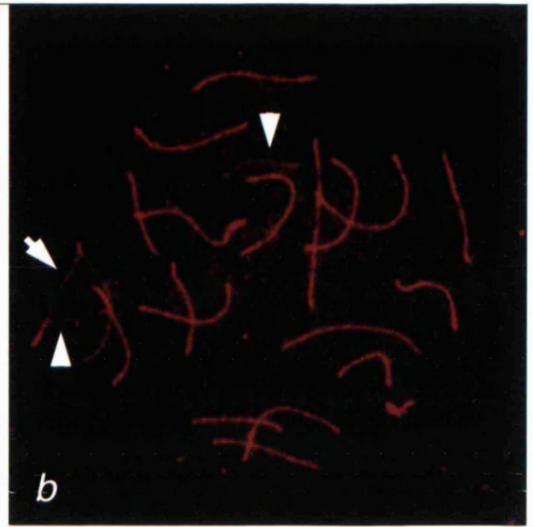
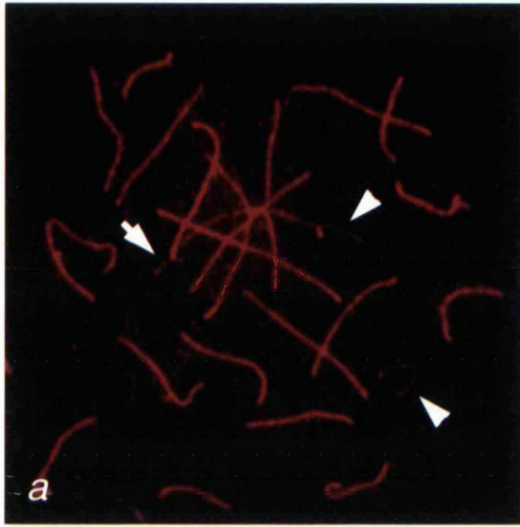
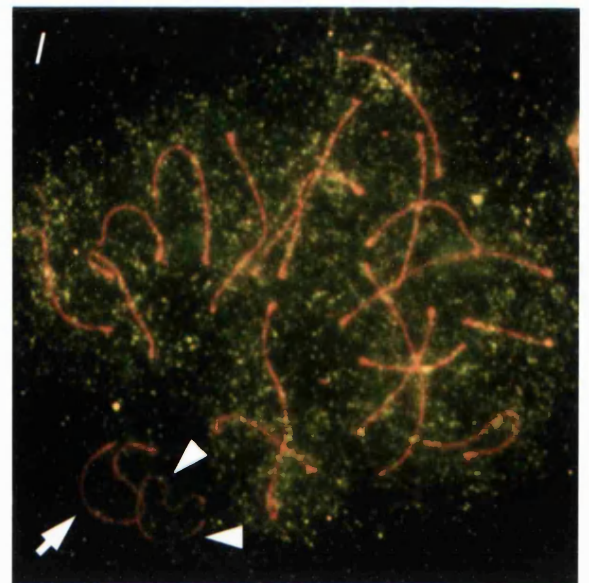
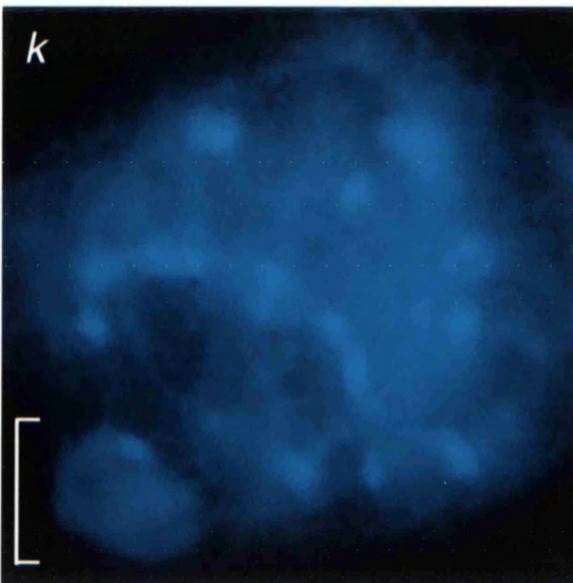
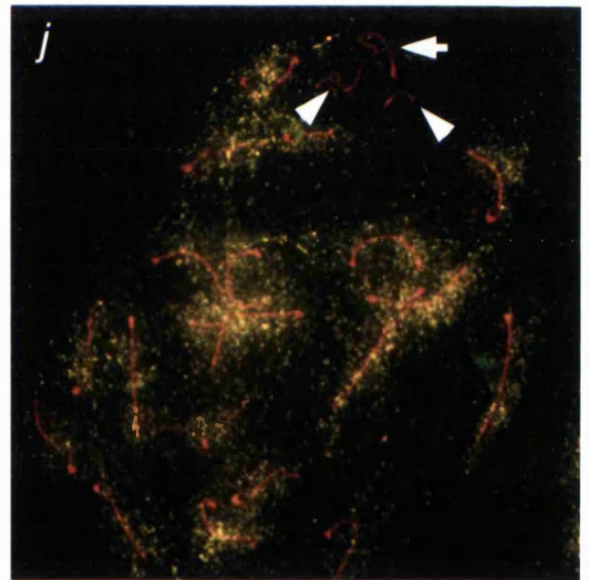
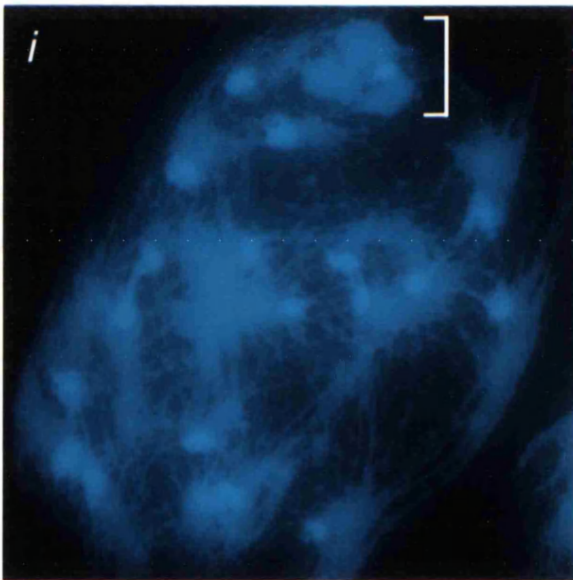
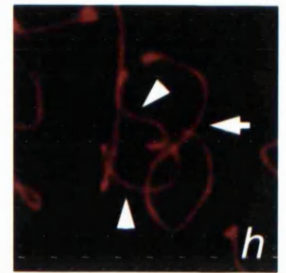
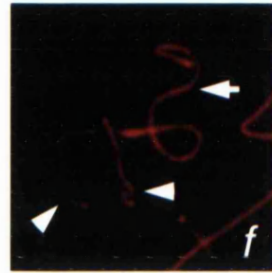
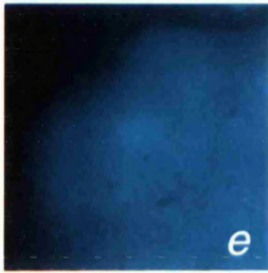
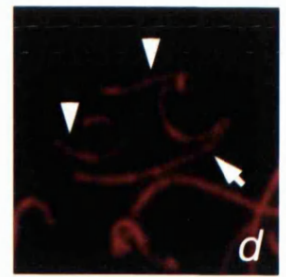
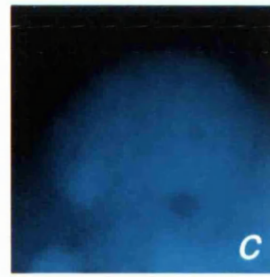
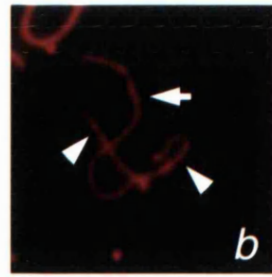


Figure 4.11. Surface spread  $XY Y^{d1}$  spermatocytes demonstrating that synapsis with the X chromosome is not a prerequisite for Y chromosome inclusion in the sex body. SCP3 = red, RNA POLII = green, DAPI = blue. Arrowhead = Y chromosome, short arrow = X chromosome.

- a) Sex body.
- b) Same nucleus showing trivalent synapsis with all sex chromosomes in the sex body.
- c) Sex body.
- d) Same nucleus showing XY bivalent plus Y univalent with all sex chromosomes in the sex body.
- e) Sex body.
- f) Same nucleus showing three univalents, all of which are in the sex body.
- g) Sex body.
- h) Same nucleus showing X univalent plus YY bivalent with all sex chromosomes in the sex body.
- i) Early diplotene nucleus stained with DAPI, showing trilobar sex body (white bracket).
- j) Same nucleus stained for SCP3 and RNA POLII, with an XY bivalent plus Y univalent. The Y chromosome is incorporated in the sex body and is RNA POLII-negative.
- k) Late pachytene nucleus stained with DAPI, showing sex body (white bracket).
- l) Same nucleus stained for SCP3 and RNA POLII with an X univalent plus YY bivalent. The YY bivalent is in the sex body and is RNA POLII-negative.





#### 4.4 DISCUSSION

The main aim of this study was to test the hypothesis that inactivation of the Y chromosome proceeds via *quasi-cis* spreading of *Xist* from the X chromosome via the synapsed PARs (Ayoub *et al.*, 1997). As discussed earlier (section 4.1) this model has been invoked by Rodriguez and Burgoyne in providing a possible explanation for unexpectedly severe meiotic failure of males with four sex chromosomes. As argued in the following discussion, the '*quasi-cis*' model is rejected on several counts.

The rationale of the '*quasi-cis*' hypothesis is that MSCI is brought about by *Xist* transcripts produced by the X chromosome, and that these transcripts can only migrate from the X chromosome to the Y chromosome if they are 'joined' via the region of PAR synapsis. However, the present results show that MSCI, as measured by a number of parameters, proceeds normally in males with an *Xist*-disruption. It has been suggested that the truncated *Xist* transcript in these mice might be sufficient for MSCI (J. Wahrman, pers.commn). However, the fact that the same truncation efficiently disrupts somatic X-inactivation (Marahrens *et al.*, 1997) together with the fact that *Xist* is transcribed at extremely low levels in the testis (Kay *et al.*, 1993) makes it unlikely that *Xist* plays a primary role in MSCI.

Even the possibility that a *quasi-cis* mechanism does operate, but that it is *Xist*-independent, is rejected by the results with  $XYY^{d1}$  mice. The  $XYY^{d1}$  surface spread analysis showed that Y chromosomes not synapsed with the X chromosome could still be incorporated in the sex body, where they appeared RNA POLII-negative. This data is consistent with that of Handel *et al* (1994), who demonstrated that interspecific hybrid males (which have high levels of PAR-pairing failure) synthesise morphologically 'normal' sex bodies, with tritiated-uridine

uptake values not statistically different from controls. Nevertheless, univalent Y chromosomes were frequently seen spatially separated from X chromosomes, yet double signals were very rarely observed in squashed  $XY Y^{d1}$  spermatocytes stained with anti-XLR. One possible explanation for the paucity of double sex bodies comes from the study of Baart *et al* (submitted), who found that the surface spreading technique frequently disrupts the association of asynapsed autosomal chromatin with the sex body. Similarly, the separation of many of the univalent Y chromosomes in the spread preparations may be artefactual; the squash method used for the anti-XLR sex body analysis is much less disruptive. It would be interesting to score the frequency of Y chromosome separation from the sex body using the fibrin clot method of Baart *et al.*, since this allows sufficient resolution to identify the sex chromosomes with minimal disruption of the three dimensional structure of the nucleus.

Although the anti-XLR staining indicated that the vast majority of  $XY Y^{d1}$  pachytene spermatocytes possessed single sex body signals, the sex bodies were frequently abnormal in shape. These 'tadpole-shaped' sex bodies were reminiscent of the condensing sex bodies of normal XY zygotene spermatocytes. The fact that they were present in early and mid pachytene spermatocytes suggested that sex body formation had been delayed relative to the synapsis of the autosomes. Analysis of surface spreads confirmed that this was the case. Frequently, the X chromosome stretched across the autosomal compartment and displayed a morphology that was earlier than that of the autosomes. Once again, these results argue against the *quasi-cis* model of sex body formation (whether or not MSCI is mediated by *Xist*), because under this model condensation of the X chromosome would be completed regardless of its synaptic status. Importantly, these sex body abnormalities were not seen in  $XY Y^{*X}$  mice, even though they have a reasonable frequency of pachytene spermatocytes in

which the Y chromosome has not synapsed with the X chromosome (Rodriguez and Burgoyne, 2000).

Although the '*quasi-cis*' model must be rejected, one prediction of the model was fulfilled in  $XY Y^{d1}$  males (but not in  $XY Y^{*X}$  males); namely, a failure of Y chromosomal MSCI in mice with univalent Y chromosomes. The Y-linked gene product RBM, which is absent from pachytene cells of normal males, was found to be highly expressed in a sub-population of  $XY Y^{d1}$  early and mid pachytene spermatocytes. Significantly, this aberrant RBM expression was not restricted to, or biased towards cells with morphologically abnormal sex bodies.

The simplest interpretation of these observations on  $XY Y^{d1}$  and  $XY Y^{*X}$  males is that the addition of extra non-PAR sex chromatin (as with an extra Y but not an extra  $Y^{*X}$ ) increases the time required to complete sex body formation, resulting in cells in which the completion of autosomal synapsis precedes that of sex body formation (under normal circumstances these processes are completed simultaneously). As a result, some pachytene cells may have incomplete X condensation/MSCI, Y condensation/MSCI, or both. If this is the case, then as well as a subpopulation of pachytene cells expressing Y-linked genes like *Rbm*, there should also be a subpopulation expressing X-linked genes like *Pgk1* that are normally inactivated. Furthermore, since the cells with morphologically abnormal sex bodies are likely to be those with incompletely condensed X chromosomes, these cells in particular should have a failure of X chromosomal MSCI. Ways of directly assessing a failure of X chromosomal MSCI are being explored.

The analysis of  $XYY^{d1}$  spermatocytes using XY77 staining, anti-XLR staining, surface spreading and RBM staining revealed that the defects in sex body formation and Y chromosome MSCI were not apparent at late pachytene. This implies either that the defects were corrected by this stage or that the cells harbouring these defects were eliminated. If cells have been unable to form sex bodies or undergo MSCI by early/mid pachytene, there is no obvious reason why they should suddenly acquire competence to do so by late pachytene. It is therefore more likely that the cells with defective sex body formation and MSCI are being eliminated prior to late pachytene. The reasons why spermatocytes with such abnormalities should be eliminated during pachytene depend on the perceived functions of sex body formation/MSCI. Should the function be to mask the asynapsed portions of the X and Y chromosomes from triggering a checkpoint monitoring synapsis or recombination (Jablonka and Lamb, 1988; McKee and Handel, 1993), then 'unmasked' X and/or Y chromatin in  $XYY$  males would be expected to trigger this arrest in the same way that asynapsed autosomes do (de Boer and de Jong, 1989). Alternatively, unmasked X and/or Y chromatin may precipitate spermatocyte death through inappropriate expression of sex chromosomally-linked genes (Lifschytz and Lindsley, 1972).

Although the present results suggest that excess non-PAR chromatin may be the cause of the breakdown in MSCI, this does not provide an explanation for why  $XYY\bar{Y}^{*X}$  males have more severe meiotic problems than  $XYY\bar{Y}$  males and  $XYY^{*X}\bar{Y}^{*X}$  males have more severe meiotic problems than  $XYY^{*X}$  males; in both cases the additional  $\bar{Y}^{*X}$  chromosome consists largely of a PAR which escapes MSCI (Burgoyne *et al.* 1998). It will therefore be important to carry out an analysis of sex body formation and MSCI in these males with four sex chromosomes in the future.

CHAPTER 5

GENETIC ANALYSIS OF A FERTILE PEDIGREE OF X<sup>Y\*</sup>O MICE

## 5.1 INTRODUCTION

$X^{Y^*}O$  males possess a single sex chromosome comprising an X chromosome and a Y chromosome attached by a shared pseudoautosomal region. The  $X^{Y^*}$  chromosome is one of two products generated by recombination in the  $XY^*$  male (Eicher *et al.*, 1991; Figure 5.1).  $X^{Y^*}O$  males are sterile, with testis weights less than half the size of controls and are usually aspermic (Burgoyne and Mahadevaiah, 1993). Histologically, there is a meiotic arrest at metaphase I accompanied by a dramatic accumulation of apoptotic MI spermatocytes (Odorisio *et al.*, 1998). Furthermore, pachytene SC analysis has demonstrated that the  $X^{Y^*}O$  univalent is incapable of achieving full self-synapsis (Burgoyne and Mahadevaiah, 1993). Since  $X^{Y^*}O$  males are not deficient in X or Y-specific gene dosage, this arrest is likely to be attributable to PAR pairing failure, providing further support for the existence of a checkpoint monitoring synapsis and suggesting the  $X^{Y^*}O$  mouse as a useful model for studying this checkpoint.

We routinely produce  $X^{Y^*}O$  males by mating  $XY^*$  males to females heterozygous for the X inversion  $In(X)1H$  (Evans and Phillips, 1975). Following the introduction of the X-linked marker *Tabby* (*Ta*) into the  $XY^*$  fathers of this production cross, in order to allow identification of their  $X^{Y^*}O$  (hemizygous *Ta*) sons without the need for karyotyping, an exceptional  $X^{Y^*}O$  male was identified that had testes greater than 100mg (c.f. the expected 30-50mg) and a sperm count of  $1.6 \times 10^6$  sperm/caput epididymis. A breeding stock of fertile  $X^{Y^*}O$  males was subsequently established. Initially, three possibilities were considered that might explain the fertility of these males: 1) that the introduction of *Ta*, or other changes in the genetic background, might have increased the ability of the  $X^{Y^*}$  chromosome to self synapse (and thereby avoid elimination), 2) that a deletion in the

pseudoautosomal region might have encompassed sequences required to precipitate elimination, or 3) that a heritable factor(s) arising through mutation, or present in the genetic background, might have circumvented the elimination mechanism. An increase in  $X^{Y^*}$  self-synapsis was ruled out based on pachytene SC analysis (Rodriguez, T.A; PhD thesis, 1997). Although it is known that the compound PAR of the  $X^{Y^*}$  chromosome is deleted for the distal PAR marker *Sts* (Burgoyne *et al.*, 1998), this is not specific to the fertile  $X^{Y^*}$  pedigree. Furthermore, since fertile  $X^{Y^*}O$  males could give rise to fertile or sterile  $X^{Y^*}O$  offspring (all of which would have inherited the same  $X^{Y^*}$  chromosome from their father) the possibility of a further PAR deletion being responsible for the fertility was rejected. Finally, since a significantly higher percentage of fertile males were produced from mating  $X^{Ta}Y^*$  males to the XO daughters of fertile  $X^{Y^*}O$  males (which inherit a maternal X chromosome) than to In(X)/X females (41% vs. 18%,  $\chi^2=8.8$ ,  $p<0.005$ ; Figure 5.2a,b), it was concluded that one or more heritable factors of autosomal origin must be involved (Rodriguez, T.A; PhD thesis, 1997).

Subsequent analysis of a large body of sperm count data indicated that at least two unlinked factors were contributing to the sperm counts. The first (termed the 'major factor') produced sperm counts of 200,000 - 800,000 sperm/caput, and when in combination with the second (termed the 'minor factor') sperm counts increased to greater than 800,000 sperm/caput (Figure 5.2c,d). Initial analysis of  $X^{Y^*}O$  mice from the second group indicated that the minor factor is dominant (7 out of 13 fertile  $X^{Y^*}O$  sons had sperm counts greater than 800,000; Rodriguez, T.A; PhD thesis, 1997).



Since the appearance of fertile  $X^{Y^*}O$  males was coincident with the introduction of *Ta*, one or both of these autosomal factors might have been introduced with this marker. *Ta* was maintained on a mixed 129, C3H, 101 and MF1 strain background. The existence of C3H in the genetic background was of particular interest in light of an analysis of the genetics of interspecific hybrid sterility by Forejt and Ivanyi (1975). Hybrid sterility is the result of a spermatogenic arrest associated with high levels of sex chromosome asynapsis (Matsuda *et al.*, 1992). Forejt *et al.* (1991) identified a chromosome 17 locus, *Hst1*, linked to the H2 complex, as being required for such sterility. Importantly, the C3H strain carries an allele at this locus that allows interspecific hybrid males to be fertile. The sperm counts of both T(14;15)6Ca and T(X;4)37H males are also augmented when on a C3H background (Forejt, 1976; Mahadevaiah *et al.*, 1988). It was therefore conceivable that inheritance of the C3H *Hst1* allele was responsible for the fertility of the  $X^{Y^*}O$  males in this study. This possibility was tested by linkage analysis of fertile and sterile  $X^{Y^*}O$  males using a marker that resided close to the *Hst1* locus. The strain source and mode of inheritance of the  $X^{Y^*}O$  fertility was also investigated in parallel by mating  $XY^*$  males with known strain inputs (e.g. MF1, C3H, 129) to In(X)/X females. Finally, the fertile  $X^{Y^*}O$  males were used as a source of the factors that abrogate the 'synapsis' checkpoint, in an attempt to circumvent this meiotic checkpoint in another sex chromosomally aberrant genotype, the  $X^{Y^*}Y^{Tdym1}$  male.

Figure 5.1. Diagrammatic representation of the  $XY^*$  rearrangement and of the products of its recombination with the X chromosome. The  $Y^*$  chromosome is essentially a Y chromosome that has been hijacked by a non-Y centromere added distally to the PAR, the original centromere being inactivated. In conjunction with this addition, there has been deletion and addition of PAR material. The resulting compound PAR consists of a region of proximal X-derived PAR (together with X-specific sequences adjacent to the X PAR boundary) and a region of proximal Y-derived PAR in opposite orientations; there is no distal PAR, and thus no *Steroid sulphatase* (*Sts*) locus. During meiosis in  $XY^*$  males, synapsis and crossing-over generates two recombinant chromosomes:  $X^{Y^*}$ , comprising the X chromosome with a Y attached via the compound PAR and that is therefore deleted for *Sts*, and  $Y^{*X}$ , comprising the non-Y centromere with the segment of X-specific DNA adjacent to the PAR boundary and a normal PAR (Burgoyne *et al.*, 1998).

XPB = X PAR boundary, YPB = Y PAR boundary,  $+^{Paf}$  = wild type allele of the *Paf* locus, that was added along with the non-Y centromere and distal X PAR.

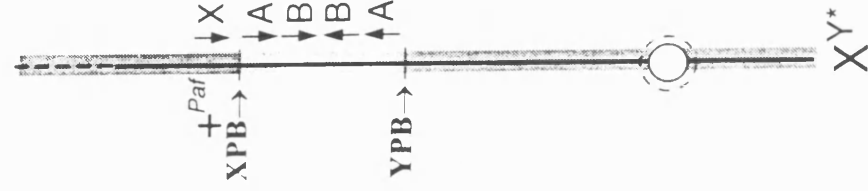
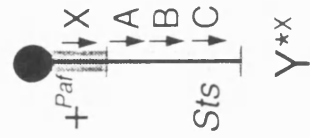
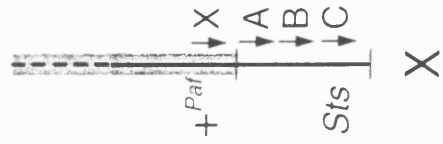
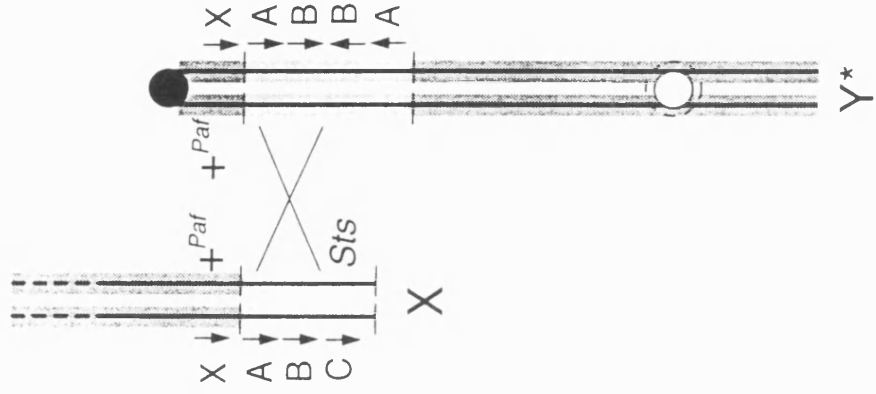


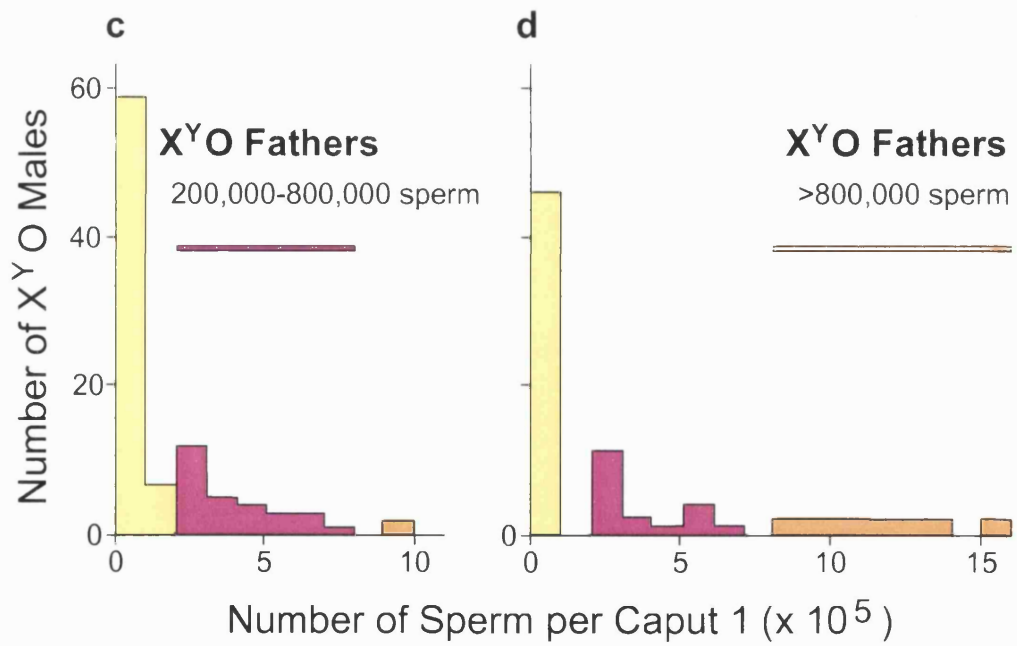
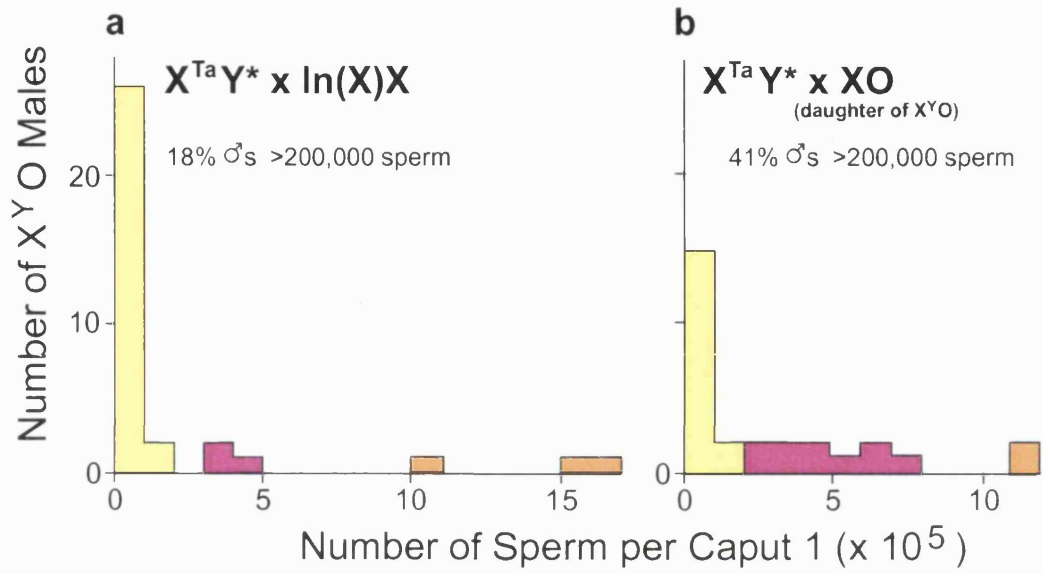
Figure 5.2. Sperm count distributions from  $X^{TaY^*}O$  males generated by the following crosses:

a)  $X^{TaY^*} \times \text{In}(X)/X$ .

b)  $X^{TaY^*} \times XO$  (daughter of fertile  $X^{TaY^*}O$ )

c) Fertile  $X^{TaY^*}O$  males with sperm counts 200,000 – 800,000 (major factor only)  $\times$   $\text{In}(X)/X$ . These males produce sterile sons or sons with the major factor.

d) Fertile  $X^{TaY^*}O$  males with sperm counts  $> 800,000$  (major and minor factors)  $\times$   $\text{In}(X)/X$ . These males produce sterile sons, sons with the major factor and sons with the major and minor factors.



## 5.2 MATERIALS AND METHODS

### 5.2.1 Breeding crosses

#### 5.2.1.1 $XY^*$ x In(X)/X

This was the cross routinely used for generating  $X^{Y^*}O$  males. In(X)/X mothers, that produce 'O' gametes following crossing over within the inversion (Evans and Phillips, 1975), are much easier to produce and are more fertile than XO mothers.  $XY^*$  males of known genetic background (either C3H/MF1, 129/MF1 or MF1) were mated to these In(X)/X females. The gametes produced by  $XY^*$  males are displayed in Figure 5.1.  $X^{Y^*}O$  offspring were distinguished from their  $XY^*$  and  $XX^{Y^*}$  brothers by bone marrow karyotyping (see Appendix 1.1) and by PCR for the steroid sulphatase (*Sts*) gene. *Sts* is a PAR-located gene that is deleted in the  $X^{Y^*}$  and  $Y^*$  chromosomes (Burgoyne *et al.*, 1998).  $X^{Y^*}O$  males are therefore *Sts*-negative, whilst  $XY^*$  and  $XX^{Y^*}$  males are *Sts*-positive. The autosomal *myogenin* gene was used as an amplification control (see section 2.2.8).

#### 5.2.1.2 $XY^*$ x XO

After determining the effect of MF1, C3H and 129  $XY^*$  paternal input on  $X^{Y^*}O$  sperm counts in matings with In(X)/X females, further crosses were carried out using XO females of known genetic background (MF1 or C3H) in order to determine the mode of inheritance of these effects. The  $X^{Y^*}O$  offspring were distinguished from their  $XY^*$  and  $XX^{Y^*}$  brothers as described in section 5.2.1.1.

#### 5.2.1.3 $X^{TaY^*}O$ (fertile) x In(X)/X or XO

Once fertile  $X^{Y^*}O$  males had been produced, these were mated to In(X)/X or XO females in order to generate more  $X^{Y^*}O$  males. These crosses also allowed an analysis of the effects of

different maternal genetic background on  $X^{Y^*}O$  sperm counts, since the  $In(X)/X$  had a mixed C3H/101/CXBH/MF1 background and the  $XO$ 's, an MF1 background. The  $X^{TaY^*}O$  offspring were distinguished from their  $X^{Ta}X^{Y^*}$  brothers because of their hemizygous  $Ta$  phenotype.

#### 5.2.1.4 $X^{TaY^*}O$ (fertile) x $XY^{Tdym1}$ or $XO$ (?carrier)

$XY^{Tdym1}$  mice are female due to a 11kb deletion encompassing the testis-determining gene *Sry* (Gubbay *et al.*, 1992). Although frequently poor breeders, they are capable of producing, amongst others, 'O' and ' $Y^{Tdym1}$ ', gametes, and as such can generate  $X^{TaY^*}O$  and  $X^{TaY^*}Y^{Tdym1}$  males when bred with fertile  $X^{TaY^*}O$  males. The initial  $XY^{Tdym1}$  females used in this cross had fertile  $X^{TaY^*}O$  fathers and hence also had a chance of carrying the factors responsible for the fertility of their fathers (hereafter termed ' $X^{Y^*}O$  fertility factors'). Four different male genotypes are generated by this cross; these are distinguished using the  $Ta$  marker and by PCR using *Sts* and *Muty3* primers to detect the  $X^{TaY^*}$  and  $Y^{Tdym1}$  chromosomes, respectively (Section 5.2.1.8):

		SPERM	MARKERS		
		$X^{TaY^*}$			
		MALE OFFSPRING	$Ta$	<i>Sts</i>	<i>Muty3</i>
E	X	$XX^{TaY^*}$	heterozygous	+	-
G	$Y^{Tdym1}$	$X^{TaY^*}Y^{Tdym1}$	hemizygous	+	+
G	$XY^{Tdym1}$	$XX^{TaY^*}Y^{Tdym1}$	heterozygous	+	+
S	O	$X^{TaY^*}O$	hemizygous	-	-

PCR for *myogenin* was used as an amplification control (see section 2.2.8). This cross was used to test whether the sperm counts of  $X^{Y^*}Y^{Tdym1}$  males could also be augmented by the  $X^{Y^*}O$  fertility factors (initial analysis on an MF1 background demonstrated that  $X^{Y^*}Y^{Tdym1}$  males are aspermic; Rodriguez, T.A; PhD thesis, 1997). In addition, intercrossing between

fertile  $X^{TaY^*}O$  males and further  $XY^{Tdym1}$  females generated by this cross, or between fertile  $X^{TaY^*}O$  sons and XO daughters was carried out to increase the chance of homozygosity for the  $X^{Y^*}O$  fertility factors.

#### 5.2.1.5 $XY^* \times XY^{Tdym1}$

This mating was used to generate control  $X^{Y^*}Y^{Tdym1}$  and  $X^{Y^*}O$  males on an MF1 background to serve as controls for the previous cross. Males were PCR-genotyped as described in section 5.2.1.4. Since the *Ta* marker was not used in this cross, males were also karyotyped using bone marrow in order to distinguish between  $X^{Y^*}Y^{Tdym1}$  and  $XX^{Y^*}Y^{Tdym1}$  males (see Appendix 1.1).

#### 5.2.2 Sperm counts

Sperm counts were estimated from the initial segment of the caput epididymis (Mahadevaiah *et al.*, 1998). Whole epididymides were dissected and then the initial segments of the capita were removed by cutting at the height of the third vein using fresh scalpel blades (Swann Morton). These segments were then placed in 0.1ml 1% trisodium citrate (BDH) before being macerated with scalpel blades. The final volume was made up to 1ml and sperm counts were estimated from these sperm suspensions using an Improved Neubauer Haemocytometer (Weber, England).

#### 5.2.3 Genomic DNA extraction

Genomic DNA was extracted from tail tips as described in Appendix 1.2



#### 5.2.4 PCR procedure

Genomic PCRs were carried out as described in Appendix 1.5. Genomic PCR primers used were:

*Sts* (STSF 5' GCT CGC TGA CAT CAT CCT C 3', STSR 5' CAC CGA TGC CCA GGT CGT C 3',  $T_m = 58^{\circ}\text{C}$ , product = 101bp; Salido *et al.*, 1996).

Muty3 (Muty3 5' GTG TCT CAA AGC CTG CTC TTC 3',  $T_m = 58^{\circ}\text{C}$ , product = 550bp; N. Vivian, pers. comm). This single primer is located within the inverted repeat that flanks *Sry* and the 11kb *Tdym1* deletion, and thus anneals to both strands. However, there is only amplification when the 11 kb stretch is deleted.

*Tbp* (TBPF 5' GAG TCA TAG CGC CCT GTG GA 3', TBPR 5' ATC CAC TTG CCT CTG CCT CC 3',  $T_m = 60^{\circ}\text{C}$ , product ~ 500bp (C3H) and ~ 400bp (other inbred strains; Gregorova *et al.*, 1996).

## 5.3 RESULTS

### 5.3.1 *Hst1* linkage analysis

In order to test whether the fertility in the  $X^{TaY^*}O$  males was due to inheritance of the C3H allele of *Hst1*, linkage analysis was carried out using primers specific for the TATA-binding protein (*Tbp*) gene (Gregorova *et al.*, 1996). The *Tbp* and *Hst1* genes lie 8.25cM from the centromere of chromosome 17 and show complete linkage with one another (Hamvas *et al.*, 1996; Gregorova *et al.*, 1996). The upstream and downstream *Tbp* primers used (Gregorova *et al.*, 1996) anneal to sequences in intron 1E and exon 2, respectively (the first five exons of the *Tbp* gene have been named 1A-1E; differential use of these exons generates a large number of testis-specific transcripts; Schmidt *et al.*, 1997). The PCR product generated using these primers is reportedly larger in C3H than B10 mice, although the exact size has not been published (Gregorova *et al.*, 1996). Amplification of genomic DNA from mice with different genetic backgrounds verified that the C3H PCR product (approximately 500bp) was larger than that of B10 and all other strains analysed (in every case approximately 400bp; Figure 5.3). For the  $X^{TaY^*}O$  analysis, PCR using *Tbp* primers was carried out on 21 fertile and 26 sterile  $X^{TaY^*}O$  males. Of the 21 fertile males, 4 had inherited the C3H *Tbp* allele, compared to 5 of the 26 sterile males. This indicates that the C3H allele of *Hst1* was not the major or minor factor responsible for the  $X^{TaY^*}O$  fertility in this pedigree.

### 5.3.2 Investigation of the strain source of the fertility factors in the $X^{TaY^*}O$ pedigree

First, MF1  $XY^*$  males were mated to In(X)/X females in order to substantiate an earlier conclusion based on testis weights, that no males with sperm counts in the fertile range were produced using  $XY^*$  fathers from the MF1 based stock. All 17  $X^{Y^*}O$  males generated had sperm counts of <200,000 sperm/caput, although one male did have 198,000 sperm/caput

(Figure 5.4a). This compared with the  $X^{Ta}Y^*$  cross, from which 6 out of 34 males (18%) had sperm counts of >200,000 sperm/caput, 3 of which had >800,000 sperm/caput (Figure 5.4b). These results indicate that both the major and minor factors arose from the stock that contributed the  $X^{Ta}$  chromosome.

As described in section 5.1, *Ta* was maintained on a mixed 129, C3H, 101 and MF1 (random bred) strain background. Since the major and minor factors were not regularly present in the MF1 stock, then they must have originated from the 129, C3H or 101 stocks. C3H/MF1<sub>F1</sub> and 129/MF1<sub>F1</sub>  $XY^*$  males were therefore produced (the 101 strain was not available at NIMR) and mated to In(X)/X females. 17  $X^{Y^*}O$  males were produced from the 129/MF1  $XY^* \times$  In(X)/X cross and all had few if any sperm (Figure 5.4c). However, from the cross with C3H/MF1  $XY^*$  males, 7 out of 24 males (29%) had sperm counts of >200,000 sperm/caput, 3 of which had >800,000 sperm/caput (Figure 5.4d). This frequency was not significantly different from that of the  $X^{Ta}Y^* \times$  In(X)/X mating (18%;  $\chi^2=1.66$ ,  $p=0.1-0.25$ ). Thus it is concluded that although neither the major nor the minor factor is *Hst1*, both factors originate from the C3H stock (Figure 5.4d).

### 5.3.3 The mode of inheritance of the C3H fertility factors

The previous crosses demonstrated that both the major and minor  $X^{Ta}Y^*O$  fertility factors had arisen from the  $X^{Ta}$  stock, and that they were both C3H in origin. The next question to be addressed was the mode of inheritance of the C3H factors. The fact that the provision of a C3H input through the father alone could give rise to fertility initially suggested that the major factor was dominant in nature. However, the In(X)/X mothers in these crosses also had a mixed genetic background that included C3H (C3H/101/CXBH/MF1), and so the C3H

factors could have been recessive, with both the In(X)/X and  $X^{Ta}Y^*$  parents providing a copy of the allele.

In order to circumvent this problem, the In(X)/X females needed to be replaced with 'non-C3H factor-carrying' females. The MF1  $XY^* \times$  In(X)/X cross in section 5.3.2 had demonstrated that neither the major nor the minor factor was present in the MF1 stock. MF1 XO females were therefore used to replace the In(X)/X females in the cross with C3H/MF1  $XY^*$  males. Once again  $X^{Y^*}O$  males with the full range of sperm counts were produced. 3 out of 9 males had sperm counts of  $>200,000$  (a frequency not significantly different from that of the C3H/MF1  $XY^* \times$  In(X)/X cross:  $\chi^2=0.05$ ,  $p=0.75-0.9$ ), and 2 had sperm counts  $>800,000$  (Figure 5.5a,b). Thus the C3H-derived major and minor factors are both dominant.

Sperm counts were also obtained for  $X^{Y^*}O$  males obtained by mating fertile  $X^{Y^*}O$  males to MF1 XO females. 5 out of 23 (22%)  $X^{Y^*}O$  sons had  $>200,000$  sperm/caput, Figure 5.5d), compared to 11 out of 34 males (32%) generated from the  $X^{Y^*}O \times$  In(X)/X cross (Figure 5.5c). These frequencies were not significantly different ( $\chi^2=0.8$ ,  $p=0.25-0.5$ ). The absence of males with sperm counts of  $>800,000$  from the cross with MF1 females simply reflects the fact that their fathers only carried the major factor.

#### 5.3.4 Evidence that a recessive MF1 factor is also required for $X^{Y^*}O$ fertility

If the C3H-derived major and minor 'fertility factors' are dominant, then using one pure C3H parent in matings to produce  $X^{Y^*}O$  males should result in all the  $X^{Y^*}O$  progeny having sperm counts of  $>800,000$ . However, when MF1  $XY^*$  males were mated to C3H XO females, or C3H  $XY^*$  males (backcrossed for three generations and hence 87.5% C3H) were

mated to MF1 XO females, all 8  $X^{Y^*}O$  males produced had very low sperm counts (range 0-3,000 sperm/caput; Figure 5.6a,b). Moreover, mating C3H/MF1  $XY^*$  males to C3H XO females also produced males with low sperm counts (Figure 5.6c). Since in all the previous matings that did produce fertile  $X^{Y^*}O$  males both parents were at least half MF1, it must be concluded that in addition to the dominant C3H factors, there is a requirement for a recessive MF1 factor. In this scenario, 25% of the  $X^{Y^*}O$  males generated by mating C3H/MF1  $XY^*$  males to MF1 females would be expected to be fertile, which is not significantly different from the observed number ( $\chi^2=0.25$ ,  $p=0.5-0.75$ ).

Since in the crosses used to define the strain requirements for fertility, fertile  $X^{Y^*}O$  males had been generated only from C3H/MF1  $XY^*$  fathers, there remained a possibility that in addition to the autosomal factors, there was a requirement for a C3H derived X-linked factor. In order to test whether this was the case, MF1/C3H  $XY^*$  males (in which the X chromosome was MF1 derived) were mated to MF1 XO females. Of the 7  $X^{Y^*}O$  males generated so far, one was fertile with a sperm count of 270,000 (Figure 5.6d). Thus  $X^{Y^*}O$  fertility did not require a C3H-derived X chromosome.

### 5.3.5 Other sex chromosomally aberrant genotypes

The question as to whether introduction of the  $X^{Y^*}O$  fertility factors into other sex chromosomally aberrant genotypes could circumvent the meiotic checkpoint, was addressed with respect to  $X^{Y^*}Y^{Tdyml}$  males. In these males, the  $X^{Y^*}$  and  $Y^{Tdyml}$  chromosomes do not synapse, due to the interstitial position of the  $X^{Y^*}$  PAR (Burgoyne and Mahadevaiah, 1993). Two males of this genotype on an MF1 background had previously proved to be aspermic (Rodriguez, T.A; PhD thesis, 1997) with mean testis weights of 46mg and 50mg. In the

present study, one additional male was generated on this background which was also aspermic, with a mean testis weight of 38mg. By continued intercrossing of fertile  $X^{Y^*}O$  males with  $XY^{Tdyml}$  females, six  $X^{Y^*}Y^{Tdyml}$  males with the potential to carry the major and minor factors were generated (Figure 5.7a). Two of these males had sperm counts of zero. The remaining four males had sperm counts of 34,000, 51,000, 60,000 and 189,000 sperm/caput. Surprisingly, the male with the 60,000 sperm/caput made one of his wives pregnant (with a single foetus). It therefore appeared that the introduction of the fertility factors from the  $X^{TaY^*}O$  stock into the  $X^{Y^*}Y^{Tdyml}$  stock could partially augment sperm counts, but this was insufficient to permit the levels of fertility observed in the  $X^{Y^*}O$  males.

Not surprisingly, continued intercrossing of  $X^{Y^*}O$  males with  $XY^{Tdyml}$  or  $XO$  females that were potential carriers of the  $X^{Y^*}O$  fertility factors (see 5.2.1.4) increased the proportion of fertile  $X^{Y^*}O$ 's, including those with sperm counts greater than 800,000. Of the 12 analysed, 10 had sperm counts ranging from 200,000 - 1,600,000 (Figure 5.7b).

Figure 5.3. Example of *Hst1* linkage analysis using *Tbp* PCR primers, for five fertile and five sterile X<sup>Y\*</sup>O males from the pedigree. Sperm counts (sperm/caput epididymis) are indicated above the gel. PCR on C3H genomic DNA generates a product that is clearly distinguishable from other commonly used strains. Asterisks denote mice that have inherited the C3H allele of *Tbp*. Arrows denote 500bp.

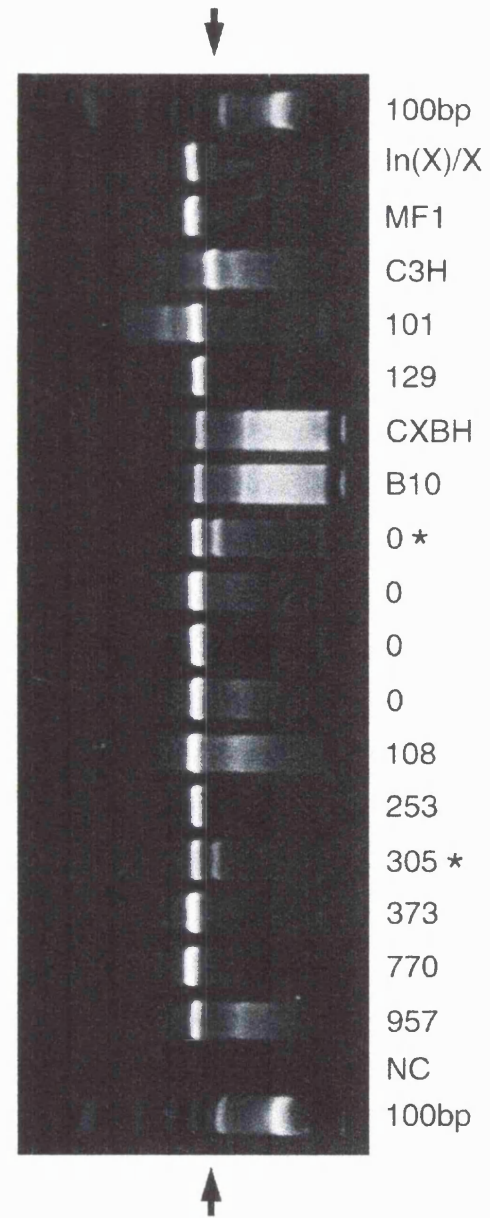
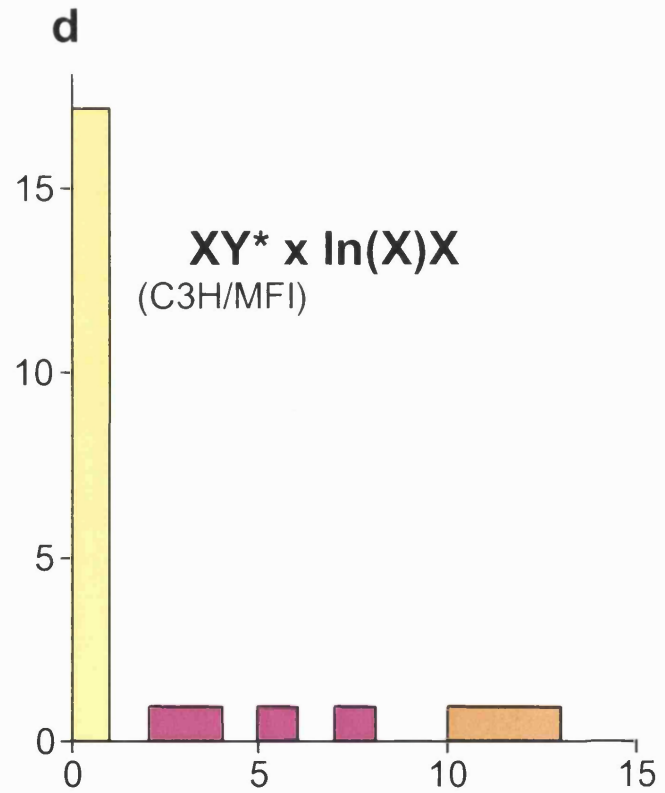
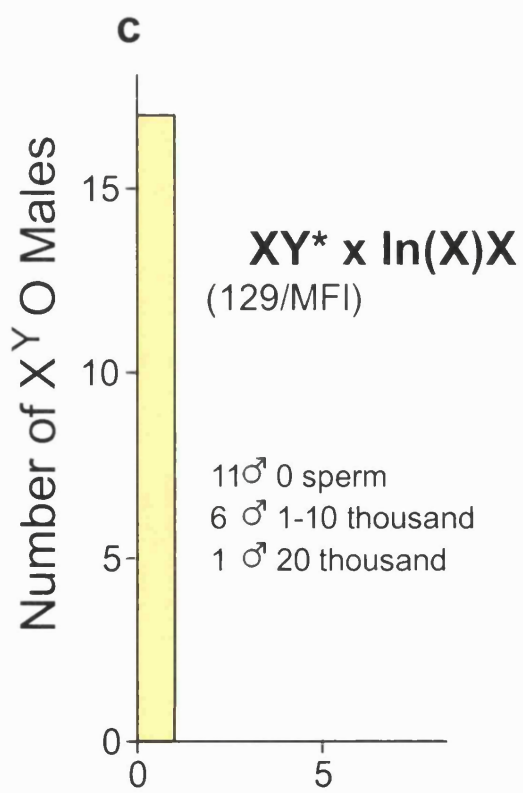
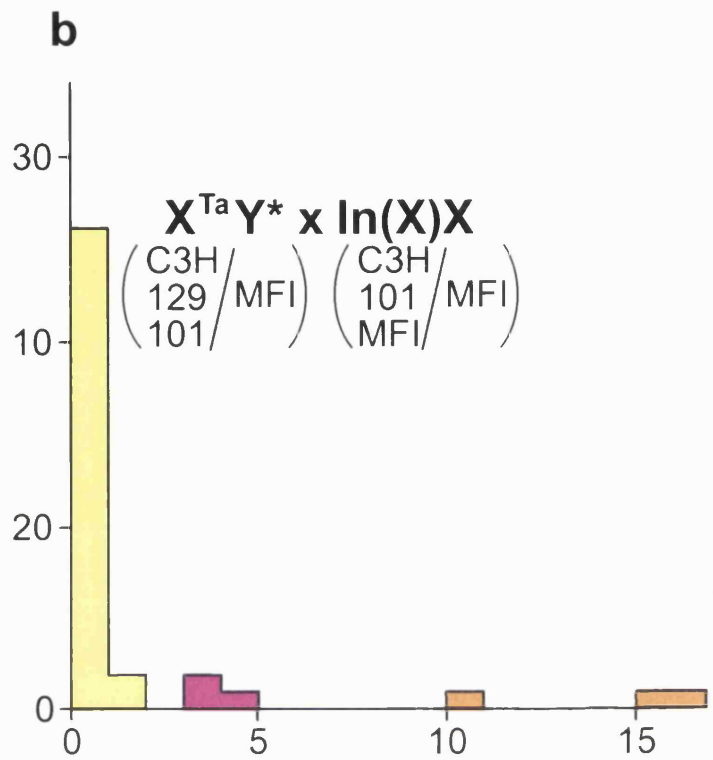
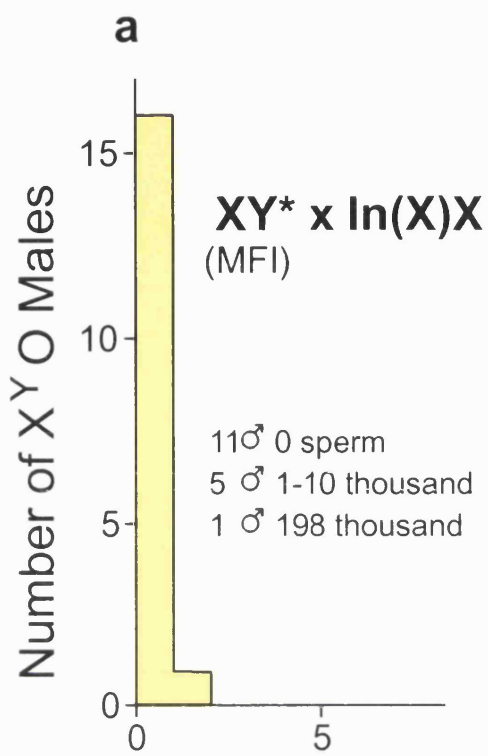




Figure 5.4. Sperm count distributions from  $X^{Y^*}O$  males generated by the following crosses:

- a) MF1  $XY^*$  x In(X)/X.
- b)  $X^{Ta}Y^*$  x In(X)/X (as seen in Figure 5.2).
- c) 129/MF1  $XY^*$  x In(X)/X.
- d) C3H/MF1  $XY^*$  x In(X)/X.



Number of Sperm per Caput 1 (x 10<sup>5</sup>)

Figure 5.5. Sperm count distributions from  $X^{Y^*}O$  males generated by the following crosses:

- a) C3H/MF1  $XY^*$  x In(X)/X (as seen in Figure 5.4d)
- b) C3H/MF1  $XY^*$  x MF1 XO
- c)  $X^{Y^*}O$  x In(X)/X.
- d)  $X^{Y^*}O$  x MF1 XO.

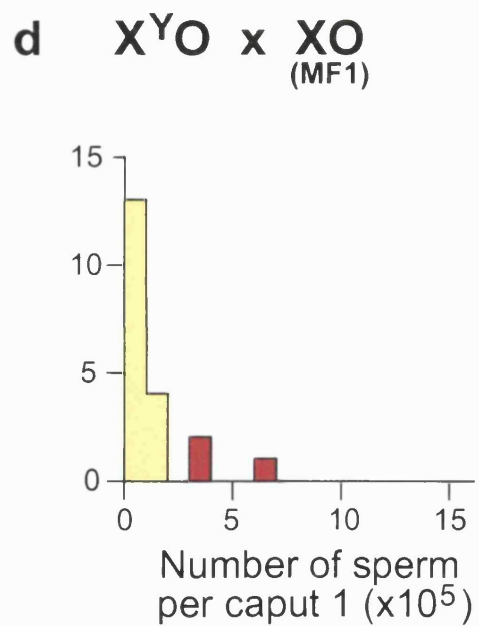
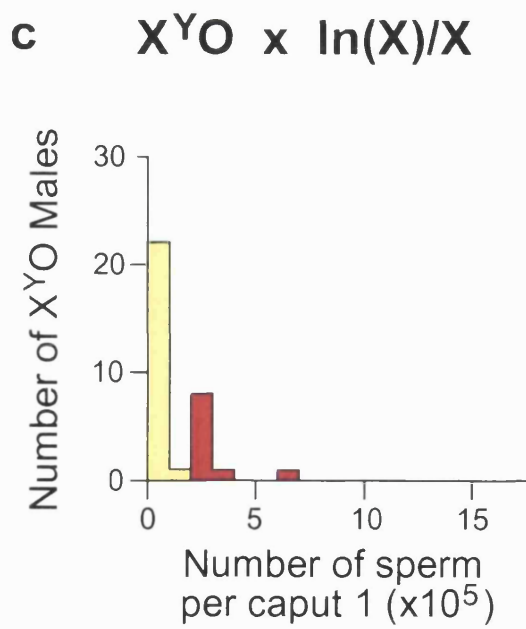
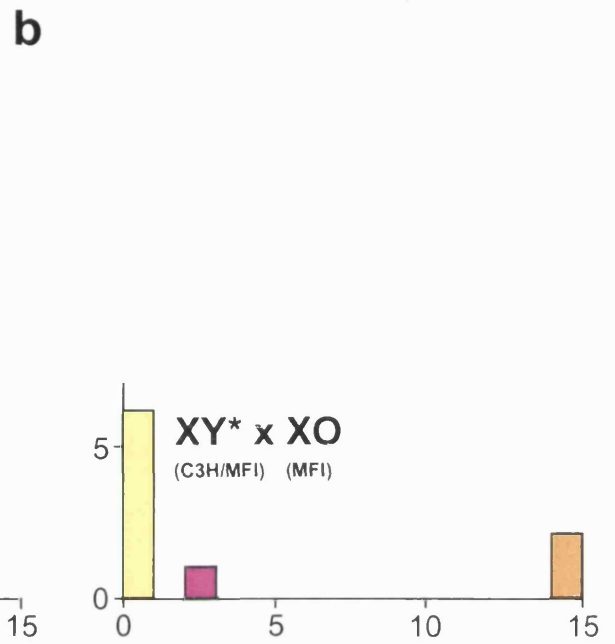
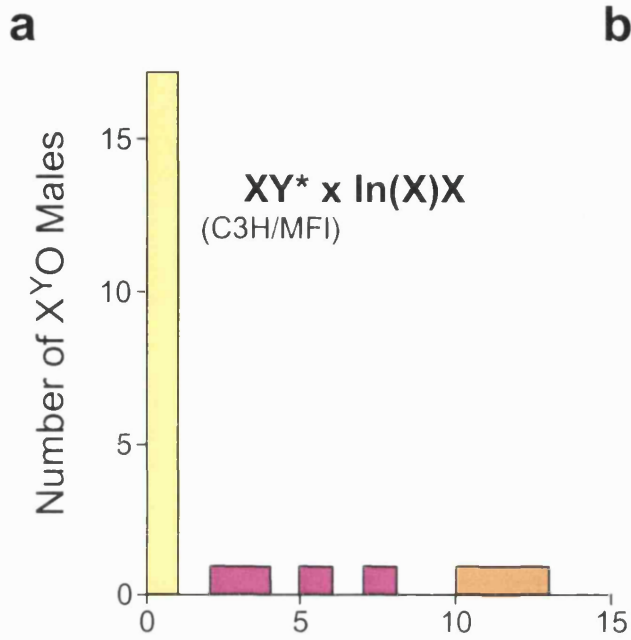
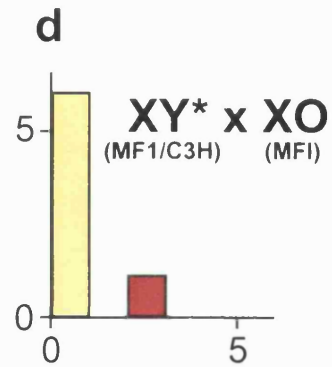
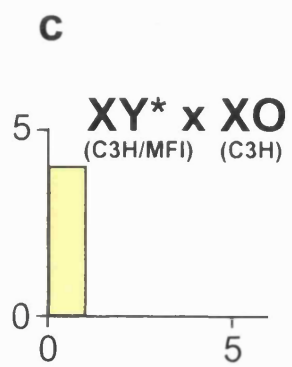
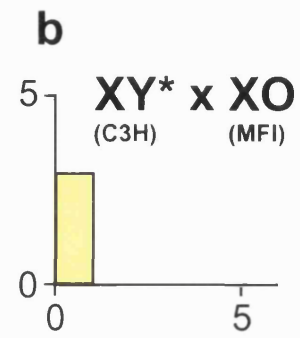
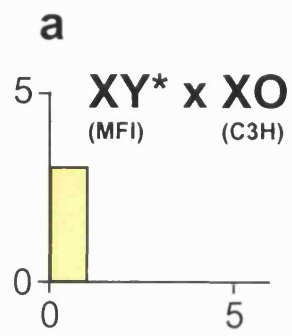


Figure 5.6. Sperm count distributions from  $X^{Y^*}O$  males generated by the following crosses:

- a) MF1  $XY^*$  x C3H XO.
- b) C3H  $XY^*$  x MF1 XO.
- c) C3H/MF1  $XY^*$  x C3H XO.
- d) MF1/C3H  $XY^*$  x MF1 XO.

Number of X<sup>Y</sup> O Males



Number of Sperm per Caput 1 ( $\times 10^5$ )


Figure 5.7. Sperm count distributions from  $X^{Y^*}Y^{Tdyml}$  and  $X^{Y^*}O$  males generated by the following crosses:

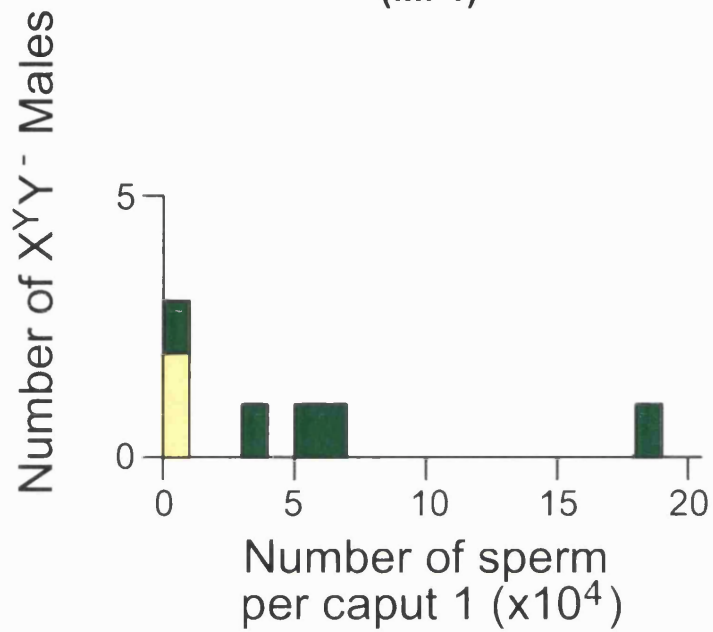
- a)  $X^{Y^*}Y^{Tdyml}$  sperm counts for males from MF1  $XY^*$  x MF1  $XY^{Tdyml}$  and  $X^{Y^*}O$  x  $XY^{Tdyml}$  crosses (the  $XY^{Tdyml}$  mothers were potential major and minor factor carriers).
- b)  $X^{TaY^*}O$  x  $XO$  or  $XY^{Tdyml}$  (the mothers were potential major and minor factor carriers).

Note that sperm/caput scales are different for a) and b).

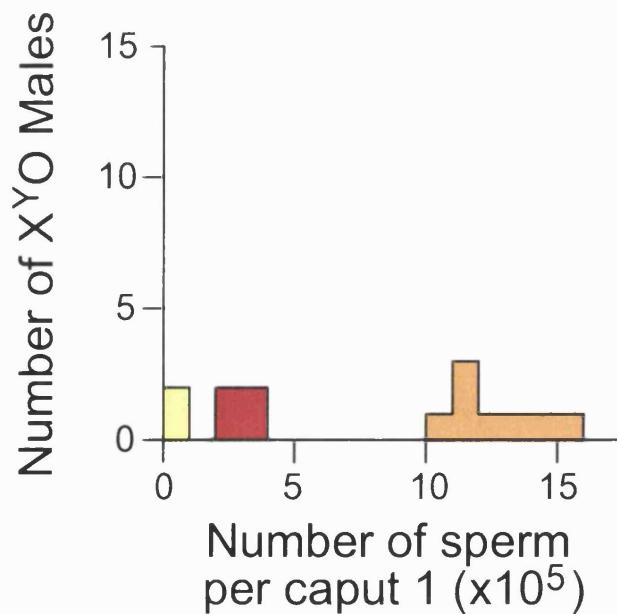
a

$XY^*$  x  $XY^-$    
(MF1) (MF1)

$X^YO$  x  $XY^-$    
(MF1)



b  $X^YO$  x  $XO/XY^-$  (?carrier)





#### 5.4) DISCUSSION

To date, a number of mouse mutants with defects in meiotic synapsis (e.g. *Dmcl*, *Pms2*, *Msh5*) have been described that invariably result in male sterility (Yoshida *et al.*, 1998; Pittman *et al.*, 1998; Baker *et al.*, 1995; Edelman *et al.*, 1999; de Vries *et al.*, 1999). Although such phenotypes support the hypothesis that a synapsis checkpoint exists in higher eukaryotes, they do not shed light on what the checkpoint proteins might be. This is in contrast to yeast, in which a number of genes (e.g. *PCH2*, *SIR2*) have been assigned a checkpoint function based on the finding that their disruption permits the meiotic progression of mutants that would otherwise arrest (e.g. *zip1*, *zip2*, *dmcl*; San-Segundo and Roeder, 1999). In light of this, the fertile X<sup>Y\*</sup>O pedigree described here represents a rare example of a mammalian mutant stock with defects in checkpoint function and so mapping the factors conferring this fertility promises to be very informative. The studies presented here were aimed at addressing three main issues: 1) the possibility that one of the fertility factors might be the C3H allele of *Hst1*, 2) the mode of inheritance and strain source of the factor/s that permitted the fertility, and 3) whether the fertility could be reproduced in other sex chromosomally aberrant genotypes.

The C3H allele of *Hst1* has previously been shown to overcome the sterility of interspecific hybrid male mice (Forejt *et al.*, 1991). Sterility in these mice is associated with a high level of sex chromosome asynapsis (Matsuda *et al.*, 1992). It is therefore likely that the cause of the sterility in these mice is recognition of asynapsed PARs by the pachytene checkpoint. By extrapolation, the *Hst1* gene product is likely to be a component of this checkpoint pathway. Perhaps the C3H *Hst1* gene product is hypomorphic with respect to that of other mouse strains. Since the fertility in the X<sup>Y\*</sup>O pedigree is also likely to be due to attenuated

checkpoint function, it was postulated that inheritance of the C3H allele of *Hst1* was giving rise to the fertility in these males. This possibility was discounted based on the *Tbp* linkage analysis.

Although the  $X^{Y^*}O$  fertility was *Hst1*-independent, it was nevertheless puzzling that inheritance of the C3H allele of *Hst1* could not make the  $X^{Y^*}O$  males fertile (5 of the 9  $X^{Y^*}O$  males that had inherited the C3H *Hst1* allele were sterile). This suggests possible differences in the molecular basis of the infertility of interspecific hybrid and  $X^{Y^*}O$  males.

Having established that neither of the  $X^{Y^*}O$  fertility factors was the C3H allele of *Hst1*, the next experiment sought to determine the source of the  $X^{Y^*}O$  fertility. It was shown that both the major and minor factors arose from the C3H stock, and that both were inherited in a dominant fashion. However, neither of the factors was inherited in a simple Mendelian fashion, indicating either that they were incompletely penetrant, or that additional factors were required in order for them to permit  $X^{Y^*}O$  fertility. The fact that all  $X^{Y^*}O$  males produced from matings in which either the mother or the father was homozygous C3H were sterile, indicated that an additional, recessive factor was required. This factor must be present in the MF1 random bred strain.

At what stage of the pachytene checkpoint might these  $X^{Y^*}O$  fertility factors be acting? Based on the fact that no other developmental abnormalities have been detected in the fertile  $X^{Y^*}O$  males, it is unlikely that these factors act in the apoptotic part of the pachytene checkpoint. It is more likely they are involved in the recognition or signalling of asynapsis. The combination of the three factors characterised above may reduce the sensitivity of the

pachytene checkpoint and thus allow small amounts of asynapsed sex chromosomal material (such as the PAR of  $X^{Y^*}O$  spermatocytes) to escape recognition.

A comparison of sperm counts of  $X^{Y^*}Y^{Tdyml}$  MF1 males with those produced using fertile  $X^{Y^*}O$  fathers revealed that although the addition of the  $X^{Y^*}O$  fertility factors could partially overcome the spermatogenic block, it was incapable of making them fertile (all  $X^{Y^*}O$  siblings of these males were fertile). This suggests that  $X^{Y^*}Y^{Tdyml}$  males are susceptible to an additional problem not experienced by the  $X^{Y^*}O$  males. This is of interest in light of the MSCI defects seen in  $XYY^{d1}$  males. Since  $X^{Y^*}Y^{Tdyml}$  males also possess an extra Y chromosome, they would also be expected to experience similarly defective MSCI. If the fertility factors described in this study do reduce the sensitivity of the pachytene checkpoint to small amounts of asynapsed sex chromosomal material, then the greater amount of asynapsed material in  $X^{Y^*}Y^{Tdyml}$  spermatocytes (at least two PARs and in the event of failure in MSCI, anything up to three sex chromosomes) may exceed this sensitivity limit, causing most cells to be recognised by the checkpoint and therefore to be eliminated.

The next step in this study will be to map and identify the three  $X^{Y^*}O$  fertility factors.

1) Mapping the MF1 factor. Fertile  $X^{Y^*}O$  males will be mated to C57/B10 XX females. C57/B10 is a useful strain for mapping purposes because the sizes of PCR products generated from this strain are generally easily distinguishable from those of other inbred strains. The XO daughters (which will be heterozygous for the MF1 factor and potential carriers of the two C3H factors) will then be mated back to the  $X^{Y^*}O$  fathers in order to generate  $X^{Y^*}O$  sons. The fertile  $X^{Y^*}O$  sons can then be used for mapping purposes. Since

fertility will require homozygosity for the MF1 fertility factor, any locus that shows heterozygosity for C57/B10 can be immediately excluded.

2) Mapping the two C3H fertility factors. C3H/MF1  $X^{Y^*}$  males will be mated to C3H/MF1 XO females to generate fertile and sterile  $X^{Y^*}$ O sons and potential fertility factor-carrying XO daughters. The  $X^{Y^*}$ O sons will be first tested for homozygosity for the MF1 factor using microsatellite markers differing between C3H and MF1, that are as tightly linked as possible to the recessive MF1 factor mapped in 1) above. Males that are homozygous for the MF1 factor will then be used to map the two C3H factors using further markers that are polymorphic between C3H and MF1. Any fertile  $X^{Y^*}$ O sons will be mated to their XO sisters, in order to generate further  $X^{Y^*}$ O males. This cycle will be repeated within each generation, in order to generate large quantities of  $X^{Y^*}$ O males for mapping of the C3H factors.

CHAPTER 6  
GENERAL DISCUSSION

Although meiotic sex chromosome inactivation (MSCI) is highly conserved amongst heterogametic males, very little is known about how it is achieved or what purpose it serves. A large number of proteins have been shown to localise to the sex body and, as a result, have been proposed to play a role in MSCI, but in no case has such a role been proven. However, one study has implicated *Xist*, a gene known to be essential for somatic X-inactivation, in the process of MSCI. Ayoub *et al.* (1997) demonstrated that *Xist* coats both the X chromosome and the Y chromosome in the sex body, leading them to speculate that *Xist* mediates MSCI and that inactivation of the Y chromosome proceeds by a spreading of *Xist* (and accompanying inactivation) from the X chromosome via synapsis at the PAR.

The primary aim of the studies described in this thesis was to investigate the validity of the *quasi-cis* model of Ayoub *et al.* (1997). In doing so, a number of other questions were addressed, most importantly the role of sex body-associating proteins and the effect of excess sex chromosome dosage on progression through meiosis.

In chapters 2 and 3, the MSCI-specificity of three proteins was analysed using females with X-Y, X, or autosomal synaptic failure. Both ASY and XMR/XLR associated with asynapsed sex chromosomes and autosomes in pachytene oocytes. It was therefore concluded that these proteins located to the sex body due to the asynaptic, rather than transcriptionally inactive nature of the sex chromosomes. These results suggest that other sex body proteins might be serving similar asynapsis-related, and not MSCI-related roles, and that all previously characterised and new sex body proteins should be subject to the same analysis in females with asynapsed chromosomes. It was suggested that ASY might function in DSB repair in the absence of synapsis or in alerting the meiocyte to asynapsis, and that XMR/XLR might

function in recombination. The fact that recombination proteins (eg XMR/XLR, MRE11, RAD50; present study and Goedecke *et al.*, 1999) accumulate in the sex body is important because it contradicts the hypothesis of McKee and Handel (1993), who proposed that MSCI serves to prevent such events from occurring in the X and Y chromosomes.

Unlike ASY and XMR/XLR, XY77 was MSCI-specific and therefore used, together with surface spread analysis, to assess the MSCI and sex body status of spermatocytes from mice with an *Xist*-disruption and from those with deficient X-Y synapsis (XYY<sup>d1</sup> males). The results opposed the predictions of the *quasi-cis* model, indicating that this model is no longer tenable. However, XYY<sup>d1</sup> spermatocytes displayed defects in both sex body formation and Y chromosome inactivation. These defects were not seen in XYY<sup>\*X</sup> spermatocytes, indicating that the addition of extra sex chromatin disrupts sex chromosome inactivation, possibly by increasing the time required to complete sex body formation and MSCI. In addition, defective spermatocytes were eliminated prior to late pachytene. These results are important because they suggest that sex body formation/MSCI is indispensable for meiosis and that excess sex chromatin, as well as asynapsis, contributes to the sterility of XYY males.

In the future, it would be interesting to examine the MSCI status of the X chromosome in XYY<sup>d1</sup> spermatocytes. This experiment was not carried out in chapter 4, because an antiserum to an X-linked protein (subject to MSCI) that would not crossreact with the corresponding autosomal back-up could not be found. A possible solution to this problem might be provided by a recently published mouse line that carries an X-linked EGFP transgene (Hadjanotonakis *et al.*, 1998). It has been reported that this transgene is subject to somatic X-inactivation (Hadjanotonakis *et al.*, 1998). Should this transgene also be subject

to MSCI, then it could be used to follow X chromosome inactivation in  $XYY^{d1}$  spermatocytes. Experiments to test this possibility are presently underway.

The finding of univalent Y chromosomes in the sex body supports a model in which inactivation of one sex chromosome is independent of another. This is intriguing when added to the many reports that asynapsed autosomal chromatin also associates with the sex body, because it tempts the speculation that MSCI might occur in response to asynapsis and independent of chromosome identity. At first sight, this may seem at variance with the sterility of  $X^{Y^*}O$  and  $XSxr^aO$  males, since in these cases the asynapsed PAR is thought to remain euchromatic and in doing so to trigger the pachytene checkpoint (Burgoyne and Mahadevaiah, 1993). However, while it has been demonstrated that the PAR-located *Sts* gene escapes MSCI in normal males (where PAR synapsis predominates; Raman and Das, 1991), the expression of this gene in  $XSxr^aO$  males and of genes on asynapsed autosomal axes that associate with the sex body has never been analysed.

It is difficult to distinguish at present whether the loss of spermatocytes in males with excess sex chromosomes is due to inappropriate sex-linked gene expression (Lifschytz and Lindsley, 1972) or to triggering of the pachytene checkpoint by uncondensed sex chromosomes (Jablonka and Lamb, 1988; McKee and Handel, 1993). This is because the former is an inevitable consequence of the latter. At first sight, the fact that spermatocytes with malformed sex bodies were eliminated regardless of their RBM status suggested that the failure to condense the sex chromosomes was sufficient to cause elimination, and therefore that the primary role of MSCI is to shield the sex chromosomes from the pachytene checkpoint, as suggested by Jablonka and Lamb (1988). However, these spermatocytes may



have been misexpressing other sex-linked genes. If many different sex-linked genes are in themselves poisonous to spermatocytes, then expression of any one of these in  $XY Y^{d1}$  spermatocytes may have caused cell death. In theory, the effect of a candidate 'poisonous' sex-linked gene on spermatogenesis could be assayed by generating males in which a transgenic copy of the gene of interest is integrated at an autosomal site and is therefore not subject to MSCI. However, in light of the dearth of such candidates, this approach is unlikely to be a particularly fruitful one.

Although Lifschytz and Lindsley (1972) formed the view that the primary function of MSCI is to silence sex-linked gene expression, a series of cogent arguments by both Jablonka and Lamb (1988) and McKee and Handel (1993; described in detail in section 1.2.2) suggest that this is not the case. To reiterate briefly, inactivation of the whole sex chromosome set may be viewed as a rather exaggerated response to the requirement to inactivate selected sex-linked genes, and organisms in which the male is the homogametic sex do not undergo MSCI. Also, a number of organisms have designed ways of compensating for the loss of sex-linked gene products during the period of MSCI, such as compensatory hyperactivation of the X chromosome prior to meiosis, or activation of autosomal backups during meiosis (reviewed by McKee and Handel, 1993). McKee and Handel (1993) provided an extensive review of the distribution of MSCI across different species, and concluded that MSCI was a feature of heterogametic, chiasmatic males. It was the relative infrequency of MSCI in achiasmatic males (eg *Drosophila*) that led to these authors suggesting a role for MSCI in preventing the initiation of recombination.

The recent finding that phosphorylated H2AX (and therefore DSBs) accumulates in the sex body (Mahadevaiah, Turner and Burgoyne, unpublished) indicate that McKee and Handel are not correct in their supposition that MSCI prevents the formation of DSBs (McKee and Handel, 1993). However, their observation that MSCI is restricted to chiasmatic species is still likely to be important in reinterpreting the possible functions of MSCI. As mentioned in section 1.2.1, KU70, a protein required in non-homologous end-joining (NHEJ), has been localised to the sex body during pachytene and diplotene (Goedecke *et al.*, 1999). It has been proposed that KU70 is recruited to the sex body in order to facilitate NHEJ (Goedecke *et al.*, 1999). This suggestion is supported by the finding of DSBs in the sex body (Mahadevaiah, Turner and Burgoyne, unpublished). Interestingly, phosphorylated H2AX also appears to assemble on the asynapsed X chromosome in  $XY^{Tdyml}$  oocytes (Mahadevaiah, Turner and Burgoyne, unpublished). Analysis of KU70 in  $XY^{Tdyml}$  oocytes will therefore be very important. Should KU70 not coat the asynapsed X chromosome in  $XY^{Tdyml}$  oocytes, then this would suggest that the sex body is a unique in its ability to attract NHEJ proteins, and thereby repair DSBs. This would explain the requirement of sex body formation in chiasmatic organisms (McKee and Handel, 1993), and would suggest that the unresolved DSBs in asynapsed autosomes or PARs provide the trigger for the pachytene checkpoint. Alternatively, if KU70 does coat the asynapsed X chromosome in  $XY^{Tdyml}$  oocytes, then this would suggest that asynapsed autosomes also possess the potential to be repaired by NHEJ. Under this model, asynapsis and not unresolved DSBs may provide the trigger for the synapsis checkpoint, and the sex body may shield the asynapsed portions of the X and Y chromosomes from checkpoint recognition, as suggested by Jablonka and Lamb (1988).

Perhaps one of the least considered but most likely roles for MSCI could be to facilitate synapsis between the X and Y PARs. As described in chapter 2, MSCI is absent in  $XY^{Tdyml}$  oocytes and X PAR-Y PAR synapsis is severely reduced. Inactivation of the X and Y non-PAR regions may focus the homology search that precedes synapsis on the X and Y PARs. In the absence of MSCI (eg  $XY^{Tdyml}$  oocytes), transient, unstable interactions between areas of weak homology in the non-PAR regions of the X and Y chromosomes may disrupt X PAR-Y PAR interactions, the result being that few meiocytes achieve any synapsis at all.

In conclusion, the present results have indicated that some of the traditional views concerning the role and genetic control of MSCI require rethinking. They have also posed a number of new questions. In particular, if not *Xist*-mediated, how is MSCI controlled? Do the sex chromosomes possess sequences that 'mark' them for inactivation, or is MSCI initiated as a response to asynapsis? If this is so, how does the cell differentiate asynapsed from synapsed axes? Also, how do non-inactivated sex chromosomes precipitate cell elimination and which sex body proteins really are involved in MSCI?

In the final chapter, a series of classical genetic experiments were described that sought to determine the basis of the circumvention of the pachytene checkpoint that occurred in an exceptional pedigree of fertile  $X^{Y^*}O$  males. The study established that at least three factors were responsible for the fertility. The first, or major factor, that was associated with the C3H background and that was inherited in a dominant fashion, produced sperm counts of between 200,000 and 800,000 sperm/caput. The second, or minor factor, which was also associated with the C3H background and was also inherited in a dominant fashion, acted as a modifier of the major factor, by producing sperm counts of greater than 800,000 sperm/caput. Neither

of these factors was the C3H allele of *Hst1*. Finally, fertility required a recessive factor present in the MF1 stock. These fertility factors were unable to augment the sperm counts of  $X^{Y^*}Y^{Tdyml}$  males to the same degree as  $X^{Y^*}O$  males, possibly as a result of the additional defects in MSCI that would be predicted to occur in  $X^{Y^*}Y^{Tdyml}$  males. Whether MSCI is compromised in these mice is now being addressed. Clearly it would be of great value to map and clone the factors that give rise to the fertility in the  $X^{Y^*}O$  males, and thereby identify the molecular components of the pachytene checkpoint.

## APPENDIX 1

## 1.1 Karyotyping of mice

- Karyotyping from liver (Mahadevaiah *et al.*, 1993).

A 2-3 mm<sup>3</sup> piece of liver obtained from freshly killed 18.5dpc female foetuses was placed in 1 ml 0.08 mg ml<sup>-1</sup> colcemid (Sigma) in Hepes-buffered DMEM (Sigma) in a round bottomed 100 X 16mm plastic tube (Sterilin). The cells were dissociated by pipetting and were incubated for 10 mins at 31<sup>0</sup>C, before being pelleted by spinning for 5 minutes at 250g. The pellet was then resuspended in 1 ml 0.56% KCl (BDH) and incubated for 20 mins at room temperature. The cells were then pelleted as described above and the pelleted cells were washed carefully with fix (3:1 methanol:glacial acetic acid; BDH) 4-5 times by running fix down one side of the tube without disturbing the pellet, before resuspending in an appropriate amount of fix (dependent on the number of cells). Three drops of cell suspension were then placed on acid alcohol (BDH) cleaned slides and were air dried at room temperature. Slides were subsequently stained with 2% Giemsa (BDH) in pH 7.6 buffered solution (BDH) for 15 mins. The karyotype was determined under a 100X objective (Olympus) with oil.

- Karyotyping from bone marrow (Mahadevaiah *et al.*, 1993).

Both femurs from freshly killed mice was dissected and flushed with 0.5 ml 0.08 mg ml<sup>-1</sup> colcemid (Sigma) in Hepes-buffered DMEM (Sigma) into a round bottomed 100 X 16mm plastic tube (Sterilin) using a 25G X 0.625'' needle (Sherwood Medical). The cells were incubated for 10 mins at 31<sup>0</sup>C and processed as described for the liver preparations (see above).

### 1.2 Genomic DNA extraction

Tail tips removed either under local anaesthetic or from freshly killed mice and digested in 100µl digestion buffer (0.1M NaCl, 0.05M Tris pH8, 0.1M EDTA pH8, 1% SDS; all BDH) and 5µl proteinase K (20mg ml<sup>-1</sup>; Sigma) overnight at 55°C. 100µl phenol/chloroform/isoamyl alcohol (25:24:1; BDH) was then added and the resulting mixture was vortexed briefly and centrifuged at 12,000g at room temperature for 5 mins. The aqueous layer was removed and transferred to a fresh 1.5 ml Eppendorf tube containing 200µl 100% ethanol (BDH). DNA was precipitated by centrifuging as described above, after which the ethanol was removed and the DNA pellets allowed to dry at room temperature for 20 mins. The pellets were then dissolved in 500µl distilled water.

### 1.3 Total RNA extraction

- Testis

Total RNA was extracted using Trizol® (Gibco BRL) by a modification of the Chomczynski and Sacchi method (1987). 80-100 mg adult testis samples were homogenised in 1 ml Trizol® using a 1 ml syringe and 19G X 1.5'' needle (Sherwood Medical). The homogenates were allowed to stand at room temperature for 10 mins, after which they were spun at 12,000g at 4°C for 10 mins. The resulting supernatants were transferred to fresh tubes and 0.2 ml chloroform (BDH) added. Tubes were shaken briefly and then left at room temperature for 3 mins. The samples were then spun as described above. The supernatant was then removed and transferred to a fresh tube, to which 0.5 ml isopropanol (BDH) was added. Samples were incubated at room temperature for 10 mins and then spun as described above. The resulting pellets were washed in 1 ml 75% ethanol (BDH), spun at 7,500g at 4°C

for 5 mins, and then allowed to dry at room temperature. The pellets were finally redissolved in 50µl water containing 2% DEPC (Sigma) and stored at  $-80^{\circ}\text{C}$  until further use.

- Ovaries

Total RNA extraction from ovaries was similar to that of testis, with added modifications due to the small amounts of tissue. One pair of ovaries was homogenised in 70µl Trizol®. There was no post-homogenisation spin, and seven pairs of ovaries (constituting 490 µl Trizol®) were pooled before adding 100 µl chloroform. 5 µl of  $2 \mu\text{g } \mu\text{l}^{-1}$  linear polyacrylamide (LPA; Gaillard and Strauss, 1990) was added to the supernatant prior to the addition of 250 µl isopropanol. Pellets were redissolved in 25 µl DEPC (Sigma) water.

#### 1.4 DNase treatment and reverse transcription of total RNA

7.5 µl total RNA was treated with 3 µl RQ DNase I ( $1 \text{ U } \mu\text{l}^{-1}$  Promega) buffered with 4.5 µl 5 X First Strand cDNA Synthesis buffer (Gibco BRL) at  $37^{\circ}\text{C}$  for 30 mins. The enzyme was inactivated by heating to  $95^{\circ}\text{C}$  for 5 mins.

For reverse transcription, 1.5 µl 5 X First Strand cDNA Synthesis buffer (Gibco BRL), 1.5 µl  $500 \mu\text{g } \text{ml}^{-1}$  oligo-dT primer (Gibco BRL), 3 µl 0.1 M DTT (Gibco BRL), 4.5 µl 15mM dNTPs (Pharmacia) and 3 µl DEPC water were added to the 15 µl post-RQ DNase mixture to give a final volume of 28.5 µl. The mixture was incubated at  $70^{\circ}\text{C}$  for 10 mins. Next, 19 µl were removed and 1 µl Superscript II (Gibco BRL) was added. For a –RT control, 0.5 µl DEPC (Sigma) was added to the remaining 9.5 µl. Both reactions were incubated at  $42^{\circ}\text{C}$  for 50 mins. The reactions were terminated by heating to  $70^{\circ}\text{C}$  for 15 mins.



### 1.5 PCR procedure

PCRs were carried out in 25  $\mu$ l reactions containing 5  $\mu$ l 5 X PCR buffer (250 mM Tris pH 9.0; BDH, 75 mM ammonium sulphate; BDH, 35 mM magnesium chloride; BDH, 0.85 mg ml<sup>-1</sup> BSA; Sigma, 0.25% NP40; BDH), 10  $\mu$ l 3.75 mM dNTPs (Pharmacia) and 0.5  $\mu$ l 5 U  $\mu$ l<sup>-1</sup> AmpliTaq® DNA polymerase (Perkin-Elmer). Genomic PCRs were carried out using 5  $\mu$ l DNA derived as described in section 1.2, with the remaining 4.5  $\mu$ l consisting of forward and reverse primers at quantities dependent upon stock concentrations (see individual chapters) plus water. RT PCRs were carried out using 2  $\mu$ l cDNA derived as described in section 1.3, with the remaining 7.5  $\mu$ l consisting of primers plus water, as described above. The standard PCR cycling procedure was

1 X 95°C for 3 mins,

30 X (95°C for 0.5 min, T<sub>m</sub> for 0.5 min and 72°C for 0.5 min, unless otherwise stated)

1 X 72°C for 5 mins

T<sub>m</sub> specified for each primer pair.

PCR products were run on 2% agarose gels in Orange G loading buffer (Searle Diagnostic) and sized using a 100bp ladder (Promega).

### 1.6 Squash procedure

- Testis

Squashes of spermatogenic cells were carried out according to the procedure of Page *et al* (1998). Testes were dissected from males killed by cervical dislocation and placed in fresh

PBS. Following removal of the tunica albuginea, the tubules were gently shaken, in order to remove adherent extratubular remnants. The tubules were then placed in fresh 2% formaldehyde (TAAB) in PBS containing 0.05% Triton X-100 (BDH) at room temperature for 10 mins. Small pieces of tubules were then placed on fresh ethanol-cleaned slides and teased apart using forceps. The resulting suspension was squashed by applying a 22 X 50mm coverslip (BDH) over the slide and pressing down briefly. The slides were then immersed in liquid nitrogen, after which the coverslips were removed and the slides taken through three 5 min washes in PBS.

- Ovaries

Ovaries were processed in a similar way to testes. Following fixation, ovaries were immediately squashed without teasing them apart first.

### 1.7 Surface spread procedure

- Testis

Surface spreading of spermatogenic cells was carried out according to the procedure of Peters *et al* (1997) with modifications. Testes were dissected from males killed by cervical dislocation and placed in fresh PBS. Following removal of the tunica albuginea, the tubules were gently shaken, in order to remove adherent extratubular remnants. The tubules were then placed in an excess of hypotonic buffer containing 30 mM Tris, 50 mM sucrose, 17 mM trisodium citrate, 5 mM EDTA (all BDH), 0.5mM DTT and 0.5mM PMSF (both Sigma) at room temperature for 30 mins. Tubules were then teased apart in fresh hypotonic solution (approximately 20mg testis tissue per 500  $\mu$ l hypotonic), and the resulting suspension transferred to a 1.5 ml Eppendorf tube, after which the cells were further disaggregated by

pipetting up and down 10 – 15 times. One drop of the solution was then placed on fresh ethanol-cleaned slides (BDH), after which 250 µl 2% formaldehyde (TAAB) in PBS containing 0.05% Triton X-100 (BDH) was pipetted on top. The cells were fixed for 30 mins, and then slides were dipped briefly in distilled water and placed on a slide rack to air-dry for 30 mins at room temperature.

- Ovaries

Ovaries were processed in a similar way to testes. Ovaries were teased apart using two 25G X 0.625’’ needles (Sherwood Medical) in 30 µl hypotonic solution.

### 1.8 Immunostaining

Following PBS washing (for squash procedure) or air-drying (spread procedure), slides were placed in PBT (0.15% BSA; Sigma, 0.1% Tween-20; BDH in PBS) for one hour at room temperature. Following slight draining of excess PBT, 100 µl of the appropriate primary antibody diluted in PBT was added and a 22 X 50mm coverslip (BDH) placed over the slide. Primary incubations were carried out in a dark, moist chamber overnight at 4°C.

Following primary incubations, slides were taken through three 5 min PBS washes and then the secondary antibody, diluted in PBT, was applied. Slides were incubated in a dark, moist chamber at room temperature for one hour. The slides were then washed three times in PBS, and dried in the dark for 30 mins. Before examination, one drop of Vectorshield® with 1.5 µg ml<sup>-1</sup> DAPI (Vector) was added and a 22 X 50mm coverslip (BDH) applied. The coverslip was stuck down with clear nail varnish (Miners). Slides were kept in the dark at 4°C until viewing.

Antibody dilutions and sources were as follows:

Primary antibody	Dilution		Secondary antibody
	Squash	Spread	
Rabbit anti-rat SCP3 (C.Heyting)	1:1000	1:1000	Sheep anti-rabbit Cy3 (C-2306; Sigma)
Rabbit anti-rat SCP1 (C.Heyting)	1:500	1:500	Sheep anti-rabbit Cy3 (C-2306; Sigma)
Rabbit anti-mouse RNA POLII (C-21; Santa Cruz)	1:100	1:10	Sheep anti-rabbit Cy3 (C-2306; Sigma)
Rabbit anti-mouse RBM (D.Elliott)	1:20	-	Sheep anti-rabbit Cy3 (C-2306; Sigma)
Mouse anti-rat ASY (2E3) (C.Heyting)	1:100	1:100	Goat anti-mouse Alexa 488 (A-11029; Molecular Probes)
Mouse anti-XLR (H.J.Garchon)	1:500	1:500	Goat anti-mouse Alexa 488 (A-11029; Molecular Probes)
Mouse anti-rat XY77 (R.Benavente)	Neat	-	Goat anti-mouse Alexa 488 (A-11029; Molecular Probes)
Fish brain tubulin hybrid.sup (C.Heyting)	1:100	1:100	Goat anti-mouse Alexa 488 (A-11029; Molecular Probes)
MOPC21 IgG (M-9269; Sigma)	1:200	1:200	Goat anti-mouse Alexa 488 (A-11029; Molecular Probes)

### 1.9 Examination

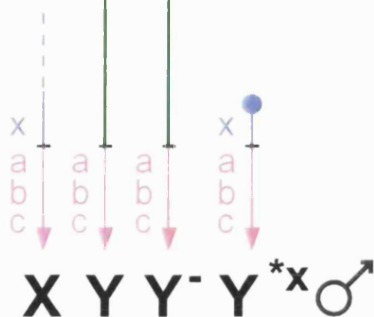
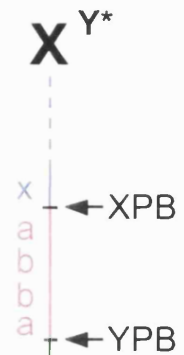
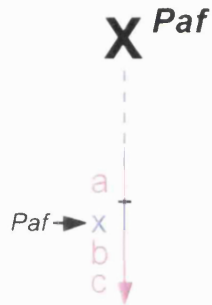
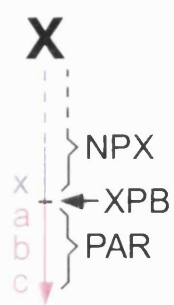
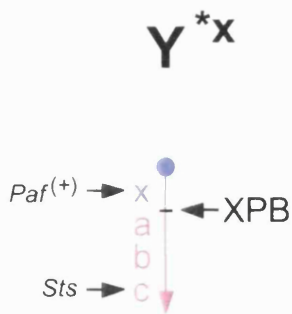
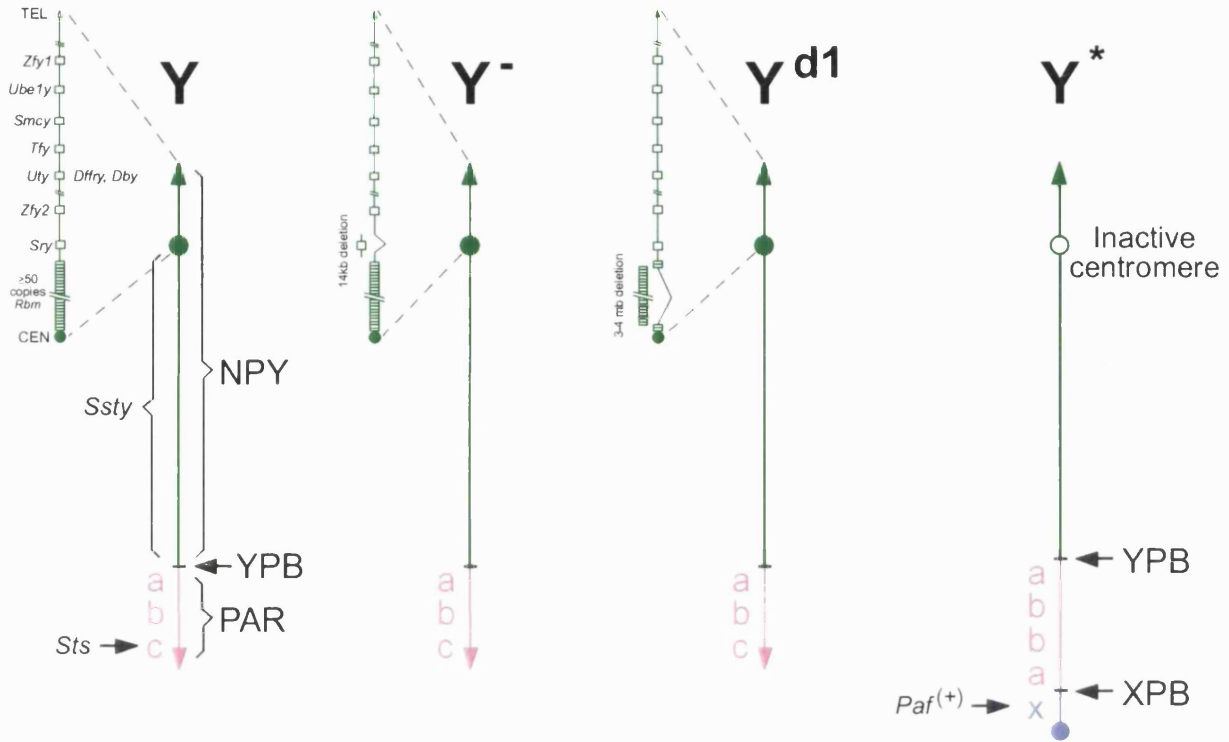
Immunostained stained cells were examined and digitally imaged on an Olympus IX70 inverted microscope with a 100W Mercury arc lamp, using either a 40 X, 0.85 NA UPL APO dry objective (for low power images) or a 100 X, 1.35 U-PLAN-APO oil-immersion objective (for high power images). Each fluorochrome image was captured separately as a 12-bit source image using a computer-assisted (Deltavision) liquid-cooled CCD (Photometrics CH350L; Sensor: Kodak KAF1400, 1317x1035 pixels). A single multiband dichroic mirror was used to eliminate shifts between different filters. Captured images were processed using Adobe Photoshop 5.0.2.

### 1.10 Sex chromosome variants

A summary of the various sex chromosome variants is shown on the following page:

(in this diagram, the  $Y^{Tdyml}$  chromosome is denoted as 'Y').

# Paul Burgoyne's Weird Sex Chromosome Guide



NPY = Non-PAR Y  
 NPX = Non-PAR X  
 YPB = Y PAR boundary  
 XPB = X PAR boundary

## REFERENCES

Abirached-Darmency, M., Zickler, D. and Cauderon, Y. (1983). Synaptonemal complex and recombination nodules in rye (*Secale cereale*). *Chromosoma* 88, 299-306.

Alani, E., Padmore, R. and Kleckner, N. (1990). Analysis of wild-type and *rad50* mutants of yeast suggests an intimate relationship between meiotic chromosome synapsis and recombination. *Cell* 61(3), 419-436.

Anderson, L. K., Stack, S. M., Todd, R. J. and Ellis, R. P. (1994). A monoclonal antibody to lateral element proteins in synaptonemal complexes of *Lilium longiflorum*. *Chromosoma* 103(5), 357-367.

Anderson, L. K., Offenberg, H. H., Verkuijlen, W, H, M, C. and Heyting, C. (1997). RecA-like proteins are components of early meiotic nodules in lily. *Proc. Natl. Acad. Sci. U.S.A* 94(13), 6868-6873.

Armstrong, S. J., Hulten, M. A., Keohane, A. M. and Turner, B. M. (1997). Different strategies of X-inactivation in germinal and somatic cells: histone H4 underacetylation does not mark the inactive X chromosome in the mouse male germline. *Exp. Cell. Res.* 230(2), 399-402.

Ashley, A. (2000). An integration of old and new perspectives of mammalian meiotic sterility. *Results Probl. Cell. Differ.* 28, 131-73.



Ashley, T. and Plug, A. (1998). Caught in the act: deducing meiotic function from protein immunolocalization. *Curr. Top. Dev. Biol.* 37, 201-239.

Ayoub, N., Richler, C. and Wahrman, J. (1997). *Xist* RNA is associated with the transcriptionally inactive XY body in mammalian male meiosis. *Chromosoma.* 106(1), 1-10.

Bahler, J., Wyler, T., Loidl, J. and Kohli, J. (1993). Unusual nuclear structures in meiotic prophase of fission yeast: A cytological analysis. *J. Cell. Biol.* 121(2), 241-256.

Baker, S. M., Plug, A., Prolla, T. A., Bronner, C. E., Harris, A. C., Yao, X., Christie, D. -M., Monell, C., Arnheim, N., Bradley, A., Ashley, T. and Liskay, R. M. (1996). Involvement of mouse *Mlh1* in DNA mismatch repair and meiotic crossing over. *Nat. Genet.* 13(3), 336-342.

Baker, S. M., Bronner, C. E., Zhang, L., Plug, A. W., Robatzek, M., Warren, G., Elliott, E. A., Yu, J., Ashley, T. and Arnheim, N. (1995). Male mice defective in the DNA mismatch repair gene *Pms2* exhibit abnormal chromosome synapsis in meiosis. *Cell* 82(2), 309-319.

Barlow, C., Liyanage, M., Moens, P. B., Deng, C. X., Ried, T. and Wynshaw-Boris, A. (1997). Partial rescue of the prophase I defects of *Atm*-deficient mice by p53 and p21 null alleles. *Nat. Genet.* 17(4), 462-466.

Barlow, C., Liyanage, M., Moens, P. B., Tarsounas, M., Nagashima, K., Brown, K., Rottinghaus, S., Jackson, S. P., Tagle, D., Ried, T. and Wynshaw-Boris, A. (1998). *Atm*

deficiency results in severe meiotic disruption as early as leptotema of prophase I. *Development* 125(20), 4007-4017.

Bauer, U. -M., Schneider-Hirsch, S., Reinhardt, S., Benavente, R. and Maelicke, A. (1998). The murine nuclear *orphan* receptor GCNF is expressed in the XY body of primary spermatocytes. *FEBS Letters*. 439(3), 208-214.

Baumann, P., Benson, F. E. and West, S. C. (1996). Human Rad51 protein promotes ATP-dependent homologous pairing and strand transfer reactions in vitro. *Cell* 87(4), 757-766.

Becak, M. L. and Becak, W. (1981). Behaviour of the ZW sex bivalent in the snake *Bothrops jararaca*. *Chromosoma* 83(2), 289-293.

Bishop, D. K., Park, D., Xu, L. and Kleckner, N. (1992). DMC1: a meiosis-specific yeast homolog of *E. coli* recA required for recombination, synaptonemal complex formation, and cell cycle progression. *Cell* 69(3), 439-456.

Bojko, M. (1983). Human meiosis. VIII. Chromosome pairing and formation of the synaptonemal complex in oocytes. *Carlsberg Res. Commun.* 48, 457-483.

Borsani, G., Tonlorenzi, R., Simmler, M. C., Dandolo, L., Arnaud, D., Capra, V., Grompe, M., Pizzuti, A., Muzny, D., Lawrence, C. Willard, H. F., Avner, P. and Ballabio, A. (1991). Characterization of a murine gene expressed from the inactive X chromosome. *Nature* 351(6324), 325-329.

Brown, C. J., Lafreniere, R. G., Powers, V. E., Sebastio, G., Ballabio, A., Pettigrew, A. L., Ledbetter D. H., Levy, E., Craig, I. W. and Willard, H. F. (1991). Localization of the X inactivation centre on the human X chromosome in Xq13. *Nature* 349(6304), 82-84.

Burgoyne, P. S. and Baker, T. G. (1984). Meiotic pairing and gametogenic failure. *Symp. Soc. Exp. Biol.* 38, 349-362.

Burgoyne, P. S. and Baker, T. G. (1985). Perinatal oocyte loss in XO mice and its implications for the aetiology of gonadal dysgenesis in XO women. *J. Reprod. Fertil.* 75(2), 633-645.

Burgoyne, P. S., Levy, E. R. and McLaren, A. (1986). Spermatogenic failure in male mice lacking H-Y antigen. *Nature* 320(6058), 170-172.

Burgoyne, P. S. (1988). Role of mammalian Y chromosome in sex determination. *Philos. Trans. R. Soc. Lond. B. Biol. Sci.* 322(1208), 63-72.

Burgoyne, P. S. and Mahadevaiah, S. K. (1993). Unpaired sex chromosomes and gametogenic failure. *Chromosomes Today* 11, 243-263.

Burgoyne, P. S., Mahadevaiah, S. K., Perry, J., Palmer, S. J. and Ashworth, A. (1998). The Y\* rearrangement in mice: new insights into a perplexing PAR. *Cytogenet. Cell Genet.* 80(1-4), 37-40.

Burgoyne, P. S., Mahadevaiah, S. K., Sutcliffe, M. J. and Palmer, S. J. (1992). Fertility in mice requires X-Y pairing and a Y-chromosomal "spermiogenesis" gene mapping to the long arm. *Cell* 71(3), 391-398.

Calenda, A., Allenet, B., Escalier, D., Bach, J. -F. and Garchon, H. -J. (1994). The meiosis-specific *Xmr* gene product is homologous to the lymphocyte XLR protein and is a component of the XY body. *EMBO*. 13(1), 100-109.

Cao, L., Alani, E. and Kleckner, N. (1990). A pathway for generation and processing of double-strand breaks during meiotic recombination in *S. cerevisiae*. *Cell* 61(6), 1089-1101.

Carpenter, A. T. (1975). Electron microscopy of meiosis in *Drosophila melanogaster* females: II. The recombination nodule - a recombination-associated structure at pachytene? *Proc. Natl. Acad. Sci. U.S.A* 72(8), 3186-3189.

Carpenter, A. T. (1988). Thoughts on recombination nodules, meiotic recombination, and chiasmata. In: *Genetic Recombination* (eds Kucherlapati, R and Smith, G. R), 529-548. American Society for Microbiology, Washington, DC.

Cattanach, B. M., Pollard, C. E. and Hawker, S. G. (1971). Sex-reversed mice: XX and XO males. *Cytogenetics* 10(5), 318-337.

Cattanach, B. M., Rasberry, C., Burtenshaw, M. D. and Evans, E. P. (1990). Illegitimate pairing of the X and Y chromosomes in Sxr mice. *Genet. Res.* 56(2-3), 121-128.

Chandley, A. C. and Fletcher, J. M. (1980). Meiosis in Sxr male mice. I. Does a Y-autosome rearrangement exist in sex-reversed (Sxr) mice? *Chromosoma* 81(1), 9-17.

Chomczynski, P. and Sacchi, N. (1987). Single-step method of RNA isolation by acid guanidinium thiocyanate-phenol-chloroform extraction. *Anal. Biochem.* 162(1), 156-159.

Chua, P. R. and Roeder, G. S. (1998). Zip2, a meiosis-specific protein required for the initiation of chromosome synapsis. *Cell* 93(3), 349-359.

Chen, Q., Pearlman, R. E. and Moens, P. B. (1992). Isolation and characterization of a cDNA encoding a synaptonemal complex protein. *Biochem. Cell. Biol.* 70(10-11), 1030-1038.

Church, K. (1979). The grasshopper X chromosome. II. Negative heteropycnosis, transcription activities and compartmentation during spermatogonial stages. *Chromosoma* 71(3), 359-370.

Cohen, D. I., Hedrick, S. M., Nielsen, E. A., D'Eustachio, P., Ruddle, F., Steinberg, A. D., Paul, W. E. and Davis, M. M. (1985). Isolation of a cDNA clone corresponding to an X-linked gene family (*Xlr*) closely linked to the murine immunodeficiency disorder *xid*. *Nature.* 314(6009). 369-372.

Cohen, D. I., Steinberg, A. D., Paul, W. E. and Davis, M. M. (1985). Expression of an X-linked gene family (XLR) in late stage B cells and its alteration by the *xid* mutation. *Nature*. *314*(6009), 372-374.

Daza, P., Reichenberger, S., Gottlich, B., Hagmann, M., Feldmann, E. and Pfeiffer, P. (1996). Mechanisms of nonhomologous DNA end-joining in frogs, mice and men. *Biol. Chem.* *377*(12), 775-786.

De Baart, E., de Rooij, D. G., Keegan, K. and de Boer, P. Distribution of ATR protein in primary spermatocytes of a chromosomal mouse mutant: a comparison of preparation techniques. Submitted.

De Boer, P. and de Jong, J. H. (1989). Chromosome pairing and fertility in mice. In: *Fertility and chromosome pairing: recent studies in plants and animals* (ed Gillies, C. B), 37-76. CRC Press, Boca Raton, Florida.

de Vries, S. S., Baart, E. B., Dekker, M., Siezen, A., de Rooij, D. G., de Boer, P. and te Riele, H. (1999). Mouse MutS-like protein MSH5 is required for proper chromosome synapsis in male and female meiosis. *Genes Dev.* *13*(5), 523-531.

Dernburg, A. F., McDonald, K., Moulder, G., Barstead, R., Dresser, M. and Villeneuve, A. M. (1998). Meiotic recombination in *C. elegans* initiates by a conserved mechanism and is dispensable for homologous chromosome synapsis. *Cell* *94*(3), 387-398.

Dobson, M. J., Pearlman, R. E., Karaiskakis, A., Spyropoulos, B. and Moens, P. B. (1994) Synaptonemal complex proteins: occurrence, epitope mapping and chromosome disjunction. *J. Cell. Sci.* *107(10)*, 2749-2760.

Edelmann, W., Cohen, P. E., Kneitz, B., Winand, N., Lia, M., Heyer, J., Kolodner, R., Pollard, J. W. and Kucherlapati, R. (1999). Mammalian MutS homologue 5 is required for chromosome pairing in meiosis. *Nat. Genet.* *21(1)*, 123-127.

Egel-Mitani, M., Olson, L. W., Egel, R. (1982) Meiosis in *Aspergillus nidulans*: another example for lacking synaptonemal complexes in the absence of crossover interference. *Hereditas.* *97(2)*, 179-187.

Eicher, E. M., Hale, D. W., Hunt, P. A., Lee, B. K., Tucker, P. K., King, T. R., Eppig, J. T. and Washburn L. L. (1991). The mouse Y\* chromosome involves a complex rearrangement, including interstitial positioning of the pseudoautosomal region. *Cytogenet. Cell Genet.* *57(4)*, 221-230.

Eicher, E. M. and Washburn, L. L. (1986). Genetic control of primary sex determination in mice. *Annu. Rev. Genet.* *20*, 327-360.

Escalier, D., Allenet, B., Badrichani, A. and Garchon, H. J. (1999). High level expression of the XLR nuclear protein in immature thymocytes and colocalization with the matrix-associated region-binding SATB1 protein. *J. Immunol.* *162(1)*, 292-298.

Evans, E. P. and Phillips, R. J. (1975). Inversion heterozygosity and the origin of XO daughters of Bpa/+ female mice. *Nature* 256(5512), 40-41.

Evans, E. P., Burtenshaw, M. D. and Brown, B. B. (1980). Meiosis in Sxr male mice: II. Further absence of cytological evidence for a Y-autosome rearrangement in sex-reversed (Sxr) mice. *Chromosoma* 81(1), 19-26.

Fawcett, D. W. (1956). The fine structure of chromosomes in the meiotic prophase of vertebrate spermatocytes. *Journal of Biophysical and Biochemical Cytology* 2, 403-406.

Forejt, J. and Ivanyi, P. (1975). Genetic studies on male sterility of hybrids between laboratory and wild mice (*Mus musculus L.*). *Genet. Res.* 24(2), 189-206.

Forejt, J. (1976). Spermatogenic failure of translocation heterozygotes affected by H-2-linked gene in mouse. *Nature* 260(5547), 143-145.

Forejt, J. (1982). X-Y involvement in male sterility caused by autosome translocations – a hypothesis. In: Genetic control of gamete production and function (eds Crosignani, P. G and Rubin, B. L), 135-151. Academic Press, New York.

Forejt, J., Vincek, V., Klein, J., Lehrach, H. and Loudova-Mickova, M. (1991). Genetic mapping of the t-complex region on mouse chromosome 17 including the Hybrid sterility-1 gene. *Mamm. Genome* 1(2), 84-91.



Freire, R., Murguia, J. R., Tarsounas, M., Lowndes, N. F., Moens, P. B. and Jackson, S. P. (1998). Human and mouse homologs of *Schizosaccharomyces pombe* rad1(+) and *Saccharomyces cerevisiae* RAD17: linkage to checkpoint control and mammalian meiosis. *Genes Dev.* *12*(16), 2560-2573.

Gaillard, C. and Strauss, F. (1990). Ethanol precipitation of DNA with linear polyacrylamide as carrier. *Nucleic Acids Res.* *18*(2), 378.

Garchon, H. -J., Loh, E. L., Ho, W. Y., Amar, L., Avner, P. and Davis, M. M. (1989). The *Xlr* sequence family: dispersion on the X and Y chromosomes of a large set of closely related sequences, most of which are pseudogenes. *Nucl. Acids. Res.* *17*(23), 9871-9888.

Goedecke, W., Eijpe, M., Offenbergh, H. H., van Aalderen, M. and Heyting, C. (1999). MRE11 and KU70 interact in somatic cells, but are differentially expressed in early meiosis. *Nat. Genet.* *23*(2), 194-198.

Goetz, P., Chandley, A. C. and Speed, R. M. (1984). Morphological and temporal sequence of meiotic prophase development at puberty in the male mouse. *J. Cell Sci.* *65*, 249-263.

Grant, M., Zuccotti, M. and Monk, M. (1992). Methylation of CpG sites of two X-linked genes coincides with X-inactivation in the female mouse embryo but not in the germ line. *Nat. Genet.* *2*(2), 161-166.

Gregorova, S., Mnukova-Fajdelova, M., Trachtulec, Z., Capkova, J., Loudova, M., Hoglund, M., Hamvas, R., Lehrach, H., Vincek, V., Klein, J. and Forejt, J. (1996). Sub-milliMorgan map of the proximal part of mouse Chromosome 1 including the *hybrid sterility 1* gene. *Mamm. Genome* 7(2), 107-113.

Gubbay, J., Collignon, J., Koopman, P., Capel, B., Economou, A., Munsterberg, A., Vivian, N., Goodfellow, P. and Lovell-Badge, R. (1990). A gene mapping to the sex-determining region of the mouse Y chromosome is a member of a novel family of embryonically expressed genes. *Nature* 346(6281), 245-250.

Hale, D. W., Hunt, P. A., Tucker, P. K. and Eicher, E. M. (1991). Synapsis and obligate recombination between the sex chromosomes of male laboratory mice carrying the Y\* rearrangement. *Cytogenet. Cell Genet.* 57(4), 231-239.

Hamvas, R. M., Artzt, K., Fischer-Lindahl, K., Trachtulec, Z., Vernet, C. and Forejt, J. (1997). Mouse chromosome 17. *Mamm. Genome* 7, Spec No:S274-S294.

Handel, M. A., Park, C. and Kot, M. (1994). Genetic control of sex-chromosome inactivation during male meiosis. *Cytogenet. Cell Genet.* 66(2), 83-88.

Hendriksen, P. J., Hoogerbrugge, J. W., Themmen, A. P., Koken, M. H., Hoeijmakers, J. H., Oostra, B. A., van der Lende, T. and Grootegoed, J. A. (1995). Postmeiotic transcription of X and Y chromosomal genes during spermatogenesis in the mouse. *Dev. Biol.* 170(2), 730-733.

Heng, H. H., Tsui, L. C. and Moens, P. B. (1994). Organization of heterologous DNA inserts on the mouse meiotic chromosome core. *Chromosoma* 103(6), 401-407.

Heng, H. H., Chamberlain, J. W., Shi, X. M., Spyropoulos, B., Tsui, L. C. and Moens, P.B. (1996). Regulation of meiotic chromatin loop size by chromosomal position. *Proc. Natl. Acad. Sci. U.S.A* 93(7), 2795-2800.

Heyting, C., Dietrich, A. J., Moens, P. B., Dettmers, R. J., Offenberg, H. H., Redeker, E.J. and Vink, A. C. (1989) Synaptonemal complex proteins. *Genome* 31(1), 81-87.

Heyting, C. and Dietrich, A. J. (1991). Meiotic chromosome preparation and protein labelling. *Methods Cell Biol.* 35, 177-202.

Hiraoka, Y., Dernburg, A. F., Parmelee, S. J., Rykowski, M. C., Agard, D. A. and Sedat, J. W. (1993). The onset of homologous chromosome pairing during *Drosophila melanogaster* embryogenesis. *J. Cell Biol.* 120(3), 591-600.

Hogg, H. and McLaren, A. (1985). Absence of a sex vesicle in meiotic foetal germ cells is consistent with an XY sex chromosome constitution. *J. Embryol. Exp. Morphol.* 88, 327-332.

Holboth, P. (1981). Chromosome pairing in allohexaploid wheat var. Chinese Spring. Transformation of multivalents into bivalents, a mechanism for exclusive bivalent formation. *Carlsberg Res. Commun.* 46, 129-173.

Hollingsworth, N. M. and Byers, B. (1989). *HOP1*: a yeast meiotic pairing gene. *Genetics* 121(3), 445-462.

Hollingsworth, N. M., Ponte, L. and Halsey, C. (1995). *MSH5*, a novel MutS homolog, facilitates meiotic reciprocal recombination between homologs in *Saccharomyces cerevisiae* but not mismatch repair. *Genes Dev.* 9(14), 1728-1739.

Hotta, Y. and Chandley, A. C. (1982). Activities of X-linked enzymes in spermatocytes of mice rendered sterile by chromosomal alterations. *Gamete Res.* 6, 65-72.

Hunt, P. A. (1991). Survival of XO mouse fetuses: effect of parental origin of the X chromosome or uterine environment? *Development* 111(4), 1137-1141.

Hunt, P. A. and Eicher, E. M. (1991). Fertile male mice with three sex chromosomes: evidence that infertility in XYY male mice is an effect of two Y chromosomes. *Chromosoma* 100(5), 293-299.

Hunter, N. and Borts, R. H. (1997). Mlh1 is unique among mismatch repair proteins in its ability to promote crossing-over during meiosis. *Genes Dev.* 11(12), 1573-1582.

Iannello, R. C. and Dahl, H. H. (1992). Transcriptional expression of a testis-specific variant of the mouse pyruvate dehydrogenase E1 alpha subunit. *Biol. Reprod.* *47(1)*, 48-58.

Ivanov, E. L., Korolev, V.G. and Fabre, F. (1992). *XRS2*, a DNA repair gene of *Saccharomyces cerevisiae*, is needed for meiotic recombination. *Genetics* *132(3)*, 651-664.

Jaafar, H., Gabriel-Robez, O. and Rumpler, Y. (1989). Pattern of ribonucleic acid synthesis in vitro in primary spermatocytes from mouse testis carrying an X-autosome translocation. *Chromosoma* *98(5)*, 330-334.

Jablonka, E. and Lamb, M. J. (1988). Meiotic pairing constraints and the activity of sex chromosomes. *J. Theor. Biol.* *133(1)*, 23-36.

Jinks-Robertson, S. and Petes, T. D. (1985). High-frequency meiotic gene conversion between repeated genes on nonhomologous chromosomes in yeast. *Proc. Natl. Acad. Sci. U.S.A* *82(10)*, 3350-3354.

Johzuka, K. and Ogawa, H. (1995). Interaction of Mre11 and Rad50: two proteins required for DNA repair and meiosis-specific double-strand break formation in *Saccharomyces cerevisiae*. *Genetics* *139(4)*, 1521-1532.

Kay, G. F., Penny, G. D., Patel, D., Ashworth, A., Brockdorff, N. and Rastan S. (1993). Expression of *Xist* during mouse development suggests a role in the initiation of X chromosome inactivation. *Cell* *72(2)*, 171-182.

Keegan, K. S., Holtzman, D. A., Plug, A. W., Christenson, E. R., Brainerd, E. E., Flaggs, G., Bentley, N. J., Taylor, E. M., Meyn, M. S., Moss, S. B., Carr, A. M., Ashley, T. and Hoekstra, M. F. (1996). The ATR and ATM protein kinases associate with different sites along meiotically pairing chromosomes. *Genes Dev.* *10(19)*, 2423-2437.

Keeney, S., Giroux, C. N. and Kleckner, N. (1997). Meiosis-specific DNA double-strand breaks are catalyzed by Spo11, a member of a widely conserved protein family. *Cell* *88(3)*, 375-384.

Kleckner, N. and Weiner, B. M. (1993). Potential advantages of unstable interactions for pairing of chromosomes in meiotic, somatic, and premeiotic cells. *Cold Spring Harb. Symp. Quant. Biol.* *58*, 553-565.

Kleckner, N. (1996). Meiosis: how could it work? *Proc. Natl. Acad. Sci. U.S.A* *93(16)*, 8167-8174.

Koopman, P., Gubbay, J., Vivian, N., Goodfellow, P. and Lovell-Badge, R. (1991). Male development of chromosomally female mice transgenic for *Sry*. *Nature* *351(6322)*, 117-121.

Kralewski, M., Novello, A. and Benavente, R. (1997). A novel Mr 77, 000 protein of the XY body of mammalian spermatocytes: its localisation in normal animals and in Searle's translocation carriers. *Chromosoma.* *106(3)*, 160-167.

Kralewski, M. and Benavente, R. (1997). XY body formation during rat spermatogenesis: an immunocytochemical study using antibodies against XY body-associated proteins. *Chromosoma*. *106*(5), 304-307.

Kundu, S. C., Winking, H. and Gropp, A. (1983). Meiosis in XY sex-reversed female mice. Abstract 271. XVth International Congress on Genetics, New Delhi. Oxford University Press and IBH Publishing Company, New Delhi.

Lammers, J. H. M., Offenbergh, H. H., van Aalderen, M., Vink, A. C. G., Dietrich, A. J. J. and Heyting, C. (1994). The gene encoding a major component of the lateral elements of synaptonemal complexes of the rat is related to X-linked lymphocyte-regulated genes. *Mol. Cell. Biol.* *14*(2), 1137-1146.

Lammers J. H., van Aalderen, M., Peters, A. H., van Pelt, A. A., de Rooij, D. G., de Boer, P., Offenbergh, H. H., Dietrich, A. J. and Heyting, C. (1995). A change in the phosphorylation pattern of the 30000-33000 Mr synaptonemal complex proteins of the rat between early and mid-pachytene. *Chromosoma*, *104*(3), 154-63.

Lane, P. W. and Davisson, M. T. (1990). Patchy fur (*Paf*), a semidominant X-linked gene associated with a high level of X-Y non-disjunction in male mice. *J. Hered.* *81*, 43-50.

LeMaire-Adkins, R., Radke, K. and Hunt, P. A. (1997). Lack of checkpoint control at the metaphase/anaphase transition: a mechanism of meiotic nondisjunction in mammalian females. *J. Cell. Biol.* *139*(7), 1611-1619.

Laval, S. H., Glenister, P. H., Rasberry, C., Thornton, C. E., Mahadevaiah, S. K., Cooke, H. J., Burgoyne, P. S. and Cattanach, B. M. (1995). Y chromosome short arm-Sxr recombination in XSxr/Y males causes deletion of *Rbm* and XY female sex reversal. Proc. Natl. Acad. Sci. U.S.A 92(22), 10403-10407.

Leu, J. Y., Chua, P. R. and Roeder, G. S. (1998). The meiosis-specific Hop2 protein of *S. cerevisiae* ensures synapsis between homologous chromosomes. Cell 94(3), 375-386.

Lifschytz, E. and Lindsley, D. L. (1972). The role of X-chromosome inactivation during spermatogenesis. Proc. Natl. Acad. Sci. U.S.A. 69(1), 182-186.

Loidl, J. (1994). Cytological aspects of meiotic recombination. Experientia 50, 185-294.

Loidl, J., Scherthan, H., Den Dunnen, J.T. and Klein, F. (1995). Morphology of a human-derived YAC in yeast meiosis. Chromosoma 104(3), 183-188.

Lovell-Badge, R. and Robertson, E. (1990). XY female mice resulting from a heritable mutation in the primary testis-determining gene, *Tdy*. Development 109(3), 635-646.

Lustig, A. J. (1999). The Kudos of non-homologous end-joining. Nat. Genet. 23(2), 130-131.

Lydall, D., Nikolsky, Y., Bishop, D. K. and Weinert, T. (1996). A meiotic recombination checkpoint controlled by mitotic checkpoint genes. Nature 383(6603), 840-843.



Mahadevaiah, S., Setterfield, L. A. and Mittwoch, U. (1988). Univalent sex chromosomes in spermatocytes of Sxr-carrying mice. *Chromosoma* 97(2), 145-153.

Mahadevaiah, S. K., Lovell-Badge, R. and Burgoyne, P. S. *Tdy*-negative XY, XXY and XYY female mice: breeding data and synaptonemal complex analysis. *J. Reprod. Fertil.* 97(1), 151-160.

Mahadevaiah, S. K., Odorisio, T., Elliott, D. J., Rattigan, A., Szot, M., Laval, S. H., Washburn, L. L., McCarrey, J. R., Cattanaach, B. M., Lovell-Badge, R. and Burgoyne, P. S. (1998). Mouse homologues of the human AZF candidate gene RBM are expressed in spermatogonia and spermatids, and map to a Y chromosome deletion interval associated with a high incidence of sperm abnormalities. *Hum. Mol. Genet.* 7(4), 715-727.

Marahrens, Y., Panning, B., Dausman, J., Strauss, W. and Jaenisch, R. (1997). *Xist*-deficient mice are defective in dosage compensation but not spermatogenesis. *Genes Dev.* 11(2), 156-166.

Matsuda, Y., Moens, P. B. and Chapman, V. M. (1992). Deficiency of X and Y chromosomal pairing at meiotic prophase in spermatocytes of sterile interspecific hybrids between laboratory mice (*Mus domesticus*) and *Mus spretus*. *Chromosoma* 101(8), 483-492.

McCarrey, J. R., Dilworth, D. D. and Sharp, R. M. (1992). Semiquantitative analysis of X-linked gene expression during spermatogenesis in the mouse: ethidium-bromide staining of RT-PCR products. *Genet. Anal. Tech. Appl.* 9(4), 117-123.

McCarrey, J. R. and Dilworth, D. D. (1992). Expression of *Xist* in mouse germ cells correlates with X-chromosome inactivation. *Nat. Genet.* 2(3), 200-203.

McKee, A. H. and Kleckner, N. (1997). Mutations in *Saccharomyces cerevisiae* that block meiotic prophase chromosome metabolism and confer cell cycle arrest at pachytene identify two new meiosis-specific genes *SAE1* and *SAE3*. *Genetics* 146(3), 817-834.

McKee, B. D. and Handel, M. A. (1993). Sex chromosomes, recombination, and chromatin conformation. *Chromosoma* 102(2), 71-80.

McKee, B. D. and Karpen, G. H. (1990). *Drosophila* ribosomal RNA genes function as an X-Y pairing site during male meiosis. *Cell* 61(1), 61-72.

McKim, K. S., Green-Marroquin, B. L., Sekelsky, J. J., Chin, G., Steinberg, C., Khodosh, R. and Hawley, R. S. (1998). Meiotic synapsis in the absence of recombination. *Science* 279(5352), 876-878.

Melton, D. W., Konecki, D. S., Brennand, J. and Caskey, C. T. (1984). Structure, expression and mutation of the hypoxanthine phosphoribosyl transferase gene. *Proc. Natl. Acad. Sci. U.S.A* 81(7), 2147-2151.

Meuwissen, R. L., Offenber, H. H., Dietrich, A. J., Riesewijk, A., van Iersel, M. and Heyting, C. (1992). A coiled-coil related protein specific for synapsed regions of meiotic prophase chromosomes. *EMBO J.* 11(13), 5091-5100.

Miklos, G. L. G. (1974). Sex chromosome pairing and male fertility. *Cytogenet. Cell Genet.* *13(6)*, 558-577.

Mills, K. D., Sinclair, D. A. and Guarente, L. (1999). MEC1-dependent redistribution of the Sir3 silencing protein from telomeres to DNA double-strand breaks. *Cell* *97(5)*, 609-620.

Miyazaki, W. Y. and Orr-Weaver, T. L. (1994). Sister-chromatid cohesion in mitosis and meiosis. *Annu. Rev. Genet.* *28*, 167-187.

Moore, D. P. and Orr-Weaver, T. L. (1998). Chromosome segregation during meiosis: building an unambivalent bivalent. *Curr. Top. Dev. Biol.* *37*, 263-299.

Moens, P. B., Chen, D. J., Shen, Z., Kolas, N., Tarsounas, M., Heng, H. H. Q. and Spyropoulos, B. (1997). RAD51 immunocytology in rat and mouse spermatocytes and oocytes. *Chromosoma* *106(4)*, 207-215.

Moens, P. B., Pearlman, R. E., Heng, H. H. and Traut, W. (1998). Chromosome cores and chromatin at meiotic prophase. *Curr. Top. Dev. Biol.* *37*, 241-262.

Moens, P. B., Tarsounas, M., Morita, T., Habu, T., Rottinghaus, S. T., Freire, R., Jackson, S. P., Barlow, C. and Wynshaw-Boris, A. (1999). The association of ATR protein with mouse meiotic chromosome cores. *Chromosoma* *108(2)*, 95-102.

Moens, P. B., Freire, R., Tarsounas, M., Spyropoulos, B. and Jackson, S. P. (2000). Expression and nuclear localization of BLM, a chromosome stability protein mutated in Bloom's syndrome, suggest a role in recombination during meiotic prophase. *J. Cell Sci.* *113(4)*, 663-672.

Monesi, V. (1965). Differential rate of ribonucleic acid synthesis in the autosomes and sex chromosomes during male meiosis in the mouse. *Chromosoma* *17(1)*, 11-21.

Monk, M. and McLaren, A. (1981). X-chromosome activity in foetal germ cells of the mouse. *J. Embryol. Exp. Morphol.* *63*, 75-84.

Moses, M. J. (1956). Chromosomal structures in crayfish spermatocytes. *Journal of Biophysical and Biochemical Cytology* *2*, 215-218.

Motzkus, D., Singh, P.B., and Hoyer-Fender, S. (1999). M31, a murine homolog of *Drosophila* HP1, is concentrated in the XY body during spermatogenesis. *Cytogen. Cell. Genet.* *86(1)*, 83-88.

Nairz, K. and Klein, F. (1997). *Mre11S* - a yeast mutation that blocks double-strand-break processing and permits nonhomologous synapsis in meiosis. *Genes Dev.* *11(17)*, 2272-2290.

Nicklas, R. B., Ward, S. C. and Gorbsky G. J. (1995). Kinetochore chemistry is sensitive to tension and may link mitotic forces to a cell cycle checkpoint. *J. Cell Biol.* *130(4)*, 929-939.

Odorisio, T., Mahadevaiah, S. K., McCarrey, J. R. and Burgoyne, P. S. (1996). Transcriptional analysis of the candidate spermatogenesis gene *Ube1y* and of the closely related *Ube1x* shows that they are coexpressed in spermatogonia and spermatids but are repressed in pachytene spermatocytes. *Dev. Biol.* *180(1)*, 336-343.

Odorisio, T., Rodriguez, T. A., Evans, E. P., Clarke, A. R. and Burgoyne, P. S. (1998). The meiotic checkpoint monitoring synapsis eliminates spermatocytes via p53-independent apoptosis. *Nat. Genet.* *18(3)*, 257-261.

Ohno, S. (1964). Life history of female germ cells in mammals. In: Proceedings 2nd International Conference on Cytogenetics. Malforma, The National Foundation, New York, 36-40.

Offenberg, H. H., Schalk, J. A., Meuwissen, R. L., van Aalderen, M., Kester, H. A., Dietrich, A.J. and Heyting, C. (1998). SCP2: a major protein component of the axial elements of synaptonemal complexes of the rat. *Nucl. Acids Res.* *26(11)*, 2572-2579.

Padmore, R., Cao, L. and Kleckner, N. (1991). Temporal comparison of recombination and synaptonemal complex formation during meiosis in *S. cerevisiae*. *Cell* *66(6)*, 1239-1256.

Page J., Suja, J. A., Santos, J. L. and Rufas, J. S. (1998). Squash procedure for protein immunolocalization in meiotic cells. *Chromosome Res.* *6(8)*, 639-642.

Pearlman, R. E., Tsao, N. and Moens, P. B. (1992). Synaptonemal complexes from DNase-treated rat pachytene chromosomes contain (GT)<sub>n</sub> and LINE/SINE sequences. *Genetics* *130*(4), 865-872.

Penny, G. D., Kay, G. F., Sheardown, S. A., Rastan, S. and Brockdorff, N. (1996). Requirement for *Xist* in X chromosome inactivation. *Nature* *379*(6561), 131-137.

Peters, A. H., Plug, A. W., van Vugt, M. J. and de Boer P. (1997). A drying-down technique for the spreading of mammalian meiocytes from the male and female germline. *Chromosome Res.* *5*(1), 66-68.

Pittman, D. L., Cobb, J., Schimenti, K. J., Wilson, L. A., Cooper, D. M., Brignull, E., Handel, M.A. and Schimenti, J. C. (1998). Meiotic prophase arrest with failure of chromosome synapsis in mice deficient for *Dmcl1*, a germline-specific RecA homolog. *Mol. Cell* *1*(5), 697-705.

Plug, A. W., Peters, A. H., Xu, Y., Keegan, K. S., Hoekstra, M. F., Baltimore, D., de Boer P. and Ashley T. (1997). ATM and RPA in meiotic chromosome synapsis and recombination. *Nat. Genet.* *17*(4), 457-461.

Plug, A. W., Peters, A. H., Keegan, K. S., Hoekstra, M. F., de Boer, P. and Ashley T. (1998). Changes in protein composition of meiotic nodules during mammalian meiosis. *J Cell Sci.* *111*(4), 413-423.

Prinz, S., Amon, A. and Klein, F. (1997). Isolation of *COM1*, a new gene required to complete meiotic double-strand break-induced recombination in *Saccharomyces cerevisiae*. *Genetics* *146*(3), 781-795.

Richler, C., Uliel, E., Rosenmann, A. and Wahrman, J. (1989). Chromosomally derived sterile mice have a 'fertile' active XY chromatin conformation but no XY body. *Chromosoma* *97*(6), 465-474.

Richler, C., Ast, G., Goitein, R., Wahrman, J., Sperling, R. and Sperling, J. (1994). Splicing components are excluded from the transcriptionally inactive XY body in male meiotic nuclei. *Mol. Biol. Cell* *5*(12), 1341-1352.

Rockmill, B. and Roeder, G. S. (1990). Meiosis in asynaptic yeast. *Genetics* *126*(3), 563-574.

Rockmill, B. and Roeder, G. S. (1991). A meiosis-specific protein kinase homolog required for chromosome synapsis and recombination. *Genes Dev.* *5*(12B), 2392-2404.

Rockmill, B., Engebrecht, J. A., Scherthan, H., Loidl, J. and Roeder G. S. (1995). The yeast *MER2* gene is required for chromosome synapsis and the initiation of meiotic recombination. *Genetics* *141*(1), 49-59.

Rodriguez, T. A. and Burgoyne, P. S. Evidence that sex chromosome asynapsis, rather than excess Y gene dosage, is responsible for the meiotic impairment of XYY mice. *Cytogen. Cell. Genet.* In Press.

Roeder, G. S. (1995). Sex and the single cell: meiosis in yeast. *Proc. Natl. Acad. Sci. U.S.A* *92(23)*, 10450-10456.

Roeder, G. S. (1997). Meiotic chromosomes: it takes two to tango. *Genes Dev.* *11(20)*, 2600-2621.

Rogakou, E. P., Boon, C., Redon, C. and Bonner, W. M. (1999). Megabase chromatin domains involved in DNA double-strand breaks in vivo. *J. Cell Biol.* *146(5)*, 905-916.

Ross-Macdonald, P. and Roeder, G. S. (1994). Mutation of a meiosis-specific MutS homolog decreases crossing over but not mismatch correction. *Cell* *79(6)*, 1069-1080.

Salido, E. C., Yen, P. H., Mohandas, T. K. and Shapiro, L. J. (1992). Expression of the X-inactivation-associated gene *Xist* during spermatogenesis. *Nat. Genet.* *2(3)*, 196-199.

Salido, E. C., Li, X. M., Yen, P. H., Martin, N., Mohandas, T. K. and Shapiro, L. J. (1996). Cloning and expression of the mouse pseudoautosomal steroid sulphatase gene (*Sts*). *Nat. Genet.* *13(1)*, 83-86.



San-Segundo, P. A. and Roeder, G. S. (1999). Pch2 links chromatin silencing to meiotic checkpoint control. *Cell* 97(3), 313-324.

Scherthan, H., Weich, S., Schwegler, H., Heyting, C., Harle, M. and Cremer, T. (1996). Centromere and telomere movements during early meiotic prophase of mouse and man are associated with the onset of chromosome pairing. *J. Cell Sci.* 134(5), 1109-1125.

Schmidt, E. E., Ohbayashi, T., Makino, Y., Tamura, T. and Schibler, U. (1997). Spermatid-specific overexpression of the TATA-binding protein gene involves recruitment of two potent testis-specific promoters. *J. Biol. Chem.* 272(8), 5326-5334.

Schwacha, A. and Kleckner, N. (1994). Identification of joint molecules that form frequently between homologs but rarely between sister chromatids during yeast meiosis. *Cell* 76(1), 51-63.

Sen, D. and Gilbert, W. (1988). Formation of parallel four-stranded complexes by guanine-rich motifs in DNA and its implications for meiosis. *Nature* 334, 364-366.

Shinohara, A., Ogawa, H. and Ogawa, T. (1992). Rad51 protein involved in repair and recombination in *S. cerevisiae* is a RecA-like protein. *69(3)*, 457-470.

Siegel, J. N., Turner, C. A., Klinman, D. M., Wilkinson, M., Steinberg, A. D., MacLeod, C. L., Paul, W. E., Davis, M. M. and Cohen, D. I. (1987). Sequence analysis and expression of an X-linked, lymphocyte-regulated gene family (*Xlr*). *J. Exp. Med.* 166(6), 1702-1715.

Smith, A. and Benavente, R. (1992). Identification of a structural protein component of rat synaptonemal complexes. *Exp. Cell Res.* 198(2), 291-297.

Smith, A. and Benavente, R. (1992). Meiosis-specific protein selectively associated with sex chromosomes of rat pachytene spermatocytes. *Proc. Natl. Acad. Sci. U.S.A.* 98, 6938-6942.

Smith, A. and Benavente, R. (1995). An Mr 51, 000 protein of mammalian spermatogenic cells that is common to the whole XY body and centromeric heterochromatin of autosomes. *Chromosoma.* 103(9), 591-596.

Smith, A. V. and Roeder, G. S. (1997). The yeast Red1 protein localizes to the cores of meiotic chromosomes. *J. Cell Biol.* 136(5), 957-967.

Solari, A. J. (1974). The behavior of the XY pair in mammals. *Int. Rev. Cytol.* 38(0), 273-317.

Solari, A. J. (1992). Equalization of Z and W axes in chicken and quail oocytes. *Cytogenet. Cell Genet.* 59(1), 52-56.

Speed, R. M. (1982). Meiosis in the foetal mouse ovary. I. An analysis at the light microscope level using surface-spreading. *Chromosoma* 85(3), 427-437.

Speed, R. M. (1986). Abnormal RNA synthesis in sex vesicles of tertiary trisomic male mice. *Chromosoma* 93(3), 267-270.

Speed, R. M. (1986). Oocyte development in XO fetuses of man and mouse: the possible role of heterologous X-chromosome pairing in germ cell survival. *Chromosoma* 94(2), 115-124.

Storlazzi, A., Xu, L., Schwacha, A. and Kleckner, N. (1996). Synaptonemal complex (SC) component Zip1 plays a role in meiotic recombination independent of SC polymerization along the chromosomes. *Proc. Natl. Acad. Sci. U.S.A* 93(17), 9043-9048.

Sung, P. (1997). Yeast Rad55 and Rad57 proteins form a heterodimer that functions with replication protein A to promote DNA strand exchange by Rad51 recombinase. *Genes Dev.* 11(9), 1111-1121.

Sutcliffe, M. J. and Burgoyne, P. S. (1989). Analysis of the testes of H-Y negative XOSxb mice suggests that the spermatogenesis gene (*Spy*) acts during the differentiation of the A spermatogonia. *Development* 107(2), 373-380.

Sutcliffe, M. J., Darling, S. M. and Burgoyne, P. S. (1991). Spermatogenesis in XY, XYSxra and XOSxra mice: a quantitative analysis of spermatogenesis throughout puberty. *Mol. Reprod. Dev.* 30(2), 81-89.

Sun, H., Treco, D. and Szostak, J.W. (1991). Extensive 3'-overhanging, single-stranded DNA associated with the meiosis-specific double-strand breaks at the ARG4 recombination initiation site. *Cell* 64(6), 1155-1161.

Sym, M., Engebrecht, J. A. and Roeder, G. S. (1993). Zip1 is a synaptonemal complex protein required for meiotic chromosome synapsis. *Cell* 72(3), 365-378.

Sym, M. and Roeder, G. S. (1994). Crossover interference is abolished in the absence of a synaptonemal complex protein. *Cell* 79(2), 283-292.

Sym, M. and Roeder, G. S. (1995). Zip1-induced changes in synaptonemal complex structure and polycomplex assembly. *J. Cell Biol.* 128(4), 455-466.

Szostak, J. W., Orr-Weaver, T. L., Rothstein, R.J. and Stahl, F. W. (1983). The double-strand-break repair model for recombination. *Cell* 33(1), 25-35.

Tease, C. and Cattnach, B. M. (1989). Sex chromosome pairing patterns in male mice of novel Sxr genotypes. *Chromosoma* 97(5), 390-395.

Tease, C. and Fisher, G. (1988). Chromosome pairing in foetal oocytes of mouse inversion heterozygotes. In: *Kew Chromosome Conference III* (ed Brandham, P. E), 293-297. HMSO, London.

Walpita, D., Plug, A. W., Neff, N. F., German, J. and Ashley, T. (1999). Bloom's syndrome protein, BLM, colocalizes with replication protein A in meiotic prophase nuclei of mammalian spermatocytes. *Proc. Natl. Acad. Sci. U.S.A* 96(10), 5622-5627.

Weiner, B. M. and Kleckner, N. (1994). Chromosome pairing via multiple interstitial interactions before and during meiosis in yeast. *Cell* 77(7), 977-991.

Weinert, T. (1998). DNA damage and checkpoint pathways: molecular anatomy and interactions with repair. *Cell* 94(5), 555-558.

West, S. C. (1992). Enzymes and molecular mechanisms of genetic recombination. *Annu. Rev. Biochem.* 61, 603-640.

White, M. J. D. (1973). *Animal cytology and evolution*, 3rd edition. Cambridge University Press, Cambridge.

Whitten, W. K., Beamer, W. G. and Byskov, A. G. (1979). The morphology of fetal gonads of spontaneous mouse hermaphrodites. *J. Embryol. Exp. Morphol.* 52, 63-78.

Wicky, C. and Rose, A. M. (1996). The role of chromosome ends during meiosis *in Caenorhabditis elegans*. *Bioessays* 18(6), 447-452.

Willison, K. W. and Ashworth, A. (1987). Spermatogenic gene expression. *Trends Genet.* 3, 351-355.

Wold, M.S. and Kelly, T. (1988). Purification and characterization of replication protein A, a cellular protein required for in vitro replication of simian virus 40 DNA. *Proc. Natl. Acad. Sci. U.S.A* 85(8), 2523-2527.

Wright, W. E., Sassoon, D. A. and Lin, V. K. (1989). Myogenin, a factor regulating myogenesis, has a domain homologous to MyoD. *Cell* 56(4), 607-617.

Xu, Y., Ashley, T., Brainerd, E. E., Bronson, R. T., Meyn, M. S. and Baltimore, D. (1996). Targeted disruption of *Atm* leads to growth retardation, chromosomal fragmentation during meiosis, immune defects, and thymic lymphoma. *Genes Dev.* 10(19), 2411-2422.

Yoshida, K., Kondoh, G., Matsuda, Y., Habu, T., Nishimune, Y. and Morita, T. (1998). The mouse RecA-like gene *Dmc1* is required for homologous chromosome synapsis during meiosis. *Mol. Cell* 1(5), 707-718.